THE

LONDON, EDINBURGH, AND DUBLIN

PHILOSOPHICAL MAGAZINE

AND

JOURNAL OF SCIENCE.

[SEVENTH SERIES.]

JULY 1936.

I. *The Inverse Method for Tapered and Twisted Wings.*

By Prof. R. C. J. HOWLAND, *M.A., D.Sc., and* B. S. SHENSTONE, *M.A.Sc., A.F.R.Ae.S.**

Introduction.

IT has for many years been recognized by aeroplane designers that tapered wings have certain obvious structural advantages. These advantages, which are definite and calculable, have been offset by some aerodynamical disadvantages, but the exact nature of these has been less clearly understood since, until recently, the difficulties of calculation have prevented a full theoretical discussion. Calculations of the characteristics of tapered wings were, it is true, undertaken by Fage, Glauert, and others † as early as 1923, but their methods lacked precision, and no more exact treatment seems to have been published until the appearance of the

* Communicated by the Authors.

† Fage, "On the Theory of Tapered Aerofoils,' Aeronautical Research Committee, R. and M. no. 806 (1923); Glauert, "A Method of Calculating the Characteristics of a Tapered Wing," R. and M. no. 824 (1923); Glauert and Gates, "The Characteristics of a Tapered and Twisted Wing with Sweep-Back," R. and M. no. 1226 (1929); Glauert, 'Aerofoil and Airscrew Theory' (Cambridge, 1930).

work of Hueber *, based on the recently published method of Lotz †.

Tapered wings, by stalling at the tips earlier than at the root, cause a loss of aileron control at high incidences. In addition, it has been shown that tapering may increase the induced drag of a wing. But it is also known that the behaviour of a wing may be improved by twisting, and, in particular, that sufficient " wash-out " may be applied to make the tips stall later than any other part of the wing. It is the object of the present paper to investigate the most favourable methods of combining twist with taper so as to improve the stalling characteristics of the wing and at the same time to obtain a low induced drag.

There are two methods of approaching such a problem, both depending upon Prandtl's fundamental equation ‡. This equation is a relation between the circulation, the chord, and the angle of incidence at each section of the wing. It is usual to regard the chord and the angle of incidence as known, and to use the equation for the determination of the circulation, and hence of the lift and the induced drag. This method we shall call the *direct* method. It has the advantage of being applicable to a wing whose form is given in advance. On the other hand, it is difficult to apply with any accuracy. When carried out systematically and accurately, as by Hueber, for an extensive class of wings it involves great labour, but gives results of much value.

It has been recognized from the first that an *inverse* method is also possible. Thus, for an untwisted wing, or for one whose twist is prescribed, we may assume the distribution of circulation and use the equation to determine the variations of the chord. This method, which has been employed by Prandtl and, later, by Roy in the papers just cited, may give interesting indications, but usually leads to wings which are structurally im-

* Hueber, " Die Aerodynamischen Eigenschaften von Doppeltrapezfoermigen Tragfluegeln," *Z. F. M.* 1933, pp. 249 and 269, and " Der Verwundene Trapezfluegel," *Z. F. M.* 1933, p. 307.

† Lotz, " Berechnung der Auftriebsverteilung beliebig geformter Fluegel," *Z. F. M.* 1931, p. 189; Shenstone, " The Lotz Method for Calculating the Aerodynamical Characteristics of Wings," Journ. Roy. Aero. Soc., May (1934).

‡ Prandtl, ' Vier Abhandlungen zur Hydrodynamik und Aerodynamik' (Berlin, 1927); " Tragfluegeltheorie," *Göttingen Nachrichten*, 1918, 1919; Roy, ' Théorie des Surfaces portantes ' (Paris, 1922).

possible, or at least undesirable *. In what follows we make use of another variety of the inverse method which is not only more favourable in its results, but is also more closely related to the way in which the problem occurs in practice. The designer will wish to be able, as far as possible, to assign in advance both the general structural form of the wing and its general aerodynamic behaviour. We therefore begin by assuming both the plan-form and the k -grading of the wing. The chord and the circulation are then known, and Prandtl's equation may be used to determine the twist.

This method has the merit of giving a direct answer to the question as to whether the characteristics desired for the wing are compatible, and, when they are, it shows how to obtain them. It has the further advantage that it gives exact and not approximate solutions, and, in some cases, these solutions are simple in form. There are, however, certain compensating disadvantages. In the first place, the twists arrived at are not linear. But, although non-linear twists are unusual, they are in no sense structurally impossible, or even very difficult. Rather more serious is the fact that the results apply only to one angle of incidence. If the incidence is changed the twist will be found to have changed also, so that the results apply to a different wing. The method cannot, therefore, by itself yield full information about the wing. It is of use mainly in the first stages of design, when it suggests the form of wing required. The investigation of the behaviour of this wing at other incidences must be made by the direct method. This is not, however, as important a defect as might appear, since, if there is exact knowledge of the performance of the wing at one important incidence, it will usually be enough to treat other incidences by a roughly approximate method, such as that of Glauert.

In the present paper we have not attempted to carry the work to its conclusion. General formulæ, mainly for straight-tapered wings, are developed in Part I., which is mathematical in character. In Part II. we summarize the relevant results of Part I. and give numerical and graphical results for some specially simple cases. It is difficult to assess the value of the results

* Compare also the discussion given by Betz in Division J of Durand's 'Aerodynamic Theory,' iv. pp. 56–62 (Berlin, 1935).

arrived at until the calculations have been extended to further types of wing. But we have been led to some interesting tentative conclusions which are discussed as they occur. We are also led to formulate a number of problems needing further investigation. When such investigation has been carried out it should be possible to present a much broader picture.

It should be observed that Part II. may be read independently of Part I. if the formulæ are accepted without proof.

Symbols to be employed.

V = velocity of wing relative to still air.

α = angle of incidence, usually a function of x.

c = chord of wing, a function of x

c_0 = chord at mid-span.

s = semi-span.

x = distance from central section measured along the span.

ξ = same as x, when a second point of the wing is indicated.

K = circulation round the wing, a function of x.

K_ξ = the same, expressed as a function of ξ.

k_L = lift coefficient, in general a function of x.

$\bar{k}_L$ = overall lift coefficient.

a_0 = slope of lift curve; its theoretical value is π.

β = angle of taper.

$\mu = (s/c_0) \tan \beta$.

θ, ϕ, defined by $x = -s \cos \theta$; $\xi = -s \cos \phi$.

a_n = coefficient in Fourier Series for k_L.

A_n = coefficient in Fourier Series for K.

L = lift of wing.

D_i = induced drag of wing.

$\delta = \dfrac{\Sigma n A_n^2}{A_1^2} - 1$, a measure of the departure from the character of an elliptic wing.

I_n, J_n, I_n', K_n, K_n', S_n, λ, are defined in Appendix to Part I.

In equations containing the ambiguous sign $\pm$, the

upper sign applies when $0 \leqslant \theta \leqslant \frac{\pi}{2}$ and the lower when $\frac{\pi}{2} \leqslant \theta \leqslant \pi$.

Part I.—General Formulæ.

The k_L grading and the plan-form are supposed given. The object is to find the twist, the lift, and the induced drag.

k_L and c are known functions of x, and V is a given constant. The circulation is then given by

$$K = k_L c V \quad . \quad . \quad . \quad . \quad . \quad . \quad . \quad (1)$$

and the angle of incidence by

$$\alpha = \frac{k_L}{a_0} + \frac{1}{4\pi V} \int_{-s}^{s} \frac{dK_\xi}{d\xi} \frac{d\xi}{x-\xi} . \quad . \quad . \quad . \quad (2)$$

The integral is to be understood as having its principal value. This exists at any point at which K has a continuous derivative ; but a discontinuity in the derivative is easily shown to lead to an infinity in α. This fact, which does not appear to have been previously noticed, is important, since it shows that c and k_L cannot always be arbitrarily chosen. For example, in the important case of a straight-tapered wing, c has a discontinuous derivative at one or more points, and k_L must also have a discontinuous derivative, the discontinuities being so related that the derivative of K is continuous. The exact relationship is easily obtained as follows.

Let c have a discontinuous derivative when $x = x_1$, so that

$$\frac{dc}{dx} \to \left(\frac{dc}{dx}\right)_+ , \quad x \to x_1 + 0 ;$$

$$\frac{dc}{dx} \to \left(\frac{dc}{dx}\right)_- , \quad x \to x_1 - 0.$$

Then

$$\frac{dK}{dx} = V\left[c\frac{dk_L}{dx} + k_L\frac{dc}{dx}\right]$$

and, with the same notation as before,

$$\left(\frac{dK}{dx}\right)_+ = V\left[c\left(\frac{dk_L}{dx}\right)_+ + k_L\left(\frac{dc}{dx}\right)_+\right],$$

$$\left(\frac{dK}{dx}\right)_- = V\left[c\left(\frac{dk_L}{dx}\right)_- + k_L\left(\frac{dc}{dx}\right)_-\right].$$

For these to be equal we must have

$$c\left[\left(\frac{dk_L}{dx}\right)_+ - \left(\frac{dk_L}{dx}\right)_-\right] = k_L\left[\left(\frac{dc}{dx}\right)_- - \left(\frac{dc}{dx}\right)_+\right]. \quad (3)$$

The Straight-tapered Wing.

If the plan of the wing is that represented in fig. 1, with a straight taper from centre to tips, we have

$$\left.\begin{aligned} c &= c_0 - x\tan\beta, \quad x>0, \\ &c_0 + x\tan\beta, \quad x<0. \end{aligned}\right\} \quad . \quad . \quad . \quad . \quad (4)$$

Fig. 1.

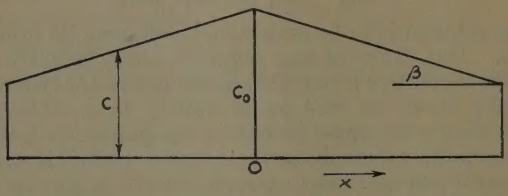

Let

$$x = -s\cos\theta, \quad . \quad . \quad . \quad . \quad . \quad . \quad (5)$$

so that $\theta = 0, \pi/2, \pi$, when $x = -s, 0, +s$.

Write also

$$s\tan\beta = c_0\mu. \quad . \quad . \quad . \quad . \quad . \quad . \quad (6)$$

Then (4) becomes

$$\left.\begin{aligned} c &= c_0(1+\mu\cos\theta), \quad \theta \geqslant \pi/2, \\ &c_0(1-\mu\cos\theta), \quad \theta \leqslant \pi/2. \end{aligned}\right\} \quad . \quad . \quad . \quad (7)$$

Now let the k_L grading be given by

$$k_L = \sum_{p=0}^{\infty} a_{2p+1}\sin(2p+1)\theta \pm \sum_{p=1}^{\infty} a_{2p}\sin 2p\theta, \quad . \quad (8)$$

where, and in later equations, the upper sign refers to the half of the wing on which $0 \leqslant \theta \leqslant \pi/2$ and the lower sign to the other half. It is, of course, possible to represent any symmetrical distribution of k_L by terms of the first type alone. But when k_L has a discontinuous deriva-

tive its Fourier Series will tend to be of a slowly converging type, and the condition of continuity in K will be an additional complication. It will be found that, by using both types of term, we can obtain appropriate solutions with only a small number of terms.

The continuity condition (3) when applied to (7) and (8) gives

$$\sum_{p=1}^{\infty} (-1)^p 2p a_{2p} = -\mu \sum_{p=0}^{\infty} (-1)^p a_{2p+1}. \quad . \quad . \quad (9)$$

When the series for k_L is infinite it may be non-differentiable, and (9) may need modification. But this possibility will be ignored since, in practice, the series will either be finite or so rapidly convergent as to be effectively finite, terms after the first few being omitted.

To find α we first write

$$\begin{aligned}
\mathrm{K} &= k_L c \mathrm{V} \\
&= \mathrm{V} c_0 \Big[\sum_{p=0}^{\infty} a_{2p+1} \{ \sin(2p+1)\theta \mp \tfrac{1}{2}\mu [\sin(2p+2)\theta + \sin 2p\theta] \} \\
&\quad + \sum_{p=1}^{\infty} a_{2p} \{ \pm \sin 2p\theta - \tfrac{1}{2}\mu [\sin(2p+1)\theta + \sin(2p-1)\theta] \} \Big] .
\end{aligned}$$

$$\begin{aligned}
\frac{d\mathrm{K}}{d\theta} &= \mathrm{V} c_0 \Big[\sum_{p=0}^{\infty} a_{2p+1} \{ (2p+1)\cos(2p+1)\theta \\
&\quad \mp \mu [(p+1)\cos(2p+2)\theta + p \cos 2p\theta] \} \\
&\quad + \sum_{p=1}^{\infty} a_{2p} \{ \pm 2p \cos 2p\theta \\
&\quad - \tfrac{1}{2}\mu [(2p+1)\cos(2p+1)\theta + (2p-1)\cos(2p-1)\theta] \} \Big] .
\end{aligned}$$

Then

$$\begin{aligned}
\int_{-s}^{s} \frac{d\mathrm{K}_\xi}{d\xi} \frac{d\xi}{x-\xi} &= \frac{1}{s} \int_0^{\pi} \frac{d\mathrm{K}_\phi}{d\phi} \frac{d\phi}{\cos\phi - \cos\theta} \\
&= \frac{\mathrm{V} c_0}{s} \Big[\sum_{p=0}^{\infty} a_{2p+1} \{ (2p+1)(\mathrm{I}_{2p+1} + \mathrm{J}_{2p+1}) \\
&\quad - \mu [(p+1)(\mathrm{I}_{2p+2} - \mathrm{J}_{2p+2}) + p(\mathrm{I}_{2p} - \mathrm{J}_{2p})] \} \\
&\quad + \sum_{p=1}^{\infty} a_{2p} \{ 2p(\mathrm{I}_{2p} - \mathrm{J}_{2p}) \\
&\quad - \tfrac{1}{2}\mu [(2p+1)(\mathrm{I}_{2p+1} + \mathrm{J}_{2p+1}) + (2p-1)(\mathrm{I}_{2p-1} + \mathrm{J}_{2p-1})] \} \Big] .
\end{aligned}$$

where

$$I_n=\int_0^{\pi/2}\frac{\cos n\phi\, d\phi}{\cos\phi-\cos\theta},\qquad J_n=\int_{\pi/2}^{\pi}\frac{\cos n\phi\, d\phi}{\cos\phi-\cos\theta}. \quad (10)$$

These integrals are evaluated in the appendix to Part I. Using the values given there, and writing

$$\left.\begin{aligned}\lambda&=\operatorname{cosec}\theta\log\tan\left(\frac{\pi}{4}+\frac{\theta}{2}\right),\\ S_n&=\pi\frac{\sin n\theta}{\sin\theta},\\ I_n'&=\sum_{p=0}^{n}\frac{S_{n-t-1}}{t+1}\sin\tfrac{1}{2}(t+1)\pi,\end{aligned}\right\}\quad . \quad . \quad . \quad (11)$$

we have, after a little reduction,

$$\int_{-s}^{s}\frac{dK_\xi}{d\xi}\frac{d\xi}{x-\xi}=\frac{Vc_0}{s}\Big[(a_1-\tfrac{1}{2}\mu a_2)S_1 + \sum_{p=1}^{\infty}(2p+1)[a_{2p+1}-\tfrac{1}{2}\mu(a_{2p}+a_{2p+2})]S_{2p+1} +2\sum_{p=1}^{\infty}\{2pa_{2p}-\mu p(a_{2p-1}+a_{2p+1})\}\{\lambda\cos 2p\theta+2I'_{2p}\}\Big]. \quad . \quad . \quad . \quad (12)$$

The values used for I_n, J_n assume $0<\theta<\pi/2$, so that (12) only applies to this half of the wing. The other half is obtainable by symmetry. The value of α is given at once by (2), (8), and (12), but there is nothing to be gained by writing down the complete expression for it.

Since λ contains factors becoming infinite when $\theta=0$ and when $\theta=\frac{1}{2}\pi$, the value given by (12) at these points must be examined.

When θ is small we have

$$\lambda\sim\frac{1}{\theta}\log(\tan\tfrac{1}{4}\pi+\tfrac{1}{2}\theta\sec^2\tfrac{1}{4}\pi)$$

$$=\frac{1}{\theta}\log(1+\theta)=1+O(\theta),$$

Hence $\lambda\to1$ when $\theta\to0$, and this point needs no further examination.

When $\theta=\frac{1}{2}\pi-\epsilon$, where ϵ is small,

$$\lambda=\sec\epsilon\log\tan\tfrac{1}{2}\epsilon\sim\log\tfrac{1}{2}\epsilon.$$

The factor multiplying 2λ is

$$\sum_{p=1}^{\infty} \{2pa_{2p}-\mu p(a_{2p-1}+a_{2p+1})\}\cos(p\pi-2p\epsilon)$$

$$= \sum_{p=1}^{\infty} p\{2a_{2p}-\mu(a_{2p-1}+a_{2p+1})\}\{(-1)^p+O(\epsilon^2)\}.$$

The product will thus have a finite limit if

$$\sum_{p=1}^{\infty} (-1)^p p\{2a_{2p}-\mu(a_{2p-1}+a_{2p+1})\}=0 \quad . \quad . \quad (13)$$

This may be written

$$\sum_{p=1}^{\infty} (-1)^p 2pa_{2p}$$

$$=\mu\left[\sum_{p=1}^{\infty}(-1)^p pa_{2p+1}+\sum_{p=0}^{\infty}(-1)^{p+1}(p+1)a_{2p+1}\right]$$

$$=-\mu\sum_{p=0}^{\infty}(-1)^p a_{2p+1},$$

and is seen to be identical with the continuity condition (9).

Fourier Series for K.

If we assume an expansion for K in the form

$$K=4sV\sum_{n=0}^{\infty} A_{2n+1}\sin(2n+1)\theta, \quad . \quad . \quad . \quad (14)$$

as in Glauert's method, we have

$$2\pi sVA_{2n+1}=\int_0^{\pi} K\sin(2n+1)\theta\, d\theta.$$

The integration is elementary, and leads to

$$2\pi sA_{2n+1}=c_0\left\{\tfrac{1}{2}\pi a_{2n+1}-\tfrac{1}{4}\pi\mu(a_{2n}+a_{2n+2})\right.$$

$$+\tfrac{1}{2}\mu\sum_{p=0}^{\infty}(-1)^{n+p-1}a_{2p+1}$$

$$\times\left[\frac{1}{2n+2p+3}-\frac{1}{2n-2p-1}-\frac{1}{2n+2p+1}+\frac{1}{2n-2p+1}\right]$$

$$\left.+\sum_{p=1}^{\infty}(-1)^{n+p}a_{2p}\left[\frac{1}{2n-2p+1}-\frac{1}{2n+2p+1}\right]\right\}. \quad . \quad (15)$$

In terms of these coefficients we have

$$\alpha = \frac{k_{\mathrm{L}}}{a_0} + \sum_{n=0}^{\infty} (2n+1)\mathrm{A}_{2n+1} \frac{\sin(2n+1)\theta}{\sin\theta} \quad . \quad . \quad (16)$$

The lift is

$$\mathrm{L} = 2\pi s^2 \rho \mathrm{V}^2 \mathrm{A}_1, \quad . \quad . \quad . \quad . \quad . \quad (17)$$

and the induced drag is

$$\mathrm{D}_i = 2\pi s^2 \rho \mathrm{V}^2 \sum_{n=0}^{\infty} (2n+1)\mathrm{A}_{2n+1}^2. \quad . \quad . \quad . \quad (18)$$

In general L and D_i are most conveniently found from (17) and (18), but the series in (16) may be rather slowly convergent, and α is then best found from (12), (8), and (2).

Special Class of Finite Solutions.

The terms in K with an ambiguous sign are

$$\mp \tfrac{1}{2}\mu \sum_{p=0}^{\infty} a_{2p+1} [\sin(2p+2)\theta + \sin 2p\theta] \pm \sum_{p=1}^{\infty} a_{2p} \sin 2p\theta.$$

If these all vanish, K is in its initial form a Fourier Series. The condition is that

$$2a_{2p} = \mu(a_{2p-1} + a_{2p+1}). \quad . \quad . \quad . \quad . \quad (19)$$

As might be expected, the continuity condition then becomes an identity. The form of α is much simplified, for in this case

$$\begin{aligned}
&\int_{-s}^{s} \frac{d\mathrm{K}_\xi}{d\xi} \frac{d\xi}{x-\xi} \\
&= \frac{\mathrm{V}c_0}{s} \Big[(a_1 - \tfrac{1}{2}\mu a_2)\mathrm{S}_1 \\
&\quad + \sum_{p=1}^{\infty} (2p+1)[a_{2p+1} - \tfrac{1}{2}\mu(a_{2p} + a_{2p+2})]\mathrm{S}_{2p+1} \Big] \\
&= \frac{\mathrm{V}c_0}{s} \Big[\{a_1 - \tfrac{1}{4}\mu^2(a_1 + a_3)\}\mathrm{S}_1 \\
&\quad + \sum_{p=1}^{\infty} (2p+1)\{a_{2p+1} - \tfrac{1}{4}(a_{2p-1} + 2a_{2p+1} + a_{2p+3})\}\mathrm{S}_{2p+1} \Big]. \\
&\qquad\qquad\qquad\qquad\qquad\qquad\qquad\qquad\qquad\qquad . \quad . \quad . \quad (20)
\end{aligned}$$

If K is written in the form (14), we now have

$$[illegible]$$

$$[illegible] \quad . \quad . \quad (27)$$

The first coefficient is exceptional, being given by

$$[illegible] \quad . \quad . \quad . \quad (28)$$

Finally, if [illegible], k, K, L, and D will all be in a finite form, and these finite solutions are exact.

The Rectangular Wing

In the special case of [illegible] it is not necessary to include the even sine terms in K. The equations reduce to

$$k = \sum [illegible] \sin (2p+1)\theta,$$

$$[illegible] \quad . \quad . \quad (29)$$

$$[illegible]$$

The Elliptic Wing

If

$$[illegible] \quad . \quad . \quad . \quad . \quad . \quad (30)$$

and if we assume

$$k = \sum [illegible] \sin (2p+1)\theta \quad . \quad . \quad . \quad . \quad (31)$$

then

$$K = [illegible] \{\cos 2p\theta - \cos (2p+2)\theta\}$$

and

$$[illegible]$$

where

$$K_n = \int_0^\pi \frac{\sin n\theta \, d\theta}{\cos\theta - \cos\theta'} \quad . \quad . \quad . \quad . \quad (32)$$

From the Appendix we have

$$\left.\begin{aligned} \mathrm{K}_n &= \frac{2\sin n\theta}{\sin\theta}\log\tan\frac{\theta}{2}+\mathrm{K}_n', \\ \text{with}\quad \mathrm{K}_n' &= \frac{4}{\sin\theta}\sum_{t=0}^{n-1}\frac{\sin(n-t-1)\theta}{t+1}\sin^2\frac{(t+1)\pi}{2}. \end{aligned}\right\} \quad (27)$$

Hence

$$\int_{-s}^{s}\frac{d\mathrm{K}_\xi}{d\xi}\frac{d\xi}{x-\xi} = \frac{\mathrm{V}c_0}{s}\Big[\sum_{p=0}^{\infty}a_{2p+1}\{p\mathrm{K}'_{2p}-(p+1)\mathrm{K}'_{2p+2}\} - \frac{2}{\sin\theta}\log\tan\frac{\theta}{2}\sum_{p=0}^{\infty}a_{2p+1}\sin(2p+1)\theta\Big]. \quad (28)$$

Since $\log\tan\theta/2$ tends to infinity when $\theta\to 0$, it is necessary that

$$\sum_{p=0}^{\infty}(2p+1)a_{2p+1}=0. \quad (29)$$

This is the condition that the derivative of k_L should vanish when $\theta=0$. The k_L curve for an elliptic wing must therefore have its tangent horizontal at the ends of the span. It also has a horizontal tangent at mid-span.

The Fourier Series for K being written, as before, in the form

$$\mathrm{K}=4s\mathrm{V}\sum_{n=0}^{\infty}\mathrm{A}_{2n+1}\sin(2n+1)\theta,$$

we easily find

$$\mathrm{A}_{2n+1}=\frac{c_0}{4\pi s}\sum_{p=0}^{\infty}a_{2p+1} \times\Big[\frac{1}{2n+2p+1}+\frac{1}{2n-2p+1}-\frac{1}{2n+2p+3}-\frac{1}{2n-2p-1}\Big]. \quad (30)$$

The special solution for an untwisted elliptic wing may be written :

$$\left.\begin{aligned} \mathrm{K} &= \tfrac{1}{2}\mathrm{V}c_0\sin\theta, \\ k_L &= a, \\ \mathrm{A}_1 &= c_0 a/8s, \\ \mathrm{A}_{2n+1} &= 0, \quad n>0. \end{aligned}\right\} \quad (31)$$

This may be added to the previous solution, a being arbitrary.

Appendix to Part I.—*Evaluation of the Integrals.*

The first two definite integrals required are

$$\mathrm{I}_n=\int_0^{\pi/2}\frac{\cos n\phi\,d\phi}{\cos\phi-\cos\theta},\qquad \mathrm{J}_n=\int_{\pi/2}^{\pi}\frac{\cos n\phi\,d\phi}{\cos\phi-\cos\theta}. \quad (32)$$

Since

$$2(\cos\phi-\cos\theta)\cos n\phi$$
$$=\cos(n+1)\phi+\cos(n-1)\phi-2\cos\theta\cos n\phi,$$

we have

$$\mathrm{I}_{n+1}-2\cos\theta\,\mathrm{I}_n+\mathrm{I}_{n-1}=2\int_0^{\pi/2}\cos n\phi\,d\phi$$
$$=\frac{2}{n}\sin\frac{n\pi}{2}.$$

Similarly,

$$\mathrm{J}_{n+1}-2\cos\theta\,\mathrm{J}_n+\mathrm{J}_{n-1}=-\frac{2}{n}\sin\frac{n\pi}{2}.$$

To find a general solution of these difference equations write them in the form

$$\left.\begin{aligned}(\mathrm{E}^2-2\mathrm{E}\cos\theta+1)\mathrm{I}_n&=\frac{2}{n+1}\sin\frac{n+1}{2}\pi,\\ (\mathrm{E}^2-2\mathrm{E}\cos\theta+1)\mathrm{J}_n&=-\frac{2}{n+1}\sin\frac{n+1}{2}\pi,\end{aligned}\right\} \quad (33)$$

where E is the operator defined by

$$\mathrm{E}\phi(n)=\phi(n+1).$$

Then *

$$\mathrm{I}_n=\mathrm{A}\cos n\theta+\mathrm{B}\sin n\theta+\mathrm{I}_n', \quad . \quad . \quad . \quad (34)$$

where A, B are arbitrary constants and

$$\mathrm{I}_n'=\frac{1}{2i\sin\theta}\left[\frac{1}{\mathrm{E}-e^{i\theta}}-\frac{1}{\mathrm{E}-e^{-i\theta}}\right]\frac{2}{n+1}\sin\frac{n+1}{2}\pi$$

* Milne-Thomson, 'Calculus of Finite Differences' (London, 1933). §§ 13.2–13.24.

$$= \frac{1}{i \sin\theta}\left[e^{(n-1)i\theta}\sum_{t=0}\frac{e^{-ti\theta}}{t+1}\sin\frac{t+1}{2}\pi \right.$$
$$\left. - e^{-(n-1)i\theta}\sum_{t=0}^{n}\frac{e^{ti\theta}}{t+1}\sin\frac{t+1}{2}\pi\right]$$
$$= \frac{2}{\sin\theta}\sum_{t=0}^{n}\frac{\sin(n-t-1)\theta}{t+1}\sin\frac{t+1}{2}\pi.$$

This may be conveniently written in the alternative forms appropriate to odd and even suffixes respectively:

$$\left.\begin{aligned} I'_{2n} &= 2\sum_{t=0}^{n-1}(-1)^t\frac{\sin(2n-2t-1)\theta}{(2t+1)\sin\theta}, \\ I'_{2n+1} &= 2\sum_{t=0}^{n}(-1)^t\frac{\sin(2n-2t)\theta}{(2t+1)\sin\theta}. \end{aligned}\right\} \quad . \quad (35)$$

To find the arbitrary constants, put $n=0$ and 1 successively in (34) and use the obvious equalities,

$$I_1 = I_0\cos\theta + \frac{\pi}{2}, \qquad I_0' = I_1' = 0.$$

Then we obtain immediately

$$A = I_0, \qquad B = \tfrac{1}{2}\pi.$$

It remains to evaluate I_0. This is an improper integral, and, as is usual in the theory, its principal value is to be taken. Writing

$$\tan\tfrac{1}{2}\phi = t, \qquad \tan\tfrac{1}{2}\theta = t_1$$

we have

$$I_0 = (1+t_1^2)\int_0^1 \frac{dt}{t_1^2 - t^2}$$
$$= \operatorname{cosec}\theta\int_0^1\left(\frac{1}{t_1+t}+\frac{1}{t_1-t}\right)dt$$
$$= \operatorname{cosec}\theta\left[\left\{\log(t_1+t)\right\}_0^1 - \lim_{\epsilon\to 0}\left\{\left[\log(t_1-t)\right]_0^{t_1-\epsilon}\right.\right.$$
$$\left.\left. - \left[\log(t-t_1)\right]_{t-\epsilon}^1\right\}\right]$$
$$= \operatorname{cosec}\theta\left[\log\frac{1+t_1}{t_1} - \lim_{\epsilon\to 0}\log\left\{\frac{\epsilon}{t_1}\,\frac{1-t_1}{\epsilon}\right\}\right]$$
$$= \operatorname{cosec}\theta\log\frac{1+t_1}{1-t_1}$$
$$= \operatorname{cosec}\theta\log\tan\left(\tfrac{1}{4}\pi+\tfrac{1}{2}\theta\right). \quad . \quad . \quad . \quad . \quad . \quad . \quad . \quad . \quad (36)$$

This is the quantity which we have already called λ; hence

$$I_n=\lambda \cos n\theta+\tfrac{1}{2}S_n+I_n', \quad . \quad . \quad . \quad . \quad (37)$$

where, as in (11),

$$S_n=\pi \frac{\sin n\theta}{\sin \theta}.$$

The first few values of I_n' written in full are

$$\left.\begin{aligned} I_0'&=I_1'=0,\\ I_2'&=2\frac{\sin\theta}{\sin\theta}=2,\\ I_3'&=2\frac{\sin 2\theta}{\sin\theta}=4\cos\theta,\\ I_4'&=2\left[\frac{\sin 3\theta}{\sin\theta}-\frac{1}{3}\right],\\ I_5'&=2\left[\frac{\sin 4\theta}{\sin\theta}-\frac{1}{3}\frac{\sin 2\theta}{\sin\theta}\right],\\ I_6'&=2\left[\frac{\sin 5\theta}{\sin\theta}-\frac{1}{3}\frac{\sin 3\theta}{\sin\theta}+\frac{1}{5}\right]. \end{aligned}\right\} \quad . \quad . \quad (38)$$

The law of formation is evident.

Treating J_n in the same way, we find

$$J_n=-\lambda \cos n\theta+\tfrac{1}{2}S_n-I_n'. \quad . \quad . \quad . \quad (39)$$

Throughout the analysis of Part I. the integrals always appear in the two combinations

$$\left.\begin{aligned} I_n+J_n&=S_n,\\ I_n-J_n&=2(\lambda \cos n\theta+I_n'). \end{aligned}\right\} \quad . \quad . \quad . \quad (40)$$

The first of these equations is well known *.

The third type of integral used may be dealt with in a similar way. Writing

$$K_n=\int_0^\pi \frac{\sin n\phi\, d\phi}{\cos\phi-\cos\theta},$$

we have

$$K_{n+1}-2\cos\theta\, K_n+K_{n-1}=2\int_0^\pi \sin n\phi\, d\phi$$

$$=\frac{4}{n}\sin^2\tfrac{1}{2}n\pi.$$

* Glauert, 'Aerofoil and Airscrew Theory,' §7.31.

Hence, by the previous method,

$$K_n = A \cos n\theta + B \sin n\theta + K_n',$$

where

$$K_n' = \frac{4}{\sin\theta} \sum_{t=0}^{n-1} \frac{\sin(n-t-1)\theta}{t+1} \sin^2 \tfrac{1}{2}(t+1)\pi, \quad n>0.$$

Since, also,

$$K_0 = K_0' = K_1' = 0, \quad K_1 = 2 \log \tan \tfrac{1}{2}\theta,$$

we obtain

$$A=0, \quad B = 2 \operatorname{cosec}\theta \log \tan \tfrac{1}{2}\theta.$$

Hence

$$K_n = \frac{2 \sin n\theta}{\sin\theta} \log \tan \frac{\theta}{2} + K_n', \quad \ldots \quad (41)$$

the first few values of K_n' being

$$\left.\begin{aligned} K_0' &= K_1' = 0, \\ K_2' &= 4, \\ K_3' &= 4 \frac{\sin 2\theta}{\sin\theta}, \\ K_4' &= 4\left(\frac{\sin 3\theta}{\sin\theta} + \frac{1}{3}\right), \\ K_5' &= 4\left(\frac{\sin 4\theta}{\sin\theta} + \frac{1}{3}\frac{\sin 2\theta}{\sin\theta} + \frac{1}{5}\right). \end{aligned}\right\} \quad \ldots \quad (42)$$

Part II.—Some Special Cases of Straight tapered Wings.

In this part we shall give formulæ and numerical results corresponding to some special classes of wing which are included in the very general types discussed in Part I. A fuller discussion, with reference to practical requirements, must be deferred until the numerical results have been obtained for a number of other cases, but some interesting conclusions will emerge. All the examples chosen are of straight-tapered wings, and the formulæ relevant to these will first be restated, so that this part of the paper may be read independently.

The plan of the wing being that shown diagrammatically in fig. 1, it has been proved that a specially simple class of

solutions exist in which k_L, K, α, L, D_i are given without approximation by the following equations * :

$$k_L = \sum_{p=0}^{n} a_{2p+1} \sin(2p+1)\theta + \tfrac{1}{2}\mu \sum_{p=1}^{n+1} (a_{2p-1}+a_{2p+1}) \sin 2p\theta,$$

$$K = 4sV \sum_{p=0}^{n+1} A_{2p+1} \sin(2p+1)\theta,$$

$$\alpha = \frac{k_L}{a_0} + \sum_{p=0}^{n+1} (2p+1) A_{2p+1} \frac{\sin(2p+1)\theta}{\sin\theta},$$

$$L = 2\pi s^2 \rho V^2 A_1,$$

$$D_i = 2\pi s^2 \rho V^2 \sum_{p=0}^{n+1} (2p+1) A_{2p+1}^2,$$

where

$$A_1 = \frac{c_0}{4s}\{(1-\tfrac{1}{4}\mu^2)a_1 - \tfrac{1}{4}\mu^2 a_3\},$$

$$A_{2p+1} = \frac{c_0}{4s}\{(1-\tfrac{1}{2}\mu^2)a_{2p+1} - \tfrac{1}{4}\mu^2(a_{2p-1}+a_{2p+3})\}, \quad p>0.$$

The coefficients a_{2p+1} and the number n of them are arbitrary, but a_{2n+3} where it is formally required by the equations must be treated as 0. The equation for k_L applies only to the half of the wing on which $\theta \leqslant \frac{1}{2}\pi$, the values on the other half being symmetrical with these.

Consider now the case of $n=2$. With a slight change of notation we may write

$$k_L = a_1[\sin\theta + a_3 \sin 3\theta + \tfrac{1}{2}\mu(1+a_3)\sin 2\theta + \tfrac{1}{2}\mu a_3 \sin 4\theta],$$

$$A_1 = \frac{c_0 a_1}{4s}\{1-\tfrac{1}{4}\mu^2(1+a_3)\},$$

$$A_3 = \frac{c_0 a_1}{4s}\{(1-\tfrac{1}{2}\mu^2)a_3 - \tfrac{1}{4}\mu^2\},$$

$$A_5 = \frac{c_0 a_1}{4s}\{-\tfrac{1}{4}\mu^2 a_3\}.$$

In order that the different members of this class of wings may be comparable, we choose a_1 so that the overall lift-coefficient $\bar{k}_L$ is the same for all. It is easily seen that this will be so if

$$a_1 = \frac{2\bar{k}_L(2-\mu)}{\pi\{1-\tfrac{1}{4}\mu^2(1+a_3)\}}.$$

* For meaning of symbols see list at end of Introduction, p. 4.

There is now only a single parameter a_3, and this may be used to adjust the form of the k_L grading curve. It is desirable for the grading to be such that at the higher angles of incidence the values of k_L are least in the neighbourhood of the wing-tips, since the part of the wing with the highest value of k_L is likely to stall first. The theory upon which our work is based does not apply after stalling commences, and the conditions then operative can only be inferred in a general way from the conditions just before the stall. But it is to be expected that if stalling commences in the neighbourhood of the ailerons lateral control will be weakened, and, perhaps, lost altogether, before the lift as a whole is lost. To remove the possibility of such dangerous conditions it is essential to keep the maximum value of k_L well in towards the root.

In fig. 2 we have given Hueber's results for untwisted tapered wings for comparison with our own results, which are given later. Hueber's curves illustrate the well-known fact that, in an untwisted wing, the maximum value of k_L approaches the tip as the taper is increased. To bring this maximum inwards twist (wash-out) must be applied, but if it is not applied with care a large increase in the induced drag may result. If, for example, the maximum value is forced inwards to the root, giving something like an elliptic distribution, the induced drag rises rapidly (*cf.* the discussion of the results shown in fig. 6). The central position of the maximum is also undesirable in other ways, for if stalling occurs first at the root the tail controls may be unfavourably affected. It is, therefore, most desirable to be able to control the position of the maximum of k_L, and we shall use the parameter a_3 for this purpose.

If the maximum occurs when $\cos\theta=\xi$, it is easily shown that

$$a_3[3\xi(4\xi^2-3)+\mu(16\xi^4-14\xi^2+1)]+[\xi+\mu(2\xi^2-1)]=0.$$

Thus a_3 is readily found for any given value of ξ, and in what follows we shall treat ξ as the parameter instead of a_3. The results of our calculations are shown in graphical form in the next few diagrams. These are very nearly self-explanatory, but a few points must receive mention.

It will be seen that the curves are drawn for four values of ξ, 0·2, 0·3, 0·4, and 0·5. Greater values of ξ would bring the maximum nearer to the wing-tip than is desirable.

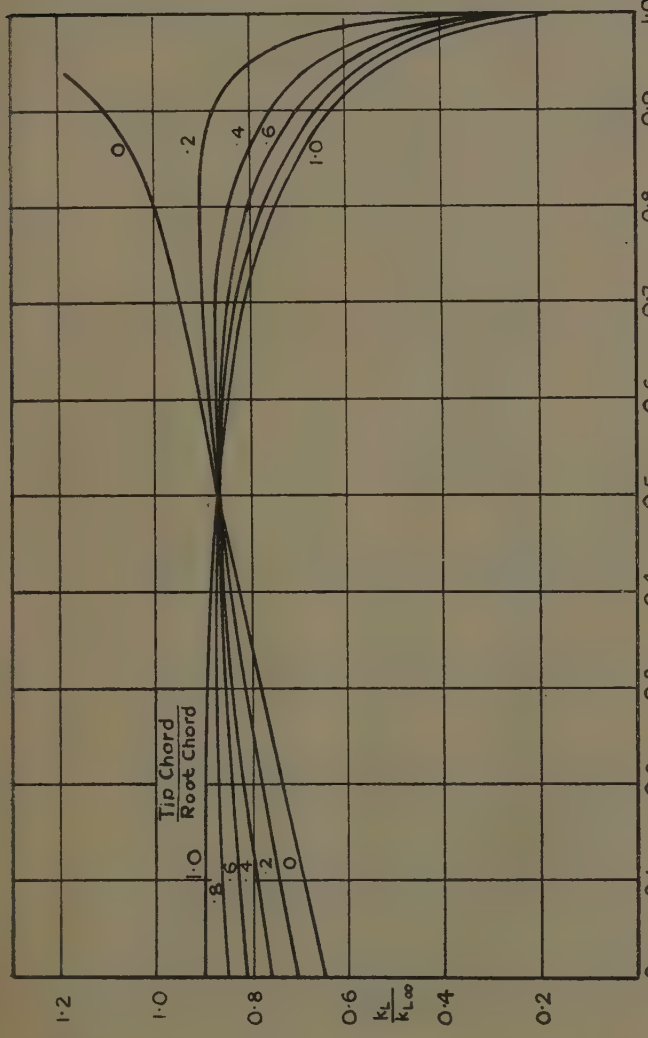

Fig. 2.

k_L gradings. Untwisted straight-tapered wings. Aspect ratio = 10. (From *Z. F. M.* 1933, p. 269.)

The calculation of k_L for any values of ξ and μ is simple, and we have thought it sufficient to give a few typical curves—those for $\mu = 0{\cdot}6$. It should be observed, however,

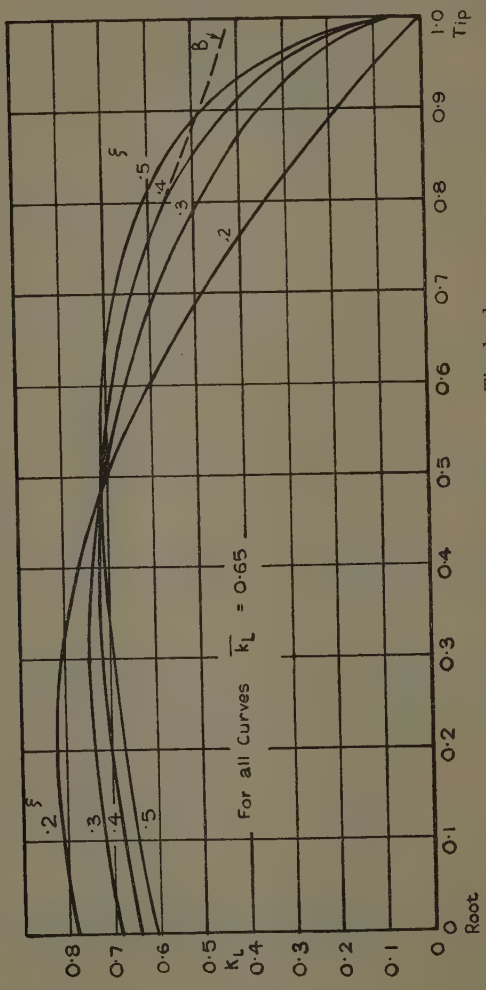

that before they can be drawn the value of the overall coefficient $\bar{k}_L$ must be specified, since upon this depends the multiplying constant a_1. In fixing this we have been

guided by the consideration that it is most important to prescribe the characteristics of the wing for high incidences. Experience shows that for normal wing sections $k_L = 0{\cdot}65$ is as high a value as can be conveniently assumed, as at slightly higher values than this the wing

Fig. 4.

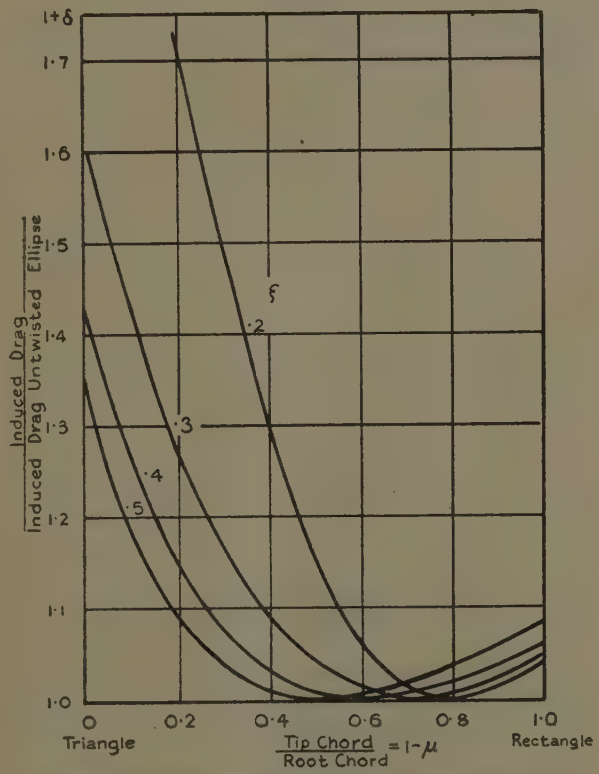

Relative induced drags. Tapered wings twisted to give k_L gradings as in fig. 3.

begins to stall. We have adopted this value, and it leads to the curves in fig. 3.

It is of the greatest importance to determine the effect on the induced drags of arranging the k_L gradings in this manner. In fig. 4 we have, following a well-known method,

shown not the induced drag itself, but the relative induced drag, taking the untwisted elliptic wing as the basis of comparison. The relative drag is defined by

$$1+\delta = \frac{\Sigma n A_n^2}{A_1^2} = \frac{D_i}{D_i\text{-ellipse}}.$$

The elliptic wing, which has the least induced drag possible, corresponds to $\delta=0$, so that δ is a measure of the departure from the best possible condition. The curves reveal the remarkable fact that in each case there is a minimum at

Fig. 5.

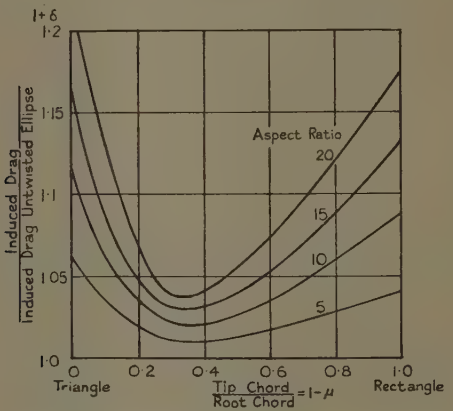

Relative induced drags. Tapered untwisted wings.
(From *Z. F. M.* 1933, p. 271.)

which δ is extremely small, so that for each value of ξ a combination of taper and twist can be found giving an induced drag scarcely greater than that of an elliptic wing.

When comparing these curves with the corresponding results for untwisted wings it should be borne in mind that the latter are dependent upon the aspect ratio. Our own curves are independent of this, the dependence being, as will be seen later, transferred to the twist. Some typical curves for untwisted wings (after Hueber) are shown in fig. 5. They show considerably greater minimum values of δ. But the advantage is not always with the

twisted wing. For moderate tapers (up to *tip chord* ÷ *root chord* = 0·4), the twisted wings have as low or lower drags than any untwisted wings. But for greater tapers the drags increase very much more rapidly for the twisted wings than for the untwisted. It would appear that tapers greater than about 1 : 3 (*tip chord* ÷ *root chord* = 0·33) are not worth using. However, in practice the question of weight has to be considered, and the optimum taper is then slightly greater than the purely aerodynamical optimum.

The formulæ that have led to the curves in fig. 4 have the advantage that they give k_L distributions of a desirable form with the use of only a finite number of terms. It must, however, be remembered that there are an infinite number of other possibilities. Larger values of n may be taken, and will lead to a great variety of solutions, some of which may lead to a modification of the conclusions we have reached. Some support is, however, given to our present conclusions by some calculations based on a different set of formulæ. These are too long to quote here, but their general nature is easily indicated. They were obtained by reducing equation (8) of Part I. to three terms arranged so as to satisfy the condition of continuity (9), but not the finiteness condition (19). The k_L curves are of the same general type as before, and the maximum can still be adjusted to any value of ξ. The formulæ for the coefficients A_n, however, now appear in the form of infinite series, and their calculation is longer. They may be obtained, however, without undue labour, and lead to values of δ which are shown in fig. 6. The curves are remarkably similar to those of fig. 4.

The other curves, shown in fig. 6, show the results of assuming k_L distributions which violate the continuity condition at the root. On this account they will lead to twists which are in part impossible, but they give δ-curves of a reasonable kind, and it is interesting to compare these with the other curves.

The first of these additional curves is obtained on the assumption that the k_L grading is elliptical *, *i. e.*,

$$k_L/k_{L_0} = \sin\theta.$$

* The curve does not agree with one given in Hueber's second paper. We have to thank Herr Hueber for having communicated to us a corrected version of his results.

A slight modification of the theory of Part I. leads to the equations

$$\frac{k_L c}{k_{L_0} c_0} = (1+\mu\cos\theta)\sin\theta = \sum_{n=0}^{\infty} A_{2n+1}\sin(2n+1)\theta,$$

where, by the usual methods of Fourier Analysis,

$$A_{2n+1} = \frac{\mu}{\pi}\left[\frac{\sin\frac{1}{2}(2n-1)\pi}{2n-1} - \frac{\sin\frac{1}{2}(2n+3)\pi}{2n+3}\right], \quad n>0.$$

Fig. 6.

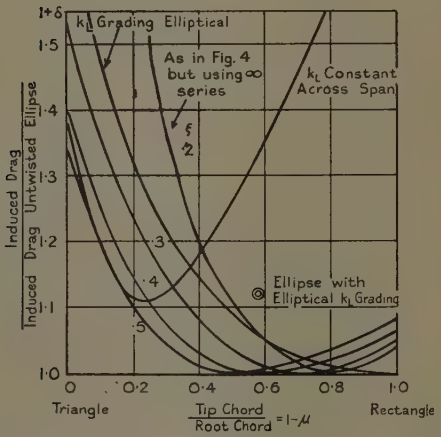

Relative induced drags. Tapered wings twisted to give various k_L gradings.

The first few coefficients are

$$A_1 = 1-\frac{4\mu}{3\pi}, \qquad A_3 = \frac{4\mu}{5\pi},$$

$$A_5 = \frac{4\mu}{21\pi}, \qquad A_7 = \frac{4\mu}{45\pi}.$$

This grading, giving an even sharper reduction of k_L along the span than the shapes assumed above, gives a higher value of δ except for the smaller tapers.

The other curve is obtained by assuming that k_L is constant across the span, as for an untwisted elliptic wing. If we write

$$k_L/k_{L_0} = \mathrm{M}\ (\text{constant}),$$

the variation of the circulation K is given by

$$\frac{k_1 c}{k_{L_0} c_0} = \mathrm{M}(1+\mu\cos\theta) = \sum_{n=0}^{\infty} \mathrm{A}_{2n+1} \sin(2n+1)\theta,$$

from which we obtain

$$\mathrm{A}_{2n+1} = \frac{2}{\pi}\left[\frac{2}{2n+1} + \mu\left\{\frac{\cos(n+1)\pi}{2(n+1)} + \frac{\cos n\pi}{2n} - \frac{1}{2(n+1)} - \frac{1}{2n}\right\}\right],$$

i. e.,

$$\mathrm{A}_1 = \frac{2}{\pi}[2-\mu], \qquad \mathrm{A}_3 = \frac{2}{\pi}\left[\frac{2}{3} - \mu\right], \qquad \mathrm{A}_5 = \frac{2}{\pi}\left[\frac{2}{5} - \frac{1}{3}\mu\right],$$

$$\mathrm{A}_7 = \frac{2}{\pi}\left[\frac{2}{7} - \frac{1}{3}\mu\right], \qquad \mathrm{A}_9 = \frac{2}{\pi}\left[\frac{2}{9} - \frac{1}{5}\mu\right].$$

This grading, besides being less favourable than the others from a control point of view, also gives very high values of δ, higher than all the others except for very large tapers, when there is little to choose between them.

So far we have given no indication of what twists are required to produce k_L gradings of the type chosen. In fig. 7 we now show the variation in the angle of incidence α for some of the gradings included in our first formula. The coefficients A_{2n+1} on which α depends contain a factor $c_0/4s$, and are, therefore, dependent upon the aspect ratio, the variable part of α decreasing as the aspect ratio increases. It is, therefore, not possible to give a complete set of curves for α without increasing the number of figures greatly. In fig. 7 we have given the curves for $\xi=0{\cdot}4$ and $\mu=0{\cdot}6$ and for aspect ratios of 5, 7, and 9. All the curves correspond to the same k_L grading, this being shown by the curve marked $\xi=0{\cdot}4$ in fig. 3.

It will be seen that as we leave the root of the wing an upward twist is first required, followed by a downward twist which becomes remarkably large near the wing-tip. This very large drop in α is due to the fact that we have combined a rapidly decreasing k_L with a square tip. Since wings are not nowadays built with square tips, it is interesting to inquire what improvement, if any, can be made by rounding off the tip. The answer to this question is remarkable, for it appears that by rounding

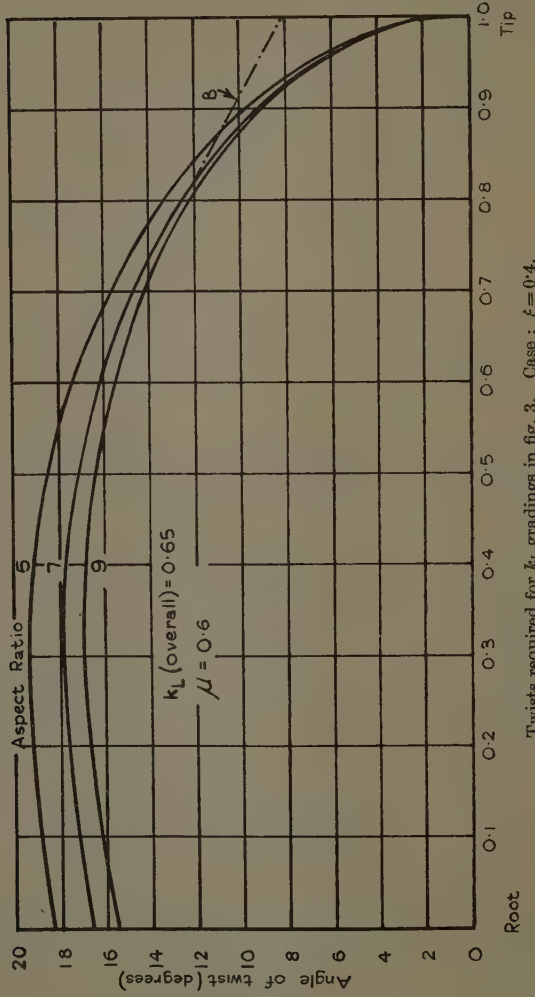

Fig. 7. Twists required for k_L gradings in fig. 3. Case : $\xi = 0{\cdot}4$.

off in the right way we can adjust the twist near the tip in any way, within reason, that we please ; and this can

be done without making any alteration in the aerodynamic properties of the wing as a whole, the only change being in the value of k_L on the part rounded off.

To accomplish this we apply, to the-wing tip only, the older inverse method of Prandtl, to which we have referred in our introduction.

The equation for α is

$$\alpha = \frac{K}{V a_0 c} + \frac{1}{4\pi V} \int_{-s}^{s} \frac{dK_\xi}{d\xi} \frac{d\xi}{x-\xi}.$$

If in this K is kept constant, while α is altered, the changes $\Delta\alpha$, $\Delta(1/c)$ in α and $1/c$ are related by the equation

$$\Delta\alpha = \frac{K}{V a_0} \Delta\frac{1}{c}$$

i. e.,

$$\Delta\frac{1}{c} = \frac{V a_0}{K} \Delta\alpha$$

$$= \frac{a_0}{k_L c} \Delta\alpha,$$

where k_L and c may be taken as either the initial or the final values, since their product does not change.

It follows that, if we change α over a selected portion of the span only, the chord will also be changed only over this portion, and the same is true of k_L. Also, since K is unchanged, the lift and drag are unchanged, and so, naturally, is δ. Suppose now that we seek to remove the large twist at the tip by making the twist linear over the last part of the span. In fig. 7 this has been done for one of the curves, the linear variation of α being shown by the dotted line B, which is tangential to the original curve at the point where $x/s = 0{\cdot}8$. The consequent reduction in chord is shown in fig. 8, which gives the old and new forms of the wing-tip.

It is important to determine to what extent k_L has now risen at the tip, since the grading initially chosen was intended to give a low k_L in this part of the wing. The new value of k_L is shown by the dotted curve B in fig. 3, and is seen to be satisfactory ; for, although it has risen, and now has a finite value at the tip, the values here are still much below the maximum. The wing may therefore be said to be in every way improved by the change.

It is remarkable that so large a change in α has here been made with only a comparatively small change in the chord and with no change in the lift. This suggests that twist applied at the extreme tip of the wing is relatively ineffective in changing the aerodynamical behaviour of the wing. Other calculations, which we do not include here, have led to rather similar conclusions. They lead us to make the tentative suggestion that the effectiveness of ailerons may be reduced if they approach the wing-tip closely. But we do not press this conclusion, except as an indication that the aerodynamical effects of the wing-tips are worthy of more study.

Fig. 8.

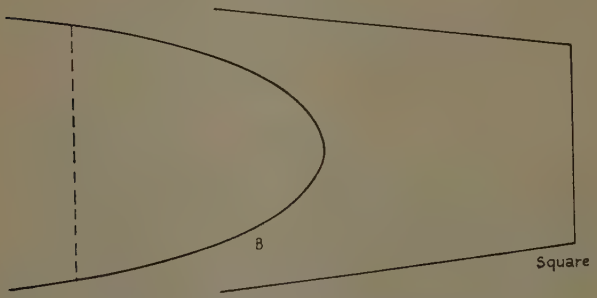

Wing-tip shapes considered. $\frac{\text{Tip chord}}{\text{Root chord}} = 0{\cdot}4$.

In conclusion, we wish to emphasize that in the present paper we have attempted no more than to indicate the type of results that can be obtained by this and similar methods. We believe that further investigation along the same lines will give results of interest and value. The special directions which appear first to call for exploration are as follows :—

(*a*) The thorough examination of the wings already described over a range of attitudes.

(*b*) An investigation of more general classes of wing obtainable from our formulæ by using a larger number of terms.

(*c*) An examination of the effects of the shape of the wing-tip upon the induced drag.

(*d*) A discussion of the effectiveness of ailerons near the wing-tip.

(*e*) An examination of the effects of small changes in plan, such as the inclusion in the tapered wing of a rectangular centre portion.

University College,
Southampton.

II. *Operational Representation of the Parabolic Cylinder Function.* *By* R. S. Varma *.

1. A GIVEN function $f(x)$ is related operationally to another function $\phi(p)$, when

$$\phi(p)=p\int_0^\infty e^{-px}f(x)\,dx, \quad . \quad . \quad . \quad . \quad . \quad \text{(i.)}$$

provided the integral converges. The relation (i.) is generally denoted as

$$\phi(p)\doteqdot f(x). \quad . \quad . \quad . \quad . \quad . \quad . \quad . \quad \text{(ii.)}$$

When the relation (ii.) holds, we have the following theorems given by Carson† :

$$\phi\left(\frac{p}{s}\right)\doteqdot f(sx) \quad (s=\text{constant}), \quad . \quad . \quad . \quad \text{(iii.)}$$

$$\frac{1}{p}\phi(p)\doteqdot\int_0^x f(x)\,dx, \quad . \quad . \quad . \quad . \quad \text{(iv.)}$$

$$\frac{p}{p+\alpha}\phi(p+\alpha)\doteqdot e^{-\alpha x}f(x), \quad . \quad . \quad . \quad . \quad \text{(v.)}$$

and

$$\int_0^\infty\frac{\phi(p)}{p}dp=\int_0^\infty\frac{f(x)}{x}dx. \quad . \quad . \quad . \quad \text{(vi.)}$$

Further, if $f_1(x)$ and $f_2(x)$ be operationally connected to $\phi_1(p)$ and $\phi_2(p)$ respectively, we have‡

$$\left.\begin{aligned}\frac{1}{p}\phi_1(p)\,\phi_2(p)&\doteqdot\int_0^x f_1(t)f_2(x-t)\,dt,\\ &\doteqdot\int_0^x f_1(x-t)f_2(t)\,dt.\end{aligned}\right\} \quad . \quad . \quad . \quad \text{(vii.)}$$

* Communicated by the Author.

† ' Electric Circuit Theory and the Operational Calculus.' (McGraw-Hill, New York, 1926.)

‡ Pol and Niessen, "Symbolic Calculus," Phil. Mag. xiii. pp. 537–577 (1932). The rule was, however, first given by Carson without proof.

The object of this paper is to study the properties of Weber's Parabolic Cylinder Function by means of Operational Calculus.

2. Goldstein* has shown that

$$\sqrt{\pi}\frac{2n!}{2^n n!}p^{\frac{1}{2}}\left(\frac{1-p}{p}\right)^n \doteq x^{-\frac{1}{2}}e^{\frac{1}{2}x}\mathrm{D}_{2n}(\sqrt{2x}), \quad . \quad \text{(viii.)}$$

and

$$\sqrt{\frac{\pi}{2}}\frac{(2n+1)!}{2^n n!}p^{-\frac{1}{2}}\left(\frac{1-p}{p}\right)^n \doteq e^{\frac{1}{2}x}\mathrm{D}_{2n+1}(\sqrt{2x}). \quad \text{(ix.)}$$

Applying (v.) to (viii.), we get

$$\sqrt{\pi}\frac{2n!}{2^n n!}\frac{p(\frac{1}{2}-p)^n}{(\frac{1}{2}+p)^{n+\frac{1}{2}}} \doteq x^{-\frac{1}{2}}\mathrm{D}_{2n}(\sqrt{2x}),$$

which gives, by virtue of (iii.), the result

$$\sqrt{\pi}\frac{2n!}{2^n n!}\frac{p(1-p)^n}{(1+p)^{n+\frac{1}{2}}} \doteq x^{-\frac{1}{2}}\mathrm{D}_{2n}(2\sqrt{x}). \quad . \quad . \quad (1)$$

Again applying first (v.) and then (iii.) to (ix.), in the manner indicated above, we arrive at the result

$$\sqrt{\pi}\frac{(2n+1)!}{2^n n!}\frac{p(1-p)^n}{(1+p)^{n+\frac{3}{2}}} \doteq \mathrm{D}_{2n+1}(2\sqrt{x}). \quad . \quad . \quad (2)$$

The result (2) has recently been deduced directly from the equation of the Parabolic Cylinder by Dr. S. C. Mitra†.

3. Now (2) can be written as

$$\mathrm{D}_{2n+1}(2\sqrt{x}) \doteq (2n+1)\frac{1}{p}\cdot\frac{p}{p+1}\sqrt{\pi}\frac{2n!}{2^n n!}\frac{p(1-p)^n}{(1+p)^{n+\frac{1}{2}}}.$$

If we use (1) and the relation

$$e^{-x} \doteq \frac{p}{p+1},$$

we obtain, by interpreting the right-hand side of the above, that

$$\left.\begin{aligned}\mathrm{D}_{2n+1}(2\sqrt{x}) &= (2n+1)\int_0^x e^{-t}(x-t)^{-\frac{1}{2}}\mathrm{D}_{2n}(2\sqrt{x-t})\,dt,\\ &= (2n+1)\int_0^x e^{-(x-t)}t^{-\frac{1}{2}}\mathrm{D}_{2n}(2\sqrt{t})\,dt.\end{aligned}\right\} \quad . \quad (3)$$

* Proc. Lond. Math. Soc. xxxiv. pp. 103–125 (1932).
† Proc. Edin. Math. Soc. iv. pp. 33–35 (1934).

4. In (vii.) let us put

$$\phi_1(p) = \sqrt{2\pi}\,\frac{2n!}{2^n n!}\,p^{\frac{1}{2}}\left(\frac{1}{p}-1\right)^n,$$

$$f_1(x) = x^{-\frac{1}{2}}e^{\frac{1}{2}x}\,\mathrm{D}_{2n}(\sqrt{2x})\,;$$

$$\phi_2(p) = \sqrt{\frac{\pi}{2}}\,\frac{(2n+1)!}{2^n n!}\,p^{-\frac{1}{2}}\left(\frac{1}{p}-1\right)^n,$$

$$f_2(x) = e^{\frac{1}{2}x}\,\mathrm{D}_{2n+1}(\sqrt{2x}),$$

we obtain

$$e^{\frac{1}{2}x}\int_0^x t^{-\frac{1}{2}}\,\mathrm{D}_{2n}(\sqrt{2t})\,\mathrm{D}_{2n+1}(\sqrt{2(x-t)})\,dt \doteqdot \pi\,\frac{(2n!)\,(2n+1)!}{2^{2n}\,(n!)^2}\,\frac{1}{p}\left(\frac{1}{p}-1\right)^{2n}.$$

Interpreting the right-hand side by means of the relation *

$$\mathrm{L}_n(x) \doteqdot n!\left(1-\frac{1}{p}\right)^n,$$

we arrive at the result

$$e^{\frac{1}{2}x}\int_0^x t^{-\frac{1}{2}}\,\mathrm{D}_{2n}(\sqrt{2t})\,\mathrm{D}_{2n+1}(\sqrt{2(x-t)})\,dt = \pi\,\frac{(2n+1)!}{2^{2n}\,(n!)^2}\int_0^x \mathrm{L}_{2n}(x)\,dx, \quad . \quad (4)$$

where $\mathrm{L}_n(x)$ stands for the Laguerre Polynomial of order n.

5. From (2), it follows that

$$\sum_{n=0}^{\infty}\frac{2^n n!}{(2n+1)!\,\sqrt{\pi}}\,\mathrm{D}_{2n+1}(2\sqrt{x}) \doteqdot \sum_{n=0}^{\infty}\frac{p(1-p)^n}{(1+p)^{n+\frac{3}{2}}}$$

$$= \frac{1}{2}\cdot\frac{1}{p}\cdot\frac{p}{\sqrt{p+1}}$$

$$\doteqdot \frac{1}{2\sqrt{\pi}}\int_0^x x^{-\frac{1}{2}}\,\mathrm{D}_0(2\sqrt{x})\,dx,$$

* Dr. B. V. D. Pol, "On the Operational Solution of Linear Differential Equations and an Investigation of the Properties of these Solutions," Phil. Mag. viii. pp. 861–898 (1929).

by the help of (iv.),

$$= \frac{1}{2\sqrt{\pi}} \int_0^x x^{-\frac{1}{2}} e^{-x}\, dx$$

$$= \frac{1}{2\sqrt{\pi}} \gamma(\tfrac{1}{2}, x),$$

where γ stands for the incomplete Gamma Function.

It follows therefore that

$$\sum_{n=0}^{\infty} \frac{2^n n!}{(2n+1)!} \mathrm{D}_{2n+1}(2\sqrt{x}) = \tfrac{1}{2}\gamma(\tfrac{1}{2}, x). \quad . \quad . \quad . \quad (5)$$

Again following the same method we get

$$\sum_{n=0}^{\infty} \frac{(-2)^n n!}{(2n+1)!} \mathrm{D}_{2n+1}(2\sqrt{x}) = \tfrac{1}{2} x^{-\frac{1}{2}} e^{-x}. \quad . \quad . \quad . \quad (6)$$

6. Again from (1), we get

$$\sum_{n=0}^{\infty} \frac{2^n n!}{\sqrt{\pi} 2n!} x^{-\frac{1}{2}} \mathrm{D}_{2n}(2\sqrt{x}) \doteqdot \sum_{n=0}^{\infty} \frac{p(1-p)^n}{(1+p)^{n+\frac{1}{2}}}$$

$$= \frac{\sqrt{1+p}}{2}$$

$$= \frac{1}{2}\frac{1}{\sqrt{1+p}} + \frac{1}{2}\frac{p}{\sqrt{1+p}}$$

$$\doteqdot \frac{1}{2\sqrt{\pi}} \gamma(\tfrac{1}{2}, x) + \frac{1}{2\sqrt{\pi}} x^{-\frac{1}{2}} e^{-x}.$$

It follows therefore that

$$\sum_{n=0}^{\infty} \frac{2^n n!}{2n!} \mathrm{D}_{2n}(2\sqrt{x}) = \tfrac{1}{2} x^{\frac{1}{2}} [\gamma(\tfrac{1}{2}, x) + x^{-\frac{1}{2}} e^{-x}]. \quad . \quad (7)$$

7. Whittaker's integral *

$$\mathrm{D}_n(z) = \frac{1}{\Gamma\left(\frac{1-n}{2}\right)} e^{-\frac{1}{4}z^2} z^n \int_0^{\infty} e^{-s} s^{-\frac{1}{2}n - \frac{1}{2}} \left(1 + \frac{2s}{z^2}\right)^{\frac{1}{2}n} ds,$$

$$\mathrm{R}(n) < 1$$

can be written as

$$2^{\frac{n}{2}} \Gamma\left(\frac{n+1}{2}\right) p^{\frac{1}{4}} e^{\frac{1}{2}p} \mathrm{D}_{-n}(\sqrt{2p}) = p \int^{\infty} \frac{e^{-px} x^{\frac{1}{2}n-1}}{(1+x)^{\frac{1}{2}n}}\, dx,$$

$$\mathrm{R}(n) > -1.$$

* Proc. Lond. Math. Soc. xxxv. pp. 417–427 (1935).

On comparison with (i.), we obtain the following new image

$$2^{\frac{n}{2}}\Gamma\left(\frac{n+1}{2}\right)p^{\frac{1}{2}}e^{\frac{1}{2}p}\mathrm{D}_{-n}(\sqrt{2p}) \doteqdot \frac{x^{\frac{1}{2}n-1}}{(1+x)^{\frac{1}{2}n}}. \quad . \quad . \quad . \quad (8)$$

The relation (vi.) now gives that

$$\int_0^\infty t^{-\frac{1}{2}}e^{\frac{1}{2}t}\mathrm{D}_{-n}(\sqrt{2t})\,dt = \frac{1}{2^{\frac{n}{2}}\Gamma\left(\frac{n+1}{2}\right)}\int_0^\infty \frac{x^{\frac{1}{2}n-\frac{3}{2}}}{(1+x)^{\frac{1}{2}n}}\,dx. \quad (9)$$

In particular when $n=2$

$$\int_0^\infty t^{-\frac{1}{2}}e^{\frac{1}{2}t}\mathrm{D}_{-2}(\sqrt{2t})\,dt = \sqrt{\pi}$$

and when $n=4$

$$\int_0^\infty t^{-\frac{1}{2}}e^{\frac{1}{2}t}\mathrm{D}_{-4}(\sqrt{2t})\,dt = \frac{\sqrt{\pi}}{6}.$$

8. Lastly, if we apply (v.) to (8), we get

$$2^{\frac{n}{2}}\Gamma\left(\frac{n+1}{2}\right)\frac{p}{\sqrt{p+\frac{1}{a}}}e^{\frac{1}{2}\left(p+\frac{1}{a}\right)} \times \mathrm{D}_{-n}\left(\sqrt{2\left(p+\frac{1}{a}\right)}\right) \doteqdot \frac{e^{-\frac{x}{a}}x^{\frac{1}{2}n-\frac{1}{2}}}{(1+x)^{\frac{1}{2}n}}.$$

Using the relation (vi.), we have, by a formula due to Nielsen*,

$$\int_0^\infty \frac{e^{\frac{1}{2}t}}{\sqrt{t+\frac{1}{a}}}\mathrm{D}_{-n}\left(\sqrt{2\left(t+\frac{1}{a}\right)}\right)dt$$

$$= \frac{e^{-\frac{1}{2a}}}{2^{\frac{n}{2}}\Gamma\left(\frac{n+1}{2}\right)}\int_0^\infty \frac{e^{-\frac{x}{a}}x^{\frac{1}{2}n-\frac{3}{2}}}{(1+x)^{\frac{1}{2}n}}\,dx$$

$$= \frac{e^{-\frac{1}{2a}}a^{\frac{1}{2}n-\frac{1}{2}}}{2^{\frac{n}{2}}\Gamma\left(\frac{n+1}{2}\right)}\Gamma\left(\frac{n-1}{2}\right)\phi\left(\tfrac{1}{2}n,\ \tfrac{1}{2}n-1\right),$$

* See G. N. Watson, Jour. Lond. Math. Soc. vi. p. 64 (1931).

where

$$\frac{\phi(\alpha,\beta)}{\phi(\alpha,\beta+1)} = 1+\cfrac{\alpha a}{1+\cfrac{(\beta+1)a}{1+\cfrac{(\alpha+1)a}{1+\cfrac{(\beta+2)a}{1+}}}}\cdots.$$

It follows therefore that

$$\int_0^\infty \frac{e^{\frac{1}{2}t}}{\sqrt{ta+1}}\,\mathrm{D}_{-n}\left(\sqrt{2\frac{ta+1}{a}}\right)dt$$

$$= \frac{1}{n-1}\,e^{-\frac{1}{2a}}\left(\frac{a}{2}\right)^{\frac{1}{2}n-1}\phi\left(\tfrac{1}{2}n,\ \tfrac{1}{2}n-1\right), \quad (10)$$

where $n>1$ and a is positive.

III. *Some High-temperature Properties of Niobium.* *By* A. L. Reimann, *Ph.D., D.Sc., and* C. Kerr Grant, *B.A., B.Sc.* (Communication from the Research Staff of the M.O. Valve Company, Limited, at the G.E.C. Research Laboratories, Wembley *.)

Introduction.

A SHORT time ago the thermionic emission from niobium was studied by Wahlin and Sordahl †. They obtained their final emission, corresponding, presumably, to a clean state of the metal surface, only after an extremely long heat treatment of their experimental tube and filament, the tube being kept on the pump the whole time. In the hope of obtaining a clean surface more quickly we have followed a rather different procedure as regards vacuum technique, and, in addition to measuring the electron emission from the filament after it appeared to have attained its final condition, we have obtained measurements of the specific resistance, total thermal radiation, and the rate of evaporation of the metal as a function of the temperature in the range 1800°–2400° K., and also of its melting point.

Preliminary Experimental Procedure.

The niobium wire used was of exceptional purity. An indication of this was its extreme softness after heat

* Communicated by C. C. Paterson, M.I.E.E.

† H. B. Wahlin and L. O. Sordahl, Phys. Rev. xlv. p. 886 (1934).

treatment. Also a sample was analysed spectroscopically, and the only impurity that could be detected at all was a trace of tin. The proportion of this was estimated at less than 0·02 per cent. It is noteworthy that no trace of tantalum, iron or titanium was found.

It was felt highly desirable to age the wire thoroughly at a high temperature before any of its various properties were determined. Not only is the gas content of the metal thus largely eliminated, but it is well known that during a prolonged heat treatment a metal develops a characteristically roughened surface, and the thermal radiation must, to some extent, depend on the degree of this roughness. At the same time, with the disappearance of internal strains there occurs a change in the electrical resistance. Furthermore, it is believed that in the final condition of heat-treated metals only certain kinds of crystal faces are exposed on the surface, and it may well be that not until the surface reaches this condition will the thermionic emission and the rate of evaporation of the metal have attained definite, final values.

Two unequal lengths of wire of about 0·3 mm. diameter, cut from the same original piece, were mounted as long hairpins on heavy nickel supports, each on a separate pinch. The lengths of wire between supports were 36·0 cm. and 55·5 cm. The object of making the lengths unequal was to enable the effects of end cooling to be eliminated in subsequent determinations of resistivity and total radiation. The filaments were not supported at the tips, being intended to hang vertically downwards. Each pinch carried, in addition to its niobium filament, two previously outgassed nickel disks to which were attached getter pellets of copper-clad barium. The pinches were sealed into long tubular bulbs which were then connected by a short, wide tube and pumped together. After the tubes had been baked at 400° C. for 30 minutes, the filaments, connected in series, were heated for several minutes at about 2000° K. One getter disk in each tube was then heated by induction until a heavy deposit of barium was formed on the glass wall near it. Finally, spectroscopically pure argon was admitted to a pressure of about 400 mm., and the tubes were sealed off from the pump.

The filaments, hanging downwards, and connected

in series, were now heated in their common atmosphere of argon for 66 hours at 1850° K., then for 44 hours at 2020° K., and finally for 110 hours at 2150° K.* The object of heating the filaments in argon instead of in a vacuum was to avoid excessive evaporation. Actually no evidence of appreciable evaporation was found, and probably the evaporation would not have been serious if the same heat treatment had been given in a vacuum. During the filament heating the getter patches became appreciably discoloured, owing to attack by gas liberated from the niobium. The filaments were examined after the heating and found to have the appearance characteristic of well-aged metals. They were thought probably to have attained their final condition, both as regards surface and freedom from internal strain, and thus to have had enough heat treatment for all the intended measurements except, possibly, the thermionic ones. Considerable further heat treatment in a vacuum, to which some of the wire was subsequently subjected, did not, in fact, produce any noticeable further change in either the surface appearance or the softness of the wire.

The tubes were now separated from one another, re-pumped, and baked, the barium in the remaining getter pellet in each tube was dispersed, and the tubes were sealed off. They were now ready for the temperature, total radiation, and resistivity measurements. The getter disks were so placed in the tubes that the patches of dispersed barium were confined to their upper ends, leaving the glass near the parts of the filaments not affected by end cooling perfectly clear.

Measurement of Temperature, Total Radiation, and Resistivity.

In making temperature measurements, care was taken to confine observations to those parts of the filaments which could not possibly have been cooled appreciably by conduction to the supports. The colour temperature (T_c) was determined as a function of heating current (I) by a visual colour-matching method, using a calibrated tungsten lamp as standard. The T_c–I relation was found to be the same for each of the two filaments,

* These temperatures are approximate only.

as it should be. The points found for the longer filament and the curve representing them are shown in fig. 1. The brightness-temperature (T_b) curve for the same filament is also shown. To obtain this a tungsten strip

Fig. 1.

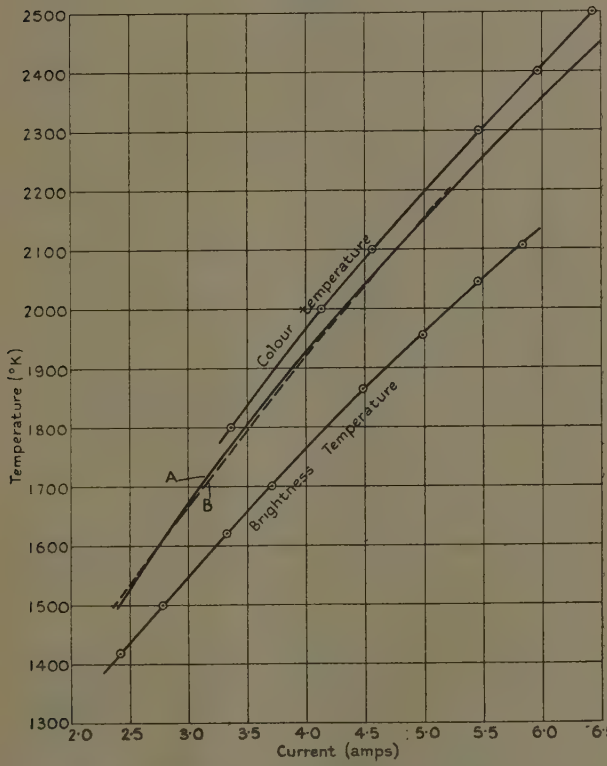

Colour, brightness, and true temperatures of a $0{\cdot}302_5$ mm. niobium wire in terms of heating current.

lamp was used as a background for the niobium filament viewed through the pyrometer telescope, and the effect of absorption and reflexion by the tube walls was experimentally determined and allowed for at each temperature. The black-body temperature scale under

lying the determinations of both T_c and T_b is that at present in use at the National Physical Laboratory.

The relation between the true temperature (T) of well-aged niobium and its brightness temperature for red radiation ($\lambda = 6670$ Å.) has recently been determined by Whitney *. From this and our T_b–I curve we have obtained a curve connecting T with I. This is the dashed curve marked B in fig. 1.

It is interesting to note that in the range of currents 3·4–5·8 amperes, where determinations of both T_c and T_b have been made, $\frac{T-T_b}{T_c-T_b}$ is very nearly the same for each value of T as, according to the data of Forsythe and Worthing † and the known relation between their black-body temperature scale and the N.P.L. scale, it is for tungsten, the values of T for niobium being taken as given by the curve B. This will be appreciated on comparing curve B with A. For currents in the range 3·4–5·8 amperes the ordinates of curve A lie between the corresponding ordinates of the colour and brightness temperature curves in the same proportion as T lies between T_c and T_b for the corresponding values of T for tungsten. It is seen that curves A and B lie so close together that, on the assumption that $\frac{T-T_b}{T_c-T_b}$ is the same at each value of T for niobium as it is for tungsten, the differences between the ordinates of the two curves could easily be due to the combined errors of pyrometry of Whitney and ourselves.

On re-plotting curve A logarithmically, for currents between 3·4 and 5·8 amperes, we have found the relation between the logarithm of its ordinates and log I to be accurately linear. This gives a convenient basis for extrapolation, and this has been done accordingly, for both lower and higher currents. The corresponding logarithmic relationship for curve B is, however, not quite linear. Now for metals of constant crystal structure we should rather expect log I to vary linearly with log T at sufficiently high temperatures, in view of the way the resistance and total radiation usually

* L. V. Whitney, Phys. Rev. xlviii. p. 458 (1935).

† W. E. Forsythe and A. G. Worthing, Astrophys. J. lxi. p. 146 (1925).

vary with temperature. We have therefore decided to choose A, rather than B, as the curve whose ordinates are to be considered to give the true temperature. We have been confirmed in this choice by the fact that the Richardson line for electron emission based on curve A is straight, as it should be, while that based on B is definitely curved. Knowing the diameter of our wire (this was found later), and using the 3/2 power law for converting to corresponding currents for a different diameter, we thus find that for a long wire of diameter d cm. in a vacuum, having the same kind of surface as ours, and receiving negligible radiation from its surroundings compared with what it gives out, the temperature is given in terms of the current by the formula

$$\log_{10} T = 0{\cdot}49254 \log_{10} I - 0{\cdot}7388 \log_{10} d + 1{\cdot}8658. \quad (1)$$

The two wires were now connected in series and the potential drop across each observed for each of several values of the current. Then by subtraction the corresponding potential drops across a wire of length equal to the difference between the two actual lengths, and of uniform temperature, were found, the end-cooling effects cancelling out. Hence, the temperature being known in terms of the current, the relation between the radiation w, in watts per cm.^{2}, and the temperature was found. This is shown as a plot of log w against log T in fig. 2. The logarithmic relation is linear, and is expressed by the formula

$$\log_{10} w = 4{\cdot}796 \log_{10} T - 14{\cdot}554. \quad . \quad . \quad . \quad (2)$$

From (1) and (2) we readily obtain the relation between the specific resistance r, in ohm cm., and the temperature. This is

$$\log_{10} r = 0{\cdot}7354 \log_{10} T - 6{\cdot}586 \quad . \quad . \quad . \quad (3)$$

It should be noted that thermal expansion has deliberately been left out of account in arriving at these formulæ, the dimensional units referred to being those at room temperature. It is felt that the equations will probably be more useful in this form.

The tubes were now opened up and those portions of the filaments which might have suffered appreciable

cooling by conduction to the supports discarded. From the remainder the weight per unit length was obtained, and hence the diameter calculated. The weight per unit length was found to be 6·166 mg. per cm. The density of a well-aged metal is most conveniently found from X-ray data and the atomic weight. Niobium has a body-centred cubic lattice, and the lattice constant of the pure, heat-treated metal has been found by Mr. H. P. Rooksby, of these Laboratories, to be

Fig. 2.

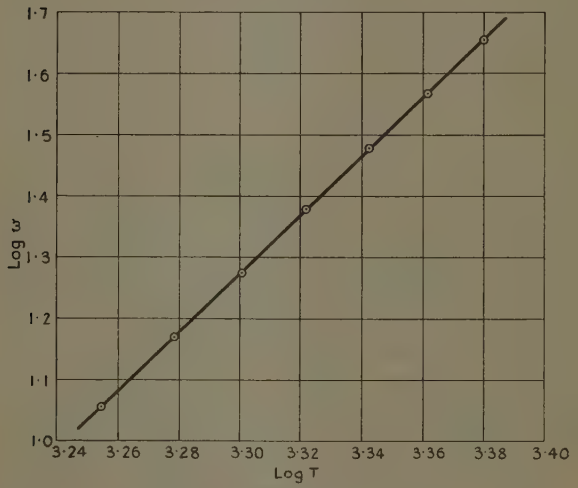

Relation between total radiation and temperature for niobium.

3·2935 ± 0·0005 Å. The atomic weight is 92·91 *. Hence the density is $8{\cdot}58_2$ g. per c.c. and the wire diameter was $0{\cdot}302_5$ mm. This result was used in obtaining the formulæ (1), (2), and (3). The wires were now cut up into suitable lengths for the remaining investigations.

The Melting Point.

Various values of the melting point of niobium are given in the literature, the highest being about 1950° C., or 2220° K. It will be noted, however, that the highest

* O. Hönigschmid, *Naturwiss.* xxii. p. 463 (1934).

temperature to which our specimens were heated in the work already described is some 200° beyond this, and we knew, in fact, from preliminary experiments, that the true melting point must be much higher than has hitherto been supposed. The too-low values given in the literature are undoubtedly due to impurities in the specimens used. The effect of impurities in lowering the melting points of metals is quite well known. Thus the presence of carbon in iron lowers the melting point by something like 50° for each 1 per cent. of impurity up to the first 3 or 4 per cent.

In order to find the melting point of pure niobium, a length of wire was mounted in a bulb, which was pumped, baked, barium gettered, and sealed off in the usual manner, and then a gradually increasing current was passed through the wire until it melted, the value of the current just as it did so being noted. When the wire melted it did so along its whole length simultaneously, except for 2 or 3 cm. at each end, where cooling by conduction to the supports was appreciable. The bulb was afterwards found not to be appreciably blackened by volatilized metal, so in finding the temperature corresponding to the melting current the extrapolated (log T)–(log I) line found for the same wire before it had been heated to such a high temperature was used. The temperature so found is 2790° K. The temperature could not have lagged behind the current by more than some 3 or 4 degrees, and when this and all other sources of error are considered it is estimated that the result is accurate to within about 20°.

To obtain a check on this, another, similar tube was prepared and the filament photoelectrically colour-matched as its temperature was gradually increased, and the last colour temperature recorded before it melted (which it did in the same manner as before) was noted. The last T_r observed was 2801° K. From an extrapolation of the T and T_c curves of fig. 1 it appears that at a T_r of 2801° K., T would be about 2730° K. We should expect this result to be too low, for two reasons. One is that 2801° K. was only the last value of T_c found before the wire melted. The other is that the radiation from the cooler ends of the wire was not eliminated in the colour matching. Experience gained in previous work of this nature indicates, however, that the combined

error due to these two causes plus the uncertainty of the actual measurement is not likely to exceed 40°.

Thus the two results are just mutually reconcilable, their difference being equal to the sum of the estimated maximum possible errors. The value of the melting point consistent with both results is about 2770° K.

Rate of Evaporation.

Three **U**-shaped filaments, each of ample length, so that several centimetres would be unaffected by end cooling, were mounted in separate bulbs, each of which was then pumped, baked, barium gettered, and sealed off. Each filament was then burned at a constant voltage until the current had fallen by some 6 or 7 per cent., the voltages being so chosen that the filaments should have suitable temperatures. When a filament of suitable length, cooled at the ends by its supports, is run at constant voltage, the temperature of its central part remains very nearly constant while it is evaporating. In the present work the lengths varied between 14 and 17 cm., and in no case did the temperature vary from beginning to end by more than 10°. The difference between the initial and final temperatures being so small, their mean was taken as the constant temperature that would have produced the same evaporation. Both initial and final temperatures were calculated from the corresponding wire diameters and currents. The final wire diameter was found by discarding as much wire at each end as might possibly have been cooled appreciably by conduction to the supports and measuring and weighing the remainder. A further piece was then cut off from each end and the remainder again measured and weighed. In this way a check was obtained both on the weight per unit length and on the assumption that the end pieces originally discarded included all the wire that had been appreciably cooled by conduction to the supports.

In fig. 3 the logarithms of the three rates of evaporation are plotted against the reciprocals of the corresponding temperatures, 2367°, 2496°, and 2681° K. In arriving at these rates the thermal expansion of the metal was taken into account, a formula for this obtained by Hidnert and Krider *, working in the temperature range

* P. Hidnert and H. S. Krider, Bur. Std. J. of Research, xi. p. 279 (1933).

−135° to +305° C., being assumed to be valid at higher temperatures also. It is seen that the points are practically collinear, as one would expect them to be.

Fig. 3.

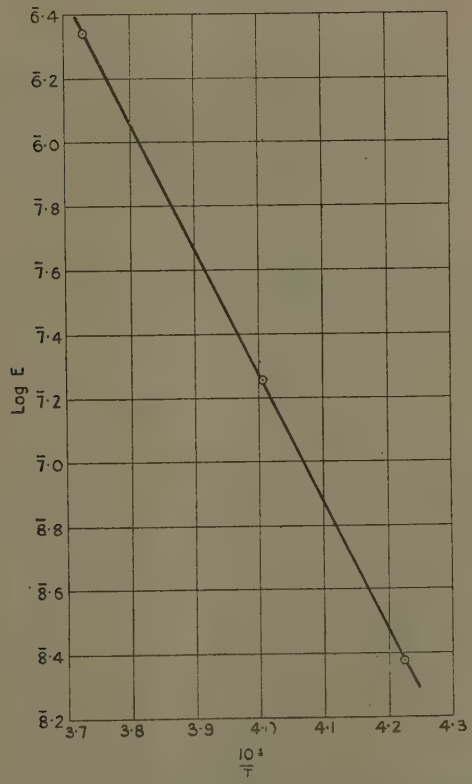

Rate of evaporation of niobium as a function of temperature.

In the temperature range covered, the rate of evaporation E in g. cm.$^{-2}$ sec.$^{-1}$ is expressed in terms of the temperature within about 2 per cent. by the formula

$$\log_{10} E = 9{\cdot}125 - \frac{39636}{T} \quad . \quad . \quad . \quad . \quad . \quad (4)$$

Now it may easily be shown thermodynamically that

$$\frac{d\log_\epsilon\left(\frac{E}{T^2}\right)}{d\left(\frac{1}{T}\right)} = -\frac{l}{R}, \quad \ldots\ldots (5)$$

where R is the gas constant and l is the internal latent heat of evaporation per gram-molecule, *i. e.*, that part of the latent heat which is not concerned with work of expansion or kinetic energy of the vapour. An empirical formula which fits the experimental data as well as (4) is

$$E = 29{\cdot}3\,T^2\epsilon^{-\frac{86234}{T}}. \quad \ldots\ldots (6)$$

Hence, by (5), the mean value of l in the experimental range covered is 86234 R, or 171,200 calories per gram-molecule.

Thermal Electron Emission.

A 20·2 cm. length of wire was mounted in the form of a hairpin on heavy nickel supports and surrounded by two electrodes of fairly open molybdenum gauze, each of length 6 cm. and of oval section (3 cm. $\times$ 1 cm.), arranged end-to-end with a 1 mm. gap between them. The electrodes were mounted in a double-ended tube, the freely hanging filament and upper molybdenum electrode being supported by the upper pinch and the lower molybdenum electrode by the lower. The length of filament (when cold) below the centre of the gap between the two molybdenum electrodes was 9·9 cm. Each filament support carried a nickel wire ending in a small nickel disk to which was attached a copper-clad barium getter pellet. The molybdenum gauze electrodes and their supports, the filament supports, and the getter disks with their supports were outgassed by vacuum furnacing at 950°–1000° C. for 15 minutes before being assembled.

The tube was first baked on the pump for 30 minutes at 400° C. and then both molybdenum electrodes were heated by induction to redness for several minutes. After this the barium was dispersed from both getter

disks and the tube was sealed off. Finally a current of 5·25 amps. was passed through the filament (temperature 2200° K.) and the two molybdenum electrodes, connected together, bombarded from it at 120 watts for 30 minutes. This was done in order to drive off some of the gas which must have settled on their surfaces during the gettering and sealing-off operations.

The main thermal conditioning of the filament for thermionic measurements was now begun, the clean-up of residual gas by the getter being assisted by passing a space current of about 20 mA. between the filament and the two molybdenum electrodes held at a suitable positive potential (more than sufficient for gas to be ionized) with respect to it. The filament was first heated for 48 hours at 2000° K., the emission from it at this temperature being measured at intervals. During the first 30 hours the emission rose at a steadily diminishing rate by a total of about 30 per cent., but thereafter remained quite constant. After completion of the 48 hours at 2000° K. the filament temperature was increased to 2100° K. and held there for a further 10 hours, but this did not produce any further change in the emission measured at 2000° K. Finally the filament was flashed for some minutes at gradually increasing temperatures up to 2700° K., the bulb being thereby caused to blacken appreciably, owing to evaporation from the filament, but still the emission remained unaffected. It was therefore taken to have reached its final, steady value, characteristic of clean niobium.

The emission from that part of the filament which was below the centre of the gap between the two molybdenum electrodes was now measured at each of a number of temperatures ranging from 1438° to 1980° K.* None of this part of the filament suffered appreciable cooling by conduction to the supports, even at the lowest temperature. At each temperature the emission was measured at a series of saturating positive potentials of the lower molybdenum electrode, the upper electrode always being made as much negative to the centre of the

* The temperatures were calculated from the heating currents and the wire diameter, the latter being found from the weight per unit length after the completion of the thermionic measurements.

filament as the lower one was positive. In this way the emission from the upper part of the filament was suppressed and the field at the filament surface was made to change from electron-retarding to electron-accelerating at the mid-point of the gap between the two molybdenum electrodes, or rather, since there was a potential drop along the filament, as much above this point in one limb as below it in the other. At each temperature the logarithm of the emission was found to vary linearly with the square root of the field, as it should do according to Schottky's law, and thus the zero-field emission was obtained by extrapolation. In arriving at the zero-field emission i' per apparent unit area of emitting surface the thermal expansion of the filament was again taken into account, as it was for evaporation, the formula of Hidnert and Krider * being used.

In fig. 4 the values found for $\log(i'/T^2)$ are plotted against the corresponding reciprocals of the temperatures, i' being in amperes per apparent cm.^{2} The points are, within the limits of experimental uncertainty, collinear. The equation of the straight line which best represents the points is

$$\log_{10}\frac{i'}{T^2} = 1{\cdot}571 - \frac{20226}{T} \quad . \quad . \quad . \quad . \quad . \quad (7)$$

Thus the constants of the empirical T^2 formula

$$i = AT^2\epsilon^{-\psi/kT}, \quad . \quad . \quad . \quad . \quad . \quad . \quad . \quad (8)$$

in which i stands for the zero-field emission per unit area of true emitting surface and is equal to i'/ρ, where ρ is the effective roughness factor for the surface, are

$$A = \frac{37{\cdot}2}{\rho} \text{ amp. cm.}^{-2} \text{ deg.}^{-2}, \quad \psi = 4{\cdot}01_3 \text{ e.v.}$$

The corresponding values obtained by Wahlin and Sordahl † are

$$A = \frac{56}{\rho} \text{ amp. cm.}^{-2} \text{ deg.}^{-2}, \quad \psi = 3{\cdot}96 \text{ e.v.}$$

The discrepancy between the two sets of values is such as might possibly be due to a difference between the temperature scales employed by them and by us.

* *Loc. cit.* † *Loc. cit.*

Just what is meant by the effective roughness factor ρ has been explained elsewhere by one of us *, and reasons were given for believing that in the case of aged tungsten the value of ρ is probably within something like 10 per cent. of 1·3. Perhaps we may assume that ρ will have about this value for other aged metal surfaces also. If we make this assumption in the case of niobium, the

Fig. 4.

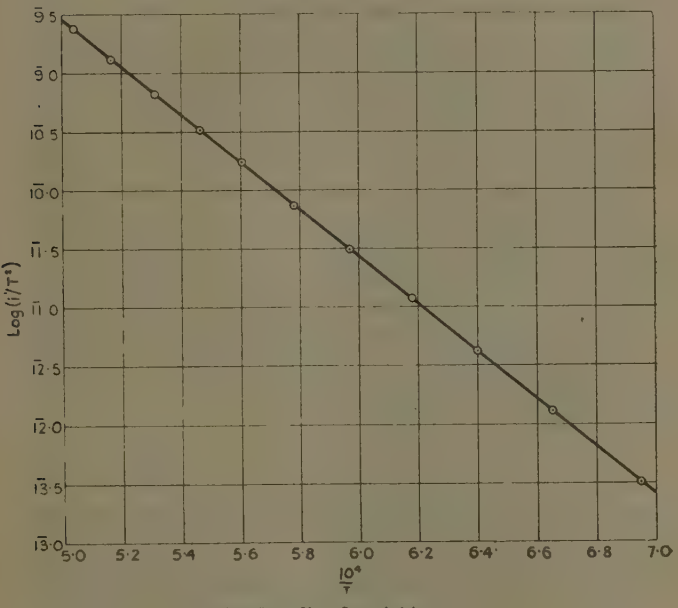

Richardson line for niobium.

value of A given by our data becomes 29 amp. cm.$^{-2}$ deg.$^{-2}$.

It is interesting to note that this value of A is about that which we should expect on the assumption that the transmission of electrons through the surface is perfect, and that the work function varies sensibly linearly with the temperature over the range covered at a rate which is determined primarily by the effect of thermal expansion

* A. L. Reimann, Phil. Mag. xx. p. 594 (1935).

on the critical energy of the Fermi distribution of the free (valency) internal electrons. It has been shown by one of us * that in such a case, where there is a constant number of free electrons per atom,

$$A = A_0 \epsilon^{-\frac{h^2\alpha}{4mk}\left(\frac{3n}{\pi}\right)^{2/3}}, \quad . \quad . \quad . \quad . \quad . \quad (9)$$

where A_0 is the universal constant of thermionic theory whose numerical value is 120 amp. cm.$^{-2}$ deg.$^{-2}$, h is Planck's constant, m is the electronic mass, n is the number of free electrons per unit volume of the emitter, and α is the coefficient of linear expansion. Let us assume that there is one valency electron per atom of the metal. Actually there may be more than one, but at the same time the effect of the periodic lattice field will be to make the electrons behave as if their mass were somewhat greater than it really is, and it is the *effective* mass in the periodic field whose value should be given to m in (9). Thus we might expect the actual state of affairs to be much the same as it would be if there were only one valency electron per atom having an effective mass equal to the true mass. Making this assumption, then, and taking Hidnert and Krider's formula for thermal expansion, we have, for the temperature range in which our thermionic data were obtained,

$$n = 5{\cdot}35 \times 10^{22}, \qquad \alpha = 1{\cdot}11 \times 10^{-5} \text{ deg.}^{-1},$$

and substituting these values, and those of the other quantities, in the right-hand side of (9), we find for A the value of 32 amp. cm.$^{-2}$ deg.$^{-2}$. This differs by only about 10 per cent. from the value arrived at experimentally, and in view of the crudeness of the assumptions made concerning the values of ρ and the equivalent n for a field-free lattice, the agreement is as good as could have been expected.

In conclusion, we wish to tender our acknowledgements to the General Electric Company and the Marconi Company, on whose behalf the work was done which has led to this publication.

* A. L. Reimann, 'Nature,' cxxxiii. p. 833 (1934). To make the notation and nomenclature of this communication agree with that of the present article, read "A" for "the apparent A" and "$A_0\bar{D}$" for "the true A."

IV. *On the Atomic Forces of Solid States.*

By WENG WEN-PO *.

PART I.

(1) IT is well known that a great part of the properties of solids is due to atomic motion. But as long as the nature of atomic force is still somewhat obscure, it is difficult to imagine how an atom in the solids actually moves. Thus, the explanation of the properties of matter is still far from complete. In the present investigation we try to study the atomic motion based on a few assumptions and to see whether the result obtained is capable of explaining all the properties of matter, and, finally, we hope to get some conception about the nature of atomic forces.

Since the atomic force, or rather the ionic force, is related nearly to all the properties of solids, we can start our investigation in many different directions. Here, however, the elastic constants are chosen, in the first step of our research, as the basis from which we deduce the field of the atomic force, because these constants give the pressure and volume relations of solids in a very simple manner. Elastic constants have early been used to study atomic forces by M. Born †. More recently, G. A. Tomlinson ‡ has also worked on an empirical repulsion formula from purely elastic data.

(2) Let us imagine an ionized atom to be acted on by a certain force in a mass of isotropic solid. Considering the rigidity of all solids, there must be a position of equilibrium at which the atom should be acted on by no force. But as soon as the atom goes beyond the equilibrium position it will be immediately acted on by a certain restoring force which depends on the displacement. The restoring force depends also on the direction of the displacement, since the neighbouring atoms are by no means arranged in the same way in all directions, although the solid is macroscopically isotropic. So the problem is really not a simple one.

But all isotropic solids have by definition the same property along all directions, since we observe nothing

* Communicated by the Author.

† *Verh. D. Phys. Ges.* xx. p. 210 (1918).

‡ Phil. Mag. xi. p. 1009 (1931).

of a solid but the average property of a number of atoms through a certain period of time. To take advantage of this we treat the average atomic force as independent of direction as a first approximation.

Let any one axis passing through the equilibrium point O of a certain ionized atom Q be x-axis as shown in fig. 1. Again, let two neighbouring atoms O_1 and O_2 at two sides of O be both on the x-axis, each distant from the point

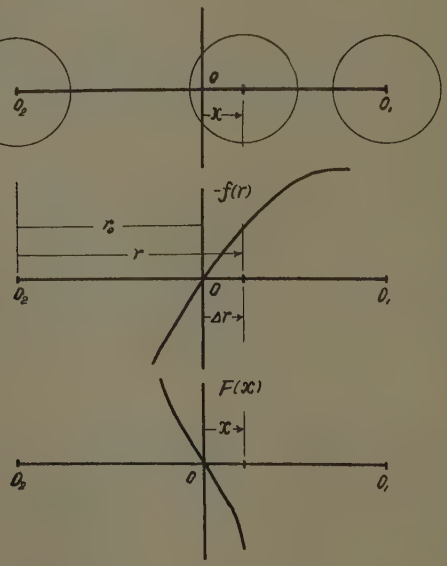

O by r_0, where r_0 is defined as the average distance of any two neighbouring atoms in the solid. The above assumptions do not make the treatment less general, since the solid is assumed to be isotropic and the neighbouring atoms O_1 and O_2 may be considered simply as mathematical artifices, no matter whether there are actually two atoms in these positions or not. It should also be noticed that the position of an atom is referred to a fixed point in the atom. For definiteness the geometrical centre of the atom is used.

Considering the rigidity of the solid, we conclude that all the atoms at one side of the perpendicular bisector of O_1 O_2 should exert zero force to the atom at O, and so are the atoms at other side, otherwise the solid will expand or contract until the above condition is satisfied. The above condition can be explained in a more substantial sense. The atom Q is attracted toward the right side by all the ions to the right of O with a certain force, say by a force $-\frac{Ae^2}{r^2}$, and repelled away from the right side by a certain repulsive force which is practically due to the atom O_1 only, since the atomic repulsion is known to decrease rapidly as the distance between atoms increases. At the position O the repulsion just neutralizes the attraction.

Let $f(r)$ be the atomic force of all the atoms at one side of O, say to the right of O, acting on the atom Q, where r is the distance measured from O_1 to Q. The force $f(r)$ is considered positive when it is a repulsion. Then $f(r_0)=0$. Furthermore, let the component of the displacement of the atom Q from the point O along the x-axis be x, which is considered as positive when it extends towards O_1. Then the restoring force $F(x)$ of Q, which is nothing but the superposition, or algebraic sum of the two $f(r)$-functions due to neighbouring atoms on both sides, becomes

$$F(x)=f(r_0+x)-f(r_0-x).$$

In fig. 1 the approximate relation between $f(r)$, $F(x)$, and x are shown. Assuming $f(r)$ to be a continuous and finite function of r, we set

$$f(r)=f_0-ar-br^2-cr^3-\ldots\ldots \quad (1)$$

where f_0, a, b, c, and d are constants. Considering $f(r_0)=0$, equation (1) becomes

$$f(r)=a(r_0-r)+b(r_0-r)^2+C(r_0-r)^3+\ldots\ldots,$$

or

$$f(r_0+\Delta r)=-a\,\Delta r+b(\Delta r)^2-C(\Delta r)^3+\ldots \quad (2)$$

Then $F(x)$ can be expanded as follows

$$F(x)=-2ax-2cx^3-\ldots\ldots \quad (3)$$

Since x is always small compared with r_0, the motion of the atom in such a field of force as represented by

equation (3) should be very near to harmonic motion, although the second order of x/r is still appreciable. This explains why Dulong and Petit's law, which is essentially a result of harmonic motion, is approximately valid at moderate temperatures.

(3) It is now desirable to see how the restoring force affects the property of the solid. If the solid is pressed by a uniform external pressure P, the atom O_2 is pushed nearer to O by an amount Δr, and the force $f(r_0-\Delta r)$ is balanced by the external pressure P, or,

$$f(r+\Delta r)=n^{\frac{2}{3}}\mathrm{P}, \quad \ldots\ldots \quad (4)$$

where n is the number of atoms per unit volume. Customarily we call the ratio of the volume strain to the applied stress the compressibility, or

$$\beta=-\frac{1}{\mathrm{V}}\frac{d\mathrm{V}}{d\mathrm{P}}, \quad \ldots\ldots \quad (5)$$

where V is the external volume. Since the external volume V is proportional to the third power of r_0, or $\mathrm{V}\propto r_0{}^3$, equations (4) and (5) can be combined into a single equation thoroughly in microscopic terms

$$f(r+\Delta r)=-\frac{3}{n^{\frac{2}{3}}\beta}\left(\frac{\Delta r}{r_0}\right).$$

Comparing with equation (2) we have

$$-a\,\Delta r+b(\Delta r)^2-\mathrm{C}(\Delta r)^3+\ldots=-\frac{3}{n^{\frac{2}{3}}\beta r_0}\Delta r. \quad (6)$$

For small strains, *i. e.*, small x, higher order terms than first power of (r_0-r) are negligible, and β approaches a constant β_0, or

$$a=\frac{3}{n^{\frac{2}{3}}\beta_0 r_0}. \quad \ldots\ldots \quad (7)$$

It follows from equation (3),

$$\mathrm{F}(x)=-\frac{6}{n^{\frac{2}{3}}\beta_0 r_0}x.$$

Then it is no longer difficult to write down the equation of motion of the atom in the field of force $\mathrm{F}(x)$,

$$\frac{d^2x}{dt^2}=\frac{2a}{m}=-\frac{6}{mn^{\frac{2}{3}}\beta_0 r_0}x,$$

where m denotes the mass of the atom. The last equation indicates a type of simple harmonic motion. Naturally the oscillation so defined is the characteristic vibration of the solid. Then the frequency of the characteristic vibration should be

$$\nu = \frac{1}{2\pi}\sqrt{\frac{2a}{m}} = \frac{1}{2\pi}\sqrt{\frac{6}{n^{\frac{2}{3}}\beta_0 r_0 m}}. \quad . \quad . \quad (8)$$

To avoid the trouble of involving n, r_0, and m, we introduce following equations of conversion which will transform equation (8) into an easily manageable form,

$$\left.\begin{aligned} mn &= \rho \\ n &= \rho N_0/W \end{aligned}\right\}, \quad . \quad . \quad . \quad . \quad . \quad (9)$$

where N is the Avogadro's number, W the atomic weight or the equivalent atomic weight, and ρ the density. In addition, we set

$$r_0 = kn^{-\frac{1}{3}}, \quad . \quad . \quad . \quad . \quad . \quad (10)$$

where k is a constant which is different for different types of lattice structures. Then, we have

$$\nu = \frac{\sqrt{6}}{2\pi} N_0^{\frac{1}{3}} \frac{1}{\sqrt{k}} W^{-\frac{1}{3}} \beta_0^{-\frac{1}{2}} \rho^{-\frac{1}{6}}. \quad . \quad . \quad . \quad (11)$$

The exponents of W, β_0, and ρ have early been discovered independently through dimensional considerations by Madelung, Sutherland * and Einstein †.

For simple cubic lattice the value k can be approximately calculated by averaging the length of the side of the diagonal and that of the diagonal of one face of a unit cube. Since among the atoms in the neighbourhood of O there are three pairs at a distance $n^{-\frac{1}{3}}$ from O, four pairs at a distance $\sqrt{3}n^{-\frac{1}{3}}$ from O, and six pairs at a distance $\sqrt{2}n^{-\frac{1}{3}}$ from O, therefore $k = 1/3(1+\sqrt{2}+\sqrt{3}) = 1{\cdot}38$ and equation (11) for cubic lattice reduces to

$$\nu = 2{\cdot}9 \times 10^7 \times W^{-\frac{1}{3}} \beta_0^{-\frac{1}{2}} \rho^{-\frac{1}{6}}. \quad . \quad . \quad . \quad (12)$$

For other types of lattice system the constant $k = 1{\cdot}38$ still holds good approximately, because in setting $r_0 = kn^{-\frac{1}{3}}$ we have transformed the other lattice types into an

* Phil. Mag. xx. p. 657 (1910).
† *Ann. der Phys.* xxxiv. p. 170 (1911); xxxv. p. 679 (1911).

equivalent cubic lattice. Equation (12) is essentially of the same form as Einstein's equation of characteristic vibration of solid, except that the constant in Einstein's equation is 2·8 instead of 2·9.

(4) From the validity of Dulong and Petit's law we may conclude that the value cx^3 in equation (3) is small, even when the temperature reaches the melting-point. This makes the calculation of the order of magnitude of the maximum displacement of the atom possible.

Let v_0 denote the X-component of the velocity of Q at position of zero force, or at the point O. It is then quite simple to get from the equation of motion the maximum amplitude of the linear oscillator, or

$$X_1 = \frac{\sqrt{m}v_0}{\sqrt{2a}} = v_0\sqrt{n^{\frac{1}{3}}\beta_0 r_0 m}/\sqrt{6}, \quad . \quad . \quad (13)$$

where x_1 is the maximum amplitude of the oscillation. Now the maximum kinetic energy of the atom in X-axis is one-third of the total heat energy of the atom, since the atom is assumed to obey the law of Equipartition of Energy. Or, in symbols,

$$\tfrac{1}{2}mv_0^2 = \int_0^T s(T)dT \times \frac{\rho}{3n},$$

where $s(T)$ is the specific heat at constant volume of the solid in ergs per gram per degree and is assumed to be a function of the absolute temperature T. Let the average specific heat of the solid be defined by

$$\bar{S}(T) = \int_0^T S(T)dT.$$

Then we have

$$v_0 = \sqrt{\frac{2}{3}\int_0^T S(T)dT} = \sqrt{\frac{2}{3}\bar{S}(T)}. \quad . \quad . \quad (14)$$

It follows that

$$X_1^2 = \frac{m\int_0^T S(T)dT}{3a} = \frac{k}{9}\frac{\beta_0\rho^{\frac{1}{3}}W^{\frac{2}{3}}}{N_0^{\frac{2}{3}}}\bar{S}T. \quad . \quad . \quad (15)$$

Since the intensity of the elastic spectra is proportional to the maximum amplitude, it is clear that the intensity of the elastic spectra should be also linearly proportional

to the absolute temperature for the same solid, and proportional to $\beta_0\rho^{\frac{1}{3}}W^{\frac{2}{3}}$ and s for different solids at the same temperature.

If we compare x_1 with r_0 equation (15) can be written as

$$\left(\frac{X_1}{r_0}\right)^2 = \frac{1}{9k}\rho\beta_0\bar{S}T. \quad . \quad . \quad . \quad . \quad (16)$$

According to Lindemann's * supposition, at melting-point of a solid the atoms are substantially in contact. Let σ be the diameter of the sphere of an atom inside of which there is substance, or rather electronic clouds. Then the value x_1/r_0 in equation (16) becomes $\frac{\hat{r}_0-\sigma}{2\hat{r}_0}$ at the melting temperature. The notation $\hat{r}_0$ denotes the distance between nearest neighbouring atoms, since as soon as a part of atoms becomes unstable the whole equilibrium breaks down. Consequently the value k should be replaced by another constant, say j

$$\left(\frac{r\hat{r}-\sigma}{2\hat{r}_0}\right)^2 = \frac{1}{3j}\rho\beta_0\bar{S}T_m = \frac{1{\cdot}40\times10^7}{j}\rho\beta_0\bar{S}_hT_m, \quad (17)$$

where j is defined by $\hat{r}_0 = jn^{-\frac{1}{3}}$ and $\bar{S}_h$ is the mean specific heat in heat unit, or in cal. per gram per degree. In equation (17) the factor 3 through the consideration of equipartition of energy is omitted, since we consider only the most favourable case of a collision instead of average case. The most favourable case of a collision is the degenerated case of linear oscillation, with the total energy concentrated into one direction. In other words, the average value of $\left(\frac{X_1}{r_0}\right)^2$ at melting-point is one-third of $\left(\frac{\hat{r}_0-\sigma}{2\hat{r}_0}\right)^2$. Evidently the value of j is unity for simple cubic lattices. For other simple lattice systems the values of j have been calculated as given below:

For face-centred cubic lattice, $n = \frac{4}{\left(\frac{2}{\sqrt{2}}\right)^3\hat{r}_0}$, $j = 1{\cdot}122$;

for body-centred lattice, $j = 1{\cdot}091$.

* *Phys. Zeits.* xi. p. 609 (1910).

Equation (17) is expected to give slightly too small values of σ which will be discussed at the end of Part II. of this paper.

In Table I. the value σ of several metals so calculated are tabulated. The supposition of Lindemann that σ/r_0 is a constant is partially proved. But with still further observation we see that this rule is not strictly right. The values of alkaline elements are practically equal to each other, but deviate away, namely 50 per cent.,

TABLE I.*

Metals.	S(50° C.) cal. per gram.	$\beta_0 . 10^{12}$.	T_m° A.	ρ.	$\left(\frac{\hat{r}_0-\sigma}{2\hat{r}_0}\right)^2 \times 10^2$.	$\sigma/2$ in Å.	$\sigma/2$ Å.
Al	0·217	1·33	933	2·7	0·90	0·405	1·16
Co	0·104	0·54	1753	8·9	1·10	0·395	0·99
Ni	0·109	0·53	1725	8·9	1·11	0·395	0·99
Cu	0·0931	0·72	1356	8·92	1·02	0·399	1·01
Ag	0·0563	0·99	1234	10·5	0·90	0·405	1·17
Pt	0·0322	0·36	2028	21·45	0·63	0·421	1·17
Au	0·0316	0·577	1336	19·3	0·59	0·423	1·22
Pb	0·0305	2·3	601	11·34	0·60	0·423	1·47
Ca.....	0·148	5·70	1083	1·55	1·77	0·367	1·46
Th	0·0276	1·82	2118	11·2	1·49	0·278	1·35
The above metals have the face-centred cubic lattice.							
Fe	0·113	0·587	1808	7·86	1·21	0·390	0·97
Mo	0·072	0·361	2893	10·2	0·99	0·400	1·09
Cr	0·110	0·52	1888	7·1	0·99	0·400	1·00
V	0·115	0·61	1983	5·96	1·07	0·397	1·04
Li	0·79	9·1	459	0·53	2·25	0·350	1·09
Na	0·308	15·8	371	0·97	2·25	0·350	1·30
K	0·192	32·1	335	0·86	2·28	0·349	1·57
Rb	0·081	40·5	312	1·53	2·01	0·358	1·77
Cs	0·48	62·0	299	1·90	2·18	0·352	1·88
The above metals have the body-centred cubic lattice.							

from the majority of elements. In Table II. the value $\sigma/2$ of alkaline metals obtained from equation (17) is compared with the similar quantities obtained from other methods.

Equation (17) also enabled us to calculate $\sigma/2$ of the

* The physical constants which we used to compute or to compile the tables, if not specially noted, are taken from International Critical Tables; Charles D. Hodgman and Norbert A. Lande; 'Handbook of Chemistry and Physics.'

anions in simple crystalline compounds. In these cases Equation (17) becomes

$$\left[\frac{\mathring{r}_0-\left(\frac{\sigma_1+\sigma_2}{2}\right)}{2\mathring{r}_0}\right]^2=\frac{1\cdot4\times10^7}{j}\rho\beta_0\mathrm{T}_m\overline{\mathrm{S}}_h,$$

TABLE II.

Metals.	$\sigma/2$.	Ionic domain from X-rays data.	Richard's radius.	Wasastjerna's radius.	Pauling's radius.
Li	1·09 Å	..	..	..	0·574 Å.
Na	1·30	..	1·07–1·10 Å.	1·01 Å.	0·873
K	1·57	1·548 Å.	1·40	1·30	1·17
Rb	1·77	1·696	1·44	1·50	1·29
Cs	1·88	1·974	1·82	1·75	1·43

TABLE III.

Substance.	S (0° C.) Joules per gram.	10^{12}.	T_m Å.	ρ.	$\left[\frac{\mathring{r}_0-\frac{\sigma_1+\sigma_2}{2}}{2\mathring{r}_0}\right]^2\times10^2$.	$\frac{\sigma_1+\sigma_2}{2}$ Å.	σ of the anion.
LiF	1·56	1·53	1143	2·30	2·08	1·47	0·38
LiCl	1·18	3·41	886	2·06	2·45	1·76	0·67
NaCl.....	0·85	4·2	1073	2·16	2·75	1·88	0·57
NaBr	0·49	5·08	1028	3·21	2·74	1·99	0·69
KF	0·83	3·31	1153	2·48	2·62	1·80	0·33
KCl	0·68	5·63	1043	1·99	2·65	2·11	0·54
KBr	0·44	6·70	1003	2·75	2·71	2·20	0·63
KI	0·31	8·54	996	3·12	2·74	2·36	0·79
RbBr	0·31	7·94	955	3·35	2·62	2·31	0·54
RbI	0·24	9·58	915	3·55	2·49	2·50	0.73

where σ_1 and σ_2 are the value σ of the components, in case it is a binary compound. Since σ of the cation, or of the metal, has been found, by a single subtraction, we can get σ of the anion. In Table III. the values σ of halogens calculated from properties of alkaline halides are tabulated. In Table IV. the average value of σ of halogens is compared with their similar quantities derived from other assumptions. The diversity in value indicates a defect of Lindemann's collision hypothesis.

So far we have discussed, the value a, or the first term of the force function, is calculated from compressibility. It is evident that the constant a can also be deduced from

TABLE IV.*

Halogens.	$\sigma/2$.	Ionic domain from X-rays data.	Richard's radius.	Wasasjerna's. radius.	Pauling's radius.
F	0·36 Å.	..	2·13 Å.	1·33 Å.	1·225 Å.
Cl	0·58	1·589 Å.	1·74	1·72	1·589
Br	0·62	1·740	1·90	1·92	1·702
I	0·76	1·974	1·19	2·19	1·867

other properties as well †, *e. g.*, from optical dispersion, from dielectric constants, or, still better, by determining experimentally the characteristic vibrations of the solid.

PART II.

(5) It is well known that the compressibility is really not a constant. It varies not only with pressure, but also with temperature. Let

$$\frac{1}{\beta_0}\left(\frac{\partial\beta}{\partial t}\right)_p = \mathrm{A}_p \quad \text{and} \quad \frac{1}{\beta_0}\left(\frac{\partial\beta}{\partial \mathrm{P}}\right)_\mathrm{T} = \mathrm{A}_t,$$

or

$$\frac{d\beta}{\beta_0} = \mathrm{A}_t d\mathrm{P} + \mathrm{A}_p d\mathrm{T}. \quad . \quad . \quad . \quad . \quad (18)$$

This equation is convenient enough for experimental purposes, but for our discussion we prefer to use the temperature and volume as arguments. Since

$$d\mathrm{P} = \left(\frac{\partial \mathrm{P}}{\partial \mathrm{T}}\right)_\mathrm{V} d\mathrm{T} + \left(\frac{\partial \mathrm{P}}{\partial \mathrm{V}}\right)_\mathrm{T} d\mathrm{V}$$

and

$$-\left(\frac{\partial \mathrm{P}}{\partial \mathrm{T}}\right)_\mathrm{V}\left(\frac{\partial \mathrm{T}}{\partial \mathrm{V}}\right)_p = \left(\frac{\partial \mathrm{P}}{\partial \mathrm{V}}\right)_\mathrm{T},$$

* Davey, ' Study of Crystal Structure and its Applications,' 1934.

† Rawlins and Taylor, ' Infra-red Analysis of Molecular Structure, p. 85 (1929).

we can transform equation (18) into

$$\frac{d\beta}{\beta_0} = \left[A_p - \left(\frac{\partial P}{\partial V}\right)_T \left(\frac{\partial V}{\partial T}\right)_p A_t \right] dT + \left(\frac{\partial P}{\partial V}\right)_T A_t dV.$$

Let α_v be the coefficient of cubical thermal expansion or $\alpha_v = \frac{1}{V_0}\frac{dV}{dT}$. Considering the definition of compressibility, we get

$$\frac{\partial \beta}{\beta_0} = \left(A_p + \frac{\alpha_v A}{\beta_0} \right) dT + \frac{A_t}{\beta_0}\frac{dV}{V_0},$$

which is an exact total differential equation and can be readily solved. The solution is

$$\beta = \beta_0 \left[1 + \left(A_p + \frac{\alpha_v A_t}{\beta_0} \right)(T - T_0) + \frac{A_t}{\beta_0}\frac{(V - V_0)}{V_0} \right], \quad (19)$$

where T_0 and V_0 are respectively the temperature and volume at the initial condition.

We can also choose volume and pressure as independent variables as well, since the operations are quite similar. In such case equation (19) becomes

$$\beta = \beta_0 \left[1 - \left(A_t + \frac{A_p \beta_0}{\alpha_v} \right)(P - P_0) + \frac{A_p}{\alpha_v}\frac{(V - V_0)}{V_0} \right]. \quad (19')$$

It is commonly believed that atomic force is dependent on nothing but dimension, or the atomic spacing. If there is any such case we may find some solid which obeys the condition

$$\alpha_v : A_p = \beta_0 : A_t. \quad . \quad . \quad . \quad . \quad . \quad (20)$$

After an examination of many solids we find that the alkaline halides satisfy this condition approximately. In Table V. the proportionality of these physical constants of several alkaline halides is shown. The proportionality of the constants has been noticed by J. C. Slater * for four salts.

The representation of atomic force by compressibility now encounters a difficulty, if the temperature and pressure correction of the compressibility is taken into consideration. But for those solids whose compressibility varies with volume only, such as alkaline halides, our representation of the restoring force still applies.

* Phys. Rev. xxiv. p. 488 (1924).

For metals the condition of equation (20) is, however, not satisfied. Therefore the atomic force cannot be exactly represented by compressibility, when the temperature and pressure corrections are to be made. This is due to the fact that in the metals there are free electrons which may exert considerable pressure and cannot be neglected as far as the second order terms of pressure are concerned. In case only thermal quantities are concerned the free electrons contribute very little. Thus it is quite reasonable to assume the function $f(r)$ for any substance changes very little with temperature. As a preliminary, let us treat the case of alkaline halides.

TABLE V.

Substance.	$\alpha_l \cdot 10^4$.	$A_p \cdot 10^4$.	$\beta_0 \cdot 10^{12}$.	$A_t \cdot 10^{12}$.	α_v/A_p.	β_0/A_l.
NaCl	1·1	7	4·2	21·9	0·16	0·19
NaBr	1·2	8	5·08	25·5	0·5	0·6
KCl	1·1	5	5·63	26·5	0·22	0·21
KBr	1·1	6	6·7	31·8	0·18	0·21
KI	1·3	6	8·54	39·1	0·22	0·22
RbI	1·2	7	9·58	43	0·17	0·22

(6) When the atom O as shown in fig. 1 is oscillating through a full period, the atom O_2 is also influenced by the relative force $f(r_0+x)$ between them. The average force between O and O_2 through a complete oscillation is, then,

$$-\nu \int_0^{\frac{1}{\nu}} f(x)\, dt;$$

where ν is the frequency of the oscillation as already defined. As far as the first and the second order terms of x are considered, the motion of O is harmonic. Thus the equation describing the motion of O can be concisely assumed as a linear harmonic oscillator along x-axis,

$$x = X_1 \sin 2\pi \nu t.$$

Substituting this into $f(r_0+x) = -ax+bx^2- \ldots$, and

taking the average, we get the average force which acts between O and O_2 as

$$\tfrac{1}{2}bX_1^2. \quad . \quad . \quad . \quad . \quad . \quad . \quad . \quad . \quad (21)$$

It is evidently the repulsive force acting between O and O_2 when O_2 is fixed. This repulsion, if there is no external pressure to offset it, will be surely neutralized by the binding force between the atoms O and O_2, resulting in a slight expansion of the lattice spacing. Then the expansion per unit length of r_0 will be given as Δx in

$$f(r+\Delta x) = -\tfrac{1}{2}bX_1^2$$

or

$$\Delta x = \frac{1}{2}\frac{b}{a}X_1^2$$

when higher order than third power of x/r_0 is neglected. The same expression has already been obtained by P. Debye * in 1913. But P. Debye assumed that the atom O in our symbols is oscillating in the field of force $f(r)$ instead of $F(x)$, and, as a result, his conclusion might be physically inapplicable to our case.

Let $\frac{\Delta l}{l}$ be the relative linear expansion of the solid, then

$$\frac{\Delta l}{l} = \frac{1}{2}\frac{b}{a}X_1^2/r_0 = \frac{1}{2k}n^{\frac{1}{3}}\frac{b}{a}X_1^2. \quad . \quad . \quad . \quad (22)$$

Now introducing equation (19) into (6), and bearing in mind the condition of equation (20), we obtain for alkaline halides

$$fr(+\Delta r) = -a\Delta r + b(\Delta r)^2 - C(\Delta r)^3$$

$$= -\frac{3\Delta r}{\beta_0 n^{\frac{1}{3}} r_0}\left[1 - \frac{A_t}{\beta_0}\frac{(-\Delta V)}{V_0}\right].$$

Since $V_0 \propto {r_0}^3$, from the last equation we get

$$\left.\begin{aligned} a &= 3/(n^{\frac{1}{3}} r_0 \beta_0), \\ b &= -\frac{9A_t}{n^{\frac{2}{3}}\beta_0^2 {r_0}^2}, \end{aligned}\right\} \quad . \quad . \quad . \quad . \quad . \quad (23)$$

* 'Vorträge über die Kinetische theorie der Materie und Elektricität.' Göttingen, 1913.

Substituting equations (23), (9), and (15) into (22), we have

$$\frac{\Delta l}{l} = \frac{-1}{6k}\rho A_t \int_0^T S(T)\,dT. \quad . \quad . \quad . \quad . \quad (24)$$

Let $\alpha_l(T)$ be the coefficient of linear thermal expansion and thereby a function of absolute temperature. It is evident, then,

$$\int_0^T \alpha_l(T)\,dT = \frac{\Delta l}{l} \quad . \quad . \quad . \quad . \quad . \quad . \quad (25)$$

Eliminating $\frac{\Delta l}{l}$ from (24) and (25) and getting rid of the integral sign, we have

$$\alpha_l(T) = \frac{-1}{6k}\rho A_t S(T).$$

If the specific heat is measured in heat units, say calories per gram per degree, the mechanical equivalent of heat J appears as a factor on the left-hand side, or

$$J\alpha_l(T) = \frac{-1}{6k}\rho A_t S_h(T), \quad . \quad . \quad . \quad . \quad (26)$$

where the subscript h denotes that the value is in heat unit. This last equation is really a very interesting one, which connects four common physical constants together in a very simple relation. Moreover, the equation is expected to be approximately true for a range of temperature.

In Table VI. a list of calculated α_l and observed α_l are tabulated. In the last column the ratios of calculated and observed values are given. These ratios show that the calculated values are generally ten to twenty per cent. too large.

We can find from Table III. that at the melting-point the mean value of x_1^2 is very roughly equal to $\frac{0{\cdot}024 r_0^2}{3}$. Then at melting-point, for all alkaline halides,

$$\left(\frac{\Delta l}{l}\right)_{\text{melting-point}} = \frac{1}{2k} n^{\frac{1}{3}} \frac{b}{a} \frac{0{\cdot}024}{3} r_0^2$$

$$= -{\cdot}012 \frac{A_t}{\beta_0}. \quad . \quad . \quad . \quad . \quad (27)$$

TABLE VI.

Substance.	T° C.	ρ.	$-A_t$.	$Cp(T)$ Joules per gram per °C.	S(T) cal. per gram per °C.	$\alpha_l \times 10^4$ calc.	$\alpha_l \times 10^4$ obs.	Ratio.
NaCl.....	−150	2·16	21·9	0·657	0·153	0·37	0·32	1·2
	−100	2·16	21·9	0·736	0·170	0·41	0·34	1·2
	0	2·16	21·9	0·853	0·196	0·47	0·38	1·2
	100	2·16	21·9	0·908	0·200	0·48	0·41	1·2
NaBr	−150	3·21	25·5	0·408	0·095	0·39	0·37	1·1
	−100	3·21	25·5	0·450	0·104	0·43	0·38	1·1
	0	3·21	25·5	0·492	0·111	0·46	0·40	1·2
	100	3·21	25·5	0·518	0·115	0·48	0·42	1·1
KCl	−150	1·98	26·5	0·588	0·138	0·36	0·31	1·2
	−100	1·98	26·5	0·634	0·147	0·39	0·32	1·2
	− 50	1·98	26·5	0·664	0·153	0·41	0·33	1·2
	0	1·98	26·5	0·680	0·156	0·41	0·35	1·2
	100	1·98	26·5	0·703	0·157	0·42	0·38	1·1
KBr	−200	2·75	31·8	0·325	0·076	0·34	0·32	1·1
	−100	2·75	31·8	0·403	0·094	0·41	0·35	1·2
	0	2·75	31·8	0·435	0·100	0·44	0·38	1·2
	100	2·75	31·8	0·452	0·101	0·45	0·41	1·1
KI	−150	3·12	39·1	0·302	0·071	0·44	0·38	1·2
	− 50	3·12	39·1	0·309	0·071	0·44	0·41	1·1
	0	3·12	39·1	0·312	0·071	0·44	0·42	1·1
RbBr	10	3·35	35	0·311	0·70	0·42	0·37	1·1
RbI	10	3·55	43	0·243	0·056	0·43	0·40	1·1

TABLE VII.

Halides.	$-A_t . 10^{12}$.	$\beta_0 . 10^{12}$.	A_t/β_0.	br_0/a.
NaCl	21·9	4·2	5·2	15·6
NaBr	25·5	5·1	5·0	15·0
KCl	26·5	5·7	4·7	14·1
KBr	31·8	6·7	4·7	14·1
KI	39·1	8·6	4·6	13·8
RbBr	35	7·9	4·4	13·2
RbI	43	9·5	4·5	13·5

Empirically we found that, $-A_e\beta_0$ for these compounds is nearly constant, as shown in Table VII. If we assume

$-A_l/\beta_0$ to be 4·5 for all these compounds, we conclude that the total relative expansion at the melting-point should be about 0·05, which is a well-known fact sometimes described as Pictet's rule.

From equation (23) the value b can be calculated in a very simple manner, *i. e.*,

$$\frac{br_0}{a} = \frac{3A_t}{\beta_0}.$$

Here b is expressed in relative magnitude with respect to a/r_0, such that the unnecessary complication of expressing in absolute unit can be avoided. In the last column of Table VII. values of br_0/a are given.

(7) For metals equation (22) still holds. Considering also equations (15) and (25), we have for metals

$$\alpha_l(\mathrm{T}) = \frac{1}{6k} n^{\frac{1}{3}} m \frac{b}{a^2} \mathrm{S(T)}, \quad . \quad . \quad . \quad . \quad (28)$$

which shows Grüneisen's rule. To find the relative value of b equation (7) is substituted into equation (28). Then

$$\frac{br_0}{a} = \frac{18k}{\rho\beta_0}\left[\frac{\alpha(\mathrm{T})}{\mathrm{S(T)}}\right]. \quad . \quad . \quad . \quad . \quad (29)$$

The value br_0/a for several metals has been calculated as shown in Table VIII. By assuming the mean value of X_1^2 for metals to be $\frac{0{\cdot}012}{3}$, as shown in Table I., equation (27) can, then, be transformed into

$$\left(\frac{\Delta l}{l}\right)_{\text{melting-point}} = \frac{1}{2k} n^{\frac{1}{3}} \frac{b}{a} \frac{0{\cdot}012}{3} r_0^2$$

$$= {\cdot}002\left(\frac{br_0}{a}\right).$$

From Table VIII. we get the average value of br_0/a for the metals listed to be about 15. Thus, the relative linear expansion at melting-point should be near to 0·030, which is in agreement with experimental fact.

(8) After we have discussed the second term of $f(r)$, let us pay some attention to the second term of $\mathrm{F}(x)$, to which the variation of specific heat with temperature at high temperature is greatly due. We have already proved that

$$\mathrm{F}(x) = -2ax - 2cx^3 - \ldots$$

or

$$\frac{d^2x}{dt^2} = -\frac{2a}{m}x - \frac{2c}{m}x^3.$$

If we suppose cx^2 to be small compared with a, and substitute expansions in powers of $2c/m$ for the displacement x, viz.,

$$\frac{d^2x}{dt^2} = x_0 + x_p\left(\frac{2c}{m}\right) + \ldots\ldots,$$

TABLE VIII.

Metals.	β_0.	ρ.	α_l/s in grams per Joule.	br_0/a.
Al	1·33	2·7	256	17·6
Co	0·54	8·9	293	15·1
Ni	0·53	8·9	292	15·3
Cu.....	0·72	8·92	431	16·8
Ag	0·99	10·5	809	19·3
Pt	0·36	21·5	655	20·9
Au	0·577	19·3	1089	24·2
Pb	2·3	11·3	2278	21·8
Ca	5·7	1·55	386	10·8
Fe	0·587	7·86	263	14·1
Mo	0·361	10·2	148	10·1
Cr	0·52	7·1	185	12·4
Li	9·1	0·53	169	8·7
Na	15·8	0·97	584	9·7
K	32·1	0·86	1120	10·2
Rb	40·5	1·53	2680	10·8
Cs	62·0	1·9	4441	9·2

we obtain in succession, by equating powers of $2c/m$, the equation

$$\frac{d^2X_0}{dt^2} = -\frac{2a}{m}x_0, \quad x_0 = X_1 \cos 2\pi\nu t\,;$$

$$\frac{d^2X_p}{dt^2} = -\frac{2a}{m}x_p - x_0^3 = -\frac{2a}{m}x_p - x_1^3 \cos^3 2\pi\nu t.$$

It indicates that the period of the motion is $1/\nu$, and its harmonics and the maximum displacement can be roughly represented as $X_1 \pm qX_1^3$, where q is a constant.

Now the instantaneous kinetic energy of the atom can be expressed as

$$\tfrac{1}{2}m\left(\frac{\partial X}{\partial t}\right)^2=\tfrac{1}{2}mv_0{}^2-ax^2-\frac{2c}{4}x^4 \quad . \quad . \quad . \quad (28')$$

It follows that the average kinetic energy $\bar{E}_{kin}$ becomes

$$\bar{E}_{kin}=4\nu\int_0^{\frac{l}{4\bar{\nu}}}\tfrac{1}{2}m\left(\frac{dx}{dt}\right)^2dt$$

$$=4\nu\int_0^{X_1+qX_1{}^3}\tfrac{1}{2}m\left(\frac{dx}{dt}\right)dx. \quad . \quad . \quad (29')$$

Substituting equation (8) and (13) and (28′) into (29′), we get

$$\bar{E}_{kin}=\tfrac{1}{2}m\frac{2\sqrt{z\bar{a}}}{\pi\sqrt{\bar{m}}}\int_0^{\frac{\sqrt{\bar{m}v_0}}{\sqrt{2a}}\pm qX_1{}^3}\sqrt{v_0{}^2-\frac{2a}{m}x^2-\frac{cx^4}{m}}$$

$$=\tfrac{1}{2}m\frac{2\sqrt{z\bar{a}}}{\pi\sqrt{\bar{m}}}\int_0^{\frac{\sqrt{mv_0}}{\sqrt{2a}}\pm qX_1{}^3}\sqrt{v_0{}^2-\frac{2ax^2}{m}}$$

$$\times\left[1-\frac{cx^4}{m\left(v_0{}^2-\frac{2a}{m}x^2\right)}\right]^{\frac{1}{2}}.$$

Since $\dfrac{cx^4}{m\left(v_0{}^2-\dfrac{2a}{m}x^2\right)}$ is small compared with unity, we may neglect its higher terms. Thus, we obtain

$$\bar{E}_{kin}=\tfrac{1}{2}m\frac{4a}{\pi m}\left[\left(\frac{x}{2}-\frac{3mcv_0{}^2x}{64a^2}\right)\sqrt{v_0{}^2\frac{m}{2a}-x^2}\right.$$

$$+\frac{mv_0{}^2}{4a}\sin^{-1}\frac{x\sqrt{2a}}{\sqrt{mv_0}}+\frac{cx^3}{4a}\sqrt{\frac{m}{2a}v_0{}^2-x^2}$$

$$\left.+\frac{3cx}{16a}\left(\frac{m}{2a}v_0{}^2-x^2\right)^{\frac{3}{2}}-\frac{3m^2v_0{}^4C}{128a^3}\sin^{-1}\frac{x\sqrt{2a}}{\sqrt{mv_0}}\right]^{\frac{\sqrt{\bar{m}}v_0}{\sqrt{2a}}+qX_1{}^3}$$

$$=\tfrac{1}{2}m\left[\frac{v_0{}^2}{2}-\frac{3mv_0{}^4C}{64a^2}\right], \quad . \quad . \quad . \quad . \quad . \quad . \quad . \quad . \quad (30)$$

when terms of higher order than $v_0{}^2$ or $X_1{}^2$ are neglected.

According to the law of equipartition of energy of particles, the mean kinetic energy corresponding to each degree of freedom of the oscillation is $1/k_0\mathrm{T}$, where k_0 is Boltzmann's constant. As we are considering the motion along, we have

$$\tfrac{1}{2}m\left[\frac{v_0^2}{2}-\frac{3mv_0^4c}{64a^2}\right]=\frac{1}{2}k_0\mathrm{T}. \quad . \quad . \quad (31)$$

Substituting equation (14) into (31), we get

$$m\int_0^{\mathrm{T}}\mathrm{S}(\mathrm{T})\,d\mathrm{T}\times\left[1-\frac{3mc}{32a^2}v_0^2\right]=3k_0\mathrm{T}. \quad . \quad (32)$$

As $\frac{3mc}{32a^2}v_0^2$ is small compared with unity, equation (32) becomes

$$\int_0^{\mathrm{T}}\mathrm{S}(\mathrm{T})\,d\mathrm{T}=\frac{3k_0\mathrm{T}}{m}\left[1+\frac{3mc}{16a^2}\frac{k_0}{m}\mathrm{T}\right]$$

or

$$\mathrm{S}(\mathrm{T})=\frac{3k_0}{m}\left[1+\frac{3mc}{32a^2}\frac{k_0}{m}\mathrm{T}\right]$$

or

$$\mathrm{WS}_h(\mathrm{T})=5{\cdot}955\left[1+\frac{3mc}{32a^2}\frac{\mathrm{RJ}}{\mathrm{W}}\mathrm{T}\right], \quad . \quad . \quad (33)$$

where R is the universal gas constant in work unit. The last equation is qualitatively in agreement with experimental facts, since the value $\mathrm{WS}_h(\mathrm{T})$, or the gram atomic heat at high temperatures, can be represented empirically by

$$\mathrm{W}\rho_h(\mathrm{T})=5{\cdot}955+\mathrm{CT},$$

where C is a constant. If C is experimentally determined we can calculate the relative magnitude of c-term by the following equation.

On introducing equations (7), (9), and (10) into the above equation, it becomes

$$\frac{cr_0^2}{a}=\frac{32\mathrm{W}r_0^2a\mathrm{C}}{3m\mathrm{RJ}}=21\times10^{-9}\times\frac{\mathrm{WC}}{\beta_0\rho}. \quad . \quad . \quad (34)$$

In Table IX. the value cr_0^2/a for a few metals are given. It is perhaps worth mentioning here that in deriving equation (17), or,

$$\left(\frac{\hat{r}_0-\sigma}{2\hat{r}_0}\right)^2=\frac{1}{3j}\rho\beta_0\bar{\mathrm{S}}\mathrm{T}_m$$

x^2- and x^3-terms are neglected. Let us now estimate to what an extent the equation is influenced by these terms of higher order in x.

Though $F(x)$ does not contain x^2-terms, yet the thermal expansion at melting-point affects the value of σ to a certain extent. As we have seen, if the thermal expansion is not corrected, $\hat{r}_0$ may be affected to about 4 per cent. Thus the absolute value of σ will be affected to a like magnitude.

TABLE IX.

Metals.	C. in* cal. per degree ^{2}.	W.	ρ.	$\beta_0 . 10^{12}$.	cr_0^2/a.
Ag	2·50	107·9	10·5	0·99	5·4
Au	1·6	197·2	19·3	0·577	6·0
Pt	5·4	195·2	21·5	0·36	29
Cu	4·4	63·6	8·92	0·72	9·3
Pb	6·8	207·2	11·3	2·3	11·4

* 'Handbuch der Experimental Physik.'—VIII. 1. Teil, p. 221.

If equation (25) is right, to equation (17) a correcting factor

$$\left[1-\frac{cr_0^2}{a}\left(\frac{X_1}{r_0}\right)^2\right] \text{ to } \left(\frac{\hat{r}_0-\sigma}{2\hat{r}_0}\right)^2$$

rises from the c-term of $F(x)$. In case of platinum, for example, $cr_0^2/a=29$, and $(X_1 r_0)^2$ at melting-point is equal to 0·0063. The correcting factor is about 0·8. Therefore the error is also not too serious.

A further discussion of the function $f(r)$ will be given in Part III. of this paper.

In concluding this part, the writer takes the opportunity to express his thanks to Dr. C. S. Yeh, of Tsin Hua University, Dr. Ny Tse-Ze, and Mr. Fang Sun-Hung, of the Institute of Physics, Academy of Peiping, for their encouragement and help.

Institute of Physics,
National Academy of Peiping,
Peiping.

V. *The Influence of Circular and Elliptical Holes on the Transverse Flexure of Elastic Plates.* *By* J. N. GOODIER, *M.A., Ph.D.**

IN the Poisson-Kirchhoff theory of thin plates [1] the differential equation for the transverse deflexion w is, in a well-known notation [1], $D\nabla^4 w = p$, p being the pressure applied to the surface. The stresses are represented by their force and couple resultants, on sections normal to the middle surface, per unit length of arc. These resultants are related to the deflexion by the formulæ

$$G_1 = -D\left(\frac{\partial^2 w}{\partial x^2} + \sigma \frac{\partial^2 w}{\partial y^2}\right), \quad G_2 = -D\left(\frac{\partial^2 w}{\partial y^2} + \sigma \frac{\partial^2 w}{\partial x^2}\right),$$

$$H_1 = -H_2 = (1-\sigma)D \frac{\partial^2 w}{\partial x \partial y}, \; N_1 = -D \frac{\partial}{\partial x} \nabla^2 w,$$

$$N_2 = -D \frac{\partial}{\partial y} \nabla^2 w. \quad . \quad . \quad . \quad . \quad . \quad . \quad . \quad . \quad . \quad . \quad (1)$$

G_1, G_2 are bending couples, H_1, H_2 torsional couples, and N_1, N_2 transverse shearing forces, per unit length on sections normal to the x- and y-axes respectively. We consider a region in which these resultants are constants (except for linear variations in G_1, G_2 necessary for equilibrium when N_1, N_2 are constant), so that the plate may be regarded as transmitting bending moments and transverse shearing forces, and seek to calculate the effects of making a hole. The general case can be built up from the solutions of a set of fundamental problems. These problems are chosen so that, but for the disturbance due to the hole,

(1) $G_1 = G$, a constant, $G_2 = \sigma G$. In the unperforated plate $w \propto x^2$. This is the state of the interior of a rectangular plate bent by couples G on the edges x = constant, the edges y = constant being free.

(2) $G_1 = \sigma G$, $G_2 = G$ (a similar state of flexure, but about the other axis).

(3) $H_1 = H$, a constant; $w \propto xy$. This state of twist is maintained by the distribution of torsional couples H on x = constant, and the complementary couples $-H$ (adopting Love's conventions) on y constant.

* Communicated by the Author.

It may be maintained alternatively by concentrated forces at the corners.

(4) $N_1=N$, a constant ($G_1=Nx$, $G_2=\sigma Nx$). The plate is transmitting shear force N, and the couple distribution G_1 is required for equilibrium. In the neighbourhood of $x=0$ there is simply shear force $N_1=N$.

(5) $N_2=N_1$ ($G_1=\sigma Ny$, $G_2=Ny$). The same as (4) except for change of axes.

For the elliptical hole these are all independent, but for the circular hole only two are independent, and for these two we may choose (2) and (5).

We may have in mind either plates with holes of limited size relative to the outer boundary, on which boundary the applied forces are as postulated in the cases 1–5, or else the region about a small hole, in a plate of greater extent, without any such restrictions on the applied forces. But then it is required that, except for the disturbance due to the hole, the stress couples and resultants in the plate vary only slightly over distances comparable with a few diameters of the hole.

In all cases there is no transverse loading p, and the deflexion w, with or without the hole, will be a plane, single-valued, biharmonic function.

Edge-conditions.—In orthogonal curvilinear coordinates, ξ, η, given by $\xi+i\eta=f(x+iy)$, we have the following formulæ, equivalent to (1), for the actions on sections $\xi=$constant:

$$J^4G_\xi=-D\left[J^2\left(\frac{\partial^2 w}{\partial\xi^2}+\sigma\frac{\partial^2 w}{\partial\eta^2}\right)-\frac{1}{2}(1-\sigma)\frac{\partial J^2}{\partial\xi}\cdot\frac{\partial w}{\partial\xi}+\frac{1}{2}(1-\sigma)\frac{\partial J^2}{\partial\eta}\cdot\frac{\partial w}{\partial\eta}\right],$$

$$J^4H_\xi=(1-\sigma)D\left[J^2\frac{\partial^2 w}{\partial\xi\partial\eta}-\frac{1}{2}\frac{\partial J^2}{\partial\xi}\frac{\partial w}{\partial\eta}-\frac{1}{2}\frac{\partial J^2}{\partial\eta}\cdot\frac{\partial w}{\partial\xi}\right],$$

$$J^5N_\xi=-D\left(J^2\frac{\partial w}{\partial\xi}-\frac{\partial J^2}{\partial\xi}\right)\left[\frac{\partial^2 w}{\partial\xi^2}+\frac{\partial^2 w}{\partial\eta^2}\right], \quad . \quad . \quad . \quad . \quad . \quad (2)$$

where $J^{-1}=|d(\xi+i\eta)/d(x+iy)|$. The actions on sections $\eta=$constant are obtained by interchanging ξ and η, except for H_η, which is simply $-H_\xi$.

On a boundary ξ=constant the actions are G_ξ, H_ξ, N_ξ, but the two latter are statically equivalent to a shear force distribution $N_\xi - \partial H_\xi/\partial s$, where s is the arc of the boundary. The edge conditions for a stress-free hole ξ=constant will be $G_\xi = 0$ and $N_\xi - \partial H_\xi/\partial s = 0$. But [1] $N_\xi = -D\partial/\partial\nu . \nabla^2 w$, where ν is the normal to the boundary. Since w is biharmonic, $\nabla^2 w$ is harmonic, and will possess a conjugate function Ω such that $\partial/\partial\nu . \nabla^2 w = \partial/\partial s . \Omega$, ν and s being so taken that they are related in the same sense as x and y. The second condition is thus equivalent to $D\partial\Omega/\partial s + \partial H_\xi/\partial s = 0$, and therefore can be fulfilled by making $D\Omega + H_\xi$ constant on the periphery of the hole.

At infinity the stress couples and resultants due to the presence of the hole must vanish; but it is not possible to obtain solutions in which the same holds for the deflexion itself. The significance of the terms which do not vanish at infinity will be discussed when the solutions have been obtained.

The Circular Hole.

Case 2: *Cylindrical Bending.*—The formulæ in polar coordinates corresponding to (2) are to be found in the text-books. With the customary conventions, we assume that the deflexion of the perforated plate has the form

$$w = -\frac{G}{2D}\left[y^2 + Aa^2 \log r + \left(Ba^2 + C\frac{a^4}{r^2}\right)\cos 2\theta\right].$$

The values of G_r and $D\Omega + H_r$ at the hole $r=a$ are

$$\tfrac{1}{2}G\{1+\sigma+(1-\sigma)A-[1-\sigma+4\sigma B-6(1-\sigma)C]\cos 2\theta\},$$

$$\tfrac{1}{2}G[1-\sigma+2(3-\sigma)B-6(1-\sigma)C]\sin 2\theta,$$

and the vanishing of these determines A, B, and C. Then

$$G_r = \frac{G}{2}\left\{(1+\sigma)\left(1-\frac{a^2}{r^2}\right) - (1-\sigma)\left(1-\frac{4\sigma}{3+\sigma}\frac{a^2}{r^2} - 3\frac{1-\sigma}{3+\sigma}\frac{a^4}{r^4}\right)\cos 2\theta\right\},$$

$$G_\theta = \frac{G}{2}\left\{(1+\sigma)\left(1+\frac{a^2}{r^2}\right) + (1-\sigma)\left(1+\frac{4}{3+\sigma}\frac{a^2}{r^2} - 3\frac{1-\sigma}{3+\sigma}\frac{a^4}{r^4}\right)\cos 2\theta\right\},$$

$$H_r = -\frac{G}{2}(1-\sigma)\left\{1-2\frac{1-\sigma}{3+\sigma}\frac{a^2}{r^2}+3\frac{1-\sigma}{3+\sigma}\frac{a^4}{r^4}\right\}\sin 2\theta,$$

$$N_r = -\frac{G}{a}\cdot 4\frac{1-\sigma}{3+\sigma}\frac{a^3}{r^3}\cos 2\theta, \quad N_\theta = \frac{G}{a}\cdot 4\frac{1-\sigma}{3+\sigma}\frac{a^3}{r^3}\sin 2\theta.$$

The most interesting quantity is G_θ. Without the hole it would have the value G along the x-axis. The form it takes when there is a hole is shown in fig. 1. It has a maximum value $G(1+\sigma)(5-\sigma)/(3+\sigma)$ at the edge of the hole. For steel this is 1·85 G, and 1·85 is thus the factor of stress concentration. This may be compared with the value 3 for a plate under tension. In either

Fig. 1.

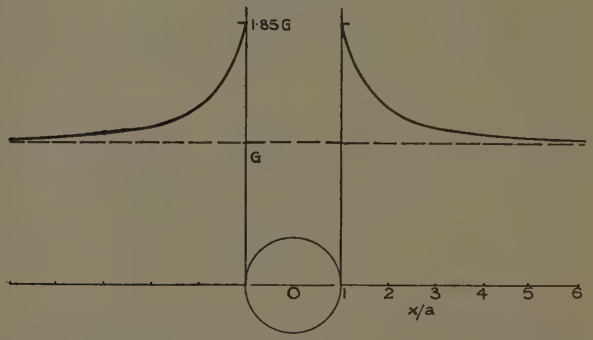

case the additional stresses are inappreciable outside a radius four or five times the radius of the hole.

It is noteworthy that the transverse shear forces N_r, N_θ are entirely due to the hole, and have maxima $G.4(1-\sigma)/a(3+\sigma)$ at the hole, inversely proportional to the radius. The shear force $N_\theta - \partial H_\theta/\partial r$, statically equivalent to N_θ and H_θ together, also has a maximum inversely proportional to the radius.

It is to be expected on dimensional grounds that, whatever the shape of the hole, there will be a maximum shear force inversely proportional to a characteristic linear dimension, c. Let the shape of the hole be specified by the ratios m, n, ... of other necessary lengths to c. The coordinates may be taken as dimensionless. The shear force N in general will be a function of G, D, σ, c, m, n, ... and the dimensionless co-ordinates. N is to be

proportional to G on account of the linearity of the fundamental equations. It follows that Nc/G must be a function of the shape factors m, n, ... and the dimensionless co-ordinates only, and consequently it will have a maximum depending only on the shape factors. Thus the maximum value of N will be proportional to G/c.

In the theory of thin plates with which we are concerned the deformation is taken as entirely due to the stress couples, the influence of the strains due to shear-stress resultants being disregarded. Evidently this restricts the application of the theory to states which involve shear forces so small that their influence on the deflexion can legitimately be ignored in comparison with that of the couples. We could not therefore conclude from the formulæ for the circular hole that very small holes may cause very high concentrations of shear force in their neighbourhood. The dimensional argument is independent of the assumptions of the detailed theory; but it is restricted to holes which are large in comparison with the thickness of the plate. Otherwise we should have to include the thickness in the dimensional argument, and it would no longer be true that the maximum shear force is inversely proportional to c.

We may now turn to the consideration of the term in $\log r$ in the deflexion. Adding a constant to secure vanishing at the points $x=0$, $y=\pm b$,

$$w=-\frac{Gb^2}{2D}\left[\frac{y^2}{b^2}-1+\frac{1+\sigma a^2}{1-\sigma b^2}\log\frac{r}{b}-\frac{1-\sigma a^2}{3+\sigma b^2}(1+\cos 2\theta)\right.$$
$$\left.+\frac{1}{2}\frac{1-\sigma a^2}{3+\sigma b^2}\left(\frac{a^2}{b^2}+\frac{a^2}{r^2}\cos 2\theta\right)\right];$$

w is accordingly the deflexion relative to the two points in question, which may be regarded as on the boundary of the plate. The hole is small in comparison with this boundary. We should therefore consider the behaviour of w for $a<<b$. Consider the deflexion at the hole itself. As $a/b\to 0$ the logarithmic term $(a^2/b^2)\log a/b$ also tends to vanish, and so do all the other terms except those representing the undisturbed deflexion—that is, the additional deflexion due to a very small hole is insignificant in comparison with the total deflexion. The logarithm is thus physically admissible in spite of its behaviour at infinity. The results may be applied without

significant error to finite plates, provided the boundary does not come within $r=5a$, say. The expression for w then leads to the conclusion that in finite plates the additional deflexion increases with the size of the (small) hole, although not in proportion to its radius. The boundary is here supposed unchanging.

The curves I and II in fig. 2 show the form of the deflexion at $x=0$ with and without the hole, and are placed at arbitrary levels. To compare them for a plate of given size they may be moved vertically so as to intersect at the boundary.

Fig. 2.

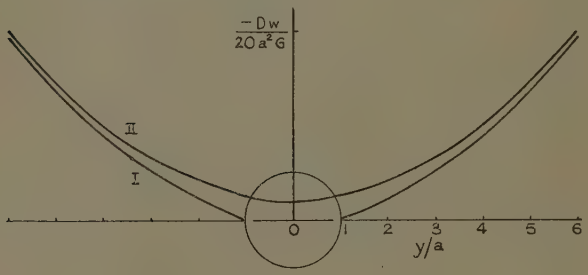

All-round Bending.—In the undisturbed plate $G_1=G_2=G$, $w\propto r^2$. The solution is deducible from the preceding by superposition, and is

$$G_r=G\left(1-\frac{a^2}{r^2}\right), \quad G_\theta=G\left(1+\frac{a^2}{r^2}\right),$$

$$H_r=H_\theta=N_r=N_\theta=0.$$

This is a result already well known from the theory of circular plates with axially symmetrical conditions. The greatest stress-couple is G_θ at the hole, with value $2G$.

Case 3 : *Twist.*—This also is deducible from Case 2 by superposition. The conditions at infinity are equivalent to a distribution of bending couples of magnitude H on two opposite sides of an infinite rectangle and $-H$ on the other two sides. The sides make angles 45° with the coordinate axes. The result is

$$G_r=H\left(1-\frac{4\sigma}{3+\sigma}\frac{a^2}{r^2}-3\frac{1-\sigma}{3+\sigma}\frac{a^4}{r^4}\right)\sin 2\theta,$$

$$G_\theta = -H\left(1+\frac{4}{3+\sigma}\frac{a^2}{r^2}-3\frac{1-\sigma}{3+\sigma}\frac{a^4}{r^4}\right)\sin 2\theta,$$

$$H_r = H\left(1-2\frac{1-\sigma}{3+\sigma}\frac{a^2}{r^2}+3\frac{1-\sigma}{3+\sigma}\frac{a^4}{r^4}\right)\cos 2\theta,$$

$$N_r = \frac{H}{a}\cdot\frac{8}{3+\sigma}\frac{a^3}{r^3}\sin 2\theta, \quad N_\theta = -\frac{H}{a}\cdot\frac{8}{3+\sigma}\cdot\frac{a^3}{r^3}\cos 2\theta.$$

$-G_\theta$ is $H.4(1+\sigma)/(3+\sigma)$ at $r=a$, $\theta=\pi/4$. This is 1·57 H for steel. H_r and H_θ reach the value $H.4/(3+\sigma)$, 1·21 H for steel, and there are again shear stress resultants with maxima varying inversely as the radius of the hole. There is no logarithmic term in the deflexion.

This solution also represents the effect of a small hole in a plane strip under torsion. For the deflexion $w \propto xy$ can be maintained, at points not near the edges, by any distributions of forces on the two ends only, equivalent to equal and opposite resultant twisting couples.

Case 5.—Taking

$$w = -\frac{N}{6D}\left[y^3+\left(\frac{A}{r}+Br\log r\right)\sin\theta+\left(\frac{C}{r^3}+\frac{D}{r}\right)\sin 3\theta\right],$$

the conditions that the periphery of the hole is free yield four equations for A, B, C, D. They give the value zero for B, so that in this case also the additional deflexion vanishes at infinity and may be described as purely local. The stress couples and resultants are found to be

$$G_r = \frac{Na}{4}\left[(3+\sigma)\left(\frac{r}{a}-\frac{a^3}{r^3}\right)\sin\theta\right.$$
$$\left.+(1-\sigma)\left(-\frac{a}{r}-\frac{1-5\sigma}{3+\sigma}\frac{a^3}{r^3}+4\frac{1-\sigma}{3+\sigma}\frac{a^5}{r^5}\right)\sin 3\theta\right],$$

$$G_\theta = \frac{Na}{4}\left\{\left[(1+3\sigma)\frac{r}{a}+(3+\sigma)\frac{a^3}{r^3}\right]\sin\theta\right.$$
$$\left.+(1-\sigma)\left[\frac{r}{a}+\frac{5-\sigma}{3+\sigma}\frac{a^3}{r^3}-4\frac{1-\sigma}{3+\sigma}\frac{a^5}{r^5}\right]\sin 3\theta\right\}.$$

$$H_r = \frac{Na}{4}\left\{\left[(1-\sigma)\frac{r}{a}+(3+\sigma)\frac{a^3}{r^3}\right]\cos\theta\right.$$
$$\left.+(1-\sigma)\left[-\frac{r}{a}+3\frac{1-\sigma}{3+\sigma}\frac{a^3}{r^3}-4\frac{1-\sigma}{3+\sigma}\frac{a^5}{r^5}\right]\cos 3\theta\right\},$$

$$N_r = N\left[\sin\theta-3\frac{1-\sigma}{3+\sigma}\frac{a^4}{r^4}\sin 3\theta\right],$$

$$N_\theta = N\left[\cos\theta + 3\frac{1-\sigma}{3+\sigma}\frac{a^4}{r^4}\cos 3\theta\right].$$

The shear force is intensified to N . $2(3-\sigma)/(3+\sigma)$(1·64 N for steel) at the hole, and falls with extreme rapidity to the undisturbed value within the plate. The maximum is here independent of the size of the hole. The same cannot be said of the flexural couples, which will have maxima proportional to the radius. They will, however, be unimportant for small holes.

The Elliptical Hole.

In the elliptical coordinates ξ, η, specified by $x+iy = c\cosh(\xi+i\eta)$ (so that $x=c\cosh\xi\cos\eta$, $y=c\sinh\xi\sin\eta$), any curve $\xi=$constant is an ellipse with foci at $x=\pm c$, $y=0$, the major axis lying along the x-axis. J^2, occurring in the formulæ (2), takes the form $\frac{1}{2}c^2(\cosh 2\xi - \cos 2\eta)$. The general form of the biharmonic function, periodic in η, in these coordinates is well-known [2], and we can select from it the biharmonics appropriate to the present problems.

Case 1.—Take

$$w = -(G/2D)[x^2 + A(e^{-2\xi} + \cos 2\eta) + Be^{-2\xi}\cos 2\eta + C\xi].$$

After substituting for x^2 its value in the elliptic coordinates, $\frac{1}{4}c^2(1+\cosh 2\xi)(1+\cos 2\eta)$, we find from (2) that J^4G_ξ can be expanded in a terminating harmonic series including terms in $\cos 0\eta$, $\cos 2\eta$, $\cos 4\eta$. Similarly the function $J^4(D\Omega + H_\xi)$ has terms in $\sin 2\eta$, $\sin 4\eta$ only. The conditions at the hole $\xi=\alpha$, namely, $G_\xi=0$, $D\Omega+H_\xi=$ constant, can be changed to

$$J^4G_\xi = 0,$$

$$J^4(D\Omega + H_\xi) = F(2+\cosh 4a - 4\cosh 2\alpha\cos 2\eta + \cos 4\eta),$$

the latter bracket representing the expansion of J^4. F is the indeterminate constant of the boundary.

There are accordingly, by equating coefficients of harmonics individually, five equations for the three constants A, B, C. These are not independent, and are all satisfied if

$$A = -\frac{c^2}{4}\cdot\frac{1+\sigma-(1-\sigma)e^{2\alpha}}{3+\sigma},$$

$$B = -\frac{c^2}{8}\left[1 - \frac{4(1+\sigma)e_{2\alpha}}{(1-\sigma)(3+\sigma)} + \frac{1-\sigma}{3+\sigma}e^{4\alpha}\right],$$

$$C = -\frac{c^2}{4} \cdot \frac{1+\sigma}{3+\sigma}\left[2+e^{-2\alpha}-\frac{3+\sigma}{1-\sigma}e^{2\alpha}\right].$$

The resulting expression for G_η at the hole is

$$G(1+\sigma)\left[1-\frac{1+\sigma-(1-\sigma)e^{2\alpha}}{3+\sigma}\cdot\frac{e^{-2\alpha}-\cos 2\eta}{\cosh 2\alpha-\cos 2\eta}\right].$$

For $\eta=0$, or the end of the major axis, this gives $G(1+\sigma+2\sigma a/b)(1+\sigma)/(3+\sigma)$ ($2a$ and $2b$ being the major and minor axes of the hole), which may be large for a slender ellipse. For $\eta=\pi/2$, or the end of the minor axis, we find $G(3-\sigma+2b/a)(1+\sigma)/(3+\sigma)$, which will always be smaller than the value for $b=a$, *i. e.*, the circular hole, in which case it is in agreement with the result obtained previously.

The term in ξ in the displacement corresponds at infinity to the term in $\log r$ for the circular hole, and its occurrence may be interpreted in the same way.

Case 2.—This can be dealt with just as in the preceding case, with y^2 replacing x^2 for the undisturbed deflexion. The values of the constants are

$$A = -\frac{c^2}{4}\cdot\frac{1+\sigma+(1-\sigma)e^{2\alpha}}{3+\sigma},$$

$$B = \frac{c^2}{8}\cdot\frac{1}{3+\sigma}\left[3+\sigma+4\frac{1+\sigma}{1-\sigma}e^{2\alpha}+(1-\sigma)e^{4\alpha}\right],$$

$$C = \frac{c^2}{4}\cdot\frac{1+\sigma}{3+\sigma}\left[2-e^{-2\alpha}+\frac{3+\sigma}{1-\sigma}e^{2\alpha}\right].$$

Then, for $\xi=\alpha$, *i. e.*, at the hole,

$$G_\eta = G(1+\sigma)\left[1-\frac{1+\sigma+(1-\sigma)e^{2\alpha}}{3+\sigma}\cdot\frac{e^{-2\alpha}-\cos 2\eta}{\cosh 2\alpha-\cos 2\eta}\right],$$

which has a maximum magnitude

$$G(3-\sigma+2a/b)(1+\sigma)/(3+\sigma)$$

at the ends of the major axes. This may be large for b/a small. It is easily verified that there are shearing forces, which are inversely proportional to c ; c determines the size of the hole, α determining merely its ellipticity.

Case 3.—The appropriate form for w is

$$\frac{H}{D(1-\sigma)}[xy+Ae^{-2\xi}\sin 2\eta+B\sin 2\eta].$$

There are no biharmonic functions other than the two appearing in this expression, which are of the form $f(\xi)\sin 2\eta$ and give stresses vanishing at infinity. The conditions at the hole in this case lead to five equations involving A, B, and F, the constant value of $D\Omega+H_\xi$. The four resulting from the elimination of F are all satisfied if

$$A=-\frac{c^2}{4}\cdot\frac{(1-\sigma)\sinh 4\alpha}{3+\sigma+(1-\sigma)e^{-4\alpha}}, \qquad B=\frac{c^2}{2}\cdot\frac{(1-\sigma)\sinh 2\alpha}{3+\sigma+(1-\sigma)e^{-4\alpha}}.$$

G_η at the hole is

$$H\,.\,4(1+\sigma)\frac{\sinh 2\alpha}{3+\sigma+(1-\sigma)e^{-4\alpha}}\cdot\frac{\sin 2\eta}{\cosh 2\alpha-\cos 2\eta}.$$

The numerical maxima occur for $\cos 2\eta=\operatorname{sech} 2\alpha$, and are of magnitude

$$H\,.\,\frac{(1+\sigma)(a+b)^2}{a^2+b^2+(1+\sigma)ab}.$$

This agrees, for $b=a$, with the result already found for the circular hole. When $b/a\to 0$ it does not, unlike Cases 1 and 2, increase indefinitely, but tends to a limit $H(1+\sigma)$.

The limiting circular case shows the greatest stress concentration of flexural couple, and the other limiting case, the crack, shows the least. This is true only while the ellipse lies along one of the axes of twist, Ox, Oy. If it has any other orientation we should need to take new axes along the axes of the ellipse, and relative to these axes the undisturbed deflexion would no longer be proportional to the product of the coordinates. The solution would involve Cases 1 and 2 as well as 3, and consequently would show concentrations of bending couple at the ends of the major axis and possibly elsewhere. For instance, when the ellipse lies at 45° to the axes Ox, Oy of the twist, the torsional couple being H as before,

$$(G_\eta)_{\xi=\alpha}=H\,.\,2\frac{1+\sigma}{3+\sigma}\cdot e^{2\alpha}\cdot\frac{e^{-2\alpha}-\cos 2\eta}{\cosh 2\alpha-\cos 2\eta}$$

with a numerical maximum $H\,.\,2(1+a/b)(1+\sigma)/(3+\sigma)$ at

the ends of the major axis, which increases without limit as the ellipse is flattened.

These results can be applied to the torsion of a strip, the argument being just as for the circular hole.

Case 4.—The deflexion of the unperforated plate, $-Nx^3/6D$, can be expressed in terms of $\cos\eta$ and $\cos 3\eta$, and it is appropriate to assume

$$w=-(N/6D)[x^3+Ae^{-\xi}\cos\eta+Be^{-3\xi}\cos 3\eta + C(e^{-\xi}\cos 3\eta+e^{-3\xi}\cos\eta)];$$

J^4G_ξ then has terms in $\cos\eta$, $\cos 3\eta$, $\cos 5\eta$; $J^4(D\Omega+H_\xi)$ in $\sin\eta$, $\sin 3\eta$, $\sin 5\eta$, so that there are six equations for A, B, and C. They are all satisfied if

$$A=\frac{3c^3}{32}\left[2e^{-2\alpha}-\frac{1-5\sigma}{3+\sigma}+4\frac{1+\sigma}{3+\sigma}e^{2\alpha}-\frac{3+\sigma}{1-\sigma}e^{4\alpha}\right],$$

$$B=\frac{c^3}{32}\left[-1+\frac{(1+3\sigma)(5-\sigma)}{(1-\sigma)(3+\sigma)}e^{4\alpha}-2\frac{1-\sigma}{3+\sigma}e^{6\alpha}\right],$$

$$C=-\frac{3c^3}{32}\left[1-\frac{1-\sigma}{3+\sigma}(2e^{2\alpha}+e^{4\alpha})\right].$$

Along the x-axis, the prolongation of the major axis, there is no shear force on account of symmetry. On the y-axis, the prolongation of the minor axis, we have, putting $\eta=\pi/2$,

$$N_\eta=-N+\frac{N}{8}\left[1-\frac{1-\sigma}{3+\sigma}(2e^{2\alpha}+e^{4\alpha})\right](e^{-3\xi}+3e^{-\xi})\operatorname{sech}^3\xi.$$

The term $-N$ is the value for the unperforated plate. The negative sign arises from the fact that, for $\eta=\pi/2$, $J^{-1}\partial/\partial\eta=-\partial/\partial x$.

It is easily seen that if α is very small, *i. e.*, the ellipse very flat, the shear force is reduced by the hole; but if α is large enough to satisfy $(2e^{2\alpha}+e^{4\alpha})(1-\sigma)>3+\sigma$ the shear force is increased by the hole.

The value at the hole, and at $\eta=\pi/2$, is

$$-N+\frac{N}{4}\left(2+\frac{b}{a}\right)\left\{\left(1-\frac{b}{a}\right)^2-\frac{1-\sigma}{3+\sigma}\left(3+2\frac{b}{a}-\frac{b^2}{a^2}\right)\right\},$$

reducing to the value already found for the circular hole, when $b=a$. For the limiting case $b/a=0$ it becomes $-N(3-\sigma)/(3+\sigma)$.

Case 5.—Starting from

$$w=-(\mathrm{N}/6\mathrm{D})[y^3+\mathrm{A}e^{-\xi}\sin\eta+\mathrm{B}e^{-3\xi}\sin 3\eta + \mathrm{C}(e^{-3\xi}\sin\eta+e^{-\xi}\sin 3\eta)],$$

all the conditions are found to be fulfilled if

$$\mathrm{A}=-\frac{3c^3}{32}\left[2e^{-2\alpha}+\frac{1-5\sigma}{3+\sigma}+4\,\frac{1+\sigma}{3+\sigma}\,e^{2\alpha}+\frac{3+\sigma}{1-\sigma}\,e^{4\alpha}\right],$$

$$\mathrm{B}=-\frac{c^3}{32}\left[1-\frac{(1+3\sigma)(5-\sigma)}{(3+\sigma)(1-\sigma)}\,e^{2\alpha}-2\,\frac{1-\sigma}{3+\sigma}\,e^{6\alpha}\right],$$

$$\mathrm{C}=\frac{3c^3}{32}\left[1+\frac{1-\sigma}{3+\sigma}(2e^{2\alpha}-e^{4\alpha})\right].$$

In this case the most interesting quantity is the shear force on the prolongation of the major axis N_η for $\eta=0$. This is

$$\mathrm{N}+\frac{\mathrm{N}}{8}\left[1+\frac{1-\sigma}{3+\sigma}(2e^{2\alpha}-e^{4\alpha})\right](e^{-3\xi}-3e^{-\xi})\,\mathrm{cosech}^3\,\xi.$$

If $(e^{4\alpha}-2e^{2\alpha})(1-\sigma)<3+\sigma$ the part of the above expression due to the hole is negative. Thus, if α is very small, that is, if the ellipse is very flat, the total shear force in the neighbourhood of the hole will be in a sense opposite to that of the original, or to the sense at infinity on the x-axis. In magnitude it will be very large. The value, whatever a or b, at the hole and on the x-axis, is

$$\mathrm{N}+\frac{\mathrm{N}}{4}\left(2+\frac{a}{b}\right)\left[\frac{1-\sigma}{3+\sigma}\left(1+\frac{a}{b}\right)\left(3-\frac{a}{b}\right)-2\left(\frac{a}{b}-1\right)^2\right],$$

which becomes negative and increases without limit as b/a decreases. When $b=a$ it reduces to the value already found for the circular hole. In that case it has the same sense as the shear force in the unperforated plate.

The validity of all the solutions involving shear stress resultants, and especially cases 4 and 5, is subject to the limitation mentioned in connexion with the circular hole.

References.

(1) A. E. H. Love, Math. Theory of Elasticity, 1927, Art. 313.
(2) (i.) E. G. Coker and L. N. G. Filon, 'Treatise on Photoelasticity,' Art. 6.20.
(ii.) A. Timpe, *Math. Zeit.* xvii. p. 189 (1923).

Ontario Research Foundation, Toronto.
November 1935.

VI. *The Specific Heat of Nickel.* *By* EDMUND C. STONER, *Ph.D.* (*Cambridge*), *Reader in Physics at the University of Leeds* *.

1. *Introduction.*

THE specific heat of nickel is of particular interest on account of the large contributions other than that associated with the lattice vibrations. The most obvious of these contributions is the "magnetic specific heat," which will be denoted by C_M, associated with the decrease of intrinsic magnetization with increase of temperature. This rises to a maximum near the Curie point and then falls fairly rapidly; a rough estimate of its magnitude may be made, for temperatures near the maximum, by extrapolating downwards the observed specific heat above (and not too near) the Curie point. This procedure gives an estimate of C_M only for a small temperature range; to obtain an estimate of C_M and its variation over any considerable temperature range, a much more detailed analysis of the specific heat variation is necessary. Even well above the Curie point, in the range where there is no longer any variation of intrinsic magnetization, the specific heat is still considerably in excess of the normal value. It has been shown that the greater part of the excess, until recently regarded as of unknown origin, may reasonably be identified with an electronic specific heat [1], [2], [3]. The order of magnitude of the excess at high temperatures is compatible with that of the electronic specific heat at very low temperatures as deduced by Keesom and Clark [4] from their measurements. The electronic specific heat will be denoted by C_E.

From the standpoint of the collective electron treatment of metals C_M may also be regarded as an electronic specific heat. It is, however, convenient to distinguish this part of the electronic specific heat as that associated with changes of spin orientation of the electrons (and so with change of intrinsic magnetization). The symbol C_E will be retained for that part of the electronic specific heat associated with changes of translational state, without changes of orientation A term corresponding

* Communicated by Prof. R. Whiddington, F.R.S.

to C_E will occur for all metals, while C_M is peculiar to ferromagnetics. The experimental results indicate that C_E is larger for ferromagnetic metals than for others. It is to be expected that above the Curie temperature the temperature variation of C_E for ferromagnetics will be of the normal type, but that below the Curie point the variation may be abnormal, since C_E may depend appreciably on the intrinsic magnetization (that is, on the number of parallel spins).

In this paper an analysis of the specific heat of nickel will be made with the aim of obtaining some indication of the variation of C_E and C_M over the whole temperature range, and so of the dependence of electronic energy on temperature and magnetization; the variation of intrinsic magnetization with temperature being known with considerable precision over the whole temperature range, except in the immediate neighbourhood of the Curie point and at the lowest temperatures.

A summary is first given of some of the more reliable experimental results for the specific heat of nickel, interpolated values being tabulated for a series of conveniently spaced temperatures (2).

It is the specific heat at constant volume, C_V, which is required, and the measured specific heat, C_P, must accordingly be corrected.

$$C_V = C_P - (C_P - C_V). \quad . \quad . \quad . \quad . \quad . \quad (1.1)$$

The $(C_P - C_V)$ correction is considered (3). The main contribution to C_V is that connected with the lattice energy; it will be denoted by C_Q, to indicate the possibility of its derivation on a quantum basis.

$$C_V = C_Q + C_M + C_E. \quad . \quad . \quad . \quad . \quad . \quad (1.2)$$

Another term should possibly be included corresponding to the Born-Brody[5] anharmonicity effect; this, however, will be small except at high temperatures, and even there may be of little importance, as suggested by a discussion by Eucken and Dannöhl[6]. It is in the C_E term that any error resulting from this neglect will be introduced.

It will be assumed that C_Q can be represented with fair approximation over most of the range by a Debye expression with a suitably chosen Debye temperature, θ_D. The possibility of a variation of the effective θ_D value

with temperature, brought out by the work of Blackman [7], will, however, be borne in mind. The values of θ_D derived from elastic constants are usually not sufficiently precise, nor are they necessarily appropriate, for giving the closest representation of the specific heat; the estimate of the effective θ_D must be made on the basis of the specific heat results themselves. It will be shown that C_E can be estimated with reasonable certainty for a considerable range of temperature (4). This leads to values for C_Q+C_M. The justifiable assumption is then made that C_M increases with increasing temperature; and it will be shown that this enables the effective θ_D value to be fixed within fairly narrow limits (5). It is then possible to obtain estimates of C_M for a wide range of temperature, and from them, the changes in quasi-magnetic energy for given changes of temperature. From the results for the variation of intrinsic magnetization with temperature the magnitude of the molecular field coefficient can then be estimated (6). Such estimates of the molecular field coefficient by a method which, in principle, appears sound are very desirable, in view of the wide discrepancies in estimates made by other methods, such as those based on measurements of the magneto-caloric effect. The problem of these discrepancies has been discussed in detail elsewhere [1], and it has been shown how they may arise from domain structure effects. These effects do not enter in connexion with the specific heat. Unfortunately it is not possible, by the present method, to obtain results of high precision for the whole temperature range, mainly on account of the large effect of comparatively small errors in the specific heat measurements. A number of definite conclusions can be drawn, however, and where they are less definite, attention may be directed to the interest of further more precise measurements.

The most comprehensive analysis of the specific heat of nickel so far made is that of Lapp [8], based on her own experimental results. The present analysis inevitably follows a somewhat similar procedure, though there are a number of differences both in the method and the conclusions drawn. Lapp virtually assumes that the value of C_M in (1.2) is known, being given by

$$C_M = -\tfrac{1}{2}N\rho(\partial\sigma^2/\partial T), \quad . \quad . \quad . \quad . \quad (1.3)$$

where $N\rho$ is given the value derived from the variation of paramagnetic susceptibility above the Curie point, and $(\partial\sigma^2/\partial T)$ is taken (as here) from the Weiss results. The value of C_E was then simply the excess of unknown origin ("terme inconnu") left over, the procedure being a not unreasonable provisional one when the possibility of a large electronic specific heat was not realized. Here this procedure is reversed, C_E being treated as approximately known, and the value of $N\rho$, in (1.3), as a quantity to be determined from the specific heat results. In a previous paper [1] the specific heat results have been considered in this way, but only for a range of some 50° below the Curie point. Here much more extensive series of measurements, which cover a range of 1000°, are taken into consideration.

Nickel is here considered as extensive and reliable data are available; but the general method would apply equally to the other ferromagnetic elements. Moreover, as an electronic term will appear for all metals, the treatment has some relevance in connexion with the specific heat of metals generally.

2. *Experimental Results.*

In the following tables are given the values of the specific heat of nickel (calories per degree per gram atom) obtained by slight interpolations from the results of Lapp [8], Grew [9], Ahrens [10], Rodebush and Michalek [11] (R.-M.), Keesom and Clark [4] (K.-C.), Eucken and Werth [12] (E.-W.), and Klinkhardt [13]. The interpolations have been made with considerable care, and errors introduced are certainly within the errors of the experiments. Such interpolated values for suitably spaced temperatures greatly facilitate the quantitative comparison of results of different investigators, and are convenient for calculations.

Although small amounts of impurities are likely to have little effect on C_Q, their effect on C_M and C_E may be considerable, and some indication of the purity of the materials used is therefore desirable. Grew used a Hilger nickel, stated to contain $<\cdot03$ per cent. impurity. Keesom and Clark used Mond nickel ($<\cdot2$ per cent. impurity), and a pure Mond nickel was also used by Lapp (no analysis is given). The Ahrens nickel was about

99·4 per cent. pure (main impurity Fe, ·20 per cent.). Rodebush and Michalek state that their nickel was better than 99 per cent. pure, the main impurities being

TABLES I. A–I. D.

Atomic Heat of Nickel, C_P
(calories per degree per gram atom).

I. A.—100°–750° K.

T.	Lapp.	Grew.	R.-M.
100	3·30	3·48	3·30
200	5·29	5·51	5·52
50	5·87	6·02	Ahrens
300	6·25	6·34	6·26
50	6·51	6·60	6·52
400	6·75	6·86	6·81
50	7·05	7·14	7·14
500	7·42	7·49	7·48
50	7·88	7·90	7·85
600	8·45	8·55	8·44
50	7·44	7·70	7·85
700	7·50	7·60	7·80
50	(7·62)	(7·72)	

I. B.—Curie Point Region. 600°–650° K.

T.	Lapp.	Grew.	Ahrens.
600	8·45	8·58	8·44
10	·67	·79	·62
20	·95	9·05	·93
2	9·04	·12	9·01
4	·13	·18	8·65
6	·23	·25	·40
7	—	·30	—
8	8·25	·05	·25
30	7·80	8·70	·15
5	·42	·25	·00
40	·43	7·98	7·90
5	·44	·82	·87
50	·44	·70	·85

I. c.—Low temperatures. 1°–200° K.

T.	K.-C.	T.	E.-W.	R.-M.
1	·00175	20	·075	..
2	356	40	·54	..
3	542	60	1·45	..
4	738	70	1·96	1·98
5	95	80	2·45	2·47
6	·0119	90	2·85	2·90
7	143	100	3·24	3·30
8	170			
9	200	120	3·83	..
		40	4·41	..
14	·0386	60	4·83	..
16	477	80	5·12	..
18	582	200	5·39	5·52

I. d.—High Temperatures. 650–1050° K.
(Klinkhardt.)

T.		T.	
650	7·31	900.....	7·88
700	7·35	50.....	8·06
50	7·42	1000.....	8·17
800	7·51	50.....	8·26
50	7·68		

iron and cobalt. The Klinkhardt nickel (the same material was used by Eucken and Werth) contained ·5 per cent. Mn. The effect of the impurities was here considerable, as shown by the maximum of the specific heat occurring some 30° lower than with Grew, Lapp, and Ahrens ; the effect will be greatest on C_M, but the values found for C_P both above the Curie point and at low temperatures may differ appreciably from those for pure nickel.

As to the accuracy of the results, Lapp and Grew both estimate that the errors should not exceed 2 per cent., though Grew states that his result for the lowest temperature (86° K.) was less reliable. It will be seen from Table I. a that there is a systematic difference

between the Grew and Lapp results, the Grew values being higher by about 2 per cent. over most of the range ; though this is a small percentage difference in C_P it leads to a large percentage difference in C_M ; and it is hardly possible to decide on which set of values the greater reliance should be placed without further comparable data. The Ahrens values are relative to an assumed standard value of $C_P = 6{\cdot}22$ at 20° C. There is little agreement in detail between the results of different observers in the region extending some 20° or 30° above the temperature of the maximum (Table I. B). Here the specific heat and the magnetic characteristics generally depend greatly on the details of the thermal treatment given to the material ; no quantitative explanation of these effects has yet been given, and in this paper they will not be considered in detail.

Keesom and Clark place less reliance on the accuracy of the measurements in the liquid hydrogen region (14°–19° K.) than on those in the helium region, which may be regarded as of considerable precision. The results of Eucken and Werth are estimated to be correct to within 2 per cent., those of Rodebush and Michalek to 0·5 per cent. (Table I. C). Klinkhardt estimates that the results obtained by his electron bombardment method (Table I. D) are probably accurate to about 3 per cent.

3. *The Dilatation Term*, $C_P - C_V$.

Values of $C_P - C_V$ are given in Table II. These values are interpolated from those given by Lapp [8] for the range 100–700° K., and extrapolated beyond this range by the method described below. The corresponding values of $\int_0^T (C_P - C_V)\,dT$ are also given in the table, these being the energies in calories per gram atom associated with the dilatation.

Lapp calculates $C_P - C_V$ from the usual expression

$$C_P - C_V = \frac{A}{J\rho}\cdot\frac{(3\alpha)^2}{\gamma}, \quad . \ . \ . \ . \quad (3.1)$$

where A is the atomic weight, J the mechanical equivalent of heat, ρ the density, α the coefficient of linear expansion, and γ the compressibility. Values for α were obtained

from the work of Chevenard. The compressibility was calculated from

$$\gamma = \frac{3(1-2\sigma)}{E}, \quad . \quad . \quad . \quad . \quad . \quad (3.2)$$

where σ is Poisson's ratio, E Young's modulus. Lapp adopted the Grüneisen values $\sigma = \cdot 309$, $E = 20 \cdot 54 \times 10^{-8}$ at room-temperature, and measured the relative values of E over the range 0°–450° C. Values are given in the

TABLE II.

$C_P - C_V$ and $\int_0^T (C_P - C_V)\, dT$.

T.	$C_P - C_V$.	$\int_0^T (C_P - C_V) dT$.	T.	$C_P - C_V$.	$\int_0^T (C_P - C_V) dT$.
100 ...	·012	·27	600...	·361	80·9
50 ...	·031	—	10...	·375	—
200 ...	·057	3·50	20...	·388	—
50 ...	·089	—	26...	·400	90·8
300 ...	·119	12·39	30...	·338	—
50 ...	·154	—	50...	·350	99·0
400 ...	·186	27·7	700...	·382	117·2
50 ...	·222	—	800...	·44	158
500 ...	·261	50·0	900...	·50	205
50 ...	·308	—	1000...	·56	258

literature of up to ·33 for σ, and from 17·1 to $23 \cdot 5 \times 10^{-3}$ for E. The deduced value of γ may thus be in error by as much as 20 per cent., but the room-temperature value obtained, $\cdot 56 \times 10^{-12}$, is in good agreement with that found by Bridgman (·54). The values of α as measured by Eucken and Dannöhl [14] are somewhat scattered, but are in general agreement with the Chevenard values. It may be concluded that the values of $C_P - C_V$ adopted by Lapp are probably correct to about 5 per cent., which is adequate for most purposes.

The downward extrapolation of $C_P - C_V$ was made by Lapp on the basis of the empirical relation

$$C_P - C_V = a(C_P - C_M)^2 T. \quad . \quad . \quad . \quad . \quad (3.3)$$

The upward extrapolation is here made on the basis of

a pure extrapolation of γ and an extrapolation of α based on the Chevenard and Eucken-Dannöhl measurements. This is considered preferable to the use of a relation of the type (3.3), partly owing to uncertainty as to the allowance which should be made for the electronic specific heat C_E. The values adopted for $(C_P - C_V)$, α and γ. are shown in fig. 1, the full lines giving the values used by Lapp, the dotted lines extrapolations. On the curve for α, which represents Chevenard's measurements, are shown the values given by Eucken and

Fig. 1.

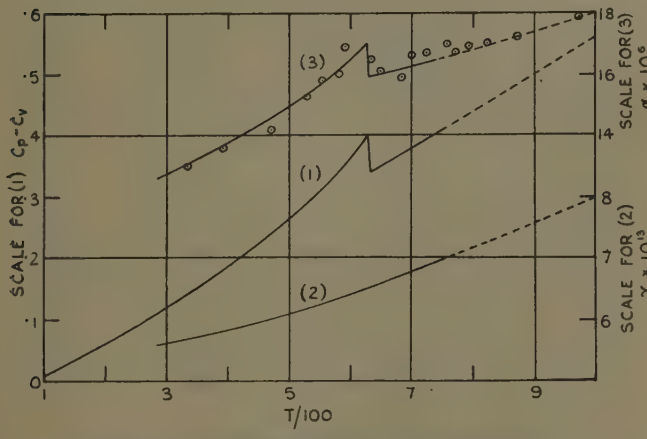

(1) $C_P - C_V$ (Lapp) (calories per degree per gram atom).
(2) Compressibility, γ. (Grüneisen, Lapp.)
(3) Coefficient of linear expansion, α. (Curve, Chevenard-Lapp. Points, Eucken and Dannöhl.)

The full parts of the curves show values used by Lapp; the dotted parts show extrapolated values.

Dannöhl [14], to indicate the degree of agreement between different observers.

4. *The Electronic Specific Heat*, C_E.

The value deduced by Keeson and Clark [4] for the electronic specific heat from measurements in the liquid helium range (1°–9° K.) is

$$C_E = \cdot 001744\, T. \quad . \quad . \quad . \quad . \quad . \quad (4.1)$$

The value used in correcting for the vibrational specific heat was $\theta_D = 413$; but the value (4·1) will be little modified by changes of θ_D of 10 or 20 degrees. Below 4° K. the vibrational specific heat is less than 6 per cent. of the total. It is difficult to see how this large low temperature specific heat can be accounted for as other than an electronic specific heat, and a linear increase with T is in accordance with theory. In the T^3 region C_Q is given by

$$C_Q = 464{\cdot}1\,(T/\theta_D)^3. \quad . \quad . \quad . \quad . \quad (4{\cdot}2)$$

With $\theta_D = 413$ the values of $C_Q + C_E$ are considerably in excess of the observed values in the liquid hydrogen region. Both the Keesom-Clark [4] values (14–19° K.) and the Eucken-Werth [12] values in the lower temperature range (up to 30° K.) are, in fact, less than the sum given by (4·1) and (4·2), except with values of the effective θ_D much higher than that appropriate for the rest of the temperature range. According to the Blackman treatment [7], a considerable increase in θ_D is possible at low temperatures. (See, for example, curve 1 of his fig. 3 for the 1-dimensional case, *l. c.*) In view of the stated uncertain accuracy of the liquid hydrogen measurements, however, it seems undesirable to attempt to draw definite conclusions from them at present. The value given by (4·1), being based on the precise liquid helium measurements, can probably be accepted as representing C_E with considerable accuracy, at least in the low temperature range.

The excess specific heat above the Curie point can be obtained by subtracting $(C_P - C_V)$ and C_Q from the observed C_P. In this region C_Q changes from about 5·85 at 650° K. to 5·91 at 1000° K., and depends little on the value chosen for θ_D with $380 < \theta_D < 420$. The values of the excess, C_E, and also of C_E/T are shown in the following table.

The values of C_E/T are of the same order as that deduced from the low temperature measurements ($100\,C_E/T = {\cdot}174$). The values of Lapp and Grew, however, are definitely greater, and the relatively low values of C_P obtained by Klinkhardt are probably in part due to the impurity of the specimen. Although at low temperatures an electronic specific heat is represented by an expression of the form (4·1), this will not form a

good approximation at the higher temperatures, and a more detailed theoretical consideration of the temperature variation is desirable.

In the ferromagnetic metals there is a superposition of the electronic bands corresponding to the d and s electrons, the top of the occupied portions of the bands at absolute zero coinciding with the top of the Fermi distribution. The saturation moment corresponds to the number of " holes " in the d-band, in nickel ·6 per atom. According to a plausible suggestion of Mott [15], the d-band is narrow and superposed on a much wider s-band.

TABLE III.

Excess Specific Heat, C_E, above the Curie Point, and C_E/T.

T.	C_E.			$(C_E/T)\times 100$.		
	L.	G.	K.	L.	G.	K.
650 ...	1·24	(1·50)	1·11	·191	(·230)	·171
700 ...	1·26	1·36	1·13	·180	·194	·161
50 ...	1·34	1·44	1·14	·179	·192	·153
800 ...	..	..	1·19	..	..	·146
50 ...	..	..	1·32	..	..	·155
900 ...	..	..	1·48	..	..	·153
50 ...	..	..	1·63	..	..	·172
1000 ...	..	..	1·70	..	..	·170
50 ...	..	..	1·75	..	..	·167

Under these conditions the electronic specific heat will be mainly due to the ·6 holes per atom in the d-band. It has been shown elsewhere [2] that these holes are energetically equivalent to the same number of electrons in an otherwise unoccupied reversed band. At low temperatures, C_E for nickel will be that for ·6 electrons per atom with parallel spins. In general, at low temperatures, the electronic specific heat for electrons with one direction of spin is given by

$$C_E = (\pi^2/3)k^2 T \nu(\epsilon_0), \quad . \quad . \quad . \quad . \quad . \quad (4.3)$$

where $\nu(\epsilon_0)$ is the number of states per unit energy range for this direction of spin at the top of the Fermi distribution. Expressing the electronic energy in volts,

let $\nu(V_0)$ be the number of electronic states per volt per atom for one direction of spin at the top of the Fermi distribution. The electronic specific heat per gram atom is then

$$C_E = 2{\cdot}835 \times 10^{-4} \nu(V_0) T. \quad . \quad . \quad . \quad . \quad (4.4)$$

The measured electronic specific heat (4.1) gives immediate information about $\nu(\epsilon_0)$ or $\nu(V_0)$. The value of $\nu(V_0)$ cannot, however, be related to the total effective number of electrons per atom, nor can the temperature variation be calculated, unless the energy distribution of states is known. To obtain an indication of the character of the temperature variation it will be assumed that $\nu(\epsilon)$ varies as $\epsilon^{1/2}$ (or $\nu(V)$ as $V^{1/2}$). The temperature dependence of the specific heat for this "normal" distribution has been obtained for the whole temperature range in a previous paper [16]. Let q be the number of effective electrons (or holes) per atom. With the normal energy distribution, and for states corresponding to one direction of spin,

$$\nu(V) = \frac{3}{2}\left(\frac{q}{V_0}\right)\left(\frac{V}{V_0}\right)^{1/2} \quad . \quad . \quad . \quad . \quad . \quad (4.5)$$

The expression for the electronic specific heat at low temperatures then becomes

$$C_E/Rq = 4{\cdot}253 \times 10^{-4}(T/V_0)[1 - 2{\cdot}20 \times 10^{-8}(T/V_0)^2]. \quad (4.6)$$

Putting $q = {\cdot}6$, as far as the first power of T,

$$C_E' = 5{\cdot}065 \times 10^{-4}(T/V_0'). \quad . \quad . \quad . \quad (4.7)$$

The experimental value (4.1) gives $V_0' = {\cdot}2904$. The straight line (1) in fig. 2 corresponds to (4.7) using this value of V_0', and so also to (4.1). The dash is used to indicate the value for parallelism of the spins. In the high temperature limit

$$C_E/Rq = 1{\cdot}5, \quad . \quad . \quad . \quad . \quad . \quad . \quad (4.8)$$

giving

$$C_E = 1{\cdot}785. \quad . \quad . \quad . \quad . \quad . \quad (4.8a)$$

In the paper above referred to [16], a table and a diagram are given showing the values of C_E/Rq for values of T/V_0 covering the intermediate range. From these, values of C_E for different values of T may be obtained for $V_0 = {\cdot}2904$ and $q = {\cdot}6$. Curve (1*a*) of fig. 2 shows C_E'

for $q=\cdot 6$, $V_0'=\cdot 2904$, the value of V_0' having been chosen as above to give agreement with the low temperature results.

As pointed out by Mott [3], the spins are no longer parallel above the Curie point, and the electronic specific heat will be larger than for parallel spins, as the effective V_0 will be smaller. Let f be the fractional number of spins pointing in one direction, $(1-f)$ in the opposite direction, V_f and V_{1-f} the corresponding values of V_0. For the low temperature specific heat

$$C_E=5\cdot 065\times 10^{-4}T\{f/V_f+(1-f)/V_{1-f}\}. \quad . \quad (4.9)$$

With the distribution of states here assumed

$$f \propto V_f^{3/2}. \quad . \quad . \quad . \quad . \quad . \quad . \quad (4.10)$$

For $f=1$, the low temperature state,

$$V_f=V_0'. \quad . \quad . \quad . \quad . \quad . \quad . \quad (4.11)$$

In general

$$f/V_f=f^{1/3}/V_0', \qquad (1-f)/V_{1-f}=(1-f)^{1/3}/V_0'. \quad (4.12)$$

For $f=1-f=\frac{1}{2}$, corresponding to the state above the Curie point, with equal numbers of oppositely directed spins, the band width and electronic specific heat will be denoted by V_0'' and C_E''. From (4.12)

$$V_0''=V_f=V_{1-f}=(\tfrac{1}{2})^{2/3}V_0' \quad . \quad . \quad . \quad (4.13)$$

$$=\cdot 1829 \quad . \quad . \quad . \quad . \quad . \quad . \quad . \quad . \quad (4.14)$$

The asymptotic low temperature value of C_E'' is greater, from (4.9) and (4.13), than that of C_E' by a factor of $2^{2/3}$ $(=1\cdot 5874)$.

$$C_E''=1\cdot 5874\, C_E'$$

$$=2\cdot 758\times 10^{-3}\,T. \quad . \quad . \quad . \quad . \quad (4.15)$$

The straight line (2) in fig. 2 corresponds to (4.15). At high temperatures C_E' and C_E'' tend to the same limit (4.8). The intermediate values of C_E'' are given by curve (2 *a*) of fig. 2.

In general, from (4.7), (4.9), and (4.12) the asymptotic low temperature value of C_E would be given by

$$C_E=C_E'\{f^{1/3}+(1-f)^{1/3}\}, \quad . \quad . \quad . \quad (4.16)$$

where C'_E is given by (4.7). Let σ_0 be the saturation moment at absolute zero, σ_T at a temperature T. Then

$$\left.\begin{aligned} f-(1-f)&=\sigma_T/\sigma_0, \\ f=\tfrac{1}{2}\{1-\sigma_T/\sigma_0)\},\quad 1-f&=\tfrac{1}{2}\{1+(\sigma_T/\sigma_0)\} \end{aligned}\right\}. \quad (4.17)$$

Use of (4.17) in (4.16) gives the asymptotic low temperature value of C_E, shown by curve (3) in fig. 2. An approximation to the curve for C_E for the whole range may be obtained from the curves (1 *a*) and (2 *a*) for C'_E and C''_E by using the asymptotic value for the ratio $(C_E-C'_E)/(C''_E-C'_E)$

$$\frac{C_E-C'_E}{C''_E-C'_E}=\phi=\frac{1}{2^{2/3}-1}\left[\{\tfrac{1}{2}(1-\sigma_T/\sigma_0)\}^{1/3}+\{\tfrac{1}{2}(1+\sigma_T/\sigma_0)\}^{1/3}\right]. \quad (4.18)$$

$$C_E=C'_E+\phi(C''_E-C'_E). \quad (4.19)$$

In fig. 2 the curve (3 *a*) corresponds to (4.19).

In fig. 2 are shown the values of C'_E, C''_E, and C_E calculated with the asymptotic expression for low temperatures (1, 2, and 3), and also the values calculated from the results for the whole temperature range, assuming a normal energy distribution of states (curves 1 *a*, 2 *a*, and 3 *a*). The experimental values for high temperatures (Table III.) are also plotted. The experimental values for low temperatures correspond to the lower part of the straight line 1.

It will be seen from fig. 2 that the experimental values at high temperatures are all higher than the calculated curve 1 *a* corresponding to parallel spins, while the Lapp and Grew values are higher than those corresponding to the low temperature result $C_E=1{\cdot}744\times10^{-3}$ T. The Grew and Lapp values are in fair agreement with those calculated for equal numbers of oppositely directed spins assuming a "normal" energy distribution of states (2 *a*). The mean of the Klinkhardt values (which are less reliable for the reasons stated above) is also in fair agreement with 2 *a*. It should be borne in mind that an error of 3 per cent. in C_P would correspond to an error from ·22 to ·25 in C_E.

In Table IV. are given the values of the electronic specific heat, C_E, and of $\int_0^T C_E dT$. These are calculated (A) from the asymptotic low temperature expression

for parallel spins (curve 1 in fig. 2), and (B) for numbers of oppositely directed spins corresponding to the observed magnetization, and assuming a normal distribution of states in calculating the temperature variation (curve 3 *a* in fig. 2). In both cases the calculations are based on the low temperature result (4.1), which corresponds to an energy width of ·2904 volts for the portion of the electronic band occupied by the ·6 virtual electrons (" holes ") per atom.

Fig. 2.

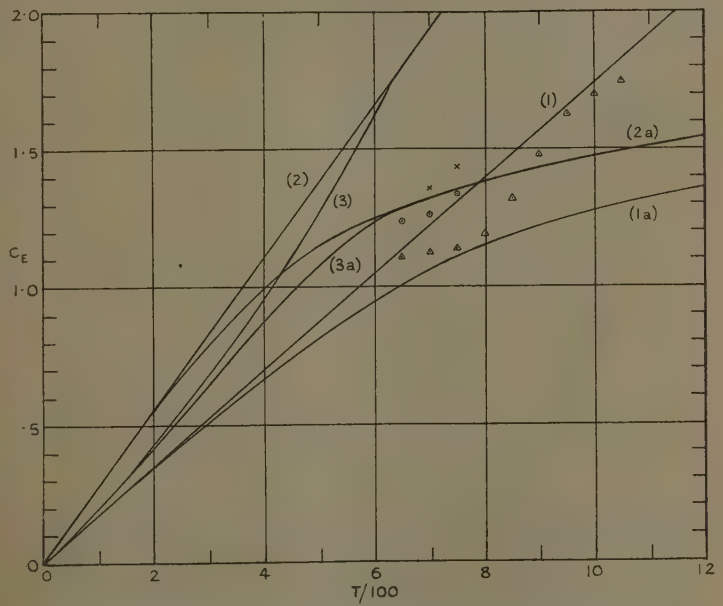

Electronic specific heat of nickel (calories per degree per gram atom). All the curves are calculated on the basis of the experimental result at low temperatures, $C'_E = 1{\cdot}744 \times 10^{-3}$ T.

1, 1 *a*, C'_E (parallel spins); 2, 2 *a*, C''_E (equal numbers of oppositely directed spins); 3, 3 *a*, C_E (relative numbers of oppositely directed spins corresponding to observed intrinsic magnetization); 1, 2, 3 correspond to the formulæ appropriate in the low temperature limit; 1 *a*, 2 *a*, and 3 *a* are calculated assuming a normal energy distribution of states. Experimental values: ⊙, Lapp; ×, Grew; △, Klinkhardt.

5. *The Lattice Vibration Term*, C_Q.

It will be assumed that the vibrational specific heat can be represented by a Debye expression with an approximately constant effective θ_D at least for the range from 100° K. upwards. Some justification for this assumption is provided by the fact that for copper, which has the same crystal structure as nickel, and similar mechanical properties, C_V is well represented by a constant θ_D considering the curve as a whole

TABLE IV.

Electronic Specific Heat, C_E, and $\int_0^T C_E\,dT$.

T.	A. C_E.	A. $\int_0^T C_E dT$.	B. C_E.	B. $\int_0^T C_E dT$.
100	·174	8·7	·20	10
200	·349	34·9	·42	40
300	·523	78·5	·65	93
400	·698	139·5	·87	169
500	·872	218·0	1·08	267
600	1·046	313·9	1·24	383
650	1·134	367·1	1·29	444
700	1·221	427·3	1·32	511
800	1·395	558	1·39	646
900	1·570	706	1·44	787
1000	1·744	872	1·48	933

($\theta_D=315$), while the value derived from the T^3 region is not very different ($\theta_D=321$). (These data are taken from Fowler [17].) For copper C_V is practically equal to C_Q, since $C_M=0$ and C_E is relatively small.

Values of θ_D given in the literature for nickel range from about 375 to 425 (excluding smaller values derived from C_V without allowing for C_E and C_M). The value used by Lapp, based on the observed C_P at 98° K., is $\theta_D=380$. (The values used in calculating C_Q were $C_P=3{\cdot}23$, $C_P-C_V=\cdot01$, $C_M=\cdot06$, $C_E=\cdot06$, giving $C_Q=3{\cdot}1$.)

For a given uncertainty in C_Q, θ_D can be fixed most precisely from the low temperature values (since at

low temperatures C_Q varies more rapidly with θ_D). It seems undesirable, however, to base the estimate of θ_D only on the results and estimates of the correcting terms for one temperature. Here the results for T=100, 200, and 300 will be considered, and use will be made of the estimated values of C_E already given. The values of C_P are taken from Table I. A. The values taken are at T=100, the Lapp, Rodebush-Michalek value, $C_P=3{\cdot}30$; at T=200, the Grew, Rodebush-Michalek value, $C_P=5{\cdot}51$; at T=300, the mean of the Grew and Lapp values, $C_P=6{\cdot}30$. The reasons for this choice have been indicated in the discussion of the experimental results.

The values of C_P-C_V are given in Table II., those of C_E in Table IV. It is the C_E values under B which will be used; at low temperatures these differ little from those under A which correspond to a pure extrapolation of the low temperature results. By subtraction C_Q+C_M is obtained

$$C_Q+C_M=C_P-(C_P-C_V)-C_E. \quad . \quad . \quad . \quad (5.1)$$

At low temperatures C_M is small, and an approximate estimate of its value is sufficient. According to the Weiss treatment

$$C_M=-\tfrac{1}{2}AN\rho(\partial\sigma_t{}^2/\partial T), \quad . \quad . \quad . \quad . \quad (5.2)$$

where σ_T is the intrinsic magnetization at the temperature T. Writing

$$N\rho=a\times 10^5. \quad . \quad . \quad . \quad . \quad . \quad (5.3)$$

C_M, in calories per degree per gram atom, is given by

$$C_M=\cdot 1402\, a\times\{-\sigma_T(\partial\sigma_T/\partial T)\}. \quad . \quad . \quad (5.4)$$

Above the Curie point, from the paramagnetic susceptibility a has the value 1·176, this being the value used by Lapp in calculating C_M, from (5.2), for the whole range. The value deduced from the specific heat in a previous paper [1] for a range of about 50° below the Curie point (300°–353° C.) was $a=\cdot 95\pm\cdot 05$; and it was concluded that at room-temperature a was probably greater than ·7. In view of the theoretical grounds for supposing a to vary little with temperature, it seems legitimate to apply (5.2) to the temperature region under consideration with $0<a<1{\cdot}5$.

The values taken for $-\sigma_T(\partial\sigma_T/\partial T)$, derived from the results of Weiss and Forrer [18], [19], and of Weiss [20],

were ·43, ·82 and 1·52 at 100, 200, and 300° K. The values of θ_D for different values of a are shown in the following table.

At the higher temperatures small differences in the estimates of C_Q lead to large differences in θ_D. Thus the Lapp and Grew results at 300° K., which differ by only 1·5 per cent., lead to θ_D values for $a=\cdot5$ of 432 and 393. The low temperature results are most suitable for determining θ_D, except for the undesirability of weighting them unduly, and the possibility that θ_D may vary with temperature. No definite conclusions can be drawn from the table as to possible variations of θ_D or

TABLE V.

Effective Debye Temperature, θ_D, for different Values of Molecular Field Coefficient, $a\times10^5$.

	a.			
T° K.	0.	·5.	1·0.	1·5.
100	390	393	396	400
200	374	388	398	410
300	369	411	456	498

of a with temperature, owing to the considerable effect of small errors in the measured C_P, or of errors in the correcting terms. From the 100° K. results, $\theta_D=390$ may perhaps be taken as a lower limit; from the table as a whole $\theta_D=400\pm10$ is suggested.

In so far as the values of C_Q corresponding to the derived θ_D are to be used in estimating C_M, it would appear superficially that the argument employed is circular, since estimates of C_M have been used in deriving θ_D. It is true that no conclusions can be drawn about C_M at low temperatures; at high temperatures, however, the values deduced for C_M depend relatively little on the precise value of θ_D within the range fixed by a very wide range of values of a at low temperatures. For this range of θ_D values, moreover, the values deduced for the total increase in the quasi-magnetic energy, $\int_0^T C_M dT$ will not

depend greatly on the precise θ_D value so long as T is appreciably greater than θ_D.

In Table VI. are given the values of C_Q and $\int_0^T C_Q dT$ for $\theta_D = 400$; the values are calculated from tables given by Simon [21].

TABLE VI.

Specific Heat, C_Q, and Energy Content, $\int_0^T C_Q dT$ for $\theta_D = 400$.

T.	C_Q.	$\int_0^T C_Q dT$.
100	3·00	109·2
200	4·92	525·3
300	5·46	1048·5
400	5·67	1606·8
500	5·77	2179
600	5·83	2759
650	5·85	3050

For $\theta_D = 390$ and 410, the values of $\int_0^T C_Q dT$ for $T = 650$ are 3068 and 3031; for $T \geq 300$ the change in C_Q for $\Delta\theta_D = 10$ is less than ·5 per cent.

As mentioned in section 4, the Keesom-Clark values of C_P for the liquid hydrogen range, and also the Eucken-Werth values up to $T = 30°$ K., appear to be lower than is compatible with a value of θ_D which seems reasonable. With $\theta_D = 400$, the value of 100 $(C_P - C_Q)/T$ is fairly constant at about ·17 up to $T = 9°$ K., falls to ·09 at $T = 20°$ K., and then increases to a value greater than ·2 for $T \geq 40°$ K. That the low values of C_P in the range 10–30° K. are not to be attributed entirely to experimental errors is suggested by the two independent sets of results leading to similar conclusions; if the experimental values are reliable, "anomalous" variations with temperature in this region of either C_Q or C_E are indicated.

6. *The Magnetic Specific Heat*, C_M.

From the preceding tables giving C_P, $C_P - C_V$, and C_Q, values of C_M may be derived. The value of a, corresponding to $N\rho \times 10^{-5}$ may then be calculated from (5.2), using values of $\partial\sigma_T^2/\partial T$ obtained from the results of Weiss. Alternatively, the mean value of a for a range of temperatures may be obtained from

$$a = \cdot 1402 \times \tfrac{1}{2} \Delta\sigma_T^2 = \int_{T_1}^{T_2} \{C_P - (C_P - C_V) - C_E\} dT. \quad (6.1)$$

TABLE VII.

Molecular Field Coefficient, a, from the Specific Heat Results of Grew, using $\theta_D = 400$.

T.	C_M.	$\frac{1}{2}\partial\sigma_T^2/\partial T$.	a.	$\int_{T_1}^{T_2} C_P dT$.	$\int_{T_1}^{T_2} C_M dT$.	$\frac{1}{2}\Delta\sigma^2$.	a.
100 ..	(·27)	·43	..	126	6	27	1·6
200 ..	·11	·82	·96	460	11	61	1·3
300 ..	·11	1·52	·52	599	14	117	·9
400 ..	·13	2·65	·35	660	11	206	·4
500 ..	·38	4·31	·65	715	23	336	·49
600 ..	1·16	8·65	·96	795	68	602	·81
650 ..	..	..	..	428	58	327	1·26
				3783	191	1676	·81

The value used for σ_0 was 57·9; this is slightly higher than the value for pure nickel [19], [20], but is compatible with the results used [18] for the range above room-temperature. The following table gives details of the values used in calculating a from the specific heat results of Grew (Table I.).

It will be apparent from this table that a high accuracy would be required in the specific heat results (even supposing the correcting terms to have been estimated with sufficient accuracy) to enable significant conclusions to be drawn as to the molecular field coefficient at the lower temperatures. At 300° K., for example, an error of about 1·5 per cent. in C_P leads to an error of about 50 per cent. in C_M. It is only at the higher temperatures that

C_M is sufficiently large for reasonably reliable estimates to be made of its value. The high value for the range 600–650° K. is partly due to the slow fall in the specific heat as measured by Grew, and also to the estimated values of C_E used being somewhat smaller than the observed values (see fig. 2). For the range 600–630° K. the value $a = \cdot 95 \pm \cdot 05$ previously obtained by extrapolation from above the Curie point is probably more reliable. Of the values given in the table most reliance

TABLE VIII.

Upper and Lower Limits for the Molecular Field Coefficient, a, from Grew's Results. ($\theta_D = 400.$)

T/100 ...	1–2	2–3	3–4	4–5	5–6	6–6·5	0–6·5
Upper ...	1·7	1·4	·8	·9	1·0	1·43	1·14
Lower ...	1·3	·9	·4	·5	·81	1·26	·81

TABLE IX.

Upper (1) and Lower (2) Limits for the Molecular Field Coefficient, a.

	Grew.		Lapp.	
θ_D.	(1).	(2).	(1).	(2).
390	1·05	·73	·74	·41
400	1·14	·81	·81	·49
410	1·21	·88	·90	·57

can be placed on the mean $a = \cdot 81$, deduced from the total change of quasi-magnetic energy for the change in intrinsic magnetization from σ_0 to 0.

If, instead of using the value of C_E under B, Table IV., those under A are used, corresponding to direct extrapolation of the low temperature results, higher values of a are obtained. These may be regarded as upper limits. The values are shown in the following table, together with the lower limit values from Table VII.

In Table IX. are shown the upper and lower limits for a derived from the Lapp and Grew results for different values of θ_D, considering the whole range 0–650° K.

Finally, for compleeness,t in Table X. are shown the values of a for the region just below the Curie point as obtained previously [1], on the assumption that C_E varied linearly with temperature up to the value observed above the Curie point, that is, taking C_E as ·18 and $\cdot 19 \times 10^{-3}$ T. for the Lapp and Grew results respectively. This method seems the most satisfactory for estimating C_M fairly near the Curie point.

By the method of analysis used here the mean values of a for the whole range are probably underestimated from Lapp's results and slightly overestimated from those of Grew. (The reasons for this will be apparent

TABLE X.

Values of a near the Curie Point by Linear Extrapolation of C_E.

T.	Lapp.	Grew.
580	$1{\cdot}0_0$	·94
90	$1{\cdot}0_0$	·95
600	·99	·97
10	·97	$1{\cdot}0_0$
20	·96	$1{\cdot}0_0$
26	·97	..
27	..	·93

from fig. 2.) The results as a whole suggest as a mean value $a = \cdot 8 \pm \cdot 2$. This corresponds to a value of $\int_0^T C_M dT$, with T greater than the Curie temperature, of 188 ± 40. The values of a, as estimated by different methods, are consistently higher at the higher temperatures than this mean value ; and this points to the conclusion that there is a definite decrease in a in the medium temperature range (where there are still considerable changes in the intrinsic magnetization) below the value in the Curie point region and above (where the value $1{\cdot}17_6$ is fairly precise). On the other hand, there is no indication of such large decreases as are suggested by a consideration of the magneto-caloric and the magnetization results without allowing for domain structure effects. (Without

allowing for these, the results indicate values of a of about ·4 at 500, ·2 at 400, and ·1 at 300° K.). Unfortunately, the limits imposed by the attainable accuracy of specific heat measurements prevent definite conclusions from being drawn as to the temperature variation of a at the lower temperatures.

In order to indicate clearly the relative magnitudes of the various terms in the specific heat, in fig. 3 are

Fig. 3.

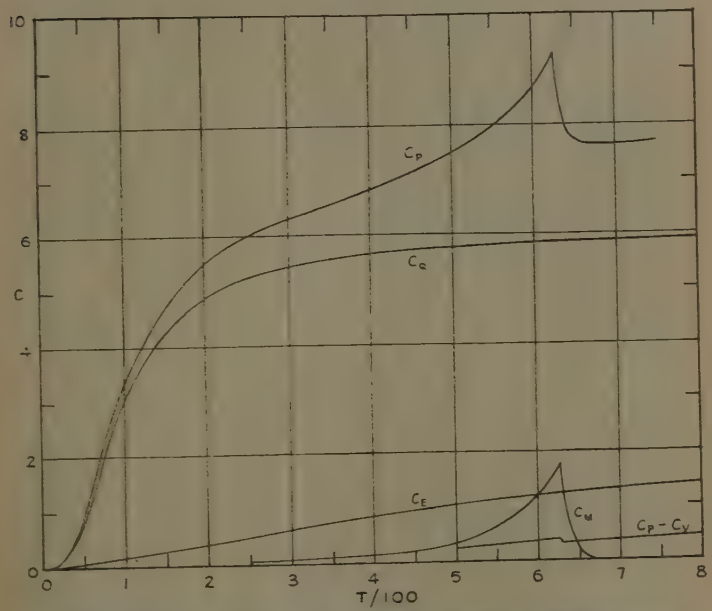

Specific heat of nickel (calories per degree per gram atom). Observed C_P (Grew), estimated $C_P - C_V$ (fig. 1) and C_E (curve 3 a, fig. 2), and derived C_M.

shown the results of Grew for C_P, the estimated values of $C_P - C_V$ and of C_E, and the deduced value of C_M.

In so far as the purpose of specific heat measurements is to enable conclusions to be drawn as to the energy changes associated with processes occurring in the material as a result of temperature change, the present analysis indicates the desirability of certain supplementary

determinations of the specific heat of nickel. Over the ordinary temperature range (say 0–450° C.) a relatively small number of precise determinations are desirable such as would serve to confirm the values in Table I. A, where these are in agreement, or to enable a choice to be made between them when they are not. At higher temperature there appear to be no precise determinations made with pure nickel, such as are desirable in connexion with the electronic specific heat term. Finally, the low temperature range (particularly 10–100° K.) requires further investigation. Here the relative importance of the C_E and C_M terms is greater; and it would be of great interest if these terms in the specific heat could be brought into relation with the low temperature variation of intrinsic magnetization, where a precise theoretical treatment has been developed, which appears to be in accordance with the more recent measurements.

On the theoretical side a detailed quantitative treatment of the temperature variation of magnetization and the associated specific heat remains to be developed. The subdivision of this specific heat into C_E and C_M is not entirely satisfactory; for although C_E corresponds to change of translational energy without change of "orientational" energy, change of orientation is not necessarily unaccompanied by change of translational state. It is possibly for this reason that there is apparently some change in the effective molecular field coefficient, a, with temperature. There is theoretical justification for expecting a to be approximately constant only so long as C_M corresponds to changes in orientational state only. The quantity $\int_0^T C_M dT$ is strictly a measure of the excess of the increase in orientational energy over the decrease in translational energy associated with the changes of orientation. The results of a theoretical treatment would depend on the energy distribution assumed for the states in the composite electronic band. (The distribution assumed here must be regarded as at best a rough approximation.) The experimental values of C_E and C_M are required to test such a theoretical treatment, but these values can only be found by a detailed analysis of the experimental results for C_P. It is such an analysis which has been made in this paper.

Summary.

A detailed analysis is made of the specific heat of nickel, which is treated as sum of four terms :

$$C_P = C_Q + (C_P - C_V) + C_E + C_M.$$

The more reliable data for the observed C_P are collected, values being given for conveniently spaced temperatures over a range of 1000°. The reliability of the measurements is discussed (2). Estimates of the dilatation term $C_P - C_V$ are given (3, fig. 1). The electronic term, C_E, is treated as corresponding to the increase in the translational energy of the collective electrons, mainly of the ·6 virtual electrons (" holes ") per atom in the *d*-electron band. From the value of C_E at low temperatures, the effective width of the unoccupied portion of the *d*-band is estimated, and a theoretical calculation is made of the variation of C_E with temperature. The calculated values at high temperatures agree reasonably well with the observed excess specific heat above the Curie point (4, fig. 2). The term C_M is the magnetic excess, an electronic specific heat associated with change of orientation of the electronic spins. It is treated as corresponding to

$$C_M = \cdot 1402\, a \times (-\tfrac{1}{2}\partial\sigma_T^2/\partial T),$$

where $a (= N\rho \times 10^{-5})$ is a molecular field coefficient, and σ_T is the intrinsic magnetization at T. Even allowing a wide range of values for a, the effective Debye temperature θ_D can be fixed from the values of C_P at 100°, 200°, and 300° K. as 400° ± 10°. This enables C_Q to be calculated for the whole range (5). Values of C_M, and hence of a, are then obtained ; there are large differences corresponding to small differences in results for C_P. The dependence of a on the values used for θ_D and C_E is considered. It is concluded that the mean value of a for the whole temperature range up to the Curie point is ·8±·2. This is lower than the value above the Curie point (1·176), but higher than values deduced by other methods. The analysis suggests that a decreases as the temperature decreases below the Curie point. The theoretical interpretation of these results is briefly discussed (6). A figure is given indicating the magnitudes of the various terms. Numerical data and results are given in a number of tables.

References.

(1) E. C. Stoner, Phil. Trans. Roy. Soc. A. ccxxxv. p. 165 (1936).
(2) E. C. Stoner, Proc. Roy. Soc. in print (1936).
(3) N. F. Mott, Proc. Roy. Soc. clii. p. 42 (1935).
(4) W. H. Keesom and C. W. Clark, *Physica*, ii. p. 513 (1935).
(5) M. Born and E. Brody, *Zeits. f. Phys.* vi. p. 132 (1921).
(6) A. Eucken and W. Dannöhl, *Zeits. f. Elektrochem.* xl. p. 789 (1934).
(7) H. Blackman, Proc. Roy. Soc. cxlviii. p. 365 (1935).
(8) E. Lapp. *Ann. de Physique*, xii. p. 442 (1929).
(9) K. E. Grew, Proc. Roy. Soc. cxlv. p. 509 (1934).
(10) E. Ahrens, *Ann. der Physik*, xxi. p. 169 (1934).
(11) W. H. Rodebush and J. C. Michalek, J. Amer. Chem. Soc. xlvii. p. 2117 (1925).
(12) A. Eucken and H. Werth, *Zeits. f. anorg. Chem.* clxxxviii. p. 152 (1930).
(13) H. Klinkhardt, *Ann. der Physik*, lxxxiv. p. 67 (1927).
(14) A. Eucken and W. Dannöhl, *Zeits. f. Elektrochem.* xl. p. 814 (1934).
(15) N. F. Mott, Proc. Phys. Soc. xlvii. p. 571 (1935).
(16) E. C. Stoner, Phil. Mag. xxi. p. 145 (1936).
(17) R. H. Fowler, ' Statistical Mechanics,' pp. 81–86 (C.U.P., 1929).
(18) P. Weiss and R. Forrer, *Ann. de Physique*, v. p. 153 (1926).
(19) P. Weiss and R. Forrer, *Ann. de Physique*, xii. p. 279 (1929).
(20) P. Weiss, *Comptes Rendus*, cxcviii. p. 1893 (1934).
(21) F. Simon, *Handbuch der Physik*, x. pp. 367–8. (Springer, Berlin, 1926.)

Physics Department,
University of Leeds.
February 1936.

VII. *On the Vibration of a Heterogeneous Circular Membrane.* *By* Prof. F. E. Relton, *D.Sc.*, *M.A.*, *Egyptian University* *.

THE equation for the vibration of a non-homogeneous circular membrane is soluble by the use of ring co-ordinates when the density varies inversely as the square of the distance from a fixed straight line in the plane of the membrane. The solution is expressible in terms of associated Legendre functions of degree half an odd integer. It gives a physical meaning to the vanishing of these functions, when regarded as functions of their order, and suggests that they vanish for a finite number of real orders and an infinite number of purely imaginary orders. The solution is shown to degenerate into the usual solution for the homogeneous membrane dependent on Bessel functions. Arithmetical values show that the frequencies are singularly little affected by the lack of homogeneity.

* Communicated by the Author.

1. The stretched circular membrane lies in the x, y-plane with its centre on the x-axis and vibrates in the z-direction. Euler's equation of motion is then

$$\rho\ddot{z}=\mathrm{T}\nabla^2 z. \quad . \quad . \quad . \quad . \quad . \quad . \quad (1)$$

T is the tension, constant throughout the membrane. The mass per unit area is ρ; it may be variable, but is usually treated as constant. ∇^2 is Laplace's operator for two dimensions. If the frequencies of the vibrations are determined by $z=\zeta \cos pt$, where t is the time, we have

$$\nabla^2\zeta+p^2\rho\zeta/\mathrm{T}=0. \quad . \quad . \quad . \quad . \quad . \quad (2)$$

2. It is customary to choose for ∇^2 a form suited to the boundary. The cases for cartesians, polars, elliptic, and parabolic coordinates are well known *. It appears that ring coordinates have not been tried. I define ring co-ordinates by the transformation †

$$\exp(\lambda-i\theta)=(b-x-iy)/(b+x+iy) \quad . \quad . \quad . \quad (3)$$

where b is a constant. The parametric curves λ, θ are two conjugate families of coaxal circles. A member of the λ-family is defined by $\exp\lambda$=the ratio (distance from b, 0 : distance from $-b$, 0) for every point on the periphery. The points $\pm b$, 0 are the limiting points for the λ-family and the real intersections for the θ-family; they correspond to $\exp(\pm\lambda)=0$. The equation (2) now takes the form

$$\frac{1}{(xh)^2}\left\{\frac{\partial^2\zeta}{\partial\lambda^2}+\frac{\partial^2\zeta}{\partial\theta^2}\right\}+\frac{p^2\rho}{\mathrm{T}}\zeta=0, \quad . \quad . \quad . \quad (4)$$

where $h=\operatorname{cosech}\lambda$, $x=-b\sinh\lambda/(\cos\theta+\cosh\lambda)$.

3. If the density is constant equation (4) furnishes the solution for the vibration of a homogeneous membrane bounded by two circles, eccentric or intersecting as the case may be. If we abandon the idea of homogeneity solutions are obtainable in certain cases. Some of these are very artificial. Thus, if the density is proportional to $(\cos\theta+\cosh\lambda)^2$ the problem reduces to the same form as the vibrating rectangular membrane. A less artificial case is one in which the density is inversely proportional to the square of the distance from a fixed straight line in the plane of the membrane. An approximation to

* Riemann-Weber, Partiellen Diff :-gleich (1919), ii. p. 261 *et seq.*
† Phil. Mag. xi. p. 129 (1931).

this condition might be achieved in practice by a wet membrane in a vertical plane. This will include, in the limit, the case where the fixed straight line is indefinitely remote, the membrane then becoming homogeneous.

4. Taking the fixed straight line as the y-axis and the density as ρ/x^2, the equation (4) becomes

$$\frac{\partial^2\zeta}{\partial\lambda^2}+\frac{\partial^2\zeta}{\partial\theta^2}+k^2h^2\zeta=0, \quad . \quad . \quad . \quad . \quad (5)$$

where $k^2=p^2\rho/\mathrm{T}$. This has solutions of the type $\zeta=\mathrm{L}\cos n\theta$, where n is integral and L is a function of λ alone, to be determined from the equation

$$\frac{d^2\mathrm{L}}{d\lambda^2}+\mathrm{L}(k^2h^2-n^2)=0. \quad . \quad . \quad . \quad . \quad (6)$$

A solution of this last equation is obtainable if we change the variable to $\nu=\cosh\lambda$. This transforms (6) to

$$(\nu^2-1)\frac{d^2\mathrm{L}}{d\nu^2}+\nu\frac{d\mathrm{L}}{d\nu}+\left(\frac{k^2}{\nu^2-1}-n^2\right)\mathrm{L}=0, \quad . \quad (7)$$

which obviously has affinities with the equation for associated Legendre functions. On putting $\mathrm{L}=\mathrm{M}(\nu^2-1)^{\frac{1}{2}}$, equation (7) becomes

$$(1-\nu^2)\frac{d^2\mathrm{M}}{d\nu^2}-2\nu\frac{d\mathrm{M}}{d\nu}+\mathrm{M}\left\{(n^2-\tfrac{1}{4})-\frac{\frac{1}{4}-k^2}{1-\nu^2}\right\}=0, \quad (8)$$

which is the equation for associated Legendre functions. The solution of (8) is accordingly an associated Legendre P or Q function, in which the argument is $\nu=\cosh\lambda>1$; the degree $n-\frac{1}{2}$ is half an odd integer; the order is $(\frac{1}{4}-k^2)^{\frac{1}{2}}$. We assume that the boundary of the membrane is the circle defined by $\lambda=c$, a constant, and that the corresponding value of ν is $\alpha=\cosh c$. The point $(b, 0)$ is inside the membrane. At this point $\exp\lambda=0$, so that $\nu=\cosh\lambda$ becomes infinite. We accordingly choose the Q-function in order that the vibrations may have a finite amplitude.

5. One set of nodal lines is given by $\cos n\theta=0$, or $\theta=s\pi/2n$ where s is an integer. These are circles through the points $\pm b, 0$; except for the fundamental of the gravest mode they always include the x-axis, and they meet the periphery of the membrane orthogonally. The other set are more interesting, as they determine the

frequencies of the fundamental and overtones. There being no amplitude at the periphery, we have

$$Q^m_{n-\frac{1}{2}}(\alpha) = 0, \quad . \quad . \quad . \quad . \quad . \quad . \quad . \quad (9)$$

where $$m = (\tfrac{1}{4} - k^2)^{\frac{1}{2}} = (\tfrac{1}{4} - p^2\rho/\mathrm{T}) \quad . \quad . \quad . \quad . \quad (10)$$

Given the degree and the argument, this is a transcendental equation to determine the order, which in turn gives the possible periods.

6. This supplies a physical meaning to the vanishing of the associated Legendre Q-function, viewed as a function of its order. I am not aware that this type of equation has ever been discussed; but it has one interesting consequence. Assuming that there is an infinity of overtones, p is capable of increase without limit; the order m ultimately becomes a pure imaginary. It seems that, given the degree and the argument, there is a finite number of real orders and an infinite number of purely imaginary orders for which the function vanishes.

7. The solution could, of course, be expressed in terms of the hypergeometric function; the change can be made by Barnes's formula. As the result is expressible in numerous forms, I think it preferable to deduce it from (6). Changing the variable to $t = \exp 2\lambda$ we have

$$\frac{d^2\mathrm{L}}{dt^2} + \frac{1}{t}\frac{d\mathrm{L}}{dt} + \frac{1}{t^2}\left\{\frac{k^2 t}{(1-t)^2} - \frac{n^2}{4}\right\}\mathrm{L} = 0. \quad . \quad (11)$$

This is of Fuchsian type with regular singularities at 0, ∞, 1. The respective exponents are $\pm\frac{1}{2}n$, $\pm\frac{1}{2}n$, $\frac{1}{2} \pm (\frac{1}{4} - k^2)^{\frac{1}{2}}$, so that the solution can be expressed as

$$\mathrm{L} = \mathrm{P}\begin{Bmatrix} 0 & \infty & 1 \\ \frac{1}{2}n & \frac{1}{2}n & \frac{1}{2}+m\,t \\ -\frac{1}{2}n & -\frac{1}{2}n & \frac{1}{2}-m \end{Bmatrix}, \quad . \quad . \quad . \quad (12)$$

where m has the same value as formerly. Since two pairs of exponents are equal, the result admits of numerous transformations *. I shall choose one that is indicated by the expression for the size of the membrane.

8. If the periphery of the membrane crosses the x-axis at distances $b+\alpha$, $b-\beta$ from the origin, we have

$$\alpha/(b+\alpha) = \exp c = \beta/(b-\beta). \quad . \quad . \quad . \quad . \quad (13)$$

* Riemann-Weber, ii. p. 53 (1919).

The diameter of the membrane is given by

$$d=\alpha+\beta=-2b \operatorname{cosech} c. \quad . \quad . \quad . \quad . \quad (14)$$

The transform of the P-function is accordingly taken to be

$$\mathrm{P}\left\{\begin{matrix} 0 & \infty & 1 & \\ \frac{1}{2}n & \frac{1}{4}+\frac{1}{2}m & 0 & \dfrac{-4t}{(1-t)^2} \\ -\frac{1}{2}n & \frac{1}{4}-\frac{1}{2}m & \frac{1}{2} & \end{matrix}\right\} . \quad . \quad . \quad (15)$$

As the amplitude of the vibration is to vanish at the periphery, where $t=\exp 2c$, we have

$$\mathrm{P}\left\{\begin{matrix} 0 & \infty & 1 & \\ \frac{1}{2}n & \frac{1}{4}+\frac{1}{2}m & 0 & -\operatorname{cosech}^2 c \\ -\frac{1}{2}n & \frac{1}{4}-\frac{1}{2}m & \frac{1}{2} & \end{matrix}\right\}=0. \quad . \quad (16)$$

Introducing the size of the membrane, and writing the P-function as a hypergeometric function, we have

$$\mathrm{F}(\tfrac{1}{4}+\tfrac{1}{2}n+\tfrac{1}{2}m,\ \tfrac{1}{4}+\tfrac{1}{2}n-\tfrac{1}{2}m\ ;\ 1+n\ ;\ -d^2/4b^2)=0, \quad (17)$$

a transcendental equation from which, given c and n, we have to determine m, and thence the periodic times.

9. It has been pointed out that, as the frequency of the overtones increases, m must ultimately become a pure imaginary. The first two constituents of F are then conjugate imaginaries, so that (17) is an equation in m^2, or p^2, with real coefficients. Viewed as an equation in p^2, it appears on physical grounds that it has an infinite number of positive roots. As an equation in m^2 it has a finite number of positive roots and an infinite number of negative roots.

10. The determination of the vibration periods for a homogeneous membrane depends, of course, on Bessel functions. It is well known, from the work of Olbricht and others *, that the associated Legendre and hypergeometric functions can be made to degenerate into Bessel functions by the confluence of singularities or otherwise. It is well, therefore, that the present solution should be tested by this criterion. The membrane must be placed at a great distance from the y-axis, making b large and exp c small, whilst the diameter

* Watson, ' Bessel Functions,' p. 158.

d remains constant. At the same time, if the density of the membrane is not to become indefinitely small ρ must be a large number of the order b^2. Accordingly we replace ρ by σb^2 ; then, by making b tend to infinity, the problem degenerates into that of a homogeneous membrane of density σ.

11. I now write equation (17) as

$$F_1(\alpha, \beta\,;\ n+1\,;\ -a^2)=0 \quad . \ . \ . \quad (18)$$

with the following meanings :—

$a =$ radius of membrane,

$$\alpha = \left(\frac{1}{4b} + \frac{n}{2b}\right) + \frac{1}{2}\left(\frac{1}{4b^2} - \frac{p^2\sigma}{T}\right)^{\frac{1}{2}},$$

$$\beta = \left(\frac{1}{4b} + \frac{n}{2b}\right) - \frac{1}{2}\left(\frac{1}{4b^2} - \frac{p^2\sigma}{T}\right)^{\frac{1}{2}},$$

and the subscript in F_1 denotes that the factors following α, β in the expansion of F_1 no longer advance by units, as in the hypergeometric series, but by $1/b$. On making b tend to infinity the equation (18) becomes

$$1 - \frac{w^2}{2(2n+2)} + \frac{w^4}{2.4.(2n+2)(2n+4)} - \ldots . = 0 = J_n(w),$$

where $w^2 = p^2a^2\sigma/T$. The vibration periods for a homogeneous membrane are determined from $J_n(ka)=0$, where $k=p/c$ and $c^2=T/\sigma$. Thus $ka = ap(\sigma/T)^{\frac{1}{2}} = w$, so that the solution for the heterogeneous membrane degenerates into the solution for the homogeneous membrane.

12. It is of interest to compare the corresponding periods for two membranes having the same mass and diameter, the one being homogeneous and the other having the mass distributed according to the inverse square law which we have adopted above. It is assumed that the tension is the same in both cases. In default of knowing the zeros of (17) the comparison can be made by substitution. Taking a known period for the homogeneous membrane, substitution in (17) will indicate whether it is above or below the corresponding zero. Suppose that we have a membrane of mass 0·1 gr./cm.^{2} and radius 5 cm., vibrating 100 times per sec. This gives $p=200\pi$, and as the smallest root of $J_0(ka)$ is 2·40483,

the tension requisite for the absence of nodal lines is $T = 1{\cdot}7066 \times 10^5$ dynes/cm.

13. If a membrane of radius a, having its centre at the point $(e, 0)$, be such that its density at any point is ρ/x^2, it is an elementary exercise in integration to show that its mass is $2\pi\rho(e-b)/b$, where $a^2+b^2=e^2$. Since a has been chosen as 5, let us take $b=25$, so that $e=5\sqrt{26}$. This membrane is to have an average mass/cm.$^2 = 0{\cdot}1$ gr., whence we derive $\rho = 63{\cdot}118$ gr. From this it follows that $m^2 = \frac{1}{4} - p^2\rho/T = \frac{1}{4} - 3{\cdot}6985 \times 10^{-4}p^2$. The equation (17) to determine p^2, as n is now zero, can be written

$$0 = 1 - \frac{x}{1{\cdot}1}(\cdot 01) + \frac{x(x+2{\cdot}3)}{(1{\cdot}2)^2}(\cdot 01)^2 - \ldots, \quad (19)$$

where $x = p^2 10^{-4} \times 3{\cdot}6985$.

14. One would expect the physical behaviour of the heterogeneous membrane to be not very different from that of the homogeneous membrane. Interpreted analytically, one would expect the graph of (19) to look rather like the graph of J_0, the roots of both being not very disparate. For the homogeneous membrane we have $p = 200\,\pi$, so that a value of x may be expected somewhere near 146·01. On substituting this value in (19) we have

$$1{\cdot}0000 - 1{\cdot}4601 + 0{\cdot}5549 - 0{\cdot}1024 + 0{\cdot}0120 - 0{\cdot}0010$$
$$= +0{\cdot}0035.$$

The adopted value is somewhat too low ; the frequency is now higher than formerly.

15. In order to ascertain how distant is the actual root I tried the value $x = 147$. This gives the figures

$$1{\cdot}00000 - 1{\cdot}47000 + 0{\cdot}56227 - 0{\cdot}10433 + 0{\cdot}01232$$
$$- 0{\cdot}00108 + 0{\cdot}00007 = -0{\cdot}00075.$$

The new value is evidently too high ; but between this and the previous value we can give the actual root as approximately 146·82. This is rather surprising. In the heterogeneous membrane the greatest density is about $2\frac{1}{4}$ times the least density, so that the redistribution of matter is distinctly drastic. Yet the proportional change in the frequency from the homogeneous membrane is only $(146{\cdot}82/146{\cdot}01)^{\frac{1}{2}} - 1$, a mere 0·28 per cent.

16. As a matter of curiosity I tried the second root of J_0, 5·52008. For the same homogeneous membrane with the same tension this raises p to 1442·2, suggesting that the corresponding value of x lies in the neighbourhood of 769·32. The substitution of this value in (19) gives not zero but −0·0016, showing that we are somewhat below the true root, as before. It suggests the speculation that all the roots of (19) are somewhat in excess of the corresponding root of J_n.

VIII. *Method of Analogy in the Theory of Structures.* *By* J. Jagn, *Professor of Structural Engineering in the Industrial Institute, formerly the Machine Designing Institute of Leningrad* *.

Short Summary.

It has been shown by Prof. Mohr † that the deflexion curve for a bar may be regarded as the diagram for the bending moments which would be produced by imaginary forces equal in magnitude to the actual bending moments divided by the rigidity of the bar. Prof. Mohr applied this analogy to certain problems in continuous beams and plane frames. Prof. Rabinovitch ‡ used the analogy in the application of the funicular polygon to continuous beams. Prof. Gorbunoff § has applied Mohr's method to a three-dimensional closed contour, consisting of rigidly jointed straight bars loaded with arbitrary forces.

In the present paper the author shows that the study of the deformation of systems of bars can in general be replaced by the study of the equilibrium of imaginary forces. By this means all problems relating to deformations and statically indeterminate forces (viz., in beams, crank-shafts, plane and three-dimensional framed structures and trusses, etc.) can be solved by the use of equations of equilibrium alone. Moreover, the existing

* Communicated by Prof. A. J. S. Pippard, M.B.E., D.Sc., M.Inst.C.E.

† *Zeitsch. des Arch. und Ingen. Ver. zu Hannover*, 1868; 'Der Eisenbau,' 1910, 1911, 1912.

‡ 'Kinematic Method in Structural Statics,' Moscow, 1928.

§ 'Frames amd Trusses' (collection of papers), Moscow, 1933.

methods of solving such problems will be shown to be particular methods of forming the equations of equilibrium for the imaginary forces. The formulæ now in use can be readily deduced. For example, there is no difficulty in forming the well-known equations of three or four moments and the equations for statically indeterminate structures due to Maxwell-Mohr and Gehler (slope-deflexion method).

Once the analogy is accepted the study of deformations can be reduced simply to the question of the rigidity of the bars. When the rigidities of the bars are known the analysis of the deformation can be completely developed by the methods of rational mechanics. The principle of virtual work can be formulated as follows, on the assumption that both the real and the imaginary systems are undeformable:—" The work done by the loads applied to a system of bars which is in equilibrium is equal to zero when the displacements are such that if they were regarded as the internal forces in the unloaded conjugate system * they would satisfy all the conditions of equilibrium."

Application of the principle of virtual work to the imaginary forces leads to a solution in a general form which enables the unknown quantities and the virtual displacements to be chosen in a way which considerably simplifies the solution.

1. *Deduction of the Analogy for a Bar with Arbitrary Form of Axis.*

THE equations of equilibrium for an arbitrary part of a bar included between two specified sections 1 and 2 (fig. 1) can be expressed in vector notation as follows :

$$\vec{V}_2 - \vec{V}_1 + \int_0^S \vec{q}\, ds + \sum_{n=1}^{n=N} \vec{P}_n = 0, \quad \ldots\ldots\ldots \quad (1)$$

$$\vec{M}_2 - \vec{M}_1 + \int_0^S \vec{m}\, ds + \sum_{k=1}^{k=K} \vec{\mu}_k + \int_0^S \left[\vec{q}\,\vec{r}\right] ds + \sum_{n=1}^{n=N} \left[\vec{P}_n \vec{r}_n\right] + \left[\vec{V}_2 r_2\right] = 0, \quad (2)$$

* The conjugate system is explained in section 3.

where $\vec{q}$ denotes the intensity of the distributed forces ;

$\vec{m}$ the intensity of the distributed moments ;

$\vec{P}_n$ the concentrated forces (equal in number to N) ;

$\vec{\mu}^k$ the concentrated moments (equal in number to K) ;

$\vec{V}_1$ and $\vec{V}_2$ the resultant forces at the terminal cross-sections 1 and 2 ;

Fig. 1.

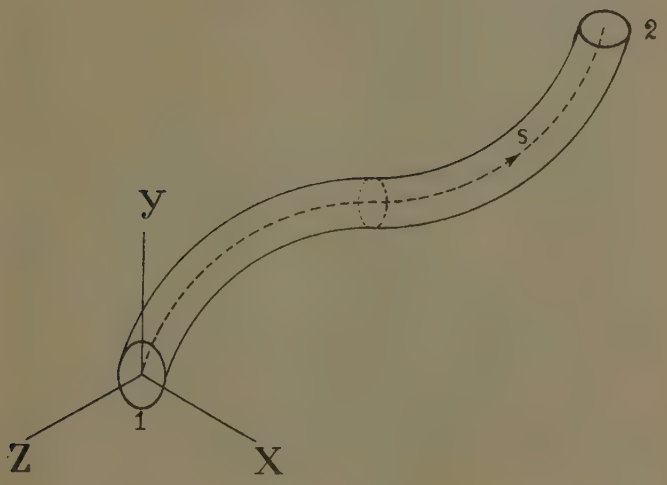

$\vec{M}_1$ and $\vec{M}_2$ the resultant moments at the terminal cross-sections 1 and 2 ;

S the distance along the axis of the bar from the terminal cross-section 1 to the terminal cross-section 2 ;

s the distance along the axis of the bar from the terminal cross-section 1 to any other cross-section, the positive direction being from the cross-section 1 toward the cross-section 2 ;

$\vec{r}$ the radius-vector of the arbitrary point on the axis of the bar from the centre of gravity of section 1.

The square brackets denote vector products. It is assumed that the vectors representing forces are directed parallel to the line of action of the forces, and that the vectors representing moments are directed so that the corresponding couples act clockwise round their positive direction. The directions of $\vec{V}$ and $\vec{M}$ are defined by considering the action of that part having greater value of s upon the remainder *.

The deformation, if small, for the same portion of the bar will satisfy the equations

$$\vec{\phi}_2 = \vec{\phi}_1 + \int_0^S \vec{\theta}\, ds + \sum_{n=1}^{n=N} \vec{\psi}_n, \quad \ldots \quad (1'a)$$

$$\vec{u}_2 = \vec{u}_1 + \int_0^S \vec{\delta}\, ds + \sum_{k=1}^{k=K} \vec{\Delta}_k - \int_0^S \left[\vec{\theta}(\vec{r}_2 - \vec{r})\right] ds - \sum_{n=1}^{n=N} \left[\vec{\psi}_n(\vec{r}_2 - \vec{r}_n)\right] - \left[\vec{\phi}_1 \vec{r}_2\right], \quad (2'a)$$

* The equations corresponding to (1) and (2) for the coordinate x-axis instead of in vector form, are as follows :

$$V_{x_2} - V_{x_1} + \int_0^S q_x\, ds + \sum_{n=1}^{n=N} P_{xn} = 0,$$

$$M_{x_2} - M_{x_1} + \int_0^S m_x\, ds + \sum_{k=1}^{k=K} \mu_{xk} + \int_0^S (q_y z - q_z y)\, ds + \sum_{n=1}^{n=N} (P_{yn} z_n - P_{zn} y_n) + V_{y_2} z_2 - V_{z_2} y_2 = 0.$$

For the components with respect to the x-axis the corresponding equations are :

$$\phi_{x_2} = \phi_{x_1} + \int_0^S \theta_x\, ds + \sum_{n=1}^{n=N} \psi_{xn},$$

$$u_{x_2} = u_{x_1} + \int_0^S \delta_x\, ds + \sum_{k=1}^{k=K} \Delta_{xk} - \int_0^S \{\theta_y(z_2 - z) - \theta_z(y_2 - y)\}\, ds - \sum_{n=1}^{n=N} \{\psi_{yn}(z_2 - z_n) - \psi_{zn}(y_2 - y_n)\} - \{\phi_{y_1} z_2 - \phi_{z_1} y_2\}.$$

where $\vec{\theta}$ denotes the intensity of angular deformation at any point on the bar;

$\vec{\delta}$ the intensity of linear deformation at any point;

$\vec{\psi}_n$ the angular deformation in the hinges which allow rotation (assumed equal in number to N);

$\vec{\Delta}_k$ the linear deformation in the hinges which allow displacements (assumed equal in number to K);

$\vec{u}_1$ and $\vec{u}_2$ displacements of the centres of the cross-sections 1 and 2;

$\vec{\phi}_1$ and $\vec{\phi}_2$ rotations of the cross-sections 1 and 2.

It is assumed that the vectors representing forces are directed parallel to the corresponding displacements, and that the vectors representing rotations are directed so that the corresponding rotations act clockwise round their positive direction.

The quantities $\vec{\theta}$, $\vec{\delta}$, $\vec{\psi}_n$, $\vec{\Delta}_k$ are defined by considering the displacements and rotations of that part having the greater value of s relative to the remainder.

On substituting the value ϕ_1 from (1′a) in (2′a) and rearranging, we obtain the following formulæ:

$$\vec{\phi}_2 - \vec{\phi}_1 - \int_0^{\mathrm{S}} \vec{\theta}\, ds - \sum_{n=1}^{n=\mathrm{N}} \vec{\psi}_n = 0, \quad . \quad . \quad . \quad (1')$$

$$\vec{u}_2 - \vec{u}_1 - \int_0^{\mathrm{S}} \vec{\delta}\, ds - \sum_{k=1}^{k=\mathrm{K}} \vec{\Delta}_k - \int_0^{\mathrm{S}} \left[\vec{\theta}\, \vec{r}\right] ds - \sum_{n=1}^{n=\mathrm{N}} \left[\vec{\psi}_n \vec{r}_n\right] + \left[\vec{\phi}_2 \vec{r}_2\right] = 0. \quad (2'$$

Comparison of the equations of deformation (1′) and (2′) with those of equilibrium (1) and (2) reveals an analogy, in consequence of which any small deformation may be regarded as a system of imaginary forces obeying conditions of equilibrium. If the same notation is used, but with a distinguishing asterisk to denote the imaginary

forces, the full analogy can be obtained by correlating the vectors as follows :—

$$\left.\begin{aligned} \vec{q}^{*} &= -\vec{\theta}\,, & \vec{\mu}_k^{*} &= -\vec{\Delta}^k\,, \\ \vec{m}^{*} &= -\vec{\delta}\,, & \vec{\mathrm{V}}^{*} &= \vec{\phi}\,, \\ \vec{\mathrm{P}}_n^{*} &= -\vec{\psi}_n, & \vec{\mathrm{M}}^{*} &= \vec{u}\,. \end{aligned}\right\} \quad . \quad . \quad . \quad . \quad (3)$$

The bar can therefore be regarded as loaded by imaginary distributed forces and moments of intensities equal to the angular and linear deformations of the elements of the bar respectively, and also by imaginary concentrated forces and concentrated moments equal to the angular and linear deformation at the hinges in the bar.

These imaginary forces and moments must be taken opposite in sign to the corresponding real deformations. When the bar is so loaded the internal forces and moments at any cross-section will be equal both in value and sign to the rotation $\vec{\phi}$ and displacements $\vec{u}$ at that cross-section. Now the quantities $\vec{\theta}$ and $\vec{\delta}$ can be expressed as functions of the real forces. In the case of elastic deformation obeying Hooke's law, provided that the bar consists of straight or only slightly curved portions, the following equations can be obtained in the directions of the principal axes :—

$$\left.\begin{aligned} q_x^{*} &= -\theta_x = -\frac{\mathrm{M}_x}{\mathrm{B}_x}, & m_x^{*} &= -\delta_x = -\frac{\mathrm{V}_x}{\mathrm{A}_x}, \\ q_y^{*} &= -\theta_y = -\frac{\mathrm{M}_y}{\mathrm{B}_y}, & m_y^{*} &= -\delta_y = -\frac{\mathrm{V}_y}{\mathrm{A}_y}, \\ q_z^{*} &= -\theta_z = -\frac{\mathrm{M}_z}{\mathrm{B}_z}, & m_z^{*} &= -\delta_z = -\frac{\mathrm{V}_z}{\mathrm{A}_z}, \end{aligned}\right\} \quad . \quad (4)$$

where B_x, B_y, B_z, A_x, A_y, A_z are the corresponding rigidities of the bars. (If the x-axis coincides with the tangent to the axis of the bar, B_x is the torsional rigidity, B_y and B_z the flexural rigidities, A_x the tensional rigidity and A_y and A_z the transverse rigidities.)

In the case of temperature variation corresponding terms expressing the influence of temperature should be added. Assuming a constant change of temperature over

the whole volume of the bar only the value of δ_x will be affected. The modified equation in (4) will be

$$m_x^* = -\delta_x = -\frac{V_x}{A_x} - \alpha l^0. \quad . \quad . \quad . \quad . \quad (4')$$

Now the imaginary concentrated forces and moments, which represent real rotations and displacements in the hinges, and also the imaginary forces and moments applied to the ends, which represent real rotations and displacements of the terminal cross-sections, remain unknown quantities which are to be determined from the conditions of equilibrium for the imaginary forces.

These imaginary forces and moments can therefore be regarded as reactions and moments corresponding to imaginary restraints. Consequently every hinge in the real bar or at its terminals transforms into a corresponding imaginary restraint. *Vice versa* all restraints in the real bar transform into corresponding imaginary hinges, because at these cross-sections the corresponding imaginary component forces and moments must be equal to zero. A change in the construction of the bar must therefore be assumed as follows :—All real hinges allowing rotation about an axis become imaginary restraints preventing displacement along the same axis, while all real hinges allowing displacement along an axis become imaginary restraints preventing rotation about the same axis, and *vice versa*. For example, a spherical hinge, permitting relative rotation of the parts of the bar round every axis, becomes a support, preventing linear displacement along any axis ; while a bearing support, allowing only rotation about its own axis, becomes a hinge which permits relative rotations and displacements of the parts of the bar in all directions except the relative displacement along the axis of the bearing. A free end transforms into a rigidly built-in end, and a rigidly built-in end becomes entirely free.

It is easy to show that if the bar has in reality only the essential restraints, the reactions at which can be found from the equations of static equilibrium alone, it transforms into an imaginary bar whose imaginary reactions can be found simply from the equations of equilibrium for the imaginary forces. In the case of redundant restraints in the real bar the imaginary bar will have supplementary hinges, *i. e.*, supplementary degrees of

freedom necessary to determine all redundant reactions in the real bar.

The equations of equilibrium for the real bar, together with the equations of equilibrium for the imaginary bar, are therefore always sufficient for the solution of the problem.

If the real bar has any elastic restraints which permit restricted displacements or rotations the hinges corresponding to these restraints cannot be shown on the imaginary bar, because at these sections the imaginary component internal forces and moments will not be equal to zero. The necessary supplementary equations in this case can be deduced from the relation between the real reactions in the elastic fastenings and the components of the imaginary internal forces at the sections considered.

2. *Generalization of the Analogy for a System of Bars.*

For every bar included between two joints it is obvious that the analogy remains the same as that described above, but that the imaginary forces applied to the terminals depend on the deformation of other bars in the system. If the attachment of one end of the bar to the joint is rigid the components of the imaginary forces at the terminal section will be equal to the corresponding displacements and rotations of the joint, but if there are hinges in any of the attachments the respective components of the imaginary forces will differ from the corresponding displacements and rotations of the joint.

The end conditions must therefore be the equality of those component imaginary forces which represent displacements of the ends of the bars at the joint which according to the construction of the joint must all be equal.

If the joint does not allow different displacements at the ends of K bars along an axis, say the x-axis, the conditions will be as follows :

$$M^*_{x1}=M^*_{x2}=M^*_{x3}=\ldots=M^*_{xk}. \quad . \quad . \quad . \quad . \quad (5)$$

If the joint does not allow different rotations at the ends of k bars round an axis, say the x-axis, the conditions will take the form :

$$V^*_{x1}=V^*_{x2}=V^*_{x3}=\ldots=V^*_{xk}. \quad . \quad . \quad . \quad . \quad (5')$$

These identities for the imaginary forces bear the same relation to the imaginary forces as the equations of equilibrium to the actual forces applied to the joints. It is these identities which the author terms " the imaginary equations of equilibrium for the joints." It can easily be shown that the complete set of equations comprising the real and imaginary equations of equilibrium for the joints, together with the equations of equilibrium for the real and imaginary forces applied to the bars, is sufficient to solve the problem, *i. e.*, to find all the components of the real and imaginary internal forces, and therefore to determine all statically indeterminate real forces and all the components of deformation.

3. *Application of the Principle of Virtual Work.*

Since the solution of all problems relating to elastic systems of bars can be obtained from the equations of statics only, the most general form for the equations may be deduced by the application of the principle of virtual work. The analogy makes it possible to set out the principle of virtual work in such a way that both systems—the real and the imaginary—can be considered as absolutely undeformable. Let the virtual work done by the imaginary forces be defined by taking every bar in the system as a rigid body. If a bar is separated from the joints, and the corresponding imaginary reactions $\vec{V}_1^*$, $\vec{V}_2^*$, $\vec{M}_1^*$, $\vec{M}_2^*$ due to the joints are introduced at the terminals, the equation of virtual work for the bar will be

$$\int_0^s \left(\vec{q}^* \vec{u}^*\right) ds + \int_0^s \left(\vec{m}^* \vec{\phi}^*\right) ds + \left(\vec{V}_2^* \vec{u}_2^*\right) - \left(\vec{V}_1^* \vec{u}_1^*\right) + \left(\vec{M}_2^* \vec{\phi}_2^*\right) - \left(\vec{M}_1^* \vec{\phi}_1^*\right) = 0, \quad (6)$$

where the values u^* and ϕ^* are arbitrary displacements and rotations of the cross-sections of the bar compatible with the condition of non-deformability of the bar and with the construction of the imaginary hinges and supports in the length of the bar. (The round brackets denote scalar product of vectors.) Now it will be seen from the analogy that if an imaginary bar is regarded as a real

bar then the real bar becomes the imaginary bar corresponding to it. It follows that the displacements of the imaginary bar can be considered as the forces at the sections of the real bar. But since it is assumed that the displacements $\vec{u}^*$ and $\vec{\phi}^*$ take place without deformation of the imaginary bar, they must correspond to the forces at the sections of a real bar which is in equilibrium without any external loading (since external loading in the real bar, according to the analogy, corresponds to deformation in the imaginary bar). Let us therefore introduce the notation

$$\vec{u}^* = \vec{\mathrm{M}}, \quad \vec{\phi}^* = \vec{\mathrm{V}},$$

where bars are used to distinguish these real internal forces which correspond to imaginary displacements.

With this new notation equation (6) becomes

$$\int_0^s \left(\vec{q}^*\vec{\mathrm{M}}\right) ds + \int_0^s \left(\vec{m}+\vec{\mathrm{V}}\right) ds + \left(\vec{\mathrm{V}}_2^*\vec{\mathrm{M}}_2\right) - \left(\vec{\mathrm{V}}_1^*\vec{\mathrm{M}}_1\right) + \left(\vec{\mathrm{M}}_2^*\vec{\mathrm{V}}_2\right) - \left(\vec{\mathrm{M}}_1^*\vec{\mathrm{V}}_1\right) = 0. \quad (6')$$

The total virtual work done by the imaginary forces applied to the system will be the sum of expressions (6′) for all the bars:

$$\sum_{\alpha=1}^{\alpha=r} \left\{ \int_0^{s\alpha} \left(\vec{q}_\alpha^*\vec{\mathrm{M}}_\alpha\right) ds + \int_0^{s\alpha} \left(\vec{m}_\alpha^*\vec{\mathrm{V}}_\alpha\right) ds + \left(\vec{\mathrm{V}}_{2\alpha}^*\vec{\mathrm{M}}_{2\alpha}\right) - \left(\vec{\mathrm{V}}_{1\alpha}^*\vec{\mathrm{M}}_{1\alpha}\right) + \left(\vec{\mathrm{M}}_{2\alpha}^*\vec{\mathrm{V}}_{2\alpha}\right) - \left(\vec{\mathrm{M}}_{1\alpha}^*\vec{\mathrm{V}}_{1\alpha}\right) = 0, \quad (7)$$

where r is the number of bars in the system.

In order to eliminate the imaginary reactions due to the joints $\left(\vec{\mathrm{V}}_{1\alpha}^*, \vec{\mathrm{V}}_{2\alpha}^*, \vec{\mathrm{M}}_{1\alpha}^*, \vec{\mathrm{M}}_{2\alpha}^*\right)$ it is necessary to subject the imaginary displacements $\left(\vec{\mathrm{V}}_{1\alpha}, \vec{\mathrm{V}}_{2\alpha}, \vec{\mathrm{M}}_{1\alpha}, \vec{\mathrm{M}}_{2\alpha}\right)$ to corresponding supplementary conditions.

The scalar products

$$\left(\vec{\mathrm{V}}_{2\alpha}^*\vec{\mathrm{M}}_{2\alpha}\right), \quad -\left(\vec{\mathrm{V}}_{1\alpha}^*\vec{\mathrm{M}}_{1\alpha}\right), \quad \left(\vec{\mathrm{M}}_{2\alpha}^*\vec{\mathrm{V}}_{2\alpha}\right), \quad -\left(\vec{\mathrm{M}}_{1\alpha}^*\vec{\mathrm{V}}_{1\alpha}\right),$$

representing the work of the reactions $\vec{\mathrm{V}}_{2\alpha}^*$, $\vec{\mathrm{V}}_{1\alpha}^*$, $\vec{\mathrm{M}}_{2\alpha}^*$, $\vec{\mathrm{M}}_{1\alpha}^*$ in the virtual displacements $\vec{\mathrm{M}}_{2\alpha}$, $\vec{\mathrm{M}}_{1\alpha}$, $\vec{\mathrm{V}}_{2\alpha}$, $\vec{\mathrm{V}}_{1\alpha}$, can be

interpreted as the work done by the real forces $\vec{M}_{2\alpha}$, $\vec{M}_{1\alpha}$, $\vec{V}_{2\alpha}$, $\vec{V}_{1\alpha}$ in the displacements $\vec{V}^*_{2\alpha}$, $\vec{V}^*_{1\alpha}$, $\vec{M}^*_{2\alpha}$, $\vec{M}^*_{1\alpha}$. If the latter are possible displacements of the cross-sections at the joints the work done by the real forces applied to these cross-sections will be zero, provided that the forces satisfy the conditions of equilibrium for the real joints. Hence the values $\vec{M}_{2\alpha}$, $\vec{M}_{1\alpha}$, $\vec{V}_{2\alpha}$, $\vec{V}_{1\alpha}$ must be governed by the following equations for every joint :—

$$\Sigma\left(\pm\vec{V}\right) = 0, \qquad \Sigma\left(\pm\vec{M}\right) = 0. \quad . \quad . \quad . \quad (8)$$

In these equations the signs will be different according as the axes s of the bars are directed outward from or inward toward the joint.

We can now state that the virtual displacements compatible with the imaginary joints in the system are those which satisfy the conditions of equilibrium for the real internal forces in the absence of real external applied loads—that is to say, we must select for our imaginary virtual displacements an arbitrary set of real internal forces compatible with no external loads being applied to the system. This statement is the exact counterpart of that for real forces. In fact, the work done by the real loads applied to the system is equal to zero if the virtual displacements do not produce breaking or deformation in the system: but according to the analogy these displacements may be represented by imaginary internal forces which are compatible with no imaginary external loads being applied to the system.

The explanation given above enables us to make the following general formulation of the principle of virtual work both for the real and imaginary systems (which we may term conjugate to one another):—"The work done by the loads applied to a system of bars which is in equilibrium is equal to zero when the displacements are such that if they were assumed as the internal forces in the unloaded conjugate system they would satisfy all the conditions for its equilibrium."

When the imaginary virtual displacements are chosen as explained above, equation (7) takes the form

$$\sum_{\alpha=1}^{\alpha=r}\left\{\int_0^{S_\alpha}\left(\vec{q}^*_\alpha\,\vec{M}_\alpha\right)ds + \int_0^{S_\alpha}\left(\vec{m}^*_\alpha\,\vec{V}_\alpha\right)ds\right\} = 0. \quad . \quad (9)$$

If we note that the imaginary forces $\vec{q}^*_\alpha$ and $\vec{m}^*_\alpha$ represent the deformation of the elements of the bar it is easy to show that equation (9) is the same as that used by Mohr in the solution of statically indeterminate problems; but Mohr considers $\vec{q}^*_\alpha$ and $\vec{m}^*_\alpha$ as the possible displacements and the values $\vec{M}_\alpha$ and $\vec{V}_\alpha$ as the forces which produce the work. We have obtained this equation from the opposite standpoint.

In the usual application of Mohr's equation it is assumed that the values $\vec{M}_\alpha$ and $\vec{V}_\alpha$ are equal to the internal forces when one of the unknown component forces is unity. From our standpoint they are arbitrary internal forces possible in the unloaded real system.

4. *Some Applications of the Analogy based on the Principle of Virtual Work.*

The writer does not intend to pay much attention to continuous beams for which the analogy affords a very simple method of treatment. The analogy simplifies considerably the solution for crank-shafts, and the solution for crank-shafts with arbitrary shape of throws can easily be obtained in the same way. In the case of crank-shafts with throws either in one plane or in two perpendicular planes the application of the principle of virtual work to the imaginary forces avoids the solution of joint equations.

The principle of virtual work done by the imaginary forces is also very useful in the application to framed structures. One method is to consider a series of closed polygons. If the axes s for all bars in the polygon have the same direction round the contour the virtual displacements of the polygon (plane or three-dimensional), when it moves as a whole as a free rigid body, will satisfy the conditions for the imaginary joints (equation (8)), and consequently the imaginary loads applied to the polygon must be in equilibrium. By assuming different virtual displacements for one or for several polygons in the framed structure more or less simple equations of equilibrium are obtained for the imaginary forces,

including the so-called statically indeterminate quantities. These equations give the solution to the problem.

The proposed method is also very useful in verifying the results obtained by other methods. When the diagrams for the bending moments, torque moment, and also tensile and transverse forces (if the latter are taken into account in the definition of imaginary forces) are obtained these diagrams can be easily verified by means of the conditions of equilibrium for the imaginary forces (defined by formula (4)) applied to every closed polygon.

The analogy also affords a simple method for determining the actual displacements which are necessary in

Fig. 2.

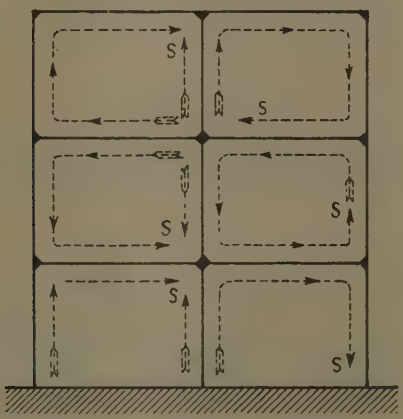

the solution of Mohr's equations in the canonical form. Let us illustrate this by an example. In a plane frame represented in fig. 2 the redundant restraints are eliminated by the knowledge of certain sections of a corresponding number of bars.

A transverse force equal to unity is assumed in the cross-section *a*. The displacements at the cross-section indicated and at other points are to be determined. Neglecting the influence of tensile and transverse forces on the deformation, let us consider only the effect of bending moment. Fig. 3 shows the bending moment diagram divided by the corresponding rigidities of the bars (the

Fig. 3.

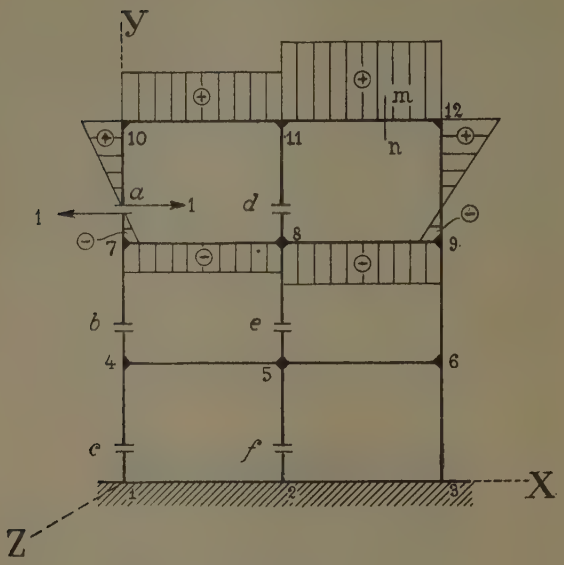
y
m
12
10
11
n
a
1
1
d
7
8
9
b
e
4
5
6
c
f
1
2
3
X
Z

Fig. 4.

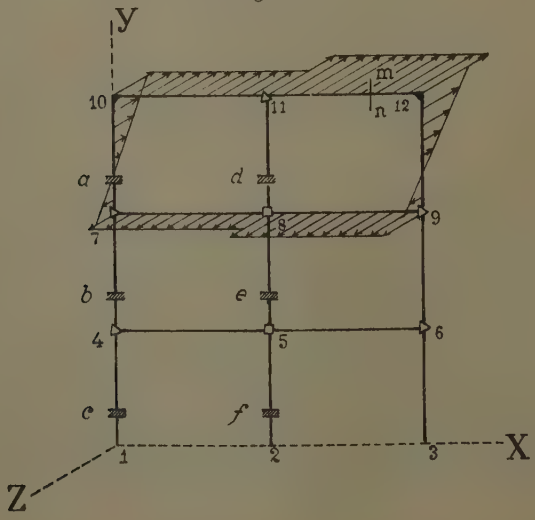
y
m
10
11
n
12
a
d
7
8
9
b
e
4
5
6
c
f
1
2
3
X
Z

rigidity of all the bars being assumed different). This diagram will also represent the imaginary forces directed parallel to the z-axis, in the negative direction if the bending moment is positive, which must be the case when it acts clockwise about the part on the positive side of the axis s. The directions of the axes s are shown in fig. 2. The imaginary structure with its loading is shown in fig. 4. Free ends become built in, and *vice versa*. Instead of joints little polygons are shown, denoting that the conditions for the imaginary joints allow displacements which obey the conditions of a closed polygon (conditions of equilibrium).

The displacements (in the generalized sense) at the six sections indicated can be obtained by considering separately the imaginary forces applied to the corresponding

Fig. 5.

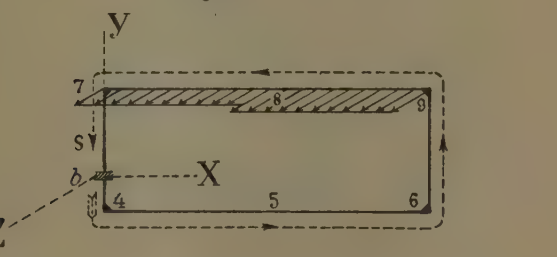

closed polygons. For example, to find the displacements at b it is necessary to consider the imaginary forces applied to the polygon 4–5–6–9–8–7–4 (fig. 5). The reactions at the imaginary restraints at b produced by the imaginary forces applied to the polygon will be equal to the relative displacements of the ends separated by the cross-section b in the real system. (The condition that the axes s have the same direction round the polygon must be observed.) The reacting moments M_x^* and M_y^* at the restraint will be equal to the relative displacements along the x- and y-axes, and the force V_z^* will be equal to the relative angle of rotation about the z-axis. By their sign they will determine the displacements of the end for which s is directed outwards relative to that for which s is directed inwards. The relative displacements at sections a, d and e can be found in the

same way by considering the corresponding closed polygons (figs. 6, 7, and 8). The displacements at the cross-sections c and f will be zero, since the corresponding polygons have no imaginary loads.

Fig. 6.

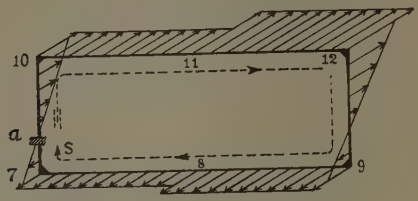

Fig. 7.

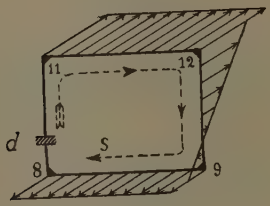

Fig. 8.

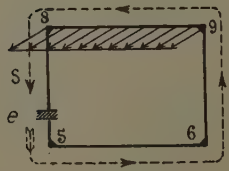

The absolute displacements at any arbitrary cross-section of a bar can be determined by considering the imaginary forces applied to the polygon between this cross-section and one of the imaginary free ends; for instance, the displacements of the cross-section mn will be equal to the components M_x^*, M_y^*, V_z^* for this cross-section, due to the imaginary forces applied to the polygon 3–6–9–12–mn (fig. 9).

In this case also, when determining the direction of the imaginary forces, it is necessary to observe the same direction for the axis s along the polygon (for this reason the directions given in fig. 2 are not suitable, but provided that the bar 6–9 is unloaded there will be no change in the direction of the imaginary forces).

In conclusion, it will be shown how easy it is to obtain the well-known formulæ used in structural statics by the application of the principle of virtual work to the imaginary forces. Let us take as an example the formation of the equation of four moments. Assuming virtual

Fig. 9.

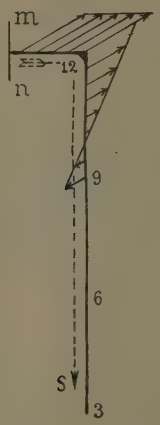

rotations of the bars about the axes y_1 and y_2 respectively (fig. 10), when the ends of the bars joined at O are displaced equally along the z-axis, we obtain directly from the equation of virtual work

$$(M_{z1}+2M'_{z0})l_1B_{z2}+(M_{z2}+2M''_{z0})l_2B_{z1}B_{z1}$$
$$+6\left(\frac{w_1a_1}{l_1}B_{z2}+\frac{w_2b_2}{l_2}B_{z1}\right)$$
$$+6B_{z1}B_{z2}\left\{\frac{M^*_{y_1 1}-M^*_{y_1 0}}{l_1}+\frac{M^*_{y_2 2}-M^*_{y_2 0}}{l_2}\right\}=0, \quad (10)$$

where M_{z1}, M'_{z0}, M''_{z0}, M_{z2} are the four moments;
B_{z1}, B_{z2} the rigidities of the bars;

Fig. 10.

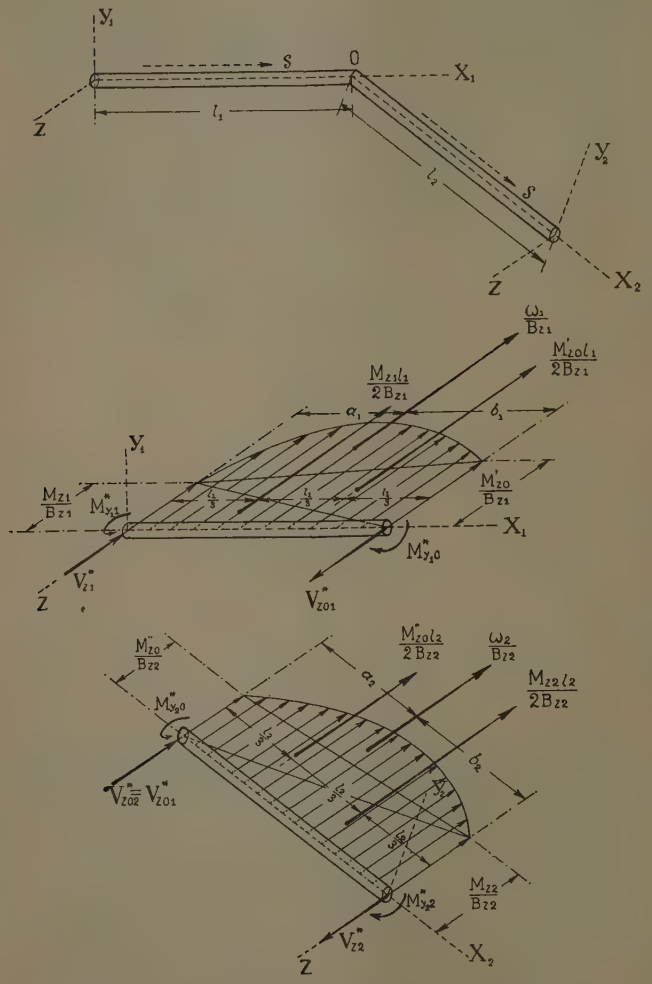

w_1, w_2 the areas of the diagrams for the bending moments determined for the bars as though each were on two-hinged supports;

a_1, b_2 the arms of the resultants $\frac{w_1}{B_{z1}}$ and $\frac{w_2}{B_{z2}}$ of the imaginary forces about the axes y_1 and y_2 respectively ;

$M^*_{y_1 1}, M^*_{y_1 0}, M^*_{y_2 2}, M^*_{y_2 0}$ the imaginary bending moments at the terminals of the bars which are equal to the corresponding displacements of the terminals parallel to the axes y_1 and y_2.

It is readily seen that the equation (10) obtained is the well-known equation of four moments.

5. *The Slope-deflexion Method from the Standpoint of the Analogy.*

When solving a statically indeterminate problem, in many cases it is better to try to eliminate the reactions at the joints in the real system and not the reactions at the joints in the imaginary system. When every bar in the real system has restraints in all directions at both ends the number of real component reactions will be twelve for each bar (six components at every terminal cross-section). Six of these can be found, from the equations of equilibrium for the real forces applied to the bar as function of six others which remain statically indeterminate in the ordinary sense. The latter, by means of six equations of equilibrium for imaginary forces, can be expressed as functions of the imaginary terminal reactions.

If there are hinges in the real system the number of unknown real component reactions will be less, and the supplementary equations of equilibrium for the imaginary forces can be used to eliminate the imaginary reactions at the imaginary supports corresponding to the real hinges. When the bars in the real system have supplementary supports, in addition to the restraints at the ends, the number of real component reactions will be greater, but there will be corresponding imaginary hinges, and consequently supplementary statical equations for the imaginary forces which will again be sufficient to find all statically indeterminate real reactions as functions of the imaginary reactions at the terminals of the bars.

In all cases, therefore, the real component reactions at the terminals of the bars can be expressed as functions of the imaginary terminal reactions by means of the

equations of equilibrium for the real and imaginary forces applied to the bars.

Now the components of the real reactions at the terminals of the bars must satisfy the equations of equilibrium for the joints. On substituting for the real terminal reactions the formulæ expressing them in terms of the imaginary terminal reactions the equations will contain only the latter. The number of equations will obviously be $6k$, where k is the number of joints. It is clear also that the number of the imaginary terminal components is $6k$, since the displacement of every joint is determined by 6 components. These equations will be the same as those used in the slope-deflexion method.

IX. *Ionospheric Height Measurements in Eastern Bengal by the Method of Signal-fading.* *By* B. Sen Gupta, *M.Sc.*, D. N. Chaudhuri, *M.Sc.*, *and* S. R. Khastgir, *D.Sc.* (*Edin.*), *Dacca University* *.

1. *Introduction.*

THE object of this investigation has been to adapt Appleton's signal-fading method to longer distances. In Appleton and Barnett's † experiment the distance had been so adjusted (50 miles) that the ground-wave was very much stronger than the wave reflected from the upper atmosphere. In our experiment the distance was 150 miles, so that the downcoming wave could no longer be considered negligible in comparison with the ground-wave. The method and results of our experiments are given in the paper. The modulated waves from the Calcutta V.U.C. station of the Indian State Broadcasting Company were received at Dacca, and the medium waves were used ($\lambda = 370{\cdot}4$ m.) for the purpose.

2. *Theory of the Method.*

In the receivers where there is cumulative grid rectification, the mean grid current due to the signal

* Communicated by the Authors.

† Appleton and Barnett, 'Nature,' cxv. p. 333 (1925); Proc. Roy. Soc. A, cix. (1925).

received on a vertical aerial during day-time is given by

$$\frac{K^2E_0^2}{4} \cdot \frac{\partial^2 i_g}{\partial v_g^2},$$

where i_g and v_g are the instantaneous values of the grid current and the grid voltage, E_0 the amplitude of the alternating electric force in the ground-wave, and K a constant. Remembering that $v_g = K.E_0 \sin pt$, and representing the grid current grid voltage characteristic by $i_g = \alpha v_g + \beta v_g^2$, the mean grid current due to the signal

$$= \frac{\beta K^2 E_0^2}{2}.$$

Now if R_g be the grid leak resistance, the voltage across the grid leak is given by

$$v = \frac{\beta \cdot K^2 E_0^2}{2} \cdot \frac{R_g}{1 + R_g\left(\frac{\partial i_g}{\partial v_g}\right)}$$

The average anode current in the detector due to the signal is then given by

$$i_v = \frac{m\beta \cdot K^2 E_0^2}{2} \cdot \frac{R_g}{1 + R_g\left(\frac{\partial i_g}{\partial v_g}\right)} = A \cdot E_0^2,$$

m being a constant for the valve.

In case of the loop aerial reception, where the magnetic vector has to be considered, the anode current will be given by

$$i_L = \frac{m'\beta' K'^2 \cdot H_0^2}{2} \cdot \frac{R_g'}{1 + R_g'\left(\frac{\partial i_g}{\partial v_g}\right)'} = A' \cdot H_0^2.$$

The dashed letters in this case correspond to the undashed letters in the other case.

For night reception the average anode currents for the two aerials should be

$$i_v = A[E_0^2 + 4E_1^2 \cos^2 \phi + 4E_0 \cdot E_1 \cdot \cos \phi \cos \theta] \quad \ldots\ldots$$

(Vertical)

and

$$i_L = A'[H_0^2 + 4H^2{}_1 + 4H_0 \cdot H_1 \cos \theta], \quad \ldots\ldots\ldots \quad \text{(Loop)}$$

where E_1 and H_1 are the amplitudes of the electric and magnetic forces in the waves reflected from the ionosphere which arrive at an angle ϕ with the ground (fig. 1). The phase difference θ can be assumed to be varying between wide limits, so that, averaged over a certain interval of time,

$$\overline{i_V} = A[E_0^2 + 4E_1^2 \cos^2 \phi]$$

and

$$\overline{i_L} = A'[H_0^2 + 4H_1^2].$$

The deviation of the signal current at any instant from the average will be in the two cases

$$\partial i_V = 4A \,.\, E_0 \,.\, E_1 \,.\, \cos \phi \,.\, \cos \theta, \quad \partial i_L = 4A' \,.\, H_0 \,.\, H_1 \cos \theta;$$

$$\therefore \quad \frac{\partial i_V}{\partial i_L} = S = \frac{A}{A'} \cdot \frac{E_0 \,.\, E_1}{H_0 \,.\, H_1} \,.\, \cos \phi.$$

Fig. 1.

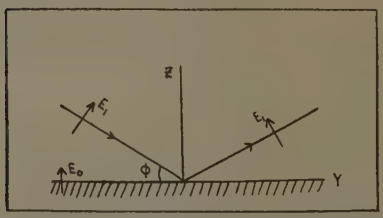

Since in electromagnetic waves the electric and magnetic forces are equal, $E_0 = H_0$ and $E_1 = H_1$.

Hence

$$S = \frac{A}{A'} \,.\, \cos \phi. \quad . \quad . \quad . \quad . \quad . \quad . \quad . \quad (1)$$

In the previous experiments of ionospheric measurements by this method * A and A′ were made equal by making the amplifications of the two sets equal, so that S became equal to $\cos \phi$. *The adjustment for equality is, however, not necessary, especially when the downcoming wave is small compared with that of the ground.* We have seen

$$\overline{i_V} = A(E_0^2 + 4E_1^2 \cos^2 \phi) \text{ and } \overline{i_L} = A'(H_0^2 + 4H_1^2).$$

* Appleton and Barnett, Proc. Roy. Soc. A, cix. (1925); Rakshit, Phil. Mag. xi. (1931).

Therefore the ratio

$$R=\frac{\overline{i_v}}{\overline{i_L}}=\frac{A}{A'}\cdot\frac{E_0^2+4E_1^2\cos^2\phi}{H_0^2+4H_1^2}. \quad . \quad . \quad . \quad . \quad (2)$$

Since $E_0=H_0$ and $E_1=H_1$,

$$R=\frac{A}{A'}\left[1-\frac{4E_1^2\sin^2\phi}{E_0^2+4E_1^2}\right]=\frac{A}{A'}\cdot K,$$

where

$$K=1-\frac{4E_1^2\sin^2\phi}{E^2{}_0+4E_1^2}.$$

Substituting this value of A/A′,

$$S=\frac{\overline{\partial i_v}}{\overline{\partial i_L}}=\frac{R}{K}\cos\phi. \quad . \quad . \quad . \quad . \quad . \quad (3)$$

When $E_0 >> E_1$, K becomes sensibly equal to unity, so that

$$R=\frac{\overline{i_v}}{\overline{i_L}}=\frac{A}{A'} \quad \text{and} \quad S=R\cos\phi. \quad . \quad . \quad . \quad (4)$$

This modification introduces simplification in the experimental technique.

The ratio $\partial i_v/\partial i_L$ for a large number of observations is plotted against the number of times a particular ratio (within a small range) was observed. The maximum of this ratio from the distribution curve gives the most frequent ratio, to which value equations (3) or (4) could be applied to obtain the value of ϕ and the height of the ionosphere.

3. *Experimental Arrangements.*

(a) *Aerial and Earth Systems.*—The vertical aerial, which was 12 metres above the roof, was tuned and magnetically coupled to one of the receiving sets through a high-frequency transformer.

The loop aerial was in the form of a triangle, permanently fixed 7 feet above the floor of the ground in a vertical plane pointing to the transmitter. The two sides of the aerial were 3 metres each, while the base was 4 metres. A shielded tuning condenser was connected in parallel to this aerial, which was connected to the receiving set.

The earth system consisted of a big iron plate buried 20 feet below the ground, where the moisture condition

was such as to make an effective earth under all weather conditions.

(b) *Receiving and Recording Systems.*—The diagrams of the two receiving sets with aerial connexions are given in fig. 2. The two sets were exactly of similar components—*i. e.*, the coils, condensers, etc. in the two sets were of the same value and same make. A Wheatstone bridge circuit was built up to balance the no-signal anode current of the detector valve. A separate H.T. battery was employed in the detector stage. Two similar reflecting moving coil galvanometers were used

Fig. 2.

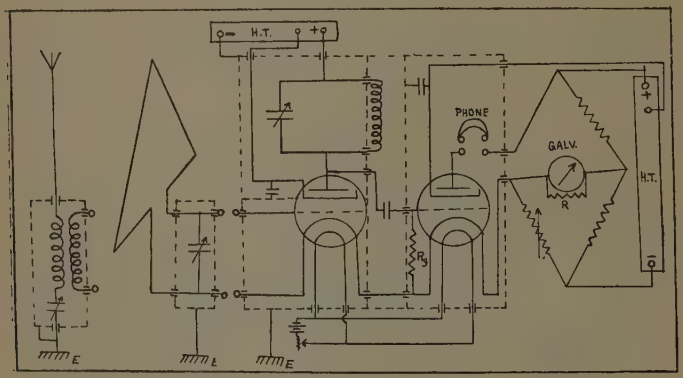

in the bridge arrangement for the two sets. Lamp and scale arrangement was used for taking galvanometer readings. The two receiving arrangements were permanently placed in two corners of the same room. The aerials were 12 feet apart, and tests were made to ascertain that there was no coupling between them. All arrangements were separately shielded in tin-lined boxes.

(c) *Experimental Procedure.*—Balancing the no-signal currents in the anode circuits of the two sets with the aerials off, readings were taken every half a minute with the aerial on. Two synchronized stop-watches were used by two observers for recording galvanometer

deflexions simultaneously, adopting ear-and-eye method. Readings were generally continued for 20 to 40 minutes.

(d) *Method of Calculations.*—From the data thus obtained, two "fading" curves, one for each aerial, were drawn. Fig 3 shows a typical case. From each pair of simultaneous observations the ratio of deviation of the deflexion at any instant in the galvanometer for the vertical aerial from the average deflexion during the whole period of observations to the corresponding deviation in the galvanometer for the loop aerial was

Fig. 3.

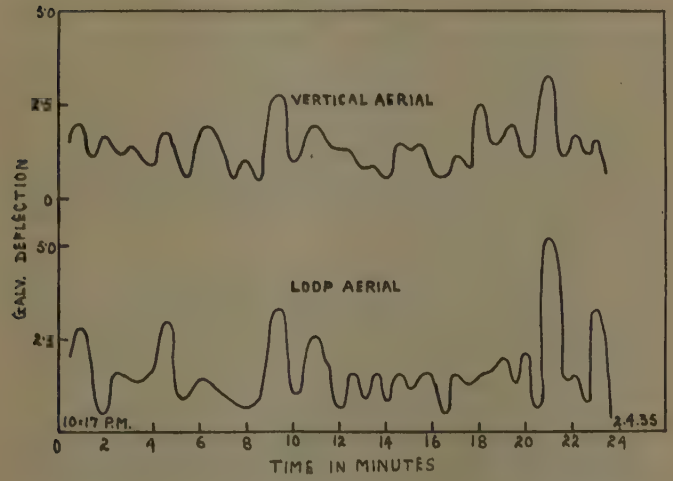

determined. The values of the glancing angle was obtained by

$$\frac{S}{R} = \cos \phi.$$

With all such values of cosine ϕ a distribution curve was drawn for each set of observations, and the most probable value of cosine ϕ was determined.

The glancing angle thus calculated needed a correction. Since in our investigation the amplitude of the down-coming waves was by no means negligible in comparison

with that of the ground-wave, the true angle would be given by the formula (3), viz.,

$$\frac{S}{R} = \frac{\cos\phi}{K}.$$

Hence the true glancing angle ϕ correcting the previous angle ϕ_u would be given by

$$\cos\phi = K\cos\phi_u, \quad \ldots\ldots \quad (5)$$

where $$K = 1 - \frac{4E_1^2\sin^2\phi}{E_0^2 + 4E_1^2}.$$

Putting $E_0 = n \cdot E_1$, $(n > 1)$ the exact value of the glancing angle would then be obtained from

$$\frac{4\cos\phi_u}{n^2+4} \cdot \cos^2\phi - \cos\phi + \frac{n^2}{n^2+4}\cos\phi_u = 0 \ldots \quad (6)$$

We have sufficient experimental evidence * to suppose that the amplitude of the wave deviated from the E-layer is about a third of the amplitude of the ground-wave, so that $\frac{E_1}{E_0} = \frac{1}{3}$ or $n = 3$.

Applying this correction to the most probable value of $\cos\phi_u$ previously determined, the effective height of the E-layer was calculated.

* It is possible to make an estimate of the ratio $\frac{E_1}{E_0}$ or $\frac{H_1}{H_0}$ from the fading curves (see Appleton and Ratcliffe, Proc. Roy. Soc. A, cxxviii. (1930).) If we assume complete *phase-fading*, i. e., if the signal variations are due to changes in the phase-angle θ, while the amplitude of the downcoming wave remains constant, we have

$$\frac{H_1}{H_0} = \frac{1}{2} \cdot \frac{H_{max.} - H_{min.}}{H_{max.} + H_{min.}}$$

for the loop-aerial observations, and

$$\frac{E_1}{E_0} = \frac{1}{2\cos\phi} \cdot \frac{E_{max.} - E_{min.}}{E_{max.} + E_{min.}}$$

for the vertical aerial observations.

Thus choosing only those values of the signal maxima and minima for which the increase above the mean value is equal to the decrease below the mean, an approximate estimate of the required ratio can be obtained. Our estimate is based on a statistical study of a large number of fading curves which is being published elsewhere.

4. *Experimental Results.*

I. *Evidence of Multiple Reflexions at the* E-*layer.*— There have been altogether sixteen sets of observations

Fig. 4.

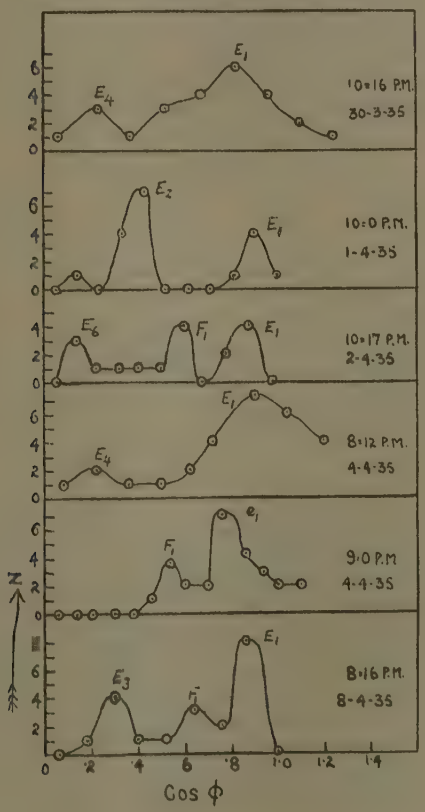

taken at night between 7.30 and 10.30 P.M. from the 23rd March to the 8th April, 1935.

The distribution curves for all the sixteen sets generally show two or more peaks. Most of the peaks can be explained as due to the reception of the E_1, E_2, E_3, and

E_4-rays *. In one case only has there been indication of the E_6-ray. The mean of all the values obtained for the effective height of the E-layer is 106 km. In many cases the height is decidedly greater than this value. The mean of such higher values, viz., 137 km., corresponds to what is called the intermediate *e*-layer. The results indicate that the E-layer may wander between these two limits. Such higher values have been obtained at Allahabad by the group retardation method by Toshniwal and Pant † *during the hours of night.* Some typical distribution curves are shown in fig. 4.

TABLE I.

Date.	Time (Dacca time).	F-layer height (in km.).
	P.M.	
23.3.35	10.19	190
1.4.35	10.20	224
2.4.35	8.45	280
	10.17	184
3.4.35	7.45	188
4.4.35	9.0	234
8.4.35	8.16	194

II. *Indication of the* F_1*-ray.*—Some of the peaks in the distribution curve cannot, however, be explained by the multiple reflexion hypothesis. There are altogether seven cases out of sixteen where there is strong suggestion of penetration of the E-layer by the upgoing wireless waves. If we assume such penetration, the reception of the F_1-ray would explain these results. The effective heights calculated on this idea are given in Table I.

According to the accepted theories of wireless propagation the penetration of the E-layer by 370 m. waves at such oblique incidence (the distance between Dacca and Calcutta is 240 km.) is not normally expected. Employing the formula $N_0 = \frac{mp^2 \sin^2 \phi}{4\pi e^2}$, where N_0 is

* The E_1-ray means the ray which is once reflected from the E-layer; similarly the E_2 and E_3 are the rays doubly and trebly reflected, the suffix denoting the number of reflexions at the layer.

† Toshniwal and Pant, Proc. Nat. Inst. Sciences, i. no. 2.

the electron density in the layer, ϕ the glancing angle, p the angular frequency, m and e are mass and charge of an electron, we find that to obtain simultaneous reception of the E_1- and F_1-rays, the electron density of the E-layer must be greater than 3×10^3 electrons/cm.^{3} and less than 6×10^3 electrons/cm.^{3}. Ionization measurements by Appleton and Naismith *, by the critical-frequency method, on the other hand, show that the electron density of the E-layer during the hours of night is of the order of 10^4 electrons/cm.^{3}, the minimum having been obtained a few hours before sunrise. Similar ionization measurements in Bengal by Mitra and his students also give the same order of values of the electron density.

The occasional "patchy" nature of the E-layer has been previously reported by Appleton †. Employing the frequency-change method with 400 metres wave over a distance of 240 km., and also over a distance of 120 km., Appleton obtained evidence of simultaneous as well as individual receptions of the E_1- and F_1-rays at midnight and in the small hours of the morning. Taking the longer distance, which is exactly equal to the Calcutta–Dacca distance, we find on calculation that the electron density should be greater than $2{\cdot}6 \times 10^3$ electrons/cm.^{3}, but less than $4{\cdot}6 \times 10^3$ electrons/cm.^{3} for the simultaneous reception of the E_1- and F_1-rays. Following the frequency-change technique, Martyn, Cherry, and Green ‡ also recorded in the early morning the unmistakable effect of the F_1-ray, simultaneous'y with E_1- and e_1-rays in their long distance observations with 212 m. waves over a distance of 700 km. They calculated that the electron density in the E-layer in the morning was greater than $2{\cdot}4 \times 10^3$ electrons per cm.^{3}, and during half the period of observations it was less than $8{\cdot}3 \times 10^3$ electrons/cm.^{3}.

III. *Tabulation of Results.*—The calculated values of the layer heights, with the dates and times of observations, are given in Table II.

In calculating the heights of the layers from the

* Appleton and Naismith, Proc. Roy. Soc. A, cxxxvii. (1932).

† Appleton, Proc. Roy. Soc. A, cxxvi. (1929).

‡ Martyn, Cherry, and Green. Proc. Phys. Soc. xlvii. pt. ii. no. 259 (March 1935).

formula (3) it is necessary to know the value of the ratio E_1/E_0 of the vertical electrical forces produced by the downcoming and the ground-waves. From a statistical study of the signal-fading observations, this ratio has been found to be about 1/3. Employing the formula given by Appleton and Barnett *,

$$\frac{E_1}{E_0} = 2\rho \cdot \cos^3 \phi \cdot e^{\frac{\alpha x}{\sqrt{\lambda}}},$$

TABLE II.

Date.	Time (Dacca time).	Layer heights (in km.). E.	e.	F.
	P.M.			
23.3.35	10.19	87 (E_1) / 74 (E_4)	—	190 (F_1)
30.3.35	10.16	122 (E_1) / 87 (E_4)	—	—
1.4.35	10.0	89 (E_1) / 109 (E_3)	—	—
	10.20	—	138 (e_1)	224 (F_1)
2.4.35	8.45	—	125 (e_1)	280 (F_1)
	10.0	—	139 (e_1)	—
	10.17	98 (E_1) / 117 (E_6)	—	184 (F_1)
3.4.35	7·45	91 (E_1) / 108 (E_4)	—	188 (F_1)
	9.46	112 (E_1) / 85 (E_3)	—	—
	10.20	107 (E_1)	146 (e_1)	—
4.4.35	8.12	91 (E_1) / 108 (E_4)	—	—
	9.0	—	120 (e_1)	234 (F_1)
	10.0	88 (E_1)	142 (e_1) / 145 (e_2)	—
8.4.35	8.16	106 (E_1) / 106 (E_4)	—	194 (F_1)
	9.25	122 (E_1)	140 (e_1)	—
	10.10	122 (E_1) / 92 (E_4)	—	—

where ρ is the reflexion coefficient of the layer, x distance between the transmitter and receiver, λ the wave-length, and, putting $\frac{E_1}{E_0} = \cdot 33$ and $\rho = \cdot 15$ (experimental values

* Appleton and Barnett, Proc. Roy. Soc. A, cix. (1925).

obtained by Appleton and Ratcliffe *), the Austin-Cohen coefficient α comes out to be equal to ·0026. This value of α is then used for the evaluation of $\frac{E_1}{E_0}$ for the *e*- and F-layers. For the *e*-layer $\phi=49°$, and we take $\rho=·15$, so that $\frac{E_1}{E_0}=\frac{1}{5}$.

Similarly for the F-layer, $\phi=55°$, and taking Appleton and Ratcliffe's value of ρ equal to ·25, we get

$$\frac{E_1}{E_0}=\frac{1}{5} \text{ nearly.}$$

5. *Summary.*

1. Experiments are described in which simultaneous observations were taken at short time intervals of the intensities of fading of the Calcutta signal ($\lambda=370·4$ m., distance=240 km.) received at Dacca on a loop and a vertical aerial. The theory of a modified form of Appleton and Barnett's method of measuring the angle of incidence of the atmospheric waves has been described. The method claims simplicity in experimental technique.

2. Evidence has been obtained of multiple reflexions at the E-layer. The average height of the E-layer has been found to be 106 km.

3. In some cases the height has been found to be distinctly greater, the mean of such values being 137 km. The result indicates that the E-layer may lie between these limits.

4. There have been strong indications of occasional penetration of the E-layer by the 370 m. waves, and of simultaneous reception of the E_1- and F_1-rays on certain occasions, indicating that the electron density of the E-layer has been on these occasions greater than 3×10^3 and less than 6×10^3 electrons/cm.^{3} during the hours of observations. This " patchy " nature has been previously reported. The average height of the F-layer has been found to be 215 km.

* Appleton and Ratcliffe, Proc. Roy. Soc. A, cxxviii. (1930). The reflexion coefficients of the E- and F-layers were determined with 400 metre waves by fading and frequency-change methods. There was no marked variation of the coefficient with the angle of incidence.

In conclusion, we record our thanks to Prof. S. N. Bose of our University for his interest in this investigation. We thank also Prof. S. K. Mitra, of the Calcutta University, for his helpful criticism and suggestions.

Physics Laboratory, Dacca University,
Sept. 21st, 1935.

X. *Note on the Relation between Internuclear Distance and Group Number for Diatomic Hydrides.* *By* H. C. Corben, *B.A., B.Sc., Queen's College, University of Melbourne, Victoria* *.

IT has been stated by Mecke † that little emphasis should be laid on the approximate linearity of the graph of r_e, the equilibrium internuclear distance for the ground state of a diatomic hydride, against n, the group number, or number of electrons outside closed shells.

On *à priori* grounds, however, it would seem likely that some relation should exist between r_e and n. Krebs has shown ‡ that the linearity is improved if $\log r_e$ be plotted against n, so that

$$r_e = a.e^{bn}. \quad . \quad . \quad . \quad . \quad . \quad . \quad (1)$$

The relation is only approximate, for with the best values of a and b it gives an error of 14 per cent. for LiH. Krebs therefore suggested that the curve should consist of two different parts, for $2 \leqslant n \leqslant 4$ and $5 \leqslant n \leqslant 8$ respectively.

If, however, the product $r_e.n$ be graphed against n an even better straight line is obtained for small n, and for large n the deviations are the same for different molecular periods. Further, the three straight lines obtained for the HK, HL, and HM periods are approximately concurrent at $n=0$. Hence for the molecules of these periods we may write

$$r_e.n = a + b.n - c.(n-1)^3, \quad . \quad . \quad . \quad (2)$$

where the last term becomes important only for $n \geqslant 6$. It is found that $a=1{\cdot}146$, $c=0{\cdot}0058$, and b depends on the molecular period, being 0·980, 1·377, and 1·653 for the HK, HL, and HM periods respectively.

* Communicated by R. C. Johnson, M.A., D.Sc.
† Mecke, *Zeits. f. Phys.* xlii. p. 394 (1927).
‡ Krebs, *Zeits. f. Phys.* lxxxi. p. 776 (1933).

Some of the values of r_e calculated from (2) are compared in the following table with those obtained experimentally*. An asterisk in the table indicates that this value of the internuclear distance is r_0, which usually differs from r_e by less than ·01 Å.U.

Molecule.	$r_{obs.}$ (Å.U.).	$r_{calc.}$	Molecule.	$r_{obs.}$ (Å.U.).	$r_{calc.}$
LiH	1·6	1·550	NaH	1·9	1·947
BeH.....	1·340	1·347	MgH.....	1·73	1·744
BH	1·226	1·227	AlH	1·644	1·624
CH	1·13*	1·135	SiH.....	1·527*	1·532
NH	1·08*	1·050	PH	1·43*	1·447
OH	0·969	0·965	ClH	1·272	1·272
FH.....	0·864	0·875	KH.....	(2·26)	2·223
			CaH	2·02	2·020

Formula (2), then, would appear to apply for all molecules of the HK, HL, or HM periods for which $n<9$. It is therefore possible to predict from it the following values of r_e for molecules for which it has not as yet been measured:

SH : 1.362. ScH : 1·90. TiH : 1·81. VH : 1·72.
CrH : 1·64. MnH : 1·55.

Information concerning the hydrides of the heavier elements is not sufficient to warrant a generalization of it into an empirical relation. There are, however, indications that for such molecules a formula of the type of (2) will still be valid.

29th November, 1935.

XI. *Distributions of Energies of Electrons.* *By* J. S. E. Townsend, *M.A., F.R.S., Wykeham Professor of Physics, Oxford* †.

1. THE experiments on the lateral diffusion of a stream of electrons in a gas which were made at the Electrical Laboratory, Oxford, show that under the action of a uniform electric force Z the electrons attain a steady

* Jevons, 'Report on Band Spectra of Diatomic Molecules.'
† Communicated by the Author.

motion in which the mean energy $\bar{E}$ of the electrons and the mean velocity $\bar{W}$ in the direction of the force depend on the ratio of force to the pressure p of the gas *.

The results of these experiments provide the data required to determine the nature of the collisions of electrons with molecules, and form a basis of theories which have been adopted to explain various phenomena associated with electric discharges. The experiments on the motion of electrons in air † are of special interest in connexion with the propagation of electromagnetic waves in the upper atmosphere.

From the values of the mean energy $\bar{E}$ and the mean velocity $\bar{W}$ which were found experimentally the mean free path l of the electrons and the mean loss of energy λE of the electrons in collisions with molecules have been determined for a large number of gases. The experiments show that the mean free path depends on the kinetic energy E of the electrons, and the coefficient λ is small and in monatomic gases is nearly constant for values of E within certain limits depending on the gas.

It follows immediately from these experiments that there are large inequalities in the energies of the electrons caused by unequal displacements by diffusion in the direction of the electric force; also there are several phenomena connected with uniform luminous columns in discharges which depend on the distribution of the energies of the electrons when the electric force and the pressure of the gas are the same as in the experiments on the determination of the energy $\bar{E}$ and the velocity $\bar{W}$.

A theory of the motion of the electrons has been given by Pidduck, in which the collisions between the electrons and molecules are assumed to be the same as the collisions between elastic spheres. The coefficient of elasticity was deduced from the values of $\bar{E}$ and $\bar{W}$, and it was found that in air the coefficient was only slightly less than that corresponding to perfect elasticity ‡.

He also investigated the distribution of the energies of the electrons when the collisions are perfectly elastic, and gave a general expression for the distribution, taking

* 'Motion of Electrons in Gases' (Clarendon Press, Oxford, 1925).
† Proc. Roy. Soc. A, lxxxi. p. 464 (1908).
‡ F. B. Pidduck, Proc. Roy. Soc. A, lxxxviii. p. 296 (1913).

into consideration all the causes of inequalities. From this expression it is seen that the distribution is the same as the Maxwellian distribution when the electric force is very small and the mean energy of the electrons is almost the same as that of the molecules of gas, but when the electric force is increased the mean energy of the electrons is also increased and the distribution changes. It is easily seen from the general expression for the distribution that the distribution is very different from the Maxwellian distribution when the mean energy of the electrons is two or three times that of the molecules, but it was considered difficult to estimate the distribution when the mean energy of the electrons is very much greater than that of the molecules *.

2. More recently, when the experiments on the conductivity of uniform luminous columns in discharges were in progress, it became of interest, in order to account for the ionization of the gas, to have a simple method of finding the distributions of the energies when the mean energy of the electrons was about fifty or one hundred times that of the molecules †.

In the first paper by the author on the theory of the distribution of the energies of the electrons under these conditions it was pointed out that, in order to obtain an approximate expression for the distribution when the mean energy of the electrons is much greater than that of the molecules of the gas, some of the causes of inequalities may be left out of consideration.

In general the inequalities in the energies of electrons are due to unequal losses and gains of energy in collisions with molecules and to unequal displacements in the direction of the electric force due to diffusion. When the ratio of the electric force Z to the gas pressure p is small, and the mean energy of the electrons is nearly the same as that of the molecules of the gas, the distribution about the mean is caused principally by inequalities in the losses and gains of energy in the collisions due to the motion of the molecules of the gas. As the force increases the mean energy of the electrons increases, and the

* F. B. Pidduck, Proc. Lond. Math. Soc. xv. p. 89 (1915).

† J. S. Townsend and R. H. Donaldson, Phil. Mag. v. p. 178 (Jan. 1928); J. S. Townsend and W. Nethercot, Phil. Mag. vii. p. 600 (March 1929); R. L. Hayman, Phil. Mag. vii. p. 586 (March 1929).

inequalities in the energies due to this cause diminish in importance when superimposed on the inequalities due to the diffusion of the electrons.

Finally, when the force is large and the mean energy of the electrons is large compared with that of the molecules of the gas the inequalities in the energies may be attributed almost entirely to diffusion in the electric field.

A theory of the motion which is obtained under these conditions was given, where it was assumed that an electron lost a small amount of energy λE in a collision, λ being a constant independent of E, also that the mean free path of the electron was independent of E.

An approximate formula for the final distribution of energy in the steady state of motion was given which was independent of the electric force Z, of the pressure p of the gas, and of the constants λ and l, so that the distribution would be the same in all gases *.

About the same time Druyvesteyn † also investigated the distribution of the velocities of electrons moving in a uniform electric field, and gave a formula for the distribution in the steady state when the electrons make perfectly elastic collisions with atoms of the gas, neglecting inequalities in the losses of energy of electrons in collisions due to the motion of the atoms. More recently ‡ he has given another method of deriving the same formula.

3. It is necessary to realize that in experiments the actual distribution differs considerably from that obtained on the hypothesis that λ and l are constants.

One of the properties of gases on which the distribution depends to a large extent is the variation of the mean free path with the energy of the electron. Thus in helium the mean free path increases as the energy increases and approaches the energy required to ionize an atom of the gas, so that in the actual distribution, when the mean energy of the electrons is about 3 or 4 volts, the number of electrons with energies of about 25 volts is much greater than the number given by the theoretical distribution where l and λ are assumed to be constant. The opposite occurs in argon, where the

* Phil. Mag. ix. p. 1145 (June 1930).
† Druyvesteyn, *Physica*, x. p. 61 (1930).
‡ *Physica*, i. p. 10 (1934).

mean free path diminishes as the energy approaches the ionizing potential *.

Many experiments on the radiation from luminous columns of direct current and high frequency discharges also afford evidence as to the energies of the electrons in the collisions which excite the line spectrum and the continuous spectrum †.

There is a general agreement between the results of these experiments and the value of l and λ which have been found experimentally for the different gases, and it becomes of interest to show more exactly how the distribution of the energies may be found by the theory of diffusion when l and λ depend on the energy of the electron.

In this paper I propose to show that the method I gave of determining the distribution of the energies when l and λ were taken to be constants may be used to determine the distributions when l and λ are functions of the energy of the electron, also to show from other simple considerations that in the steady motion under a uniform electric force the energies of the electrons are in all cases widely distributed about a mean energy.

4. The simplest equations of motion of electrons are those which have been obtained by Maxwell's theory of the interdiffusion of gases, and it is by means of these equations that the mean energy E of the electrons has been deduced from the experiments on the lateral diffusion of a stream of electrons in a uniform electric field. Omitting terms of minor importance in the theory of interdiffusion simple equations of motion are obtained which apply either to the motion of ions or of electrons in gases. They are the same as those originally used to deduce the coefficient of diffusion of ions from experiments on the loss of conductivity of a gas moving in a narrow tube ‡.

In this method of investigation the mean velocities

* Phil. Mag. xx. p. 242 (Aug. 1935).

† J. S. Townsend and F. Ll. Jones, Phil. Mag. xi. p. 1148, and xii. p. 815 (1931); J. S. Townsend and M. H. Pakkala, *loc. cit.* xiv. p. 418 (Sept. 1932); P. Johnson, *loc. cit.* xiii. p. 487 (1932); S. P. McCallum, L. Klatzow, and J. E. Keyston, 'Nature,' cxxx. p. 810 (1932); J. E. Keyston, Phil. Mag. xv. p. 1162 (June 1933), and xvi. p. 625 (Sept. 1933).

‡ Phil. Trans. A, cxciii. p. 129 (1899).

of the electrons in the directions of the axes are expressed in terms of the partial pressure P of the electrons and the electric force Z by equations of the form

$$Pw/\overline{K} = -dP/dz + neZ, \quad . \quad . \quad . \quad . \quad (1)$$

where n is the number of electrons in unit volume, e the atomic charge, m the mass of an electron, and mnw the momentum in the direction z of the electrons in unit volume.

Excepting the coefficient $\overline{K}$ the terms in this equation are independent of the distribution of the energies and the lengths of the free paths of the electrons. The partial pressure P is $mn\overline{U}^2/3$, and the mean energy of agitation of the electrons is $m\overline{U}^2/2$, $\overline{U}^2$ being the mean square of the velocity of agitation of the electrons.

In the steady motion of electrons, where the mean energy $m\overline{U}^2/2$ is the same at all points of a stream of electrons *, the term dP/dz may be written as $m\overline{U}^2/3 \times dn/dz$, and equation (1) becomes

$$n\bar{w}/\overline{K} = -dn/dz + 3neZ/m\overline{U}^2. \quad . \quad . \quad . \quad . \quad (2)$$

The principal difference between this equation and the corresponding equation for the motion of ions is that the mean energy $m\overline{U}^2/2$ of the electrons depends on the force Z and may exceed the energy of agitation of the molecules of the gas by a large factor.

The mean velocity $\bar{w}$ is made up of two parts; the one represented by the first term on the right of the equation, $\overline{K}dn/ndz$, is due to diffusion, and the other is the mean velocity $\overline{W}$ due to the action of the electric force. This velocity is given by the equation

$$\overline{W}/\overline{K} = 3Ze/m\overline{U}^2. \quad . \quad . \quad . \quad . \quad . \quad (3)$$

It may be seen that this equation implies a velocity distribution and would not be satisfied if all the electrons had the same kinetic energy.

5. The coefficient of diffusion K for a group of electrons all with the same energy of agitation $m\overline{U}^2/2$ is $l\overline{U}/3$, l being the mean free path of the electrons, but the expression $Zel/m\overline{U}$, which is usually given for the mean velocity W

* Proc. Roy. Soc. A, lxxxi. p. 464 (1908).

of the group due to the electric force, is only an approximation. It differs by a factor 2/3 from the correct value of W, as may be seen by direct calculation when W is small compared with U. In this case the energy gained by an electron in moving under the electric force between two consecutive collisions with molecules of the gas is small compared with the energy $m\mathrm{U}^2/2$, and in order to simplify the calculation the kinetic energy of an electron after a collision is taken to have the constant value $m\mathrm{U}^2/2$.

The velocity W may be found by supposing that each electron traverses a large number C of free paths of lengths $l_1, l_2 \ldots . l_c$ in the same order and approximately in the same time $l\mathrm{C}/\mathrm{U}$, l being the mean free path.

Let u, v, and w be the components in the directions of the axes of coordinates of the velocity U after a collision. Since all directions of motion are equally probable the mean value of each of the velocities u, v, and w for a large number of electrons is zero, and the mean value of w^2 is $\mathrm{U}^2/3$.

The acceleration f of an electron in the direction of the force Z is Ze/m, and the displacements of the electron in the directions of the axes in the time t between two collisions are ut, vt, and $wt+ft^2/2$. It is assumed that the distance $ft^2/2$ is small compared with the free path l, so that the trajectory is only slightly curved and the length l is $(\mathrm{U}^2t^2+wft^3)^{\frac{1}{2}}$. The free path l in terms of t is therefore $\mathrm{U}t+wft^2/2\mathrm{U}$, omitting terms in higher powers of f.

For a first approximation t may be taken to be l/U, but this simplification, which is often adopted, introduces a considerable error in estimating the mean velocity W. To obtain a more correct value of W it is necessary at this stage of the calculation to retain the term in f, and since this term is small compared with l/U the time t to the first power of f is

$$t=l/\mathrm{U}-wfl_1^2/2\mathrm{U}^4. \quad . \quad . \quad . \quad . \quad . \quad (4)$$

The displacement z_1 of the electron in the direction of the force, after traversing a free path l_1 in the time t_1, is therefore given in terms of l_1 by the equation

$$z_1=wl_1/\mathrm{U}-w^2fl_1^2/2\mathrm{U}^4+fl_1^2/2\mathrm{U}^2, \quad . \quad . \quad . \quad (5)$$

the terms in f being the displacement δ_1 due to the electric force.

The mean value of w for a large number of electrons is zero and the mean value of w^2 is $U^2/3$, so that the mean displacement $\bar{\delta}_1$ of a large number of electrons after each has traversed a free path of length l_1 is

$$\bar{\delta}_1 = f l_1^2/3U^2 ; \quad . \quad . \quad . \quad . \quad . \quad . \quad (6)$$

also, since the sum of the squares of a large number C of free paths is $2l^2C$, l being the mean free path *, the mean displacement $\bar{\delta}$ after each electron has traversed the free paths $l_1, l_2 \ldots l_c$ is

$$\bar{\delta} = 2fCl^2/3U^2. \quad . \quad . \quad . \quad . \quad . \quad . \quad (7)$$

Fig. 1.

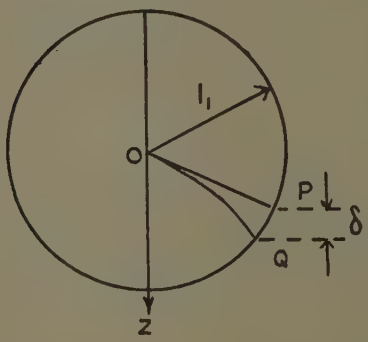

The time required for each electron to traverse the free paths is lC/U, and the mean velocity W in the direction of the force is

$$W = 2Zel/3mU. \quad . \quad . \quad . \quad . \quad . \quad . \quad (8)$$

6. This result, which depends on the mean displacement given by equation (6), may also be obtained by simple geometry.

If a large number of electrons start from the centre of the sphere of radius l_1, fig. 1, the distance through which an electron is deflected by an electric force while it moves from the centre to the surface of the sphere depends on the direction of motion. If θ be the angle between the direction of the force Z and the direction

* 'Electricity in Gases,' p. 83.

of motion OP of an electron at the centre of the sphere, Q the point at which the electron arrives at the surface of the sphere, the displacement PQ is $ft_1^2 \sin\theta/2$, and the displacement δ_1 of the electron in the direction of the force is $ft_1^2 \sin^2\theta/2$, t_1 being approximately l_1/U. Since all directions of motion at the centre of the sphere are equally probable the mean value of $\sin^2\theta$ for a large number of electrons is 2/3, and the mean displacement $\bar{\delta}_1$ is $fl_1^2/3U$, which is the same as in equation (8).

7. Since the coefficient of diffusion of electrons with the same velocity of agitation U is $lU/3$, the ratio W/K is $2Ze/mU^2$, which is two-thirds of the ratio $\bar{W}/\bar{K}$ for electrons in steady motion.

Thus the state of motion in which all the electrons have the same energy is unstable, and as the electrons move through the gas inequalities in the energies are developed, and a final steady state of motion is attained in which the ratio $\bar{W}/\bar{K}$ is $3Ze/m\bar{U}^2$.

Since the mean energy $m\bar{U}^2/2$ has been determined experimentally, it is convenient to express the mean velocity W and the mean coefficient of diffusion $\bar{K}$ in terms of root-mean-square of the velocity of agitation, which is greater than the mean velocity. If $g\bar{U}$ be the mean velocity, the coefficient $\bar{K}$ is $lg\bar{U}/3$, and if $h/\bar{U}$ be the mean of the reciprocals (1/U) of the velocities, the mean velocity $\bar{W}$ is $2Zelh/3m\bar{U}$. The coefficients g and h depend on the distribution of the velocities, and in order to satisfy equation (3) h must be $3g/2$.

For the Maxwellian distribution of velocities the coefficient * g in the expression for $\bar{K}$ is ·92, and of h in the expression for W is $\cdot 92 \times 3/2$, so that this distribution satisfies the condition required for steady motion †.

* J. S. Townsend and V. A. Bailey, Phil. Mag. xliv. p. 1033 (Nov. 1922).

† In the paper on the energies of electrons (Phil. Mag., June 1930) a mistake was made in stating that the coefficient g for a Maxwellian distribution was ·815. This number is the value of the coefficient deduced from Langevin's formulæ for the velocity $\bar{W}$ and the coefficient of diffusion K for ions. In his calculation the Maxwellian distribution was introduced in a particular manner, and his formulæ, which give the values of $\bar{W}$ and $\bar{K}$ for ions, do not apply in so far as the distribution of velocities is concerned to electrons.

8. In the previous investigation of the distribution * the energies were expressed in terms of the mean energy $\bar{E}$ as found experimentally, but from a theoretical point of view it is simpler to adopt a notation which does not involve the mean energy $\bar{E}$ or the mean velocity $\bar{W}$, and to rely on the general results of the experiments, which show that the collisions of electrons with molecules closely resemble the collisions between spheres not necessarily perfectly elastic. The principal difference is that the mean free path of an electron depends on the energy of an electron, but with spheres the mean free path is constant.

In the following investigations the original equations for determining the inequalities in the energies are expressed in terms of the force Z and the constants e and m, so as not to have numerical constants such as g and h, which depend on the distribution of energies.

In this method of finding the distribution of the energies the actual displacements of different groups of electrons are obtained by superimposing the small displacements δ due to the velocity W on the large displacements due to diffusion, as if the two displacements were completely independent. The method therefore applies accurately to cases where the mean velocity $\bar{U}$ is large compared with $\bar{W}$ and the loss of energy in a collision λE is a small fraction of the energy E.

In monatomic gases there is a considerable range of energies in which the coefficient λ is a constant, depending on the gas.

In helium when the mean energy of the electrons is 50 or 100 times that of the molecules of the gas λ is about $2{\cdot}5\times10^{-4}$ and the velocity $\bar{U}$ as found experimentally is about $100\times\bar{W}$. Also in neon and in argon λ is small and U large compared with $\bar{W}$.

In diatomic gases the values of λ are much greater and increase with the energy of the electrons. In hydrogen when the mean energy of electrons is about 50 times that of a molecule of the gas the velocity $\bar{U}$ is about $20\times\bar{W}$ and λ is 9×10^{-3}. In nitrogen when the electrons have the energies 50 times that of a molecule the velocity U is about $17\times\bar{W}$ and λ is 9×10^{-3}. The investigations

* Phil. Mag., June 1930.

in which λ is taken to be very small are therefore of particular interest in connexion with a type of motion of electrons which has been observed in monatomic gases.

9. The displacements of electrons due to diffusion are found by considering the movements of a large number Q_0 of electrons when there is no electric force, and the electrons have the same velocity of agitation U during the motion.

Let the initial positions of the electrons be very near the plane $z=0$, and let $q\,dz$ be the number between the two planes z and $z+dz$ at the time t.

The equation of continuity for q is

$$dq/dt = \mathrm{K}d^2q/dz^2, \quad . \quad . \quad . \quad . \quad . \quad (9)$$

and the solution which satisfies the initial conditions is

$$q = \mathrm{Q}_0(4\pi\mathrm{K}t)^{-\frac{1}{2}}\epsilon^{-z^2/4\mathrm{K}t}. \quad . \quad . \quad . \quad . \quad (10)$$

Instead of considering the distribution about the plane $z=0$ in terms of the time t it is more convenient to consider the distribution in terms of the number of free paths C traversed by each electron ($\mathrm{U}t=l\mathrm{C}$).

If each electron traverses the number of free paths C in the time T, the total distance UT is lC, and the product K . T when expressed in terms of C is l^2C/3. The equation for the distribution about the plane $z=0$ may therefore be written in the form

$$q = \mathrm{Q}_0(4\pi l^2\mathrm{C}/3)^{-\frac{1}{2}}\epsilon^{-3z^2/4l^2\mathrm{C}}. \quad . \quad . \quad . \quad . \quad (11)$$

The values of q after each electron has traversed a given number of free paths are represented by the curves, fig. 2, the ordinates being proportional to q and the abscissæ the values of z/l. Curve 1 gives the distribution after each electron has traversed 100 free paths and curve 2 after 400 free paths.

The number q may also be expressed as a function of a single variable S given in terms of z and C by the equation

$$\mathrm{S}^2 = 3z^2/4l^2\mathrm{C}, \quad . \quad . \quad . \quad . \quad . \quad . \quad (12)$$

and dQ number of electrons in the space between the two planes at distances z and $z+dz$ from the origin is given by the equation

$$d\mathrm{Q} = q\,dz = \mathrm{Q}_0\pi^{-1/2}\epsilon^{-\mathrm{S}^2}\,d\mathrm{S}. \quad . \quad . \quad . \quad . \quad (13)$$

In the notation the displacement z due to diffusion is $Sl\sqrt{4C/3}$, and the number of electrons Q which are displaced to distances greater than z from the plane $z=0$ is obtained in the convenient form

$$Q=Q_0\pi^{-\frac{1}{2}}\int_S^\infty \epsilon^{-s^2}\,ds. \quad . \quad . \quad . \quad . \quad . \quad (14)$$

The number Q corresponding to any value of S is given by the curve, fig. 3, where the ordinates are the values of Q/Q_0 and the abscissæ the values of S.

Fig. 2.

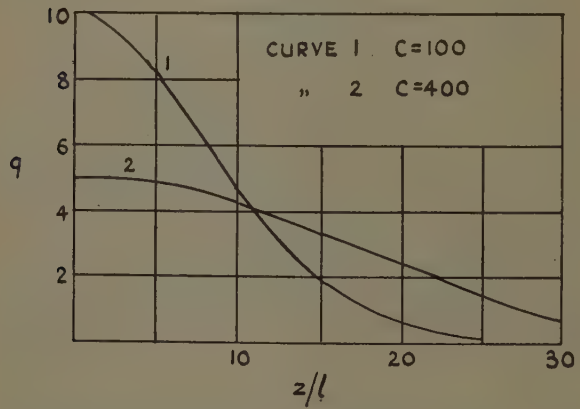

The group dQ, equation (13), will be referred to briefly as the group S or $\dot{S}$ with a suffix to denote a particular value of S.

(More generally, when there is a change in the mean free path of the electron with the distance z due to any cause, the variable S is given in terms of z by the equation

$$\sqrt{4C/3}\;dS=dz/l,$$

and equation (9) becomes

$$4C\;dq/dc=d^2q/dS^2.$$

The solution of this equation becomes $q=q_0\epsilon^{-s^2}$ when c has the value C, which is the same as in equations (13) and (14).)

The displacements z of the electrons due to diffusion, given by the curves, figs. 2 and 3, are independent of the velocities of the electrons. They represent the distances of the electrons from their initial position $z=0$ after each electron has traversed the given number of free paths C when the free paths are straight lines.

In order to find the positions of the electrons when moving under the action of an electric force the displacements δ caused by the slight curvature of the

Fig. 3.

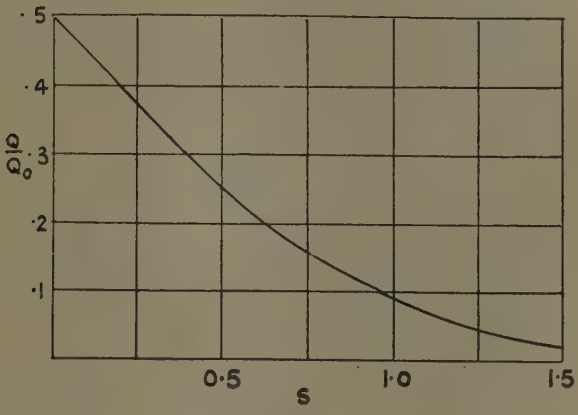

$S=z\sqrt{3/4l^2}C.$

free paths which give rise to the velocity W are added to the displacements z.

10. In general when electrons begin to move with the same kinetic energy E ($mU^2/2$) in a gas under the action of a uniform force, the mean energy of the group after each electron has traversed a small number of free paths is either greater or less than E.

The mean velocity W of the group in the direction of the force is $2Zel/3mU$, and the mean increase in the energy due to the displacement $W\,dt$ in the time dt is $WZe\,dt$. The number of collisions of each electron with molecules in the time dt is $U\,dt/l$, and the mean loss of energy in these collisions is $\lambda EU\,dt/l$.

In general one of these quantities exceeds the other so that the mean energy either increases or diminishes, but for one particular value A of the energy the gain of energy is equal to the loss, and the mean energy remains constant for a short time. This energy is determined by the equation

$$WZel = \lambda EU/l, \quad \text{or} \quad 2Z^2e^2l^2 = 3\lambda E \times mU^2,$$

which gives

$$A = Zel/\sqrt{3\lambda}. \quad . \quad . \quad . \quad . \quad . \quad . \quad (15)$$

Thus the electrons with energies A retain a constant mean energy for a short time, but owing to the motion of agitation one-half of them diffuse in the direction of the electric force and acquire energies greater than A and the remainder diffuse in the opposite directions and their energies become less than A.

The group of electrons $q\,dz$ (equation (10)), which are at the mean distance z from the plane $z=0$ at the time T, has an average velocity z/T in the direction z due to diffusion during the time T. It has already been shown that if the electrons have the same velocity of agitation U throughout the motion the mean position of the group at a time t less than T is at the distance zt/T from the plane $z=0$, so that the mean position moves with uniform velocity z/T during the time T *.

If C be the number of collisions of an electron with molecules during the time T, c the number during the time t, the mean position of the group is at the distance zc/C from the plane $z=0$ when the electrons have traversed the number of free paths c. The mean position zc/C thus expressed in terms of c is independent of the velocity of agitation or of changes in the velocity of agitation as c increases from the value $c=0$ to $c=C$.

11. Let E_1 be the energy of each of the electrons initially at the plane $z=0$, z the displacement due to diffusion of the group S in the direction of the force, and E_2 the mean energy of the electrons in the group after each electron has traversed the number of free paths C. The positions of the electrons in the group S in passing from the initial position $z=0$ to the final position z are represented by the curves, fig. 4. Curves 1 and 2 represent the initial and final positions, and curve 3 the positions after

* Phil. Mag. ix. p. 1145 (June 1930).

each electron has traversed a number of free paths c less than C. At this stage the electrons are distributed symmetrically about a plane d at a distance cz/C from the plane $z=0$.

For small values of C (less than $1/10\lambda$) curve 3 lies close to the plane d, and in the final position (curve 2) all the electrons in the group have almost exactly the same energy E_2. As C increases the distribution about the plane d becomes wider, so that in passing from the initial to the final position the loss of energy in collisions is not exactly the same for each electron in the group. Thus for large values of C of the order $1/\lambda$ there is an appreciable distribution of the energies of the electrons in the group about the mean energy E_2.

Fig. 4.

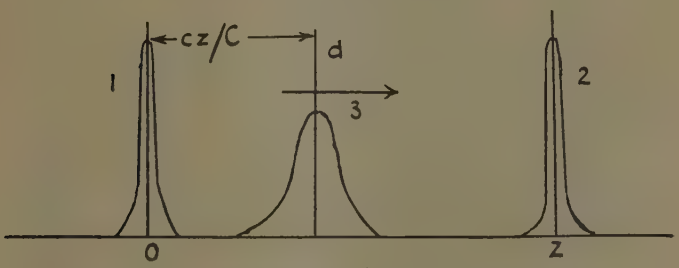

In the following calculations, where C is greater than $1/10\ \lambda$, it will be assumed that all the electrons in a group have approximately the same energy when each electron has traversed the full number of free paths C.

12. Let E be the mean energy of the group S after each electron has traversed the number of free paths c, and the displacement due to diffusion is cz/C, $(z=2Sl\sqrt{C}/3)$.

The increase in the energy due to the increase of this displacement when c increases to $(c+dc)$ is $zeZdc/C$, which may be written in the form $2SA\sqrt{\lambda C}\,.\,dc/C$.

In addition there is an increase in energy due to the displacement Wdt which is $ZeWdt$, where dt is ldc/U. This increase in energy is $2Z^2e^2l^2\,dc/3mU^2$, or $A^2\lambda\,dc/E$.

The loss of energy in the number of collisions dc is $\lambda E dc$. Thus the total increase of energy dE of the electrons in the group S when the number of collisions

of each electron with molecules increases from c to $c+dc$ is given by the equation *

$$dE=(\lambda C(A^2/E-E)+2S\sqrt{\lambda C}\,A)\,dc/C. \quad . \quad . \quad (16)$$

The increase in the energy (E_2-E_1) of any group S is found by integrating from $c=0$ to $c=C$, and the number Q of electrons which acquire energies greater than E_2 is given in terms of S by equation (14) or by the curve, fig. 3.

The integral from $c=0$ to $c=C$ obtained by substituting $(y-1/y)\sqrt{\lambda C}$ for S is

$$y^2 \log (Ay-E_1)/(Ay-E_2)+\log (A+E_1y)/(A+E_2y) = \lambda C(1+y^2), \quad (17)$$

and this equation may be used to calculate E_2.

TABLE I.

S.	5.	1·0.	2.	3.	4.
Q/Q_0	·24	$7{\cdot}8\times10^{-2}$	$2{\cdot}4\times10^{-3}$	$1{\cdot}14\times10^{-5}$	—
$\lambda C=\cdot1$, E_2/A .	1·27	1·57	2·15	2·73	3·35
$\lambda C=\cdot2$, E_2/A .	1·35	1·73	2·53	3·32	4·15
$\lambda C=\cdot4$, E_2/A .	1·44	1·92	2·92	3·94	4·96
$\lambda C=\cdot8$, E_2/A .	1·48	2·01	3·16	4·36	5·6
$\lambda C=1{\cdot}0$, E_2/A.	1·48	2·01	3·17	4·37	5·7

The values of E_2 when the initial energy of the electrons E_1 is equal to A.are given in Table I. for different values of the number λC.

The values of S are given in the first line and the corresponding values of Q/Q_0, equation (14), in the second line of the table.

The values of E_2/A when λC is 1/10 are given in the third line, and represent the energies of the different groups after each electron has traversed 400 free paths in helium (the value of λ for helium being approximately $2{\cdot}5\times10^{-4}$). The groups considered are those which diffuse in the direction of the electric force (S positive), so that the energies E_2 are greater than A.

* Equation (16) is the same as equation (17) in the first paper, Phil. Mag., June 1930.

The rate at which the distribution is extended as C increases is shown by the values of E_2/A for the larger values of C ($\cdot 2/\lambda$, $\cdot 4/\lambda$, $\cdot 8\lambda$, and $1/\lambda$) given in the lower lines of the table.

13. The figures show that a certain proportion of the electrons acquire large energies, even for small values of C. For a group S, containing a number of electrons dQ, the energy E_2 is approximately $(1+2S\sqrt{\lambda C})A$ when the product λC is small, but the rate of increase of E_2 with C diminishes as C increases, and there is very little change in the distribution when C approaches the value $\cdot 8/\lambda$.

The values of E_2/A in the last two lines of the table are almost exactly the same, which shows that a final constant distribution is attained when each electron has traversed a large number of free paths after starting with the energy A. This distribution is independent of λ, C. and Z, and is therefore the same in all gases.

It has already been stated that the energy E_2 is the mean energy of the electrons in the group S, and with values of C of the order $1/\lambda$ there is an appreciable distribution of the energies of the group about the mean energy E_2. For this reason the number of electrons with energies greater than E_2 exceeds the number Q given in the table. Thus the direct method of finding the inequalities of the energies by the solution of equation (16) also gives approximately the final distribution which would be obtained if l and λ were constant, and there were no large losses of energy in the collisions of the electrons with the sides of the envelope or from other causes.

These conditions, however, are not realized in uniform luminous columns of discharges.

The loss of energy by the lateral diffusion of electrons to the surface of the tube and other actions tend to diminish the number of electrons with large energies, and even when the mean energy of the electrons is much less than the energy required to excite radiation the variation of the mean free path with the energy has a considerable effect on the distribution of the energies.

It is impossible to take all these actions into consideration, but the effect of a variation in the mean free path may be found by direct integration of equation (16).

For this purpose it is necessary to make changes in the terms of equation (16) which involve the mean free path.

14. When the mean free path l is a function of the energy $\psi(E)$ the energy A of the group S_0 is the value of E which satisfies the equation

$$E = Ze\psi(E)/\sqrt{3\lambda}.$$

For simplicity l may be assumed to be a linear function of the energy and written in the form $l = a(1+b(E/A-1))$, a being the mean free path of an electron with the energy A.

(In helium, where the mean free path increases with the energy, the coefficient b is about ·2 when the mean energy of the electrons is about 4 volts. In argon, where the mean free path diminishes with the energy, b is negative and is about ·25.)

When a group of electrons S moves from its initial position $Z=0$ to its final position z, as shown in fig. 4, the distance traversed in the direction of the force is $2Sl\sqrt{C}\,dc/C$ when the number of free paths traversed by each electron increases from c to $c+dc$ and the energy acquired by the electrons is $(2S\sqrt{\lambda C}\,Al/a)\,dc/C$. Thus the necessary change in the last term of equation (16) is made by writing Al/a for A. Also in the first term it is necessary to substitute Al/a for A.

With these substitutions the terms have different coefficients, but the number of terms is not changed when l is a linear function of A.

The integral is therefore of the same form as equation (17), and the values of E_2 may be calculated for any value of the coefficient b.

15. If the electrons start from the plane $z=0$ with the energy A ($E_1=A$) the terms with the multiplier λC in the transformed equation (16) may be neglected when λC is very small (less than 1/10), and the energy E_2 of the group after the electrons have traversed the number of free paths is given approximately by the equation

$$E_2 = A(1+2S\sqrt{\lambda C}(1+bS\sqrt{\lambda C})),$$

which shows that when b is positive there is a considerable increase in the energies E_2 for the larger values of S.

The energies obtained when the number C is $\cdot 8/\lambda$ and the coefficient b is taken to be $\cdot 2$ are shown in Table II. The values of S are given in the first line of the table, and the corresponding values of E_2 when l is constant (as in Table I.) are given in the second line for comparison. The values of Q/Q_0 corresponding to the values of S are the same as in Table I.

The energies E_2 when the mean free path increases with the energy and the coefficient b is $+\cdot 2$ are given in the third line, and the energies E_2 when the mean free path diminishes as the energy increases and b is $-\cdot 2$ are given in the fourth line of the table.

TABLE II.

$C=\cdot 8/\lambda$.

S.	·5.	1.	2.	3.	4.
$b=0$, E_2/A	1·48	2·01	3·16	4·36	5·6
$b=\cdot 2$, E_2/A	1·55	2·29	4·5	6·9	11·3
$b=-\cdot 2$, E_2/A	1·41	1·85	2·6	3·2	3·6

Thus when the mean free path depends on the energy as in the equation

$$l=a(1+b(E/A-1))$$

the distribution of the energies depends to a large extent on the coefficient b. In general the energy G of any group S may be expressed in the form $G(1-\theta b)=E_2$, E_2 being given in the second line of Table II. and θ, a numerical constant to be determined from the values of E_2, in the third and fourth lines of the table.

For the group S_3 ($E=4\cdot 36$ A) the value of θ is 1·8 and for the group S_2 ($E=3\cdot 16$ A) θ is 1·3, which shows that variation in the mean free path affects the large energies much more than small energies.

16. The values of E_2/A given in Table I. are the energies of different groups of electrons after each electron has traversed the same number of free paths C, and since the electrons that acquire large increases in energy traverse the free paths in less time than those that acquire small increases the energies E_2 are not the energies of all

the groups at the same instant. At the time the full number C of free paths have been traversed by electrons which have acquired a large increase of energy the number of free paths traversed by electrons which tend to acquire smaller increases is less than C, and the energies of these groups are somewhat less than values of E_2 given in Table I. The numbers in the tables may be corrected so as to give the energies of the groups at any time. When C is $\cdot 8/\lambda$ the energies E_2 greater than $1\cdot 8 \times A$ at the time the electrons in the group S_4 have traversed the full number of free paths $\cdot 8/\lambda$ are given in terms of S by the equation

$$E_2/A = 1\cdot 27 \times S + \cdot 53, \quad . \quad . \quad . \quad . \quad (18)$$

and the number of electrons dQ with energies from E to $E+dE$ is obtained by substituting $(E/A - \cdot 53)/1\cdot 27$ for S in equation (13). The distribution thus obtained is expressed by the equation

$$dQ = q_0 \epsilon^{-(E/A - \cdot 53)^2/1\cdot 6} \times dE. \quad . \quad . \quad . \quad . \quad (19)$$

This expression is an approximate representation of the distribution of the energies greater than 1·8 A when λ and l are constants, and it may be used as a first step towards obtaining the actual distribution under ordinary conditions.

17. In the steady motion which is observed in the uniform luminous columns in discharge-tubes there are collisions of electrons with the surface of the tube and collisions with atoms of the gas where the losses of energy are greater, and in consequence of these losses the number of electrons with the larger energies is diminished. The effect is much the same as if the mean free path diminished with the energy. In fact if λ and l are both functions of E the distribution depends almost entirely on the ratio λ/l^2. For a first approximation therefore it may be assumed that the various processes which cause the actual distribution to differ from that given by equations (14) and (16) may be accounted for by taking the actual energy G of a group S to be related to the energy E_2 in equation (18) by an equation of the form

$$G(1 - \theta b) = E_2, \quad . \quad . \quad . \quad . \quad . \quad . \quad (20)$$

where b is an unknown constant and θ a numerical factor to be deduced from the numbers in Table II. by the method indicated above.

The energy G therefore depends only on two constants, A and b, which must be determined experimentally.

The constant A is nearly the same as the mean energy E which has been found in terms of the ratio Z/p by the experiments on the lateral diffusion of a stream of electrons, and A may be taken to be $\cdot 9 \times E$.

The constant b may be deduced from observations of the intensities of a spectral line in a uniform luminous column of a discharge in a gas at different pressures when the energy G_1 required to excite the line is known. The intensity of the line is proportional to the number of electrons Q_1 with energies greater than G_1, and the values of S_1 in equations (14) and (19), corresponding to the number Q_1, is deduced from the changes in the intensity of the line due to changes in $\bar{E}$, and b is found by the equations (18) and (20).

These equations may then be used to find the mean energy G of the electrons which excite other lines or parts of the continuous spectrum.

18. The distribution of the energies of the electrons in the steady motion acquired in a uniform electric field may be deduced by an indirect method from equations (13) and (16), when both the mean free path l and the coefficient λ are taken to be any functions of the energy of the electron.

Let $n(E)dE$ be the number of electrons in a current with energies in the range between E and $E+dE$ at any time, and U the velocity $\sqrt{2E/m}$. The electrons with energies E_1 move in all directions through distances $U_1 dt_1$ in the time dt_1, and a certain proportion $h_1 n(E_1) dt_1$ of the electrons with energies in the range between E_1 and (E_1+dE) at the time $t=0$ have energies outside that range at the time dt_1.

The factor h_1 depends on the ratio of the energy dE to the energy $ZeU_1 dt_1$.

Similarly, a certain proportion $h_2 n(E_2) dt_2$ of the electrons with energies in the range from E_2 to (E_2+dE) at the time $t=0$ have energies outside this range at the time dt_2, and the factors h_1 and h_2 are equal if the distances $U_1 dt_1$ and $U_2 dt_2$ are equal. Let $Q_1 dt$ be

the number of electrons that have energies from E_1 to (E_1+dE) at the time $t=0$ and energies outside this range at the time dt, $Q_2 dt$ the corresponding number for the range from E_2 to (E_2+dE). The ratio of the quantities Q_1 and Q_2 is given by the equations

$$Q_1 dt_1 = h_1 n(E_1) dE$$

and

$$Q_2 dt_2 = h_2 n(E_2) dE,$$

with the condition $h_1=h_2$ when $U_1 dt_1 = U_2 dt_2$. Thus

$$Q_1/Q_2 = U_1 n(E_1)/U_2 n(E_2). \quad . \quad . \quad . \quad . \quad (21)$$

The electrons in the group $Q_1 dt$ acquire energies considerably different from E_1 after traversing several free paths, and the changes of energy after each electron has traversed the same number of free paths C are given by equations (14) and (16). The number that acquire energies in the range from E_2 to (E_2+dE) is proportional to $Q_1 \epsilon^{-S_2^2} dS_2$, S_2 being given in terms of (E_2-E_1) by equation (16) and

$$dS_2 = (dE/Zl_2)\sqrt{3/4C},$$

where l_2 is the mean free path of electrons, with energies E_2 (dE/Z being the distance dz in section 9).

The number that acquire energies in the range from E_2 to (E_2+dE) is therefore proportional to $Q_1 \epsilon^{-S_2^2} dE/l_2$. In the same time there are corresponding changes in the energies of the electrons in the group $Q_2 dt$, and after traversing the same number of free paths C the number that acquire energies in the range from E_1 to E_1+dE is proportional to $Q_2 \epsilon^{-S_1^2} dE/l_2$. In these calculations it is necessary to consider the number C to be comparatively small, of the order $1/100 \times \lambda$, so that all the electrons included in the numbers $Q \times \epsilon^{\xi^2} ds$ may have the actual changes of energy given by equation (16) (not changes distributed about an average).

19. The simplest condition under which the distribution remains constant is obtained where there are very few collisions in which the electrons lose energy in very large amounts and the flow of electrons due to diffusion from one group to another is the same in both directions. The numbers $Q_1 \epsilon^{-S_2^2}/l_2$ and $Q_2 \epsilon^{-S_1^2}/l_1$ are

then the same for all pairs of groups, and the expression for $n(E)$ is obtained from the equation

$$\frac{l_1 U_1 n(E_1)}{l_2 U_2 n(E_2)} = \frac{l_1 Q_1}{l_2 Q_2} = \epsilon^{S_2^2 - S_1^2}. \quad . \quad . \quad . \quad (22)$$

This equation for the flow of electrons from one group to another would apply to uniform columns of discharges in wide tubes when the gas is at a high pressure and the radiation from the current is very faint; but as the pressure is reduced the mean energy of the electrons increases, and there is a large increase in the intensity of the radiation.

For the currents at these pressures it is necessary to take into consideration the collisions in which there are large losses of energy and the transfer of electrons from groups with large energies to groups with small energies by this process. In these currents the constant distribution is maintained when the flow of electrons due to diffusion from groups with small energies to groups with large energies is greater than the corresponding flow in the opposite direction.

20. The effect of this process on the distribution is the same as an increase in the coefficient λ with the energy of the electron on the value of $(S_2^2 - S_1^2)$ in equation (22). It is therefore necessary to assume that both l and λ are functions of E, and to substitute for A in equation (16) its original value $Zel/\sqrt{3\lambda}$. When this change is made, and F written for $Z \times e$, that equation becomes

$$dE = (C(F^2 l^2/3E - \lambda E) + 2S.F.l.\sqrt{C/3})dc/C. \quad . \quad (23)$$

Most of the electrons have energies not much different from the energy A, which is the value of E given by the equation $E = Fl/\sqrt{3\lambda}$, and is approximately the mean energy $\bar{E}$ found experimentally.

If E_2 be greater than E_1 and E_1 greater than A the number S_2 for the electrons which have energies increased from E_1 to E_2 is positive, since the electrons diffuse in the direction of the force. The number S_1 for the electrons that have their energies diminished from E_2 to E_1 is negative, and S_1^2 is less than S_2^2 by an amount which depends on λ.

For a first approximation when λC is small the first two terms on the right of equation (23) may be neglected,

and the value of S_2 for the electrons that have increases of energy from E_1 to E_2 obtained by integrating from $c=0$ to $c=C$ is given by the equation

$$2.S_2.F.\sqrt{C/3}=\int_{E_1}^{E_2} dE/l = I_2-I_1, \quad . \quad . \quad (24)$$

I_2 and I_1 being functions of E_2 and E_1 respectively.

Thus dc/C is given in terms of dE by the equation

$$dc/C=dE/l(I_2-I_1),$$

and for a second approximation this value of dc/C may be taken with the first two terms on the right of equation (23).

21. The equation for dE thus becomes

$$dE/l=C(E^2/3E-\lambda E/l^2)dE/(I_2-I_1)+2S_2F\sqrt{C/3}\times dc/C. \quad (25)$$

The integral

$$\int_{E_1}^{E_2}(F^2/3E-\lambda E/l^2)\,dE$$

may be written in the form

$$F^2(J_2-J_1)/3,$$

and the integral of (25), which gives a close approximation to the value of S_2, is

$$I_2-I_1-CF^2(J_2-J_1)/3(I_2-I_1)=2S_2F\sqrt{C/3}. \quad . \quad (26)$$

Similarly the number S_1 for electrons with energies E_2 which are diminished to E_1 is given by the equation

$$I_1-I_2-CF^2(J_2-J_1)/3(I_2-I_1)=2S_1F\sqrt{C/3}, \quad . \quad (27)$$

and $(S_1^2-S_2^2)$, obtained by eliminating C from equations (26) and (27), is (J_2-J_1).

The integral (J_2-J_1) may be written in the form

$$(\log E_2/E_1+H_1-H_2),$$

where H_1 is a function of E_1 and H_2 a similar function of E_2.

Substituting this expression for $S_1^2-S_2^2$ in equation (22), the following relation between the values of $n(E_1)$ and an $n(E_2)$ is obtained:

$$\frac{l_1U_1n(E_1)}{l_2U_2n(E_2)}=\frac{E_1}{E_2}\times\epsilon^{(H_2-H_1)}. \quad . \quad . \quad . \quad . \quad (28)$$

Since this equation is satisfied for all values of E_1 and E_2 the expression for $n(E)$ is

$$n(E)=N\sqrt{\bar{E}}\,\epsilon^{-H}/l, \quad . \quad . \quad . \quad . \quad . \quad (29)$$

where N is a constant depending on the number of electrons in the current, l the mean free path of electrons with energies E, and $H\times F^2/3$ the integral $\int^{E}(\lambda E/l^2)dE$. As before, it is necessary to assume λ/l^2 to be a simple function of E in order to obtain a formula for the distribution of energies which would provide a means of comparing the energies of the electrons that excite different parts of the spectrum of the uniform positive columns of a discharge.

22. In the preceding calculations it has been assumed that electrons with the energy E lose the same amount of energy λE in each collision, and since there may be large inequalities in the amounts of energy which are lost or gained by electrons in collisions with molecules of gases at ordinary temperatures due to the motion of the molecules it is necssary to consider to what extent these inequalities may affect the distribution of the energies of electrons moving in a uniform field. For this purpose it will be supposed that the collisions between electrons and molecules resemble the collisions between perfectly elastic spheres. As far as molecules consisting of single atoms are concerned this hypothesis with regard to their structure is consistent with the small values of λ deduced from the energies $\bar{E}$ and the velocities $\bar{W}$ of electrons in monatomic gases. The values of E and W as found experimentally thus lead to conclusions with respect to the elasticity and spherical symmetry of atoms, which are in accordance with similar conclusions deduced from the values of the specific heats of monatomic gases.

It may be seen that in these collisions there are large inequalities in the changes of the energies of electrons which depend on the relative velocities of the electrons and molecules.

23. Let m/M be the ratio of the mass of an electron to the mass of the molecule, k the ratio of the energy, E of the electron to the energy of the molecule.

The range of possible changes of energy due to a collision lies between the limits

$$4m\mathrm{E}(1-1/k\pm\sqrt{\mathrm{M}/mk})/\mathrm{M},$$

the actual change of energy depending on the directions of the motions of the electron and the molecules with respect to the normal to the molecule at the point of impact. The maximum loss of energy occurs in normal collisions when the electron and the molecule are moving in the same direction before the collisions, and the maximum gain of energy when the electron and molecule are moving in opposite directions.

If the gas be helium at 15° C. and the energy E be 3·7 volts the mean energy of agitation of the molecules is E/100, so that in the normal collisions of the electrons with molecules moving with the mean energy the electron may lose the amount of energy $38m\mathrm{E}/\mathrm{M}$ or gain the amount $30\ m\mathrm{E}/\mathrm{M}$.

For large values of k the mean loss of energy of the electron in all types of collision is $2\ m\mathrm{E}/\mathrm{M}$.

24. The complete distribution of the losses of energy of electrons after several collisions depends on inequalities due to different causes, but an approximate estimate of the distribution may be found by considering those collisions in which the direction of motion of the electron is inclined at an angle of about 45° to the normal to the atom.

It has been shown that the distribution of the energies of electrons after several such collisions may be estimated in the same manner as the distribution due to diffusion *.

The result may be expressed as follows, taking λ to be $2m/\mathrm{M}$ and B the energy of the molecules.

If a large number of electrons Q_0 with the same energy E collide with molecules of the gas the losses of energy of different groups S after each electron has made the same number C of collisions are given by the expression

$$\lambda\mathrm{EC}\pm 1{\cdot}6\sqrt{\lambda\mathrm{C}}\,.\,\mathrm{S}\sqrt{\mathrm{E}\,.\,\mathrm{B}},\ .\ .\ .\ .\ (30)$$

the number $d\mathrm{Q}$ in the group S being given by equation (13).

25. The actual distribution includes the additional inequalities due to differences in the inclinations of

* Phil. Mag. xvi. p. 729 (Oct. 1933).

the direction of motion of the electron to the normal to the molecule and to differences in the energies of the molecules. The effect of these inequalities may be expressed approximately by taking a larger numerical factor, 2 instead of 1·6, for second term in the above expression, and B as the mean energy in the molecules.

Let the gas be at 15° C. and A, the mean energy of the electrons, about 3·7 volts (B = A/100). The distribution of the changes of energy (due to the motion of the molecules) of electrons with energies E four times the mean is given approximately by the expression

$$\lambda EC \pm \cdot 4 \times S \,.\, \sqrt{\lambda C}\, A \quad . \quad . \quad . \quad . \quad . \quad (31)$$

for small values of C of about 100.

The inequalities in the energies given by the second term in this expression are much smaller than the inequalities due to diffusion of the electrons which, as shown by equation (16), are given by the expression $2 \,.\, S \,.\, \sqrt{\lambda C} \,.\, A$ for small values of C.

The inequalities in the changes of energy due to the motion of the molecules after a number of collisions C_1 are therefore the same as the inequalities due to the diffusion of the electrons in a much smaller number of collisions C_2, C_2 being $C_1/25$. Thus for a small number of collisions C the combined effect of the two independent causes of inequalities is the same as that due to diffusion alone in the number of collisions $1 \cdot 04 \times C$. The complete distribution due to both causes is therefore obtained by taking $\cdot 96 \times H$ for H in equation (28).

This small correction has the same effect as a change in the value of λ/l^2 in the expression for H, and is of little importance as far as the distribution of energies is concerned, when the value of λ/l^2 is determined experimentally by a method depending on the distribution.

XII. *Notes on the Relative and Absolute Values of Atomic Levels.* *By* Arne Eld Sandström *.

THE author † has recently published new measurements of the wave-lengths of the L-absorption spectra in the region 29 Cu–52 Te. It is of considerable

* Communicated by Prof. Manne Siegbahn, D.Sc.

† Arne Sandström, "Inaugural Dissertation," *Nova Acta Reg. Soc. Scient. Upsaliensis*, IV. ix. no. 11 (1935).

interest to compare the spectroscopically obtained energy-values of X-ray absorption edges with the values of the corresponding energy-levels obtained by magnetic deflexion of secondary electrons. By using the latter method Robinson * has measured the values of the L- and M-levels of 29 Cu, 47 Ag, and 50 Sn with a fairly high precision. He also made a comparison with the energy-values from the X-ray spectroscopic data then available, but without considering the fundamental, though slight, difference between the two sets of values.

Fig. 1.

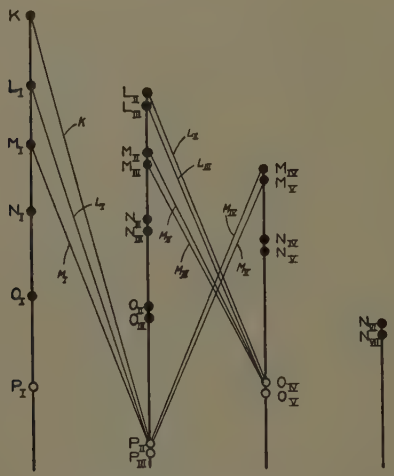

Level diagram of the absorption of 74 W.

X-ray Edges and X-ray Levels.

Through recent investigations into X-ray absorption spectra it has been shown that an absorption edge represents transitions from an inner, normally completely filled, atomic level to the first incomplete or empty outer level allowed by the selection rules. The influence of these rules is to be understood more clearly from fig. 1, in which the transitions are illustrated according to Siegbahn.

* H. R. Robinson, Phil. Mag. (7) xviii. p. 1086 (1934).

It is then evident that the energy-value of an edge equals the difference between the energy-values of two levels. Therefore, if the energy-value of an absorption edge is used as the energy-value of the initial level, this latter value is reckoned relative to the end-level of the electron transition, that is, the end-level in question is selected as a zero-level. We may then build up our system of levels in an atom by assuming the energy-value of an edge, say the L_{III}-edge, for the energy of the corresponding level (L_{III}) and calculate all the other levels from this with the aid of emission-lines only. In Siegbahn's table of the atomic levels * the L_{III}-edge is taken as a base for the elements above 50 Sn and the K-edge for the lower elements The author has published a table † for the elements 29 Cu-52 Te, where the level-values were calculated from the energy-value of the L_{III}-edge.

From spectroscopic data we accordingly obtain only relative values of the levels. On the other hand, the absolute values are given by the magnetic deflexion of secondary electrons, although with far less accuracy. We may then obtain the absolute value of the end-level of transitions from the L_I-level (or K, M_I, N_I-levels, etc.) by calculating the difference between the absolute energy-value of the L_I-level, obtained by measurements on secondary electrons (Robinson's "magnetic values") and the energy-value of the L_I-edge, and analogously the value of the end-level of transitions from the levels of the *p*-electrons may be found from the corresponding values of L_{II} and L_{III}. The values obtained from the secondary electrons ought then to be slightly higher than the energy-values of the corresponding edges obtained from the wave-length measurements. For some time it has been known, however, that the crystal scale of X-ray wave-lengths does not coincide with the absolute one owing to the fact that the lattice constant of calcite was calculated with too low a value of the electronic charge *e*. A more correct *e*-value necessitates not only a recalculation of the X-ray wave-lengths, but also of the level-values obtained from magnetic deflexion of secondary electrons.

* M. Siegbahn, 'Spektroskopie der Röntgenstrahlen,' 2. Aufl. Berlin, 1931, Table 176, pp. 346–348.

† Arne Sandström, *Nova Acta Reg. Soc. Scient. Upsaliensis*, IV. ix. no. 11, Table 45, p. 71 (1935).

Values of e and h.

In connexion with his investigations into the magnetic spectra of secondary electrons Robinson * tried to select the true value of the electronic charge by applying a value of e, which gave the same energy-value to a level for two different primary radiations (CuKα and CrKα). He concluded that Millikan's value $e = 4{\cdot}768 \cdot 10^{-10}$ e.s.u. was to be preferred to values obtained from the ruled-grating measurements of X-ray wave-lengths. As regards the latter, however, the early results have been confirmed through recent investigations. Bäcklin † obtained $e = 4{\cdot}805 \cdot 10^{-10}$ e.s.u. and Söderman ‡ $e = 4{\cdot}806 \cdot 10^{-10}$ e.s.u. Furthermore, von Friesen § has developed a very interesting method for the determination of the electronic charge by means of the de Broglie waves. He found that $e = 4{\cdot}796 \cdot 10^{-10}$ e.s.u. Bearden has earlier published several e-determinations. His latest value is $e = 4{\cdot}804 \cdot 10^{-10}$ e.s.u. ‖. It must be remembered, too, that Shiba¶ has shown that, by applying more recent values of the viscosity of air, Millikan's e-value increases to $4{\cdot}803 \cdot 10^{-10}$ e.s.u. Kellström ** has recently published new measurements on the viscosity of air. He obtained a value that will raise Millikan's e-value to $4{\cdot}818 \cdot 10^{-10}$ e.s.u. We will, however, use the average between von Friesen's value and the value from the latest X-ray measurements with ruled gratings. Thus we may assume an e-value of $4{\cdot}801 \cdot 10^{-10}$ e.s.u. If combined with the conventional value of h this e-value does not give the same value of an energy-level for the two primary radiations used by Robinson. However, as all determinations of h depend on e, we certainly have to select a value of h, which combined with $e = 4{\cdot}801 \cdot 10^{-10}$ gives the same energy-level values for the two primary radiations. By using those of Robinson's measurements, which he has given as being his most accurate, we obtain the values in Table I. The

* H. R. Robinson, Phil. Mag. (7) xviii. p. 1086 (1934).
† Erik Bäcklin, *Zeits. f. Phys.* xciii. p. 450 (1935).
‡ Martin Söderman, *Nova Acta Reg. Soc. Scient. Upsaliensis*, IV. ix. no. 8 (1935).
§ Sten von Friesen, 'Nature,' cxxxv. p. 1035 (1935). "Dissertation," Upps. Univ. Årsskr. 1935, p. 14.
‖ Bearden, Phys. Rev. xlviii. p. 385 (1935).
¶ K. Shiba, Inst. of Phys. and Chem. Res. Tokyo, xix. p. 97 (1932); xxi. p. 128 (1933).
** 'Nature,' cxxxvi. p. 682 (1935),

mean of all the 61 determinations is $(6{\cdot}619 \pm 0{\cdot}016) \cdot 10^{-27}$. Fig. 2 shows that most of the values fall close together, and if the error is put to $\pm 0{\cdot}016$ extreme values only fall outside the limits of error. If we calculate h from the Rydberg-constant, we find $h = 6{\cdot}624 \cdot 10^{-27}$ in good agreement with the value obtained from Robinson's measurements. Shiba * calculated $h = 6{\cdot}624 \cdot 10^{-27}$ corresponding to an e-value of $4{\cdot}803 \cdot 10^{-10}$. Further, a new measurement of h was recently published by Schaitberger †. His results were calculated with $e = 4{\cdot}774 \cdot 10^{-10}$ e.s.u. giving $h = 6{\cdot}554 \cdot 10^{-27}$ erg sec. If we assume $e = 4{\cdot}801 \cdot 10^{-10}$

TABLE I.

N.	Number of determ.	Levels, from which the secondary electrons emanated.	h-value giving equal level values for CuK_{α_1} and CrK_{α_2}.
79 Au..	17	$M_I - M_V$, $N_I - N_{III}$, N_V	6·621
78 Pt ..	17	$M_I - M_V$, $N_I - N_{III}$, N_V	6·618
74 W ..	9	$M_I - M_V$, $N_I - N_{III}$, N_V	6·618
50 Sn ..	6	$L_I - L_{III}$, M_I, M_{III}, M_V	6·629
47 Ag ..	10	$L_I - L_{III}$, M_I, M_{III}, M_V	6·613
29 Cu ..	2	L_I, L_{III}	6·621

Schaitberger's value will be $h = 6{\cdot}604 \cdot 10^{-27}$ erg sec. Evidently there is a tendency towards high h-values. For the recalculation of the level-values we will use the h-value, obtained from Robinson's measurements.

The application, described here, of the results from measurements on secondary electrons is really a rather circuitous method of determining e/h. The advantage of the method is that a constant high-tension for the acceleration of the electrons together with its measurement becomes unnecessary. The disadvantage is that the calculations involve the difference between two numbers.

* K. Shiba, *ibid.*

† G. Schaitberger, *Ann. d. Physik* (5) xxiv. p. 84 (1935).

The Absolute Energy-values of the Levels compared with the Energy of the Absorption-transitions.

For the recalculation of our energy-values we use $e = 4{\cdot}801 \,.\, 10^{-10}$ e.s.u. and the h-value, which gives the same level-values for both the primary radiations, viz., $6{\cdot}620 \,.\, 10^{-27}$ erg sec. The *energy-values*, which were obtained from X-ray spectra, have to be reduced to

Fig. 2.

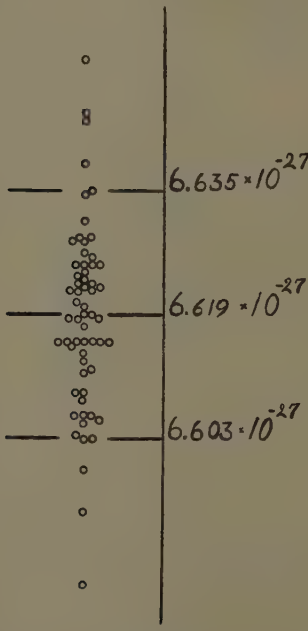

the absolute scale by multiplying by a factor 0·99812. Naturally, this also includes the energy of the two primary radiations for the excitation of secondary electrons. The energy of the latter (Robinson's ν/R^*-values) have to be multiplied by a factor 0·99582.

The energy-values of the levels and the edges together with these same values, recalculated to the absolute scale, are to be found in Table II. Unfortunately the

differences are of the same order of magnitude as the error, which may arise from the uncertainty in e and h.

TABLE II.

N.	Edge.	ν/R of initial level.	ν/R of edge.	ν/R of initial level recalc. to the abs. scale.	ν/R of edge recalc. to the abs. scale.	Difference.	Uncertainty of values.
50 Sn ..	L_I	328·9	328·80	328.7	328·2	+0·5	±0·5
	L_{II}	305·9	306·18	305·8	305·6	+0·2	±0·5
	L_{III}	289·2	289·34	289·2	288·8	+0·4	±0·5
29 Cu ..	L_{III}	68·4	68·703	69·3	68·57	+0·7	±1·2

However, the tendency is undeniably the right one, the values of the levels being slightly higher than those of the corresponding edges. The difference between the energy-values of the end-levels of the s- and p-electrons is equal to the difference between the energy-value of the L_I-level calculated from the L_{III} -edge and that of the L_I-edge. For tin this difference is 0·07 frequency-units *, which is far too low to appear in the differences tabulated above.

It is to be regretted that there are so few very accurate measurements on secondary electrons carried out in this region, where the edges have been studied with a spectrograph of high resolving power. Robinson's other precision-measurements were carried out in the M- and N-series of Au, Pt, and W, where a comparison may be made with Lindberg's measurements † of the M-edges. In the case of tungsten the different transitions of absorption are to be found in the diagram fig. 1. For transitions from the M_{III}-level of W and Pt the end-level is $O_{IV,V}$ ‡. Transitions from M_{IV} and M_V end at a lower level which, in this case, is really the completely empty $P_{II,III}$. Robinson has compared his values with those in Siegbahn's

* Arne Sandström, *Nova Acta Reg. Soc. Scient. Upsaliensis*, IV. ix. no. 11 (1935), table 44, p. 70 & fig. 33 *a*, p. 80.

† Ernst Lindberg, *Nova Acta Reg. Soc. Scient. Upsaliensis*. V. vii. no. 7 (1931).

‡ Arne Sandström, *Zeits. f. Phys.* lxvi. p. 784 (1930).

table. As the latter are calculated from the energy-value of the L_{III}-edge they give the energy-difference between the M-levels and the $O_{IV,\,V}$-level. In the case of the M_{IV}- and M_V-edges this difference is lower than the energy-value of the corresponding edge.

The absolute level-values and the energy of the M_{III}-, M_{IV}-, and M_V-transitions are to be found in Table III.

TABLE III.

N.	Level or edge.	ν/R of levels.	ν/R of edges.	ν/R of levels recalc. to the abs. scale.	ν/R of edges recalc. to the abs. scale.	Difference.	Uncertainty of the values.
79 Au ..	M_{III}	201·4	202·2	202·0	201·8	+0·2	±0·8
	M_{IV}	168·1	171·0	168·8	170·7	−1·9	±0·8
	M_V	161·6	164·8	162·4	164·5	−2·1	±0·8
78 Pt ..	M_{III}	193·9	194·9	194·7	194·5	+0·2	±0·7
	M_{IV}	161·4	164·4	162·1	164·1	−2·0	±0·8
	M_V	155·2	158·6	156·0	158·3	−2·3	±0·8
74	M_{III}	167·4	167·9	168·0	167·6	+0·4	±0·8
	M_{IV}	137·5	140·5	138·0	140·2	−2·2	±0·9
	M_V	132·5	136·0	133·3	135·7	−2·4	±0·9

We find that the difference has a positive sign as far as the M_{III}-level is concerned, but in the case of the M_{IV}- and M_V-levels we get negative values. The negative sign cannot possibly arise from errors of measurement only, as the absolute values of the differences are so much alike as to intimate a systematic influence.

The M-edges of the elements in question were measured with a spectrograph with low resolving power (60 X.U. pro mm.). It is possible, therefore, that an eventual structure in the edge may not have been resolved. This does not apply to the M_{III}-edge of Pt and W, which represents transitions to the $O_{IV,\,V}$-level, and is followed

by a white line *. In the case of the other edges, on the contrary, a structure is to be expected. The author has found that in certain cases †, when the end-level of the absorption transitions has a very low energy-value and is situated outside already incompletely filled levels, the edge does not appear single, but is followed by edges, which may be caused by transitions to levels belonging to the crystal lattice. These edges lie comparatively close to the main edge, and in cases of low resolving power they may cause that the edge is measured erroneously. In the case of tin the L_{II}- and L_{III}-edges show such structure-edges. The edges of highest energy give differences of $-1{\cdot}3$ (L_{II}) and $-1{\cdot}1$ (L_{III}) with the absolute level-values. The uncertainty is $\pm 0{\cdot}5$. It seems to be certain that the end-levels of the transitions, represented by these edges, is situated outside the zero-level, thus giving negative differences. Now, if such an unresolved structure influences the above M-edges, their differences with the absolute level-value may readily assume negative values.

In connexion with the above discussion we must not forget that after the accomplishment of the absorption transition there is one electron missing in the initial orbit. The end-level then ought to have an energy-value near that of the same level of the next element. There is in this case, however, one electron too much in the end-level, and thus again the energy-value is lowered. Anyhow, it is possible that in this way the energy of our end-level acquires too high a value. As the energy of the outermost levels increases with very small amounts, the error arising from this cause cannot exceed one or two-tenths of a frequency-unit.

Thus, we may disregard the values obtained in connexion with the M-edges of the heavy elements and reckon with those of tin and copper only, as they may be regarded as the most reliable. In a recent paper Robinson ‡

* J. Veldkamp was the first to draw attention to the fact that in cases where the end-level of an absorption-transition is the first incomplete one, the edge is followed by a white line (*Physica*, II., i. p. 25, 1935). The author has been able to confirm this (*Nova Acta Reg. Soc. Scient. Up.* IV., ix. no. 11, p. 85, 1935.)

† Arne Sandström, *Nova Acta Reg. Soc. Scient. Ups.* IV. ix. no. 11, (1935).

‡ H. R. Robinson & C. J. B. Clews, Proc. Roy. Soc. Lond. A, cxlix. p. 587 (1935).

writes that " it is necessary to retain the ' crystal ' values of the X-ray wave-lengths, as the agreement, already imperfect, is made worse if the ' grating ' values are taken." As is found in the above discussion this conception cannot be right. If all the recalculations are made, which become necessary from the new e-value, we find that the agreement is good. In the only case where the two sets of values really disagree (the M-edges of the heavy elements), they will disagree even more, when the " crystal " values are retained.

It is to be regretted that there is so little material on the absolute values of the atomic levels. However, the relative values obtained from X-ray data have the advantage of possessing higher accuracy. Not only are the errors of measurement somewhat higher for the absolute values, but errors are also introduced from the values of the fundamental constants, which values certainly are less accurate than hitherto has been supposed.

Summary.

A comparison has been made between the relative energy-values of the atomic levels obtained from X-ray absorption spectra and the absolute values obtained by magnetic deflexion of secondary electrons. Contrary to what has been supposed by Robinson, it was found that, if the fundamental difference between the two sets of values is duly recognized, the agreement is good, when the values are recalculated with an e-value of $4{\cdot}801 . 10^{-10}$ e.s.u. (the average of von Friesen's value and the value from ruled grating measurements) and a corresponding h-value of $6{\cdot}619 . 10^{-27}$ erg sec. (calculated from Robinson's measurements).

Finally, I wish to express my thanks to Prof. Siegbahn for the kind interest he always has shown in my work.

Physical Laboratory,
University of Uppsala.
Oct. 1935.

XIII. *The Influence of Capillarity on the Free Discharge of Sharp-edged Orifices.* *By* R. J. Cornish, *M.Sc.* *

List of Symbols.

h = head measured above the centre of pressure of the orifice.
Q = volume discharged in unit time.
A = area of orifice.
d_m = hydraulic mean depth of orifice (= area/perimeter).
k = coefficient of discharge ($=Q/A\sqrt{2g\bar{h}}$).
ν = kinematic viscosity.
ρ = density.
γ = capillarity constant (surface tension).
R_e = Reynolds number ($=d_mQ/\nu A$).
N_γ = capillarity number ($=d_m\rho Q^2/\gamma A^2$).

Summary.

Experiments were made to find the effect of temperature changes on the coefficient of discharge of small, square, sharp-edged orifices. A satisfactory correlation of the results was not obtained by plotting the coefficients against the Reynolds number, but a good curve was given when they were plotted against a "capillarity number," $d_m\rho Q^2/\gamma A^2$. The corresponding curves for a 1 inch by $\frac{1}{2}$ inch rectangular orifice and a 5/16 inch circular orifice agreed closely with those for the square orifices.

Introduction.

It was felt that a possible explanation of the difference in coefficients of free discharge of small and large orifices might lie in the influence of capillarity. Some experiments were therefore conducted on a range of square sharp-edged orifices, the capillarity being varied by varying the temperature. An investigation by means of the Principle of Dynamical Similarity led to the conclusion that, if both the capillarity and viscosity are to be taken into account, the coefficient of discharge k must be a function of R_e and of N_γ (see List of Symbols). In the following pages this conclusion has been applied to the results of the experiments.

* Communicated by the Author.

Apparatus.

The orifices were fixed in the end of a tank 2 ft. 9 in. wide by 3 ft. 9 in. deep, the centre of the orifice being 6 inches from the bottom of the tank. The orifices were cut in circular brass plates 3 inches in diameter; the

Fig. 1.

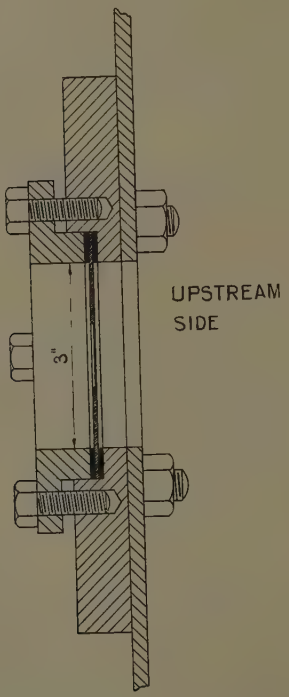

method of fixing the plates is shown in fig. 1. The water was circulated by a small centrifugal pump, and baffles were used to ensure a smooth surface above the orifice. The head, which was measured by a hook-gauge, was kept constant by an overflow funnel. In view of the small dimensions of the orifices relative to the cross-sectional area of the tank the velocity of approach was negligible. By means of a switch the water could be diverted to

a tank in which the quantity discharged during a period measured by a stop-watch could be weighed. The temperature of the water could be raised about 20° C. by electric immersion heaters, and care was taken to maintain the circulation until the temperature of the whole body of water was reasonably uniform.

The dimensions of the orifices, as obtained by a travelling microscope with vernier reading to ·002 cm., are given in the table. The edges were by no means perfect, and the dimensions used in the calculations were the average of a large number of determinations at different points on each orifice. The greatest variation from the mean was 1 per cent.

Nominal size of orifice.	Measured dimensions.	Area (A).	Hydraulic mean depth (m).
	cm	sq. cm.	cm.
¼ inch square	0·637 × 0·636	0·405	0·159
½ „ „	1·269 × 1·278	1·622	0·318
¾ „ „	1·899 × 1·907	3·624	0·476
1 „ „	2·555 × 2·544	6·500	0·637
1 in. × ½ in. rect.	2·517 × 1·263	3·179	0·420
5/16 inch circular	0·791 (diam.)	0·491	0·198

A rise of temperature of 20° C. corresponds to an increase in linear dimension of about 1 in 1000. An approximate allowance for the change of area of the orifice when passing warm water was made, though the standard of accuracy of the observations hardly justified such a correction. In any case it was very small.

The values adopted for ν and ρ were taken from the International Critical Tables (1926), and those for γ from Physikalisch-Chemische Tabellen (Landolt, Börnstein, Roth, and Scheel, 1923).

Results.

In fig. 2 the coefficient of discharge k has been plotted against the Reynolds number. The curves with cold water agree together reasonably well when R_e is greater than about 1500, but this is not the case with those with warm water, especially with the larger orifices.

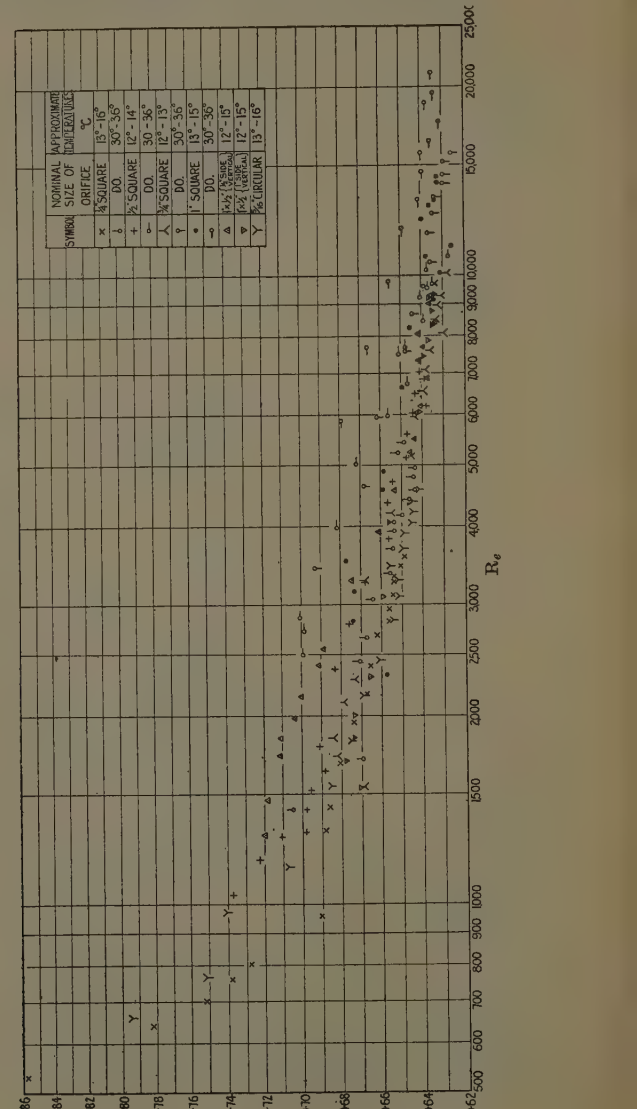
SYMBOL
NOMINAL SIZE OF ORIFICE
APPROXIMATE TEMPERATURES °C
× ¼" SQUARE 13°-16°
○ DO. 30°-36°
+ ½" SQUARE 12°-14°
○ DO. 30-36°
△ ¾" SQUARE 12°-13°
○ DO. 30°-35°
• 1" SQUARE 13°-15°
○ DO. 30°-35°
△ 1½"x¾" SIDE (VERTICAL) 12°-15°
▽ 1½"x¾" (HORIZONTAL) 12°-15°
Y ⅝" CIRCULAR 13°-16°
f
Re

Fig. 2.

In fig. 3, where k is plotted as a function of the capillarity number, N_γ, a remarkably good correlation has been obtained in spite of the large scale adopted for k. The curve seems to suffer a sudden change of slope at $N_\gamma = 10$,

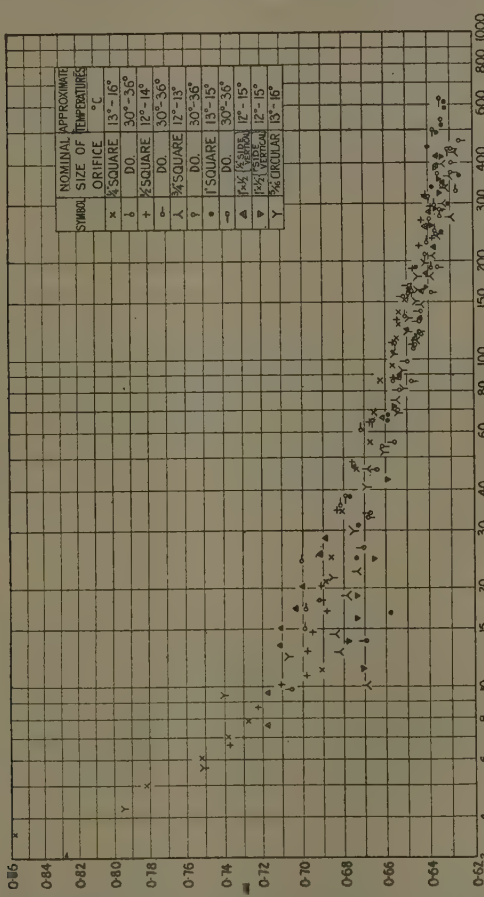

Fig. 3.

and in this region the values of k for the various orifices differ considerably. This might be due to one or more of the following causes :—

(1) The head is relatively low in this region, so a small error would have a big effect.

(2) According to the dynamical similarity calculation both R_e and N_γ should be constant to obtain a constant coefficient of discharge. This would imply that, for the same value of N_γ, k should vary systematically with the Reynolds number, but such a systematic variation was not evident.

(3) There may be instability in this region, corresponding to the condition at the change from streamline to turbulent flow in pipes. The author is inclined to think that this last explanation is the correct one.

When N_γ is greater than 100 the agreement between the results with the various orifices is within the range of experimental error.

The results of some experiments with cold water only on the discharge of a 1 inch by $\frac{1}{2}$ inch rectangular orifice and of a 5/16 inch circular orifice were available, and have been plotted in figs. 2 and 3. It is interesting to compare the two curves for the rectangular orifice. From $N_\gamma = 10$ to $N_\gamma = 50$ the curve obtained with the $\frac{1}{2}$ inch side vertical practically marks the upper boundary of the distribution of points in fig. 3, while that with the 1 inch side vertical almost coincides with the lower boundary. As N_γ increases the curves converge, and from $N_\gamma = 100$ are coincident.

Conclusion.

The experiments show that capillarity has a greater effect than viscosity on the coefficient of free discharge of sharp-edged orifices. It seems likely that the same would be true of discharge over sharp-crested weirs; unfortunately temperatures are not usually available in the published results of such observations, and the author would be glad to receive details of any experiments whereby the above suggestion could be tested.

Acknowledgment.

The author has pleasure in expressing his thanks to his research assistants, Messrs. F. H. Chandler, M.Sc. (Tech.) and T. Coates, M.Sc. (Tech.), who carried out the experimental portion of the work.

XIV. *The Exploration of Stress in the Neighbourhood of an Isotropic Point in an Elastic Plate. By* L. N. G. Filon, *C.B.E., F.R.S., Professor of Applied Mathematics and Mechanics in University College, London* *.

1. In an elastic plate under plane stress in its own plane there exist not infrequently certain points for which the two principal stresses P and Q are equal, so that the stress at such a point is the same all round and the directions of principal stress are indeterminate ; also at such points no shear-stress exists in any direction. Such points are known as *isotropic points*.

If the plate is one of transparent material and is viewed in a circular polariscope † the isotropic points are immediately recognized, as they are usually shown by isolated black patches in a brilliantly coloured field ; in a plane polariscope they form nodes through which pass a family of isoclinic lines, that is, loci of points at which the directions of principal stress are parallel to the axes of the polariser and analyser. For any given position of the latter the corresponding isoclinic appears as a black band in the field, and this passes through all the isotropic points, when such exist. As we rotate the polariser and analyser the black band coincides with the corresponding isoclinics in succession. All these have then the isotropic points in common.

In the photo-elastic method of exploration of stress difficulties arise when such an isotropic point is approached, and it is of considerable assistance to know the course of the lines of principal stress in their neighbourhood.

It is often assumed that normally the lines of principal stress at an isotropic point must approximate to a pencil of lines radiating from the point and concentric orthogonal circles. Experimental results, however, have indicated other distributions, and this suggested that a theoretical investigation of the distributions to be expected in such a case might be useful. This is the object of the discussion which follows. It has led incidentally to the conclusion that what might have been thought *a priori*

* Communicated by the Author.

† For a description of the circular polariscope see Coker and Filon, ' A Treatise on Photo-Elasticity ' (Cambridge University Press, 1931), pp. 73–77.

the most probable arrangement of the lines of principal stress is, in fact, impossible.

2. Let the isotropic point be taken as origin, and let $\widehat{xx}$, $\widehat{yy}$, $\widehat{xy}$ be the stress-components at any point, referred to axes of coordinates Ox, Oy. Let χ be the stress-function for plane stress, so that

$$\widehat{xx}=\frac{\partial^2\chi}{\partial y^2}, \quad \widehat{yy}=\frac{\partial^2\chi}{\partial x^2}, \quad \widehat{xy}=-\frac{\partial^2\chi}{\partial x\,\partial y}. \quad . \quad (1)$$

It is well known that χ satisfies the equation

$$\nabla^4\chi=0, \quad . \quad . \quad . \quad . \quad . \quad . \quad . \quad (2)$$

where $\nabla^2\equiv\partial^2/\partial x^2+\partial^2/\partial y^2$.

Now, at an isotropic point

$$\widehat{xx}=\widehat{yy}, \quad \widehat{xy}=0,$$

so that

$$\frac{\partial^2\chi}{\partial y^2}=\frac{\partial^2\chi}{\partial x^2}, \quad (3.1); \qquad \frac{\partial^2\chi}{\partial x\,\partial y}=0. \quad . \quad (3.2)$$

Developing χ in powers of x, y, and dropping the constant term and the terms linear in x, y, which cannot affect the stress in any case, we obtain the following development:

$$\begin{aligned}\chi=&\tfrac{1}{2}\mathrm{R}(x^2+y^2)+\tfrac{1}{6}(\mathrm{A}_1x^3+3\mathrm{B}_1x^2y+3\mathrm{C}_1xy^2+\mathrm{D}_1y^3)\\&+\tfrac{1}{24}[\mathrm{A}_2(x^4-6x^2y^2+y^4)+4\mathrm{B}_2(x^3y-xy^3)\\&+2\mathrm{C}_2(x^2+y^2)(x^2-y^2)+4\mathrm{D}_2(x^2+y^2)xy]+\ldots, \quad (4)\end{aligned}$$

where R is the value of the all-round stress at the isotropic point and A_1, B_1, C_1, D_1, A_2, B_2, C_2, D_2 etc. are constants depending on the general stress-distribution considered.

Except in the very special case where $\mathrm{A}_1=\mathrm{B}_1=\mathrm{C}_1=\mathrm{D}_1=0$, we may neglect all terms in (4) after the first two.

3. We have now

$$\left.\begin{aligned}\widehat{xx}&=\mathrm{R}+\mathrm{C}_1x+\mathrm{D}_1y,\\ \widehat{yy}&=\mathrm{R}+\mathrm{A}_1x+\mathrm{B}_1y,\\ \widehat{xy}&=-(\mathrm{B}_1x+\mathrm{C}_1y),\end{aligned}\right\} \quad . \quad . \quad . \quad . \quad . \quad (5)$$

and the differential equation of the lines of principal stress is

$$\tan 2\phi=2\widehat{xy}/(\widehat{xx}-\widehat{yy}), \quad . \quad . \quad . \quad . \quad (6.1)$$

where $\tan\phi = dy/dx$, so that, writing $dy/dx = p$,

$$p/(1-p^2) = -(B_1x+C_1y)/\{(C_1-A_1)x+(D_1-B_1)y\}, \quad (6.2)$$

whence

$$y/x = \{(A_1-C_1)p-B_1(1-p^2)\}/\{(D_1-B_1)p+C_1(1-p^2)\} \quad (6.3)$$

This equation is of the homogeneous type, so that the complete primitive is a system of similar and similarly situated curves, the origin being a centre of similarity. The tangents from the origin to any one curve of the system touch all the curves of the system and so form part of the envelope, and they are accordingly singular solutions of the differential equation.

If $y=\gamma x$ be such a tangent, then $y=\gamma x$, $p=\gamma$ must satisfy the equation (6.3), and we have

$$C_1\gamma^3-(D_1-2B_1)\gamma^2+(A_1-2C_1)\gamma-B_1=0. \quad . \quad (7)$$

This equation has three roots, γ_1, γ_2, γ_3, one of which is always real. On the character of these roots depends the nature of the lines of principal stress in the neighbourhood of O. We obtain at once

$$\left.\begin{aligned} (D_1-2B_1)/C_1 &= \gamma_1+\gamma_2+\gamma_3, \\ (A_1-2C_1)/C_1 &= \gamma_2\gamma_3+\gamma_3\gamma_1+\gamma_1\gamma_2, \\ B_1/C_1 &= \gamma_1\gamma_2\gamma_3, \end{aligned}\right\} \quad . \quad . \quad (7.1)$$

so that the original differential equation (6.3) takes the form

$$(y/x)\{(\gamma_1+\gamma_2+\gamma_3+\gamma_1\gamma_2\gamma_3)p+1-p^2\} = (1+\gamma_2\gamma_3+\gamma_3\gamma_1+\gamma_1\gamma_2)p-\gamma_1\gamma_2\gamma_3(1-p^2). \quad . \quad (8)$$

If we write in this $y/x=\gamma_1$ it is easily verified that the two values of p are γ_1, $-1/\gamma_1$, so that the curves of the system either touch $y/x=\gamma_1$ or are orthogonal to it.

Obviously the three lines $y=\gamma_n x$ ($n=1, 2, 3$) are lines of principal stress through O.

4. We now proceed to solve the differential equation (8). It will be convenient to treat it as of the modified Clairaut's form ($y=xf(p)$) and to obtain x and y in terms of p as parameter. Differentiating with regard to x in the usual manner, we obtain, after some straightforward reductions,

$$\frac{dx}{x} = \frac{(1+\gamma_2\gamma_3)(1+\gamma_3\gamma_1)(1+\gamma_1\gamma_2)(1+p^2)\,dp}{(\gamma_1-p)(\gamma_2-p)(\gamma_3-p)\{(\gamma_1+\gamma_2+\gamma_3+\gamma_1\gamma_2\gamma_3)p+1-p^2\}}, \quad . \quad . \quad . \quad (9)$$

and, breaking up the right-hand side into partial fractions

$$\frac{dx}{x} = \frac{k_1}{p-\gamma_1} + \frac{k_2}{p-\gamma_2} + \frac{k_3}{p-\gamma_3} + \frac{\gamma_1+\gamma_2+\gamma_3+\gamma_1\gamma_2\gamma_3-2p}{(\gamma_1+\gamma_2+\gamma_3+\gamma_1\gamma_2\gamma_3)p+1-p^2}, \quad (9.1)$$

where

$$k_1=(1+\gamma_1^2)(1+\gamma_2\gamma_3)/(\gamma_3-\gamma_1)(\gamma_1-\gamma_2), \quad . \quad . \quad (10)$$

k_2, k_3 being obtained by cyclic interchange.

Integrating, we find easily

$$x = C\{(\gamma_1+\gamma_2+\gamma_3+\gamma_1\gamma_2\gamma_3)p+1-p^2\} \times (p-\gamma_1)^{k_1}(p-\gamma_2)^{k_2}(p-\gamma_3)^{k_3}, \quad (11.1)$$

whence, from (8),

$$y = C\{(1+\gamma_2\gamma_3+\gamma_3\gamma_1+\gamma_1\gamma_2)p-\gamma_1\gamma_2\gamma_3(1-p^2)\} \times (p-\gamma_1)^{k_1}(p-\gamma_2)^{k_2}(p-\gamma_3)^{k_3}. \quad (11.2)$$

In the above C is an arbitrary constant.

Clearly when p increases through one of the three critical values γ_1, γ_2, γ_3, the corresponding factor on the right-hand side of equations (11·1) (11·2) will be affected by a complex factor, so that, for *real* lines of principal stress, the value of C must be changed when we cross such a value, being taken such that x and y are real in all cases. We shall suppose that this is done, so that we get real points corresponding to every value of p.

It will be noticed that the leading factors

$$(\gamma_1+\gamma_2+\gamma_3+\gamma_1\gamma_2\gamma_3)p+1-p^2$$

and

$$(1+\gamma_2\gamma_3+\gamma_3\gamma_1+\gamma_1\gamma_2)p-\gamma_1\gamma_2\gamma_3(1-p^2)$$

cannot in general vanish simultaneously, for these expressions, in virtue of (7.1), are proportional to

$$(D_1-B_1)p+C_1(1-p^2)$$

and

$$(A_1-C_1)p-B_1(1-p^2).$$

These cannot simultaneously vanish unless

$$\frac{B_1-D_1}{C_1} = \frac{A_1-C_1}{B_1},$$

This would imply that in equation (6.2)

$$p/(1-p^2)=\text{const.}$$

throughout, or that the lines of principal stress (to this approximation) form an orthogonal network of straight lines. Moreover, when $B_1x+C_1y=0$, so is $(A_1-C_1)x+(B_1-D_1)y=0$, and therefore on this locus $\widehat{xy}=0$, $\widehat{xx}-\widehat{yy}=0$ and every point is an isotropic point. We have thus then the case of a *neutral line*, which is highly exceptional, although in fact it does occur, as in the case of a straight strip under pure flexure in its own plane, when the neutral line is the usual neutral axis.

Putting aside this exceptional possibility it follows that a line of principal stress other than one of the three singular lines cannot pass through the origin unless we approach the values $p=\gamma_1$, γ_2, or γ_3.

The behaviour of the curves in the neighbourhood of such values depends upon the signs of the indices k. For clearly $(p-\gamma_n)^{k_n}$ tends to zero or infinity according as k_n is positive or negative. In the first case the relevant curves pass through the origin and touch $y=\gamma_n x$ there. Thus $y=\gamma_n x$ is a common tangent at O to these curves. In the second case the curves move away to infinity as we approach $y=\gamma_n x$, which then gives a common asymptotic direction.

5. Consider first the case (I.) where γ_1, γ_2, γ_3 are real. We may, without loss of generality, suppose that $\gamma_1>\gamma_2>\gamma_3$, so that k_1 has the opposite sign to $1+\gamma_2\gamma_3$, k_2 has the same sign as $1+\gamma_3\gamma_1$, and k_3 has the opposite sign to $1+\gamma_1\gamma_2$.

If we write

$$\nu_1=(1+\gamma_1\gamma_2)(1+\gamma_3\gamma_1)/(\gamma_3-\gamma_1)(\gamma_1-\gamma_2), \quad . \quad (12)$$

with a similar notation for ν_2, ν_3, it is easily shown that

$$\nu_n=k_n+1, \quad . \quad . \quad . \quad . \quad . \quad . \quad (13)$$

and also that

$$k_1+k_2+k_3+2=0, \quad . \quad . \quad . \quad . \quad . \quad (14)$$

so that

$$\nu_i+\nu_j+k_n=0, \quad . \quad . \quad . \quad . \quad . \quad (15)$$

where i, j, n is any permutation of the suffixes 1, 2, 3.

If $i=1$, $j=2$, $n=3$, we have

$$\frac{1+\gamma_1\gamma_3}{(\gamma_3-\gamma_1)(\gamma_1-\gamma_2)}+\frac{1+\gamma_2\gamma_3}{(\gamma_1-\gamma_2)(\gamma_2-\gamma_3)}+\frac{1+\gamma_3^2}{(\gamma_2-\gamma_3)(\gamma_3-\gamma_1)}=0. \quad \ldots \quad (16.1)$$

In order to obtain (16.1) we have had to divide by $1+\gamma_1\gamma_2$. This assumes that no two of the singular lines are at right angles. But, if $\gamma_1\gamma_2=-1$, then

$$\frac{1+\gamma_2\gamma_3+\gamma_3\gamma_1+\gamma_1\gamma_2}{\gamma_1\gamma_2\gamma_3}=-(\gamma_1+\gamma_2+\gamma_3+\gamma_1\gamma_2\gamma_3),$$

or

$$\frac{A_1-C_1}{B_1}=\frac{B_1-D_1}{C_1},$$

and we fall back on the case of a neutral line, already excluded. The assumption involved is thus justified.

It follows from (16.1), having regard to the relative magnitudes of γ_1, γ_2, γ_3, that we cannot have $1+\gamma_3\gamma_1$ positive and $1+\gamma_2\gamma_3$ negative. Similarly, taking $i=2$, $j=3$, $n=1$, we see that the combination $1+\gamma_3\gamma_1$ positive and $1+\gamma_1\gamma_2$ negative is impossible, and taking $i=1$, $j=3$, $n=2$, we see that the combination $1+\gamma_1\gamma_2$, $1+\gamma_2\gamma_3$ both negative is impossible.

Hence the only possible combinations of sign are as follows :—

$1+\gamma_2\gamma_3$: + − + +	k_1 : − + − −
$1+\gamma_3\gamma_1$: − − + −	k_2 : − − + −
$1+\gamma_1\gamma_2$: + + + −	k_3 : − − − +

We have thus two fundamental subcases :

I. (*a*) k_1, k_2, k_3 all negative ; the three critical lines $y=\gamma_n x$ give common asymptotic directions.

I. (*b*). Two only of k_1, k_2, k_3 are negative ; the corresponding critical lines $y=\gamma_n x$ give common asymptotic directions, the third critical line gives a common tangent at the origin.

6. We next take the case (II.) where γ_1 is real but γ_2 and γ_3 are conjugate imaginary.

Let

$$\gamma_2=\gamma+i\delta, \quad \gamma_3=\gamma-i\delta.$$

We have

$$k_1=-(1+\gamma_1^2)(1+\gamma^2+\delta^2)/\{(\gamma-\gamma_1)^2+\delta^2\},$$

so that $k_1<0$ and $y=x\gamma_1$ gives an asymptotic direction.

The curves are given by the parametric equations

$$\left.\begin{aligned} x &= C\{[\gamma_1+2\gamma+\gamma_1(\gamma^2+\delta^2)]p+1-p^2\}(p-\gamma_1)^{k_1} \\ &\quad\times\{(p-\gamma)^2+\delta^2\}^{\frac{1}{2}(k_2+k_3)}\times\exp\left\{i(k_3-k_2)\tan^{-1}\frac{\delta}{p-\gamma}\right\}, \\ y &= C[(1+2\gamma\gamma_1+\gamma^2+\delta^2)p-\gamma_1(\gamma^2+\delta^2)(1-p^2)](p-\gamma_1)^{k_1} \\ &\quad\times\{(p-\gamma)^2+\delta^2\}^{\frac{1}{2}(k_2+k_3)}\times\exp\left\{i(k_3-k_2)\tan^{-1}\frac{\delta}{p-\gamma}\right\}, \end{aligned}\right\} \quad . \quad . \quad . \quad (17)$$

where

$$k_2+k_3=[(1-\gamma_1{}^2)(1-\gamma^2-\delta^2)+4\gamma\gamma_1]/\{(\gamma-\gamma_1)^2+\delta^2\}, \quad (17.1)$$

$$i(k_3-k_2)=(1+\gamma^2+\delta^2)[(\gamma-\gamma_1)(1+\gamma\gamma_1) +\gamma_1\delta^2]/\delta\{(\gamma-\gamma_1)^2+\delta^2\}. \quad . \quad . \quad . \quad . \quad . \quad (17.2)$$

As before, the first factors on the right-hand sides of (17) cannot vanish together, nor can either the exponential factor or the factor $\{(p-\gamma)^2+\delta^2\}^{\frac{1}{2}(k_2+k_3)}$ vanish or become infinite, whatever the signs and relative magnitudes of γ_1, γ, δ may be. Accordingly no line of principal stress other than $y=\gamma_1 x$ can pass through the origin, nor can there be any asymptotic direction other than $y=\gamma_1 x$.

7. The general run of the lines of principal stress may now be inferred from the following considerations.

To simplify the discussion we will suppose that the axes of reference have been chosen so that the axis of x falls upon the line $y=\gamma_2 x$, so that $\gamma_2=0$.

We have therefore $\gamma_1>0$, $\gamma_2=0$, $\gamma_3<0$.

This reduces case I. (*b*) to the single type $k_1<0$, $k_2>0$, $k_3<0$, and cases I. (*a*) and I. (*b*) occur according as $1+\gamma_3\gamma_1\lessgtr 0$, *i. e.*, according as that angle between the lines $y=\gamma_1 x$, $y=\gamma_3 x$, which contains the third critical line is greater than, or less than, a right angle.

Further, we find, since

$$y/x=(1+\gamma_3\gamma_1)p/\{(\gamma_1+\gamma_3)p+1-p^2\},$$

that

$$\frac{d}{dp}(y/x)=\frac{(1+\gamma_3\gamma_1)(1+p^2)}{\{(\gamma_1+\gamma_3)p+1-p^2\}^2}. \quad . \quad . \quad (18)$$

Accordingly $d(y/x)/dp$ retains the same sign throughout. In case I. (*a*) y/x always diminishes algebraically as

p increases, but in case I. (b) y/x increases algebraically as p increases.

It is to be noted that, if $p=0$, γ_1 or γ_3, y/x has the same value as p.

For brevity the critical lines $y=\gamma_1 x$, $y=\gamma_2 x$, $y=\gamma_3 x$ will be referred to by the numbers 1, 2, 3 respectively.

Take first case I. (a) (3 asymptotes); the angle between 1 and 3 which includes 2 is then obtuse; those between 1 and 2, 2 and 3, which include 3 and 1 respectively, are also obtuse.

If p is $\pm\infty$, $y/x=0$, so that we can start with a point $x>0$, $y=0$, and with a branch crossing the axis of x at right angles; as p diminishes from $+\infty$ to γ_1, y/x increases from 0 to γ_1; as p increases from $-\infty$ to γ_3, y/x diminishes from 0 to γ_3. Thus such a branch, which is orthogonal to 2, approaches 1 and 3 asymptotically.

To such branches which cross 2 on the x-positive side correspond branches symmetrical with respect to O and crossing 2 on the x-negative side.

In this case the line 2 is not in any sense special, and we may equally well take the axis of x along 1 or 3. It follows that we get sets of curves lying in the obtuse angles between any pair of asymptotic rays and orthogonal to the third asymptotic ray. These sets of curves, none of which passes through the origin, are mutually orthogonal in the sectors of overlap. This case is shown in fig. 1.

Take next case I. (b) (2 asymptotes). Here the angle between 1 and 3 which includes 2 is acute, whereas the angles between 1 and 2, 2 and 3, which include 3 and 1 respectively, are still obtuse.

If p approaches zero the curves pass through O and touch the axis of x at O. As p increases from γ_3 to 0 y/x increases from γ_3 to 0, and we have a line of principal stress asymptotic to 3 and moving inwards until it touches 2 at O. As p increases from 0 to γ_1, y/x increases from 0 to γ_1, and we have a line of principal stress starting from O and touching 2 moving outwards until it approaches 1 asymptotically. Symmetrical curves exist in the vertically opposite angle.

If p increases from γ_1 to ∞, y/x increases from γ_1 to ∞, and then from $-\infty$ to 0; as p then increases from $-\infty$ to γ_3, y/x increases from 0 to ∞, and then from $-\infty$ to γ_3, the radius-vector from O revolving continu-

ously in the counter-clockwise sense. No points at infinity occur, and we have a set of lines of principal stress describing a bend round O in the reflex angle opposite to the acute angle containing the positive half of the x-axis.

A symmetrical set of lines exist in the reflex angle opposite to the acute angle between 1 and 3, which includes the negative half of the x-axis.

Fig. 1.

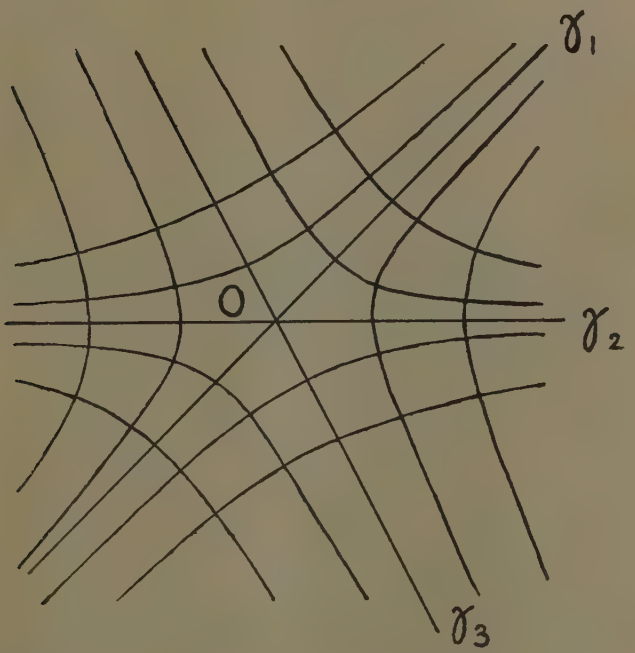

Case I. (α). Three real asymptotes.

Both these sets are asymptotic to 1 and 3 and mutually orthogonal. They are also orthogonal to the set previously mentioned, which touch 2 at the origin. The case in question is illustrated by fig. 2.

Finally, we have case II. (one asymptote). Here we take $\gamma_1=0$ and $y/x=(1+\gamma_2\gamma_3)p/\{(\gamma_2+\gamma_3)p+1-p^2\}$. We have $\gamma_2\gamma_3=\gamma^2+\delta^2$, $\gamma_2+\gamma_3=2\gamma$; the formula corresponding

to (18) then shows that y/x increases as p increases. Here no curve touches the axis of x at the origin. If we start from a point $x>0$, $y=0$, the corresponding line of principal stress is orthogonal to 1. As p varies from $-\infty$ to 0 y/x increases from 0 to ∞, and then from $-\infty$ to 0; as p decreases from $+\infty$ to 0 y/x decreases from 0 to $-\infty$, and then from $+\infty$ to 0. The vectorial angle varies continuously from π to $-\pi$, and the line of

Fig. 2.

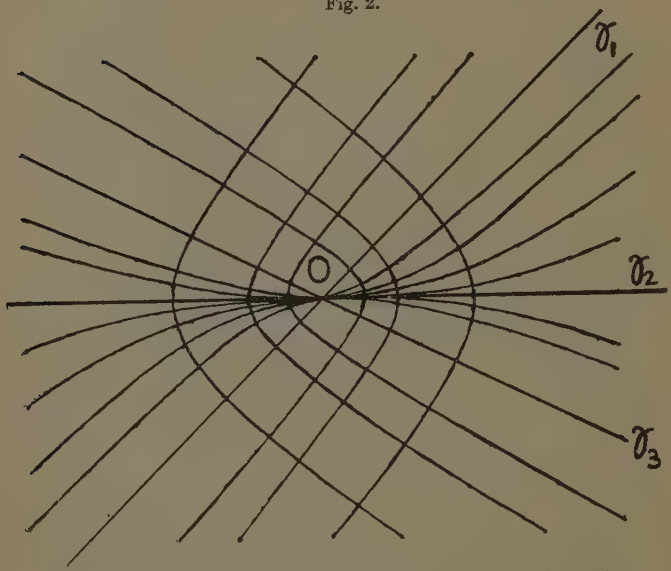

Case I. (*b*). Two real asymptotes and one real common tangent.

stress makes a half-turn round the origin, being asymptotic to the axis of x on both sides. A symmetrical set, which cross the x-axis on the negative side of O, are orthogonal to the first set, the two forming a network somewhat similar to that formed by a family of confocal parabolas, which indeed are a particular case of the present system of lines, corresponding to $\gamma=0$, $\delta=1$. The curves for case II. are shown in fig. 3.

8. So far it has been assumed that the roots γ_1, γ_2, γ_3 of the fundamental cubic were all different.

Consider now case III., when two of the roots, which we may take to be γ_2, γ_3, are equal. We may choose our axes so that the axis of y corresponds to the coincident critical directions. γ_2, γ_3 are then infinite, and the coefficients of γ^2, γ^3 in (7) both vanish, so that

$$C_1=0, \quad D_1=2B_1.$$

Fig. 3.

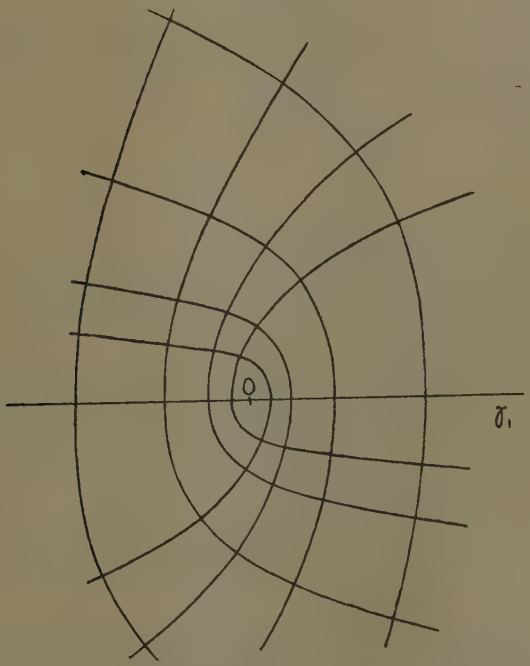

Case II. One real asymptote. $\gamma_1=0$; $\gamma=1/2$; $\delta=3/2$.

The differential equation (6.3) then takes the form

$$y/x=A_1/B_1-(1-p^2)/p=1/\gamma_1-1/p+p. \qquad (19)$$

From (19) we obtain

$$\frac{dx}{x}=\frac{\gamma_1(p^2+1)}{p(\gamma_1-p)}\,dp=\left(-\gamma_1+\frac{1}{p}+\frac{1+\gamma_1^2}{\gamma_1-p}\right)dp,$$

and $$x = Cpe^{-\gamma_1 p}(p-\gamma_1)^{-(1+\gamma_1^2)}, \quad . \quad . \quad . \quad . \quad . \quad (20.1)$$

$$y = C\left(p^2-1+\frac{p}{\gamma_1}\right)e^{-\gamma_1 p}(p-\gamma_1)^{-(1+\gamma_1^2)}. \quad . \quad (20.2)$$

We can always arrange the *sense* of our x and y axes so that $\gamma_1>0$. Fig. 4 illustrates a case where γ_1 has had to be made positive by taking the positive sense of x *to the left.*

If $\gamma_1>0$, $p=+\infty$ makes $x=0$, $y=0$, so that the y-axis is a common tangent at O. But since $p=-\infty$ makes $x=\infty$, $y=\infty$, with $|\,y/x\,|=\infty$, the y-axis is also an asymptotic ray.

$y=\gamma_1 x$ is always an asymptotic ray.

As before

$$\frac{d}{dx}(y/x) = 1+\frac{1}{p^2} > 0,$$

so that y/x steadily increases with p.

If we start at infinity on the positive side of $y=\gamma_1 x$, and make p increase from γ_1 to $+\infty$, we have a set of curves asymptotic to the ray 1 and coming in to O tangentially along the axis of y. There is a symmetrical set in the vertically opposite angle.

If now p changes to $-\infty$ we pass to a point at infinity in the direction of the y-axis. Starting from $y=+\infty$, the curves come down, make a bend round O, and finish at infinity on the y-negative side of the ray 1. The symmetrical set start from $y=-\infty$, make a bend round O, and finish on the y-positive side of the ray 1.

Fig. 4 shows the lines of principal stress for this case, when $\gamma_1=\mp 1$ according as the positive sense of x is to the right or to the left.

9. The calculation of the points (x, y) from the formulæ (11.1), (11.2), and (17) is laborious. In practice it is simpler to trace the lines graphically from the differential equation. To do this refer to any one of the critical rays (say 2) as axis of x. Then $\gamma_2=0$.

If we write $p=\tan\phi$, $y/x=\tan\theta$, the differential equation (8) takes the form

$$(y/x)\{(\gamma_1+\gamma_3)p+1-p^2\}=(1+\gamma_1\gamma_3)p$$

or

$$(\gamma_1+\gamma_3)+2\cot 2\phi=(1+\gamma_1\gamma_3)\cot\theta. \quad . \quad . \quad (21)$$

Let C (fig. 5) be the point $(\gamma_1+\gamma_3, \gamma_3\gamma_1-1)$, AU the line $y=1+\gamma_3\gamma_1$, D the foot of the perpendicular from C on AU. Then CD = 2. With C as centre and radius 2 units describe a circle, which touches AU at D, and on it take points E, F on a diameter parallel to the x-axis. If now a point Q is taken on this circle (it is sufficient to consider only points Q on the semicircle EDF) and CQ meets AU

Fig. 4.

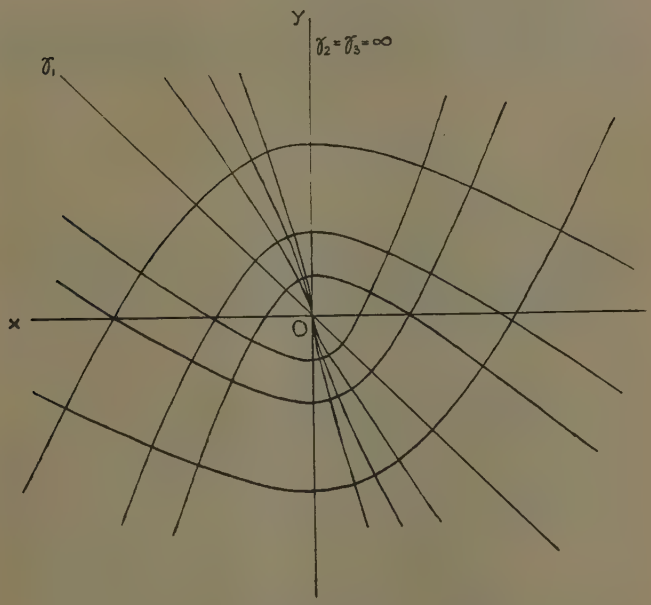

Case of two coincident asymptotes.

at P then the tangents to the lines of principal stress at the points where they cross OP are parallel to EQ, FQ.

For, if ϕ is the angle QEF, then FCP $= 2\phi =$ DPC, so that DP $= 2 \cot 2\phi$ and AP $= (1+\gamma_1\gamma_3) \cot\theta = \gamma_1+\gamma_3+ 2 \cot 2\phi$. The lines are then most easily drawn if we divide the semicircle EDF with a protractor into an even number of equal arcs, and draw the rays OP corresponding to the odd divisions. Construct a polygon whose sides lie between these rays OP, so that a side joining rays

OP_1, OP_3, say, is parallel to the line EQ_2 (or FQ_2) joining E to the even division Q_2 falling halfway between Q_1, Q_3. This side is then, to a high order of accuracy, a chord of a line of principal stress, and the vertices of the polygon are points on such a line. This largely eliminates the cumulative error due to such a step-by-step construction. The curves of figs. 1–4 have been drawn by this method, which applies also when γ_1, γ_3 are conjugate imaginaries or when they are equal.

10. We have now examined all possible cases when there are terms of the third degree in the development

Fig. 5.

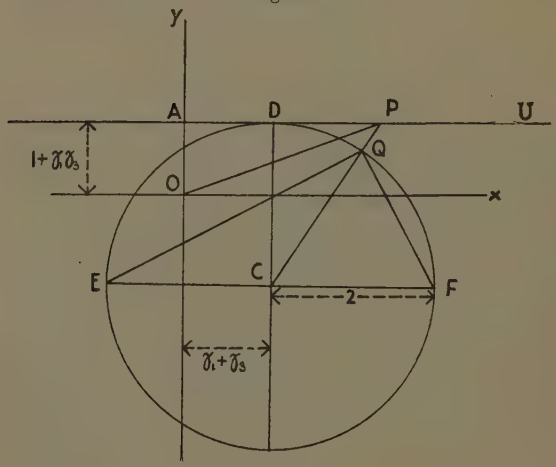

of the stress function χ. In the highly special case where $A_1=B_1=C_1=D_1=0$, we find, using (4), that

$$\widehat{xx}-\widehat{yy}=-\{(A_2+C_2)x^2+(C_2-A_2)y^2+2B_2xy\},$$

$$2\widehat{xy}=-\{(B_2+D_2)x^2+(D_2-B_2)y^2-2A_2xy\},$$

so that the differential equation of the lines of principal stress is

$$\frac{2p}{1-p^2}=\frac{(B_2+D_2)x^2+(D_2-B_2)y^2-2A_2xy}{(A_2+C_2)x^2+(C_2-A_2)y^2+2B_2xy}. \qquad (22)$$

Although (22) can be integrated, it leads to extremely complicated results, and it is hardly worth the work involved in view of the highly exceptional character of this case.

We may, however, show that it can never lead to a system of radial lines through O and concentric circles, for the differential equation must then reduce to

$$\frac{2p}{1-p^2}=\frac{2xy}{x^2-y^2}, \quad \ldots \ldots \quad (23)$$

and the right-hand sides of (22) and (23) can never be identical unless

$$B_2=D_2=0$$

and $C_2-A_2=-(A_2+C_2)$, *i. e.*, $C_2=0$, leaving

$$\frac{2p}{1-p^2}=-\frac{2xy}{x^2-y^2}. \quad \ldots \ldots \quad (24)$$

But (24) and (23) are clearly incompatible, so that this possibility does not exist, and we cannot have a distribution of stress symmetrical about an isotropic point unless the latter is a singularity, where infinite stresses are introduced.

11. The practical application of the above results to the photo-elastic exploration of the stresses in the neighbourhood of an isotropic point is important.

The photo-elastic data give the loci $P-Q=$const. (the *isochromatic* lines) and the loci $\phi=$const. (the *isoclinic* lines), where $\tan\phi=p$, as before. From the isoclinic lines the lines of principal stress are obtained by a well-known construction.

There is a method * of obtaining the separate principal stresses, proceeding from a point on a free edge, where these are known, along a line of principal stress, by integration step by step, using the equation

$$\frac{dP}{ds_1}=\frac{(Q-P)\Delta\phi}{\Delta s_2}, \quad \ldots \ldots \quad (25)$$

where ds_1 is the element of arc of the line of principal stress P and Δs_2 is the intercept perpendicular to this line of principal stress between two near isoclinics in the neighbourhood whose parameters differ by $\Delta\phi$.

* See Coker and Filon, ' Photo-Elasticity,' pp. 143–146.

Hitherto this method has been unavailable in the neighbourhood of an isotropic point, for two reasons.

In the first place, as we approach an isotropic point the actual tracing of the lines of principal stress from purely experimental data is difficult, and the results, in the absence of *a priori* theoretical knowledge as a guide, are apt to be irregular and uncertain.

In the second place, in the neighbourhood of such a point p is a function of y/x. If θ is the vectorial angle of any point, so that $y/x = \tan\theta$, ϕ is a function of θ alone. Thus the isoclinic lines ($\phi = \text{const.}$) are a set of radial lines ($\theta = \text{const.}$) passing through the origin. If follows that Δs_2, the intercept between two near isoclinics, approaches zero as we approach the isotropic point and is extremely difficult to measure. Thus, in working out the solution of equation (25) by quadratures, the values of the integrand are affected by large errors in the denominator, and equally so in the numerator, for small values of Q—P are always uncertain, owing to the presence in the material of some (usually small) residual stress.

For these two reasons the method ceases to be practicable.

The new results, however, enable us to use the method in question theoretically and to obtain the stress at the isotropic point itself and, as we shall see, also in its neighbourhood.

By rotating the polariser and analyser through known angles we obtain a series of black brushes through the isotropic point. The azimuth θ of these black brushes (which are the isoclinic lines) is readily measured, and ϕ is known from the inclination of the polariser and analyser.

A series of simultaneous values of θ and ϕ, where ϕ is varied by definite steps between 0° and 180°, can be obtained, and the values of θ plotted to ϕ on a diagram.

It will then be found that if the line $\theta = \phi$ is drawn on this diagram it will meet the curve of θ to ϕ at three real points, or at one only, according as we are dealing with case I. or with case II. The values of $\tan\theta$ or $\tan\phi$ corresponding to these intersections are then the γ_1, γ_2, γ_3 of the previous discussion. One at least of these is real, and the corresponding isoclinic is then an approximately rectilinear line of principal stress which passes through the isotropic point O.

Suppose now that we select a point A on this line of principal stress as far as possible from O consistent with

the condition that the line in question is sensibly straight. The test for this is that the curvature of the corresponding isoclinic is not appreciable up to A. In practice this is found to give quite a satisfactory range.

Now A can be reached by the standard method, and we may assume the principal stresses P_0, Q_0 at A to be known.

Applying now equation (25), then, since the line of principal stress in question is straight, $ds_1=dr$. Also the two isoclinics corresponding to parameters ϕ, $\phi+\Delta\phi$, which include ϕ_1 between (tan $\phi_1=\gamma_1$, say) are straight lines converging to O at an angle $\Delta\theta$. Accordingly $\Delta s_2=r\Delta\theta$ approximately, and we have

$$\frac{dP}{dr}=\frac{(Q-P)\Delta\phi}{r\Delta\theta},$$

$\Delta\phi$, $\Delta\theta$ remaining constant throughout the integration with regard to r.

Since from (5) $\widehat{xx}-\widehat{yy}$ and $\widehat{xy}$ are linear functions of x, y, it follows that, as we move away from O in a fixed direction, $\widehat{xx}-\widehat{yy}$ and $\widehat{xy}$ are proportional to r, and therefore

$$Q-P=\sqrt{(\widehat{xx}-\widehat{yy})^2+4\widehat{xy}^2}$$

is also proportional to r. Hence

$$Q-P=Kr,$$

where K is a constant throughout the integration.

We have therefore

$$\frac{dP}{dr}=K\frac{\Delta\phi}{\Delta\theta}=\text{const.},$$

so that, if R is the all-round stress at O,

$$P-R=rK\cdot\frac{\Delta\phi}{\Delta\theta}=(Q-P)\frac{\Delta\phi}{\Delta\theta}. \quad . \quad . \quad (26)$$

Put into this equation the values of P, Q corresponding to the point A, then, making $\Delta\phi$, $\Delta\theta$ tend to zero,

$$R=P_0+(P_0-Q_0)\frac{d\phi}{d\theta}, \quad . \quad . \quad . \quad . \quad (27)$$

which gives R if $d\phi/d\theta$ is known for a critical direction.

12. If we now differentiate the equation (8) with regard to p we find easily

$$\frac{d(y/x)}{dp} = \frac{\sec^2\theta\, d\theta}{\sec^2\phi\, d\phi} = \frac{(1+p^2)(1+\gamma_2\gamma_3)(1+\gamma_3\gamma_1)(1+\gamma_1\gamma_2)}{[(\gamma_1+\gamma_2+\gamma_3+\gamma_1\gamma_2\gamma_3)p+1-p^2]^2}. \quad . \quad . \quad . \quad (28)$$

Let the axis of x be taken to coincide with direction γ_1, so that $\gamma_1=0$. Then, when $\theta=0$, $\phi=0$ and

$$\frac{d\theta}{d\phi} = 1+\gamma_2\gamma_3. \quad . \quad . \quad . \quad . \quad . \quad (29)$$

This gives $\left(\frac{d\theta}{d\phi}\right)_1$ when γ_2, γ_3 are known.

If there are *three* real critical lines, found as in the last section, then γ_2, γ_3 are at once obtained from $\tan\phi_2$ and $\tan\phi_3$; but if there is only one critical line the constants γ_2, γ_3 are immediately obtained from the observations and the diagram of fig. 5, γ_1 replacing γ_2 in the notation of § 9. The construction is as follows.

Draw a circle centre C and radius 2 units. Through C draw a diameter EF parallel to the critical direction corresponding to γ_1 and therefore to the coincident isoclinic and line of principal stress under observation. Let ADU be a tangent to the circle parallel to EF. Take two values ϕ', ϕ'' and the corresponding values θ', θ''. Through E draw two rays of inclinations ϕ', ϕ'' meeting the circle again at Q′, Q″. Let CQ′, CQ″ meet ADU at P′, P″ and through P′, P″ draw two lines of inclinations θ', θ'' respectively; these inclinations ϕ', ϕ'', θ', θ'' are measured from any standard direction and are not necessarily referred to EF.

The lines last drawn through P′, P″ meet at some point, which is the O of fig. 5. If now A is the foot of the perpendicular from O on ADU, $OA=1+\gamma_2\gamma_3$, $AD=\gamma_2+\gamma_3$.

Thus OA gives at once the required value of $\left(\frac{d\theta}{d\phi}\right)_1$.

It can be scaled off with quite good accuracy, for O is well determined if ϕ', ϕ'' have been suitably chosen. Thus the value R of the stress at the isotropic point is immediately deduced.

13. The results of §12 enable us, however, to go a great deal further, for they give both $\gamma_2\gamma_3$ and $\gamma_2+\gamma_3$; thus γ_2, γ_3 are found as the roots of the quadratic

$$\gamma^2-(\gamma_2+\gamma_3)\gamma+\gamma_2\gamma_3=0,$$

and the coefficients of this quadratic being known its roots, whether real or imaginary, are readily calculated.

Here γ_2, γ_3 are referred to axes for which $\gamma_1=0$; but, if required, they are readily deduced for axes making an angle α with these by adding (or subtracting) α from 0, $\tan^{-1}\gamma_2$, $\tan^{-1}\gamma_3$.

Using now equations (7.1) (where $\gamma_1=0$), we have

$$B_1=0,\quad D_1=(\gamma_2+\gamma_3)C_1,\ A_1=(2+\gamma_2\gamma_3)C_1, \quad . \quad (30)$$

and, from (5),

$$\widehat{xx}-\widehat{yy}=\{-(1+\gamma_2\gamma_3)x+(\gamma_2+\gamma_3)y\}C_1,$$
$$\widehat{xy}=-C_1y.$$

Along the line of principal stress $y=0$ ($\tan\theta=\gamma_1$)

$$\widehat{xx}-\widehat{yy}=-C_1(1+\gamma_2\gamma_3)x,$$
$$\widehat{xy}=0;$$

$$\therefore \qquad P-Q=-C_1(1+\gamma_2\gamma_3)r,$$

since here $\widehat{xx}=P$, $\widehat{yy}=Q$, $x=r$.

Substituting the values at A, where $r=r_0$ say, a quantity known from measurement

$$(Q_0-P_0)/\{(1+\gamma_2\gamma_3)r_0\}=C_1. \quad . \quad . \quad . \quad . \quad (31)$$

Accordingly all four constants A_1, B_1, C_1, D_1 are known, and the stress-distribution in the neighbourhood of the isotropic point is fully determined, without any need to have recourse to step-by-step integration or to indirect methods.

14. One case requires special consideration, namely, that in which *two* critical directions only are found from the ϕ, θ diagram. This corresponds to case III., where $\gamma_2=\gamma_3$. In this case the line $\phi=\theta$ *touches* the curve of the experimental ϕ, θ diagram.

It is then an advantage to take the point A on the *double* critical line, for then we have immediately, either

from the ϕ, θ diagram or from equation (28), where $\gamma_2=\gamma_3=0$, $\theta=\phi=0$, and $p=0$,

$$\frac{d\theta}{d\phi}=1$$

and

$$R=2P_0-Q_0.$$

The method of §12 is still valid to find γ_1, but in this case γ_1 is always real and is best found from the ϕ, θ diagram. We have, referring to the coincident directions γ_2, γ_3, as x-axis

$$B_1=0,\quad D_1=\gamma_1 C_1,\quad A_1=2C_1,$$

$$\widehat{xx}-\widehat{yy}=(-x+\gamma_1 y)C_1,$$

$$\widehat{xy}=-C_1 y,$$

and along the x-axis

$$P-Q=-C_1 r,$$

so that

$$C_1=(Q_0-P_0)/r_0.$$

15. As the result of the present investigation it appears not only that the lines of principal stress in the neighbourhood of an isotropic point can be easily identified in general with one of three standard types, but that the occurrence of an isotropic point in a photo-elastic problem, far from being a stumbling block, is a very real help towards the stress exploration. It may, in fact, be advantageous to create artificially such points in a problem by superimposing a known stress-system which, in combination with the one which is being explored, will introduce such points into the field of observation.

XV. *On a Case of Self-Reciprocity in the Cosine Transform.* *By* Alan Johnson, *B.Sc., and* E. G. Phillips, *M.A., M.Sc., University College of North Wales, Bangor* *.

PAIRS of functions which are reciprocal in the Fourier transform have many applications in Applied Mathematics and Physics, and lengthy tables of such

* Communicated by the Authors.

pairs have been compiled by G. A. Campbell *. In recent years considerable attention has been given to self-reciprocal functions. If $\nu \geqslant -\frac{1}{2}$ and

$$\phi(x) = \int_0^\infty (xt)^{\frac{1}{2}} \mathrm{J}_\nu(xt)\phi(t)\,dt \quad . \quad . \quad . \quad . \quad . \quad (1)$$

then $\phi(x)$ is self-reciprocal in the Hankel transform (described as R_ν). If $\nu = \pm\frac{1}{2}$, (1) reduces to the result that

$$\phi(x) = \sqrt{\left(\frac{2}{\pi}\right)} \int_0^\infty \begin{matrix}\sin \\ \cos\end{matrix} xt\phi(t)\,dt$$

and $\phi(x)$ is self-reciprocal in the Fourier sine or cosine transform (described as R_s or R_c).

The problem of what types of functions are transforms has been so completely examined by Hardy and Titchmarsh † that particular examples can be readily written down; but an examination both of Campbell's tables and of the recent literature reveals the fact that very few self-reciprocal functions exist which have a simple functional character. Two such functions, which are R_c, are listed by Campbell; they are

$$\cos\tfrac{1}{2}\left(x^2 - \frac{\pi}{4}\right), \quad . \quad . \quad . \quad . \quad . \quad . \quad . \quad (2)$$

and

$$(a^2+x^2)^{-\frac{1}{4}}\mathrm{K}_{\frac{1}{4}}\{a\sqrt{(a^2+x^2)}\}. \quad . \quad . \quad . \quad . \quad (3)$$

The second of these suggests a new example of a function which is R_ν, and this has been discussed by one of us in a paper to be published elsewhere ‡. There does not appear to be any explicit reference in the literature to the function (2).

That (2) is R_c can be readily seen by putting $\nu = -\frac{1}{2}$, $u = 1$ in the result given by Bailey § that if $-1 < \mathrm{R}(\nu) < \frac{1}{2}$

$$\int_0^\infty \mathrm{J}_\nu(xt)t^{\nu+1}\cos\{\tfrac{1}{2}u^2t^2 - \tfrac{1}{4}(\nu+1)\pi\}dt$$
$$= x^\nu u^{-2\nu-2}\cos\tfrac{1}{2}\{x^2/u^2 - \tfrac{1}{4}(\nu+1)\pi\}.$$

* Bell System Technical Journal, vii. (1928).
† Quarterly Journal of Math. (Oxford) i. pp. 196–231 (1930).
‡ Phillips, Proc. Edinburgh Math. Soc.
§ Journ. London Math. Soc. v. p. 260 (1930).

It is, however, interesting to observe that in the paper by Hardy and Titchmarsh * in which they consider the known examples of self-reciprocal functions neither (2) nor (3) is mentioned.

The first formal solution of Hardy and Titchmarsh states that $f(x)$ is R_c if

$$f(x) = \frac{1}{2\pi i}\int_{c-i\infty}^{c+i\infty} 2^{\frac{1}{2}s}\Gamma(\tfrac{1}{2}s)\psi(s)x^{-s}\,ds$$

and $\psi(s)$ is an even function of $s-\frac{1}{2}$.

If $c=\frac{1}{2}$, $\psi(s)=\cos\frac{\pi}{4}(\frac{1}{2}-s)$ and we write $\frac{1}{2}s=-t$, $y=\frac{1}{2}x^2$, we get

$$f\{\sqrt{(2y)}\} = \frac{1}{\pi i}\int_{-\frac{1}{2}-i\infty}^{-\frac{1}{2}+i\infty} \Gamma(-t)\cos\frac{\pi}{2}(\tfrac{1}{4}+t)y^t\,dt,$$

and on calculating the residues at the poles $t=n$ ($n=0$, 1, 2, ...), the contour being supposed drawn so that these poles are all inside it, we get

$$f\{\sqrt{(2y)}\} = -2\sum_{n=0}^{\infty}\cos\frac{\pi}{2}(\tfrac{1}{4}+n)\frac{(-y)^n}{n!} = -2\cos\left(\frac{\pi}{8}-y\right)$$

and so

$$\cos\tfrac{1}{2}\left(x^2-\frac{\pi}{4}\right)$$

is R_c.

It is interesting to see where this example fits into the general theory. Since $f(x)$ is not $L^2(0,\infty)$ it cannot come under the theorems of Hardy and Titchmarsh † which concern functions of this class. It is easy to show, however, that it comes under Theorem 13 ‡.

* *Loc. cit. ante.*
† *Loc. cit.* p. 201–8.
‡ *Loc. cit.* pp. 214.

[*The Editors do not hold themselves responsible for the views expressed by their correspondents.*]